

The Feasibility of using Biomass for Energy for a Typical (African) Rural Community



Munyeowaji Ernest Mbikan

Supervisor: Dr. Christopher A. Gould

Prof. Tarik T. Al-Shemmeri

School of Creative Arts and Engineering

Staffordshire University

This dissertation is submitted for the degree of

Doctor of Philosophy

Abstract

To evaluate the biomass potential to provide thermal energy to drive an absorption refrigeration system, a computer aided model was developed. The subroutines that constitute the model agree with ASHRAE standards and reflect the underlying thermodynamic principles, but introduces a shorter method of analysing Aqua-Ammonia absorption refrigeration cycle by eliminating the need for finding the specific volume from charts or computation of the rigorous parameter components of the equations of state. Parametric evaluation from the model shows that at constant evaporator, condenser and absorber temperatures, the COP decreases with increase in generator temperature. The COP ranges between 0.84 for generator temperature of 60 °C and 0.76 for 90 °C, beyond which the variation is insignificant. The concentration of the refrigerant exiting the generator is dependent on the solution mass flow and temperature, and varies between 0.9 to 0.98 for the simulated data. This quantity is usually assumed to be 100%. The biomass consumption varies with generator temperature and the flow of hot water, but also depends on the fuel density, load and heating hours, as well as the efficiency of the biomass combusting system. The rationale a typical (African) rural community with access to biomass is based on the characteristics of these communities; one of which is the access to renewable energy in a dimension that is apt to support the production and efficient utilisation of the energy to a large scale, and the need for a refrigeration system that demands little or no extra energy but capable of conditioning indoor climate to suit human comfort, maintain and support the viability of agricultural seedlings and medical drugs in healthcare facilities and related amenities. The conventional vapour compression refrigeration systems, although efficient, use refrigerants that are not environmentally friendly and high energy consuming. The study highlights some of the limitations of the uptake, and efficient utilisation of renewable energy in the region. It also presents a review of energy in the region from a global and historical perspective and focuses on the influence on the regional economy from a state of the art review of the literature. It shows the relation between energy access and economic development. Causality study shows that this might be unilateral or bilateral, but the influence of one on the other does exist. The theory of biomass for energy was explored to highlight measures of enhancing the energy yield of a biomass species, suitability and selection.

Table of contents

	Page
List of figures	xii
List of tables	xv
Nomenclature	xvii
1 Background	1
1.1 Introduction	1
1.2 Project Objectives and Scope	3
1.3 Thesis and Contribution to Knowledge	5
1.4 Work Outline	6
2 Literature Review	8
2.1 Biomass for Energy	8
2.1.1 Global Energy Demand	8
2.2 Energy: Africa Situation	11
2.2.1 Economy	12
2.2.2 Demography	13
2.2.3 Energy Access	13
2.3 Biomass To Energy	15
2.3.1 Biomass Logistics	19
2.4 Biomass for Power Generation	20
2.4.1 Thermochemical Conversion Technology	20
2.5 Biomass Refrigeration	22
2.5.1 Absorption Refrigeration Cycles	22
2.5.2 Absorption Refrigeration Working Fluids	25
2.6 Biomass for Cooling and Power	26
2.6.1 Combined Dual Systems (CHP/CCH)	27
2.6.2 Trigeneration	28

TABLE OF CONTENTS

2.6.3	Prime Movers	29
2.7	Summary	30
3	Theory of Biomass Refrigeration	31
3.1	Introduction	31
3.2	Theory of Biomass Combustion	31
3.2.1	Properties of Biomass fuels	32
3.2.2	Stoichiometric Air and Flue Gas Calculations	35
3.2.3	Adiabatic Flame Temperatures	36
3.3	Theory of Heat Exchanger	37
3.3.1	Overall Heat Transfer Coefficient	37
3.3.2	Analysis of Heat Exchanger	40
3.4	Theory of Absorption Refrigeration	42
3.4.1	Single Stage Absorption Refrigeration Cycle	42
3.4.2	Thermodynamic Properties	43
3.4.3	Theoretical Performance Evaluation	43
3.5	Summary	46
4	Absorption Cooling and Analytical Modelling	47
4.1	Introduction	47
4.2	MATLAB Interface	48
4.3	TCA - Experimental Evaluation/Modelling	49
4.3.1	Introduction	49
4.3.2	Theoretical modelling	50
4.3.3	Experimental Evaluation	58
4.4	Aqua-Ammonia VARC - Modelling	64
4.4.1	Mass and Energy Balance	65
4.4.2	Governing Equation	68
4.4.3	Modelling	72
4.5	Summary	81
5	Biomass Performance Evaluation	82
5.1	Introduction	82
5.2	Solid Biomass Fuel Properties	83
5.2.1	Moisture content	83
5.2.2	Energy content	83
5.3	Biomass Combustion for Energy	86

TABLE OF CONTENTS

5.3.1	Biomass Combustion System	87
5.3.2	Biomass Source to Drive Absorption Refrigeration	91
5.3.3	Biomass Quantity Estimation	94
5.4	Feasibility of Nigeria's Reliance on Biomass	96
5.4.1	Biomass Energy Potential	96
5.5	Summary	99
6	Result and Discussion	101
6.1	Introduction	101
6.2	TCA – Results and Analyses	102
6.2.1	Results - Modelling	102
6.2.2	Results - Experimental	107
6.3	Aqua-Ammonia VARC - Model Validation	114
6.3.1	Sample Calculation Compared with Simulation	114
6.3.2	Manual Solution Procedure	115
6.3.3	Results of sample calculation from model	116
6.4	Model Validation	117
6.4.1	Comparison with empirical results and analysis	118
6.4.2	Comparison with theoretical results	135
6.5	Solid Biomass Fuel Properties	140
6.5.1	Moisture Content	140
6.5.2	Calorific Value	141
6.6	Biomass to Drive Absorption Refrigeration	143
6.7	Feasibility of Nigeria's reliance on Biomass	147
6.8	Other System Considerations	152
6.9	Summary	154
7	Conclusions and Recommendations	155
7.1	Conclusions	155
7.2	Recommendation	157
	References	158
	Appendix A Absorption Cooling and Analytical Modelling	173
A.1	TCA Evaluation	173
A.1.1	Technical Data	173
A.1.2	Operational Data	174

TABLE OF CONTENTS

A.1.3	MATLAB Code: TCA Evaluation	175
A.2	MATLAB Code: NH_3-H_2O VARC	178
A.2.1	Sub-routine: NH_3-H_2O VARS	181
Appendix B	Biomass Cooling	246
B.1	Oxygen Bomb Experiment	247
B.2	Time Series Analysis	248
Appendix C	Drax Power Station - Biomass Power Plant	249
C.1	Drax - Reduced Carbon Footprint	249
C.2	Drax - Biomass Power Plant	251

Validation Matrix

This matrix is a summary of the absorption refrigeration model validation

Table 1 Aqua-ammonia vapour absorption refrigeration system validation

References & Parameters					
Reference	COP	Qe/Te	Qg/Tg	Qa/Ta	Qc/Tc
Du et. al. [58]	X	X	-	-	-
El-Shaarawi et. al. [64]	X	-	X	X	X
Du et. al. [59]	XX	X	XX	XX	XX
Abdulateef et. al. [2]	X	XX	XX	XX	XX
Horuz [80]	X	X	X	X	X
Lazarin et. al. [117]	X	X	X	X	X
Karamangil [97]	X	X	X	X	X
Sun [183]	X	-	XX	-	-
Kaushik [102]	X	XX	XX	-	-

Where:

- COP - Coefficient of performance
- Qe - Evaporator energy
- Qg - Generator energy
- Qa - Absorber energy
- Qc - Condenser energy

TABLE OF CONTENTS

- T_e - Evaporator temperature
- T_g - Generator temperature
- T_a - Absorber temperature
- T_c - Condenser temperature
- X - One parameter checked
- XX - Both parameters checked

Glory to God Almighty, the source of all inspiration, strength and grace.

Declaration

I, Munyeowaji, declare that this thesis titled, "The Feasibility of using Biomass for Energy for a Typical (African) Rural Community" and the work presented in it are my own. I confirm that:

- This work was done wholly or mainly while in candidature for a research degree at this University.
- Where any part of this thesis has previously been submitted for a degree or any other qualification at this University or any other institution, this has been clearly stated.
- Where I have consulted the published work of others, this is always clearly attributed.
- Where I have quoted from the work of others, the source is always given. With the exception of such quotations, this thesis is entirely my own work.
- I have acknowledged all main sources of help.
- Where the thesis is based on work done by myself jointly with others, I have made clear exactly what was done by others and what I have contributed myself.

Munyeowaji Ernest Mbikan
September 2019

Acknowledgements

I would like to express my sincere gratitude to my supervisor Dr Christopher A. Gould for accepting the responsibility of providing, for me, guidance, technical support and insightfulness in a friendly manner and atmosphere, amidst his very tight schedules. Though short the period, the impact is huge and the memory will last in the spectrum of time. Thank you, Dr Chris.

I would like to acknowledge the invaluable moral, professional and academic support from my supervisor, prof Tarik T. Al-Shemmeri. Your trust, constant encouragement, access to your personal library and general lead has greatly impacted on me and this achievement. I would like to thank your family for the mind-blowing reception at all times of my visit. This memory is indelible. I am immensely grateful. Thank you, prof.

I would like the Dean of the school of Creative Arts and Engineering and the head of department of the engineering faculty for the financial support.

I would like to thank all my friends who have stood by me in no little way. Rev and Mrs Albert Addai, Mr and Mrs Frederick Bampo, the family at Gracefields Chapel and Mr and Mrs Kumbe. Thank you.

Finally, I would like to acknowledge my family for their patience, prayers and support. My parents chief and mrs E. D. Mbikan, my brothers Eneile and Mowon, and my sisters Ayi, Owajima, Atainu and Helen. Thank you all very much indeed.

List of figures

2.1	Energy Consumption by Source [62]	9
2.2	World Energy Consumption [63]	10
2.3	World Energy Consumption by Region [63]	11
2.4	World fossil fuel Consumption [62]	12
2.5	SSA Population (World Bank data)[206]	14
2.6	2012 statistics of people without access to electricity by country [81]	16
2.7	Schematic of biomass conversion technology	18
3.1	Double pipe heat exchangers	38
3.2	Cross-sectional view of a tube	39
3.3	Vapour absorption refrigeration cycle schematic	44
4.1	External Features of TCA [24]	49
4.2	Internal Feature of Complete Unit of TCA ([26])	50
4.3	Schematic of a single unit of TCA	51
4.4	TCA computer model flow chart	57
4.5	TCA Experiment Set-up	62
4.6	TCA Experiment Set-up (AHU)	63
4.7	Schematic of TCA test rig	64
4.8	Schematic of VARC	66
4.9	Aqua-ammonia solution temperature-composition diagram	74
4.10	Temperature-concentration (Range: 2.00MPa–2.09MPa)	74
4.11	Simulink model block showing absorber input and output parameters	75
4.12	Simulink model block showing solution heat exchanger input and output parameters	76
4.13	Simulink model block showing generator input and output parameters	77
4.14	Simulink model block showing condenser input and output parameters	78
4.15	Simulink model block showing evaporator input and output parameters	79
4.16	Simulink model block showing system performance parameters	80

LIST OF FIGURES

4.17	Computational model of aqua-ammonia absorption refrigeration system . . .	81
5.1	PARR bomb calorimeter set up	86
5.2	Windhager biomass boiler, feed unit and buffer tank	88
5.3	Windhager biomass boiler: inside view	89
5.4	Boiler Maintenance	90
5.5	Boiler Maintenance - scooping up ash remains	91
5.6	Schematic of system heat transfer	92
6.1	Variation of cooling rate with evaporator inlet temperature at 7 kW discharge power for cooling	103
6.2	Variation of cooling rate with evaporator inlet temperature at 12 kW discharge power for cooling	104
6.3	Variation of cooling rate with evaporator inlet temperature at 15 kW discharge power for cooling	104
6.4	Variation of cooling rate with evaporator inlet temperature at 18 kW discharge power for cooling	105
6.5	Variation of cooling energy with set cooling temperature at 18 & 20 °C inlet temperature	105
6.6	Variation of cooling energy with set cooling temperature at 22 & 25 °C inlet temperature	106
6.7	Variation of cooling energy set cooling temperature (Exp1)	110
6.8	Variation of cooling energy set cooling temperature (Exp2)	111
6.9	Variation of cooling energy set cooling temperature (Exp3)	111
6.10	Variation of cooling energy set cooling temperature (Exp4)	112
6.11	Variation of cooling energy set cooling temperature (Exp5)	112
6.12	Variation of cooling energy set cooling temperature (Exp6)	113
6.13	Variation of cooling energy set cooling temperature (Exp1)	113
6.14	Variation of COP with evaporator temperature	119
6.15	Variation of Cooling capacity with evaporator temperature	119
6.16	Comparison of absorber heat capacity	120
6.17	Comparison of condenser heat capacity	121
6.18	Comparison of generator heat capacity	121
6.19	Comparison of COP	122
6.20	Comparison of the variation of COP with evaporator temperature	127
6.21	Comparison of the variation of COP with condenser temperature	128
6.22	Comparison of the variation of COP with generator temperature	128

LIST OF FIGURES

6.23	Comparison of the variation of COP with evaporator temperature	129
6.24	Comparison of the variation of absorber energy with evaporator temperature	130
6.25	Comparison of the variation of condenser energy with evaporator temperature	130
6.26	Comparison of the variation of evaporator energy with evaporator temperature	131
6.27	Comparison of the variation of generator energy with evaporator temperature	131
6.28	Comparison of the variation of absorber energy with cooling temperature .	132
6.29	Comparison of the variation of condenser energy with cooling temperature .	133
6.30	Comparison of the variation of cooling energy with cooling temperature . .	133
6.31	Comparison of the variation of cooling energy with cooling temperature . .	134
6.32	Comparison of the variation of the COP with heat exchanger effectiveness .	135
6.33	Comparison of the variation of the flow ratio with generator temperature . .	136
6.34	Comparison of the variation of the COP with generator temperature	136
6.35	Comparison of the variation of the COP with condenser temperature	137
6.36	Comparison of the variation of the COP with condenser temperature	138
6.37	Comparison of the variation of the COP with evaporator temperature	139
6.38	Comparison of the variation of the COP with generator temperature for set absorber temperature	139
6.39	Bomb calorimeter experiment temperature profile of biomass fuels	142
6.40	Calorific value for the different fuel samples	142
6.41	Variation of mass of fuel and energy output with FLHE (at $\Delta T = 20\text{ }^{\circ}\text{C}$) . .	144
6.42	Variation of mass of fuel and energy output with FLHE (at $\Delta T = 30\text{ }^{\circ}\text{C}$) . .	144
6.43	Relation between energy output and ΔT on generator input temperature at $T_{c1} = 40\text{ }^{\circ}\text{C}$)	145
6.44	Relation between energy output and ΔT on generator input temperature at $T_{c1} = 35\text{ }^{\circ}\text{C}$)	145
6.45	Energy utilisation with boiler efficiency	146
6.46	Nigeria population projected	149
6.47	Comparison of energy consumption (Excerpt from Wold Bank [205])	150
6.48	Nigeria population projected (Data source: World Bank [206])	150
6.49	Comparison of consumption based on study with current trend	151
A.1	ClimateWell Solar Chiller Technical Data	173
A.2	ClimateWell Solar Chiller Operational Data	174
B.1	Computation of HHV from test data	247
B.2	Energy access projection	248
C.1	Biomass Sample - Drax Power Station	249

C.2	Biomass Sample - Drax Power Station	250
C.3	Drax carbon footprint reduction	250
C.4	Biomass combustion unit - Drax Power Staion	251
C.5	Steam turbine unit - Drax Power Staion	251

List of tables

1	Aqua-ammonia vapour absorption refrigeration system validation	vii
2.1	Electricity access 2014 Regional aggregates [34]	17
4.1	System connection for charging and discharging	56
4.2	Recorded Parameters	61
4.3	TCA test plan	61
4.4	Coefficients for Equation (4.60)	69
4.5	Coefficients for Equation (4.61)	70
4.6	Coefficients for Equations (4.74) and (4.75)	71
4.7	Coefficients for Equation (4.77)	72
5.1	Parameters for estimating biomass fuel	95
5.2	μ_i values for equation (5.22)	98
5.3	Yearly production of some energy crops in Nigeria - excerpt from reference [68]	99
5.4	Nigeria Forest and wood stock (courtesy: Global Forest Resources - Country Report, Nigeria [13])	99
6.1	Comparison of COP and Cooling Power	103
6.2	TCA experiment 1	107
6.3	TCA experiment 2	108
6.4	TCA experiment 3	108
6.5	TCA experiment 4	109
6.6	TCA experiment 5	109
6.7	TCA experiment 6	110
6.8	Operating condition	114
6.9	Comparison of results	117
6.10	Comparison of input energies variation with COP (1) (reference [59])	123

LIST OF TABLES

6.11	Comparison of input energies variation with COP (2) (reference [59])	124
6.12	Comparison of input energies variation with COP (3) (reference [59])	124
6.13	Comparison of input energies variation with COP (4) (reference [59])	125
6.14	Comparison of input energies variation with COP (5) (reference [59])	125
6.15	Comparison of input energies variation with COP (6) (reference [59])	126
6.16	Sold fuels samples tested	140
6.17	Sold fuels moisture content tests results	140
6.18	Estimation of biomass energy content from thermal characteristics	148
6.19	Estimation of biomass energy potential	148
6.20	Comparison of 5-yearly estimate: energy potential of agro-residue in Nigeria	149
6.21	Projection of 5-yearly energy potential to 2050	149

Nomenclature

Roman Symbols

A_c	Ash content
C_p	Heat capacity ($J/kg/K$)
C	Carbon
C_m	Moisture Content
C_{md}	Moisture content - dry basis
F_d	Mass of fuel - dry basis (g)
H	Hydrogen
M_{wc}	Mass of water in fuel (g)
N	Nitrogen
n	number of moles
O	Oxygen
F	Correction factor
Q	Heat energy transfer (J)
q	Heat flux density (Wm^{-2})
R	Gas constant ($8.314JK^{-1}mol^{-1}$)
r, R	radius (m)
S	Sulphur

Nomenclature

t, T	Temperature ($^{\circ}\text{C}, K$)
U	Heat energy transfer (J)
V	Volume
v	specific volume

Greek Symbols

δ, Δ	difference, time rate of change
δt_i	time step
ε	effectiveness of heat exchanger
η	efficiency
μ	viscosity (Ns/m^2)
Φ	Equivalence ratio
ψ	function
ρ	density (kg/m^3)

Subscripts

ad	Adiabatic
amb	ambient
B	Boiler
cx	condenser heat exchanger
i	in/inlet
o	out/outlet
ref	reference
rx	reactor heat exchanger
$stoi$	Stoichiometric
vap	vapour

Other Symbols

ΔH	Enthalpy difference
ΔT	Temperature difference
E_R	Energy required (J/kg)
F_d	fuel density (MJ/m^3)
h, H	Enthalpy (kJ/kg)
k	thermal conductivity ($W/(mK)$)
\dot{m}	Mass flow rate (kg/s)
M_{LiCl}	Mass of Lithium Chloride (kg)
M_{ssrb}	Mass of salt solution in the reactor bottom (kg)
M_{ssrt}	Mass of salt solution in reactor top (kg)
M_{w0}	Initial mass of water in water storage (kg)
M_{wcbi}	Initial mass of water in condenser bottom (kg)
M_{wcti}	Initial mass of water in condenser top (kg)
M_{wsrt}	Mass of water-salt solution in reactor top (kg)
Nu	Nusselt number
Pr	Prandtl number
QA	Absorber heat transfer
QC	Condenser heat transfer
\dot{Q}	rate of heat transfer (J/s)
QE	Evaporator heat transfer
QG	Generator heat transfer
Re	Reynolds number
R_{fi}	Fouling factor - inner surface

Nomenclature

R_{fo}	Fouling factor - outer surface
ρ_{LiCl}	density of lithium chloride (g/cm^3)
t_a	Absorber temperature
t_c	Condenser temperature
T_{cx0set}	cooling power set temperature ($^{\circ}C, K$)
t_e	Evaporator temperature
t_g	generator temperature
t_m	Solution temperature
t_R	Refrigerant temperature
T_{rx0set}	heating power set temperature ($^{\circ}C, K$)
UA	Overall heat transfer coefficient ($W/(m^2K)$)
V_{rt0}	Initial volume of reactor top (m^3)
w_p	pump work (W)
X	Solution concentration
x	Solution mass fraction

Acronyms / Abbreviations

<i>AHP</i>	Absorption Heat Pump
<i>BS</i>	British Standard
<i>CCHP</i>	Combined Cooling, Heating and Power
<i>CCP</i>	Combined Cooling and Power
<i>CEN</i>	Comité European de Normalisation
<i>CFCs</i>	Chlorofluorocarbons
<i>CHP</i>	Combined Heating and Power
<i>CHPP</i>	Combined Heating and Power Plant

Nomenclature

<i>COP</i>	Coefficient of Performance
<i>CWCS</i>	ClimateWell Solar Chiller
<i>DEGDME</i>	diethylene glycol dimethyl ether
<i>EIA</i>	Energy Information and Administration
<i>FLHE</i>	Full load heating hours equivalent
<i>GCV</i>	Gross calorific value
<i>GDP</i>	Gross Domestic Product
<i>HCFCs</i>	Hydrochlorofluorocarbons
<i>HFCs</i>	Hydrofluorocarbons
<i>HHV</i>	High heating value
<i>ISO</i>	International Organization for Standardization
<i>LCA</i>	Life-cycle Assessment
<i>LHV</i>	Low heating value
<i>LMTD</i>	Logarithmic mean temperature
<i>MDG</i>	Millennium Development Goals
<i>NBP</i>	Normal boiling Point
<i>NCV</i>	Net calorific value
<i>NO_x</i>	Nitrate oxides
<i>OECD</i>	Organisation for Economic Co-operation and Development
<i>OEM</i>	Original Equipment Manufacturer
<i>PPP</i>	Purchasing Power Parity
<i>SOFC</i>	Solid Oxide Fuel Cell
<i>SO_x</i>	Sulphur oxides
<i>SRC</i>	Short rotation coppice

Nomenclature

<i>SSA</i>	Sub-Saharan Africa
<i>TCA</i>	Thermochemical Accumulator
<i>UN</i>	United Nations
<i>VARC</i>	Vapour absorption refrigeration cycle
<i>VCRC</i>	Vapour compression refrigeration cycle

Chapter 1

Background

1.1 Introduction

The lack of access to modern energy, reliance on traditional biomass and fossil based fuels in meeting a greater fraction of the energy needs of rural communities of about 2,722 million people across the globe, and the effects are well known. About 70% of this population live in developing Asia and 28% in Sub-Saharan Africa (SSA). Since the industrial revolution energy has been the driving force of the development of both human and modern civilization while technology has been a base for increase in energy consumption and human population [127]. The population of SSA is about 1 billion with electricity consumption of about 40TWh, equivalent to the consumption of New York with a population of about 19.5 million [187, 206]. This implies that the electric energy available for use by one in New York is shared by about forty in SSA. The supply is usually sporadic and epileptic due to fossil fuel price volatility, high maintenance cost of over-stretched existing facilities, growing population and high rate of urbanization amidst the prevailing economic situation of most countries in the region. Hence, individuals and businesses have resorted to electric generating sets of various types and sizes that run on fossil fuels (an uneconomical, unsustainable and environmentally unfriendly option) to meet their energy needs. In Nigeria – one of the largest African nation – for instance, an estimated 60 million use petrol or diesel generating set of various sizes in large cities like Lagos with annual fuelling amounting to about £8b per annum, economic losses following power outages is put at £470.34M in 2012 and a loss in GDP of £76.72b by 2020 is forecasted [3]. The energy situation hampers economic development and the thrust of energy poverty is worse-felt in the rural communities where 25% of the monthly income is spent on fuel [29]. With little infrastructure and often difficult terrains, connection to main grid is usually economically challenging. The UN recognises that the lack of access to modern energy entrenches poverty, constrains the delivery of social services,

limits opportunities for women, and erodes environmental sustainability at local, national and global levels [100, 193]. Also, it is argued that for the UN Millennium Development Goals (MDG) of poverty alleviation to be achieved in set time, 395 million people will need to be provided with access to electricity and an additional 1 billion to clean modern energy for cooking [186]. The need for the production of energy to meet the demands of rural communities is obvious [10, 174, 29]. But to do this entirely or to a greater percent via the conventional fossil energy production path despite its future falling below economic levels, price volatility, and environmental harshness, will further limit the viability of the economies of the communities, and will constitute an oblivious sense to a current and great global challenge – climate change – and to contribute to it rather than mitigate it. Human activities have largely been responsible for the climate change across our planet resulting in significant reduction in the mass balance in most land ice mass and Arctic sea ice, change in the chemistry of sea water, and increased concentration of important greenhouse gases such as carbon dioxide, methane, nitrous oxide, CFCs (now banned), HCFCs and HFCs. The absorption capacity of these gases, due to their molecular structure and resident time in the atmosphere, affect the globe temperature. Warming of the climate has been unequivocal, and observation indicates that each of the last three decades has been successively warmer at the earth's surface than any preceding decade since 1850 to which the contribution of anthropogenic emissions have been substantial especially through fossil-fuelled energy generation and utilization [74]. Hence, it makes sense to take this important consideration into account in the course of energy development and energy related activities especially in the rural communities where the need for energy is urgent [83].

The demand for refrigeration and cooling is global and even more in the tropics where the average temperature is over 20°C. The technology is vital for indoor climate control for human comfort and food preservation. It is also a sine qua non in the agricultural, medical and manufacturing industries. However, it is one that is rarely considered for the rural areas even though it is a vital need for the thriving of their occupation (mostly fishing and farming), food preservation and comfort at home. Conventional refrigeration and air-conditioning are systems with intensive energy consumption [171, 172]. They usually run on vapour compression refrigeration cycles (VCRC) and fossil energy; the resulting climatic impact is two-fold - the effect of carbon dioxide emission from fossil fuel, and the ozone depletion effect from Hydrochlorofluorocarbons (HCFCs) and Hydrofluorocarbons (HFCs) refrigerants used in these systems. Therefore, an alternative source of cooling is necessary to meet the cooling needs of the region. Research and development of technologies aimed at reducing both the energy consumption and environmental impact of conventional refrigeration and air conditioning systems are on course [192, 67]. Ground source heating

and cooling is one such emerging technologies [27]. This involves exploring the ground's huge capacity to receive and supply heat for space heating and cooling. Others are solar powered refrigeration systems (mechanical compression or thermal sorption), ground coupled solar panel cooling and passivhaus heating and cooling ([111, 66], [167], [171, 54]). Passive heating and cooling involves strategic control of thermal conditions in buildings to improve indoor atmospheric conditions with near-zero energy consumption. The technology promises a huge energy benefit. However, its impact falls outside heavy refrigeration demands, and its application to existing buildings will be capital intensive, where possible. The vapour absorption refrigeration cycle (VARC) is a thermally driven system with very low electrical energy demand compared with the VCRC. VARC uses ozone depletion-free and environmentally friendly refrigerants. The thermal requirement of the VARC system can be met by inexpensive sources such as waste heat from industrial processes, and exhaust heat from engines, solar and biomass. As part of a trigeneration system, VARC is driven by hot water generated in the boiler and split in three ways by three separate valves leading to the three applications. Operation of VARS with solar and waste heat has been investigated substantially [175, 66, 55, 168, 173, 23, 128], [96, 126, 6, 119]. However, studies and literature on biomass driven absorption cooling is scarce.

1.2 Project Objectives and Scope

This research looked at the technical and technological aspects of utilising biomass as a renewable energy source for providing cooling energy. The project is made up of several distinct objectives:

- To contribute towards the potential of biomass as a renewable energy
- To develop and verify computer models of vapour absorption refrigeration systems
- To demonstrate the potential of biomass as an energy source to drive the vapour absorption refrigeration system
- To undertake a regional-based evaluation of the potential of biomass for energy production.

This work is carried out in three key stages:-

- The current and potential of biomass production for energy purposes and its compliance with global legislations and protocols is explored through the review of literature in relevant areas such as Biomass for Energy, Vapour Absorption Refrigeration System, Refrigerant Pairs amongst others.

- The development of a computer model succeeds the review of literature. The model shall be used to analyse and investigate the performance of a vapour absorption refrigeration system using biomass as its primary source of energy.
- The model shall be validated by comparing results with published data in the literature.

The investigation of the current and potential of biomass for energy shall be conducted through vigorous literature review of the global energy implications, and with an inclination to the African situation. The conclusion of the review will lead into the theoretical analysis of the key elements of the study, which will be applied in developing computer models. Laboratory testing of the models and comparison of simulation results with published data in the literature shall be used to validate the models. They can then be used in future works as models to obtain preliminary results without extensive testing and/or procedures.

1.3 Thesis and Contribution to Knowledge

Overall the aim of this project is:

To investigate the feasibility of using biomass as the energy source for providing cooling in rural communities with access to the resource.

Attention to biomass as a renewable source of energy has been global and considerable. However, there is no commensurate investigation of biomass as an energy source for cooling, especially for rural communities in Africa with access to biomass. Equally biomass-driven absorption cooling compared to solar, waste heat from industrial processes, engine exhaust heat and other energy sources, has not be fully understood or explored. This thesis goes, in some way to address this knowledge-gap.

The scientific interest of the project and its importance are based on preliminary review of a literature. The results and models from this project will contribute towards R&D work in the area of renewable energy, vapour absorption refrigeration systems, increased and efficient utilisation of biomass as fuel that can contribute towards carbon emission and global warming mitigation. Of particular interest is the efficient utilisation of the available resource to meet the dire need of cooling in the rural tropics without adversely impacting the environment. The following is a list of papers and a book contribution that have been published or currently under review based on the work presented in this thesis.

- Book Contribution
 - Mbikan, M. and Al-Shemmeri, T.T. 2018. Biomass for Energy Country Specific Show Case Studies. *energies*. ISBN 978-3-03842-911-1
- Conference
 - Mbikan, M. 2017. Theoretical Evaluation of a Biomass-Driven Absorption Refrigeration System. *Proceedings of the PGR Conference*. 26 May, 2017. Staffordshire University, United Kingdom
- Journal papers
 - Al-Shemmeri, T. and Mbikan, M. 2019. The Feasibility of Nigeria's Reliance on Biomass. *energies*, *under review*
 - Mbikan, M. and Al-Shemmeri, T. 2017. Computational Model of a Biomass Driven Absorption Refrigeration System. *energies*

1.4 Work Outline

This thesis consists of seven chapters with relevant appendices. Chapter two introduces biomass combustion for energy, Africa energy outlook and absorption cooling and their merits and deficiencies via a literature review of previous and current work to put in perspective the formative knowledge for this project.

Chapter three looks at the underlying scientific theory for the application of the technologies encountered in this thesis. Analyses of the mathematical concept of biomass combustion, heat exchanger and vapour absorption refrigeration cycle are considered in this chapter.

Chapter four is on modelling of vapour absorption refrigeration systems for parametric analysis and performance simulation. Experimental and theoretical evaluation of the thermo-chemical, and the modelling of a single stage aqua-ammonia absorption refrigeration cycle are presented in this chapter.

Chapter five contains the evaluation of biomass for energy. An experimental study of the properties characterising biomass solid fuels is presented. Systems for the combustion of biomass for energy and the estimation of the output energy was considered. Furthermore, the chapter presents a feasibility study to evaluate the sustainability of biomass as an energy source.

Chapter six presents and discusses the results of the tests carried out on the refrigeration system, biomass solid fuels properties, and the results and comparisons from the simulation of the aqua-ammonia absorption refrigeration system. The chapter also contains the results and discussion on the regional-based feasibility study and discusses the general challenges to the uptake of the system with the existing and emerging technologies used to address the challenges.

The general conclusion drawn from the work, as well as some suggestions for further work in this area of renewable energy will be presented in chapter seven.

Summary of work outline:

- Chapter 1 Background
- Chapter 2 Literature Review
- Chapter 3 Theory of Biomass Refrigeration
- Chapter 4 Absorption Cooling and Analytical Modelling
- Chapter 5 Biomass Energy Evaluation
- Chapter 6 Results and Discussion

- Chapter 7 Conclusions and Recommendations

Chapter 2

Literature Review

Biomass Combined Generation Technology

Amongst the measures in place to mitigate the global warming and its potential effect on lives and human activities, the use of alternative energy ranks in the bracket of the highs. Alternative energy refer to renewable energy sources whose energy flows are constantly being replenished as opposed to fossil fuels with accumulated stocks that are depleted over time. This chapter is a state of the art review of biomass to energy technologies as well as an outlook of biomass to energy - Africa situation. It also, includes reviews of other related technologies considered in this work.

2.1 Biomass for Energy

2.1.1 Global Energy Demand

Biomass refers to fuels produced directly or indirectly from organic materials. This includes plants, agricultural, domestic and industrial wastes. Biomass is carbon neutral and has been in use for energy production since the beginning of human existence; at the time it was the only source of energy for cooking and keeping warm [189]. For many parts of the world it is still the main source of heat. Energy source has moved from the single primary use of biomass (wood) to include other sources that are more convenient with greater potency. Coal played an important part of the energy evolution and it is still very relevant in the global energy production and consumption which at the height of the low-technology industrial revolution in about 1850 – 1870, led to the surge of per capita daily energy consumption of about 70000 kilocalorie in England, Germany and the United States (Fig. 2.1).

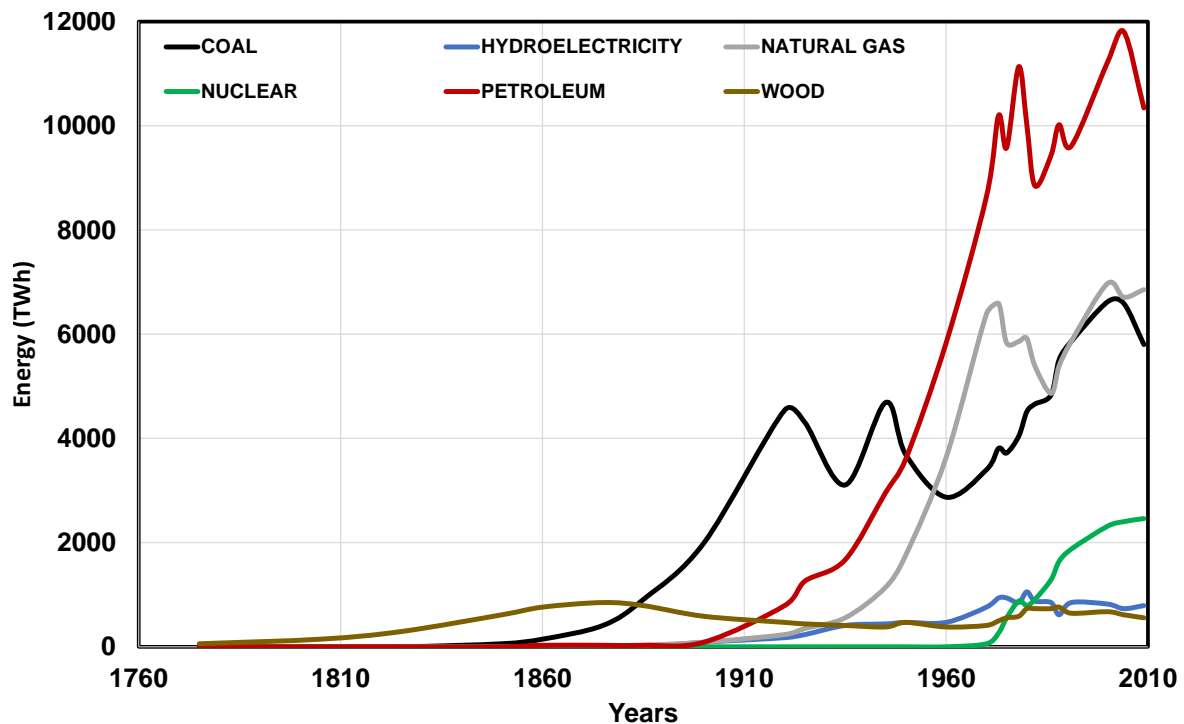


Fig. 2.1 Energy Consumption by Source [62]

Following this energy surge, was the era of the high-technology industrial revolution ushered in by the development of central power stations enhancing the availability of power for use in homes and the rapid growth in the production of automobiles which increased the use of energy in the transport sector. At the beginning of the 20th century, the per capita energy consumption further increased, reaching highs of 230,000 kilocalorie about the end of 1970 [49]. Energy demand witnessed dramatic increase with continued growth in human population, expansion, advances in technology and technology-enhanced demographic transformations. The energy demand has been met mostly by fossil fuels. Fossil fuels are non-renewable. This implies that they are not replenished and ready for use on a meaningful time-scale and the economic reserves are fast depleting below sustainable levels. This setback coupled with market fluctuations and the political instability of most production regions further constrain the sustainability of the fuel [189]. The current reserves were produced between 50 and 350 million years ago and the EIA estimates oil reserves to last till about the end of the century. The total world marketed energy consumption over the 28-year period from 2012 to 2040 is expected to reach 238 TWh from the anticipated 160 – 184 TWh projected from 2012 – 2020. Fig. 2.2 shows an increase of 48% in the global energy consumption with most of the world's increase occurring among the developing non-OECD regions due to strong economic growth and expanding population (Fig. 2.3). The increase in

demand is projected to reach 71% within the 28 – year period under projection. [63]. The projections are based on the current energy consumption and population growth profiles Fig. 2.4. The dotted projections based on estimates which requires a reduction of CO_2 production to curb global temperature rise of $2^\circ C$. The implication is a significant reduction in the consumption of fossil fuel in the near future. The exponential rise in the consumption of fossil fuel in the last 50 years is vivid from the graph, a rise of about 15% from 1997 to 2007. Considering the dwindling reserve of fossil fuel, major political problems fostered by fight over the remaining reserve may occur [145]. Fossil fuel is the major source of CO_2 emission. Although the current set of emission scenarios used by the Intergovernmental Panel on Climate Change have been challenged as unrealistic and biased by optimistic expectations on the future of fossil fuel production based on the fact that the models employed have been detached from supply and related inherent problems, it is well known that harmful emissions with short and long term devastating effects on humans and nature are synonymous with fossil fuels combustion [84, 85], [79]. Most of the increase in energy demand occurs in the non-OECD regions due to the emergence of strong economy and increase in population growth. Africa lies in this region and has been the epicentre of the global challenge of energy poverty. Ironically, the economy is developing and population is growing with the demand for energy out-pacing supply. The next section looks at Energy: Africa situation.

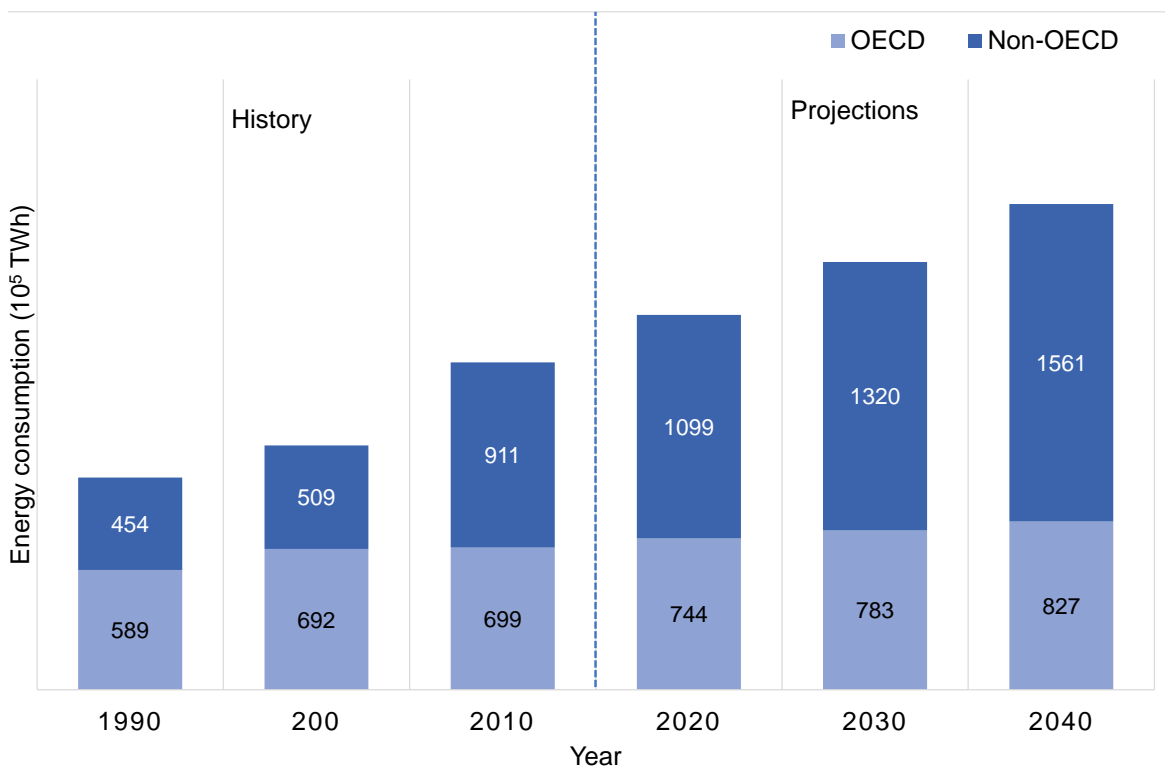


Fig. 2.2 World Energy Consumption [63]

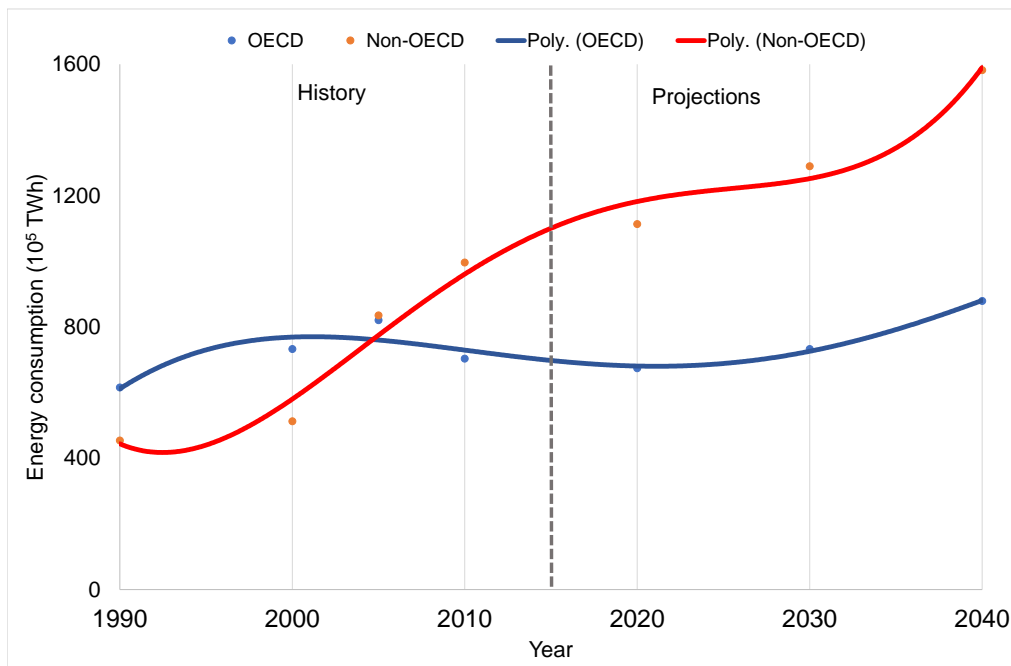


Fig. 2.3 World Energy Consumption by Region [63]

2.2 Energy: Africa Situation

Africa is endowed with the widest possible range of energy resources, large enough to meet its domestic energy needs and to substantially impact supply to meet global energy demand [81, 86, 204]. However, the economic growth in the last thirteen years owing to factors including improved macroeconomic management, a relative period of stability and security, growing middle class, increased demand for Africa's resources, growing population and urbanisation, have not guaranteed sufficient energy access as the demand for energy has grossly increased. GDP per capita has also increased but more slowly. The extent of energy access in Africa divides the continent into two broad categories - "energy-rich" and "energy-impooverished regions". The former is made up of countries in the North and South of Africa. Countries in the middle of these ends make up the SSA nations. These are the main constituent nations in the energy-impooverish region. The SSA is the main focus of this review.

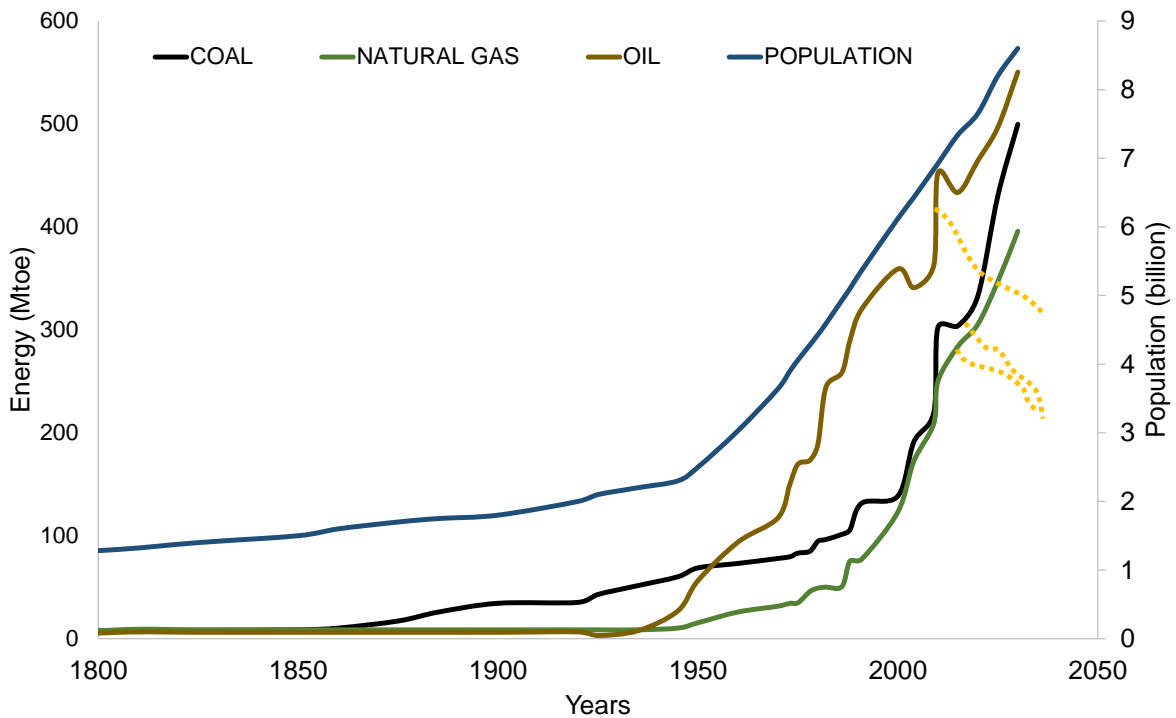


Fig. 2.4 World fossil fuel Consumption [62]

2.2.1 Economy

The relationship between economic growth and energy consumption can hardly be disengaged. The discovery of coal allowed the industrial revolution to emerge in the United Kingdom in the later part of the 18th century. Prior to the industrial revolution, energy has played an important role in human development and the quality of life. Studies of various economies at varied but defined periods have complimented this historical fact. Kraft and Kraft established the empirical relationships between energy consumption and economic growth, and causality between these two variables by applying Granger causality test to U.S. data for a period of 1947 – 1974 [113]. Other economies studied include Asian industrialised nations [44, 212]. Ozturk et. al. studied the gross domestic product (GDP) and energy consumption relationship of fifty-one countries from 1971 – 2005 [151]. The disparity in literature lies in the direction of the relation - whether the relation is bilateral or unilateral. While the order of influence is important especially for policy makers and investors, what is clear is that both variables are closely related. Similar study across seventeen Africa nations shows that there is a long standing relationship between energy consumption and GDP per capita. While some countries showed a unidirectional relationship, for others, the relation was bilateral in the causality test [203].

Sub-Saharan Africa is one of the worst energy impoverished region of the world, houses the

poorest nations. The UN Millennium Development Goal considers the provision of energy as the fundamental process to alleviate poverty in the region. The effect of the insufficient access to energy in the region entrenches poverty, limits the economy, constrains the delivery of social services, limits opportunities especially for women and children and it erodes environmental stability at all levels [100]. The economy of the region has doubled in size to reach \$2.7 trillion in 2013 (in terms of PPP of 2013) from 2000, and yet still, it is behind Germany (\$3.2 trillion), despite being about twelve times bigger in terms of population [81]. Although the development caused a lift of a large number of people out of absolute poverty (i.e. those living on less than \$1.25/day), GDP growth has been very slow. The impairment of the economy of the region is to a great extent related to energy production and consumption [50, 61, 149, 5]. Ebohon analysis of the state of the economic growth and energy consumption doubts the ability of achieving sustainable economic growth and development due to energy problem [60].

2.2.2 Demography

The increasing population of Sub-Saharan Africa plays a significant role in its energy development, demand and consumption. The population has hit the one billion mark; an increase of about 300 million from year 2000 (Fig. 2.5) [81, 205]. Although the increase opens up new frontiers for business development hinged on the rising working-age population, it pins an increasing pressure on the energy problem which has been a huge challenge for the region and enormously magnifying the task of resolving the energy menace. About 63% of the population live in the rural areas where the dependency on traditional biomass is high and the difficult task of manually fetching and processing the fuel erodes economic productivity and educational development especially for women. Also, the distribution of modern energy sources in the region is grossly uneven with the highly populated rural areas being the most neglected [28, 105]. Ideally, with a 5.5 increase in the average life expectancy since 2002 to reach 55years, increasing young working-age population and available labour force should positively reflect the economy. However, this remains an illusion largely due to the energy situation of the region.

2.2.3 Energy Access

The effect of the lack of access to modern energy in Sub-Saharan Africa is evident in the quality of life and the rate of economic development in the region. The situation has been a major constraint in the realisation of the goals of the UN's MDP geared towards poverty eradication in the region. Consequently, it has attracted several studies and allied

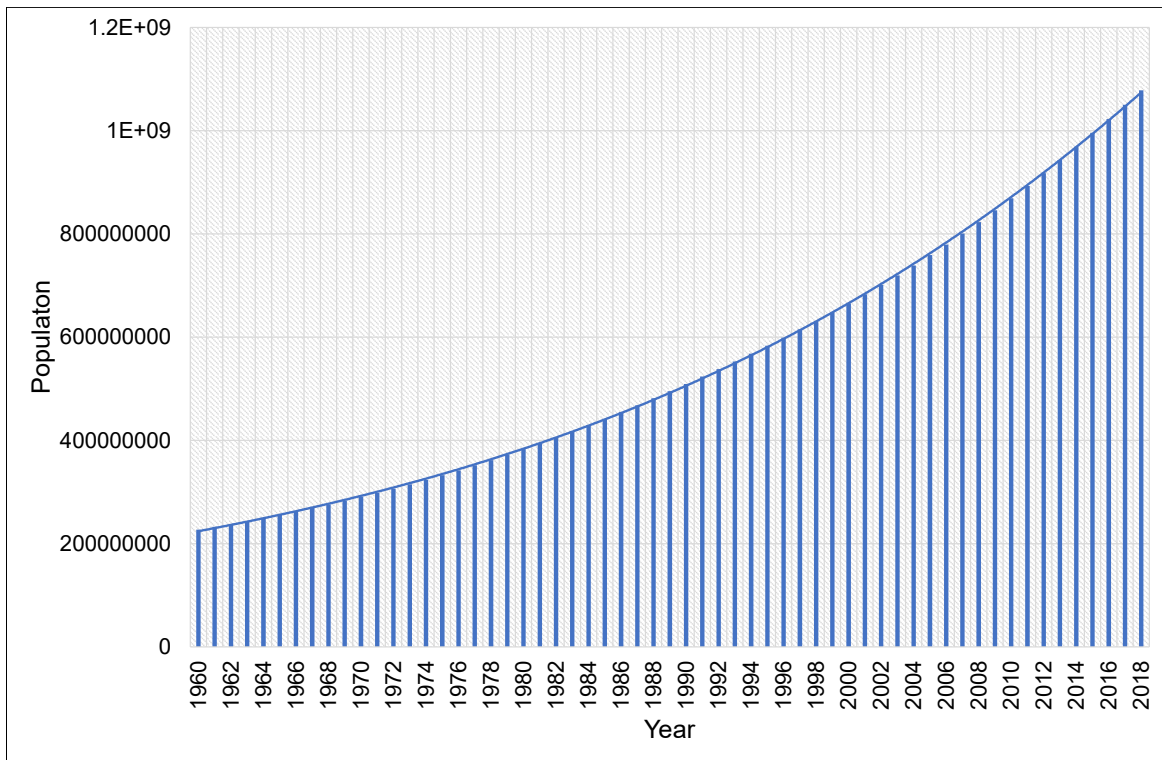


Fig. 2.5 SSA Population (World Bank data)[206]

studies, looking at the different dimensions of the situation categorized into four main areas [142] - the evaluation of rural electrification projects and programs, monitoring progress of electrification projects, relationship between energy demand, consumption and economic development, and modelling of scenarios to facilitate planned solutions in a bid to proffer solution that is both realistic and sustainable. Notably, it has captured the opening section of literature and publications related to the subject for well over the last decade with little or no significant change [191, 99, 204, 138, 107, 199, 140, 20, 139]. It is the only region in the world where the number of people living without electricity is decreasing rather slowly as rapid population growth is outpacing the effort to provide energy access. Sub-Saharan Africa houses the poorest nations of the world with an increase of about 100 million people in 37 countries without electricity since 2000. With a total of about 634 million people living without electricity [200], it is the most impoverished region of the world as per energy access, holding nearly half of the global total (Fig 2.6) with a generation capacity of 68 gigawatt (GW) of which about one-third (approximately 33%) is generated by South Africa. Most of the population without electricity live in the rural areas (Table 2.1).

The complexity of the energy problem in the African sub-region explains why the issue has lingered for so long with a sustainable solution still obscured or very vague. The

readily identified problems centre on economic, government policies and management, infrastructure, and energy generation and distribution [30, 52, 148, 157]. There is also the problem of demand and supply resulting from insufficient supply or inability to consume energy supplied. Agreeably the solution will require robust planning across government and private sectors, national and international organisations, over a defined time period. Consequently, scenarios have been modelled to project the road map to modern energy access [81] in SSA. In west Africa were access rate varies from 20% in Liberia to over 70% in Ghana, Nigeria, for instance, has a target of making reliable electricity accessible to 75% of the population by 2020 and 100% in the next 10 years following. 2030 is projected as the target for universal energy access by most scenarios. The realisation of this time period has not been unanimously accepted, as the rate of population growth in Sub-Saharan Africa is projected to leave about 25% without access by 2040 following the current effort to tackle the energy problem [81], and also, a tenfold energy generation increase, equating to 13% annual growth rate, will be needed, as against the threefold projected [30]. However, there is a convergence in the defined-pathway to realisation of universal modern energy in the region. Firstly, there is no gainsay to the fact that SSA is richly endowed with energy resources, and the need for a mix of large-scale projects and distributed generation [136, 157, 52]. Secondly, government transparency, policy and policy implementation need to improve, in addition to access to finance and increase in regional trade [20, 157, 148], and thirdly, the exploitation and integration of the renewable energy resources of the region in the energy mix is inevitable [194, 99, 101]. The pointer for the future of global stable, clean and sustainable energy inclines towards renewable energy sources of which biomass is a huge part.

2.3 Biomass To Energy

Biomass includes plant and animal wastes and remains. It is a renewable source of energy. In comparison to fossil fuels which takes thousands or millions of years for reproduction, it is reproduced annually or in several years. This makes it renewable. The CO_2 , a major contributor of green house gas (GHG) emission causing climate change, released during the production of energy from biomass will be absorbed again during the growing period of the plant for biosynthesis. Therefore, it is carbon neutral. The degree of neutrality of biomass fuel is determined by carrying out a detailed life cycle analysis (LCA).

Fig. 2.7 shows biomass-to-energy conversion technologies and end use. The two main process technology involved in the biochemical treatment of biomass are fermentation and anaerobic digestion. In the former yeast is used to ferment the biomass feedstock, converting the sugar content into ethanol. Anaerobic digestion uses bacteria to transform the organic matter into

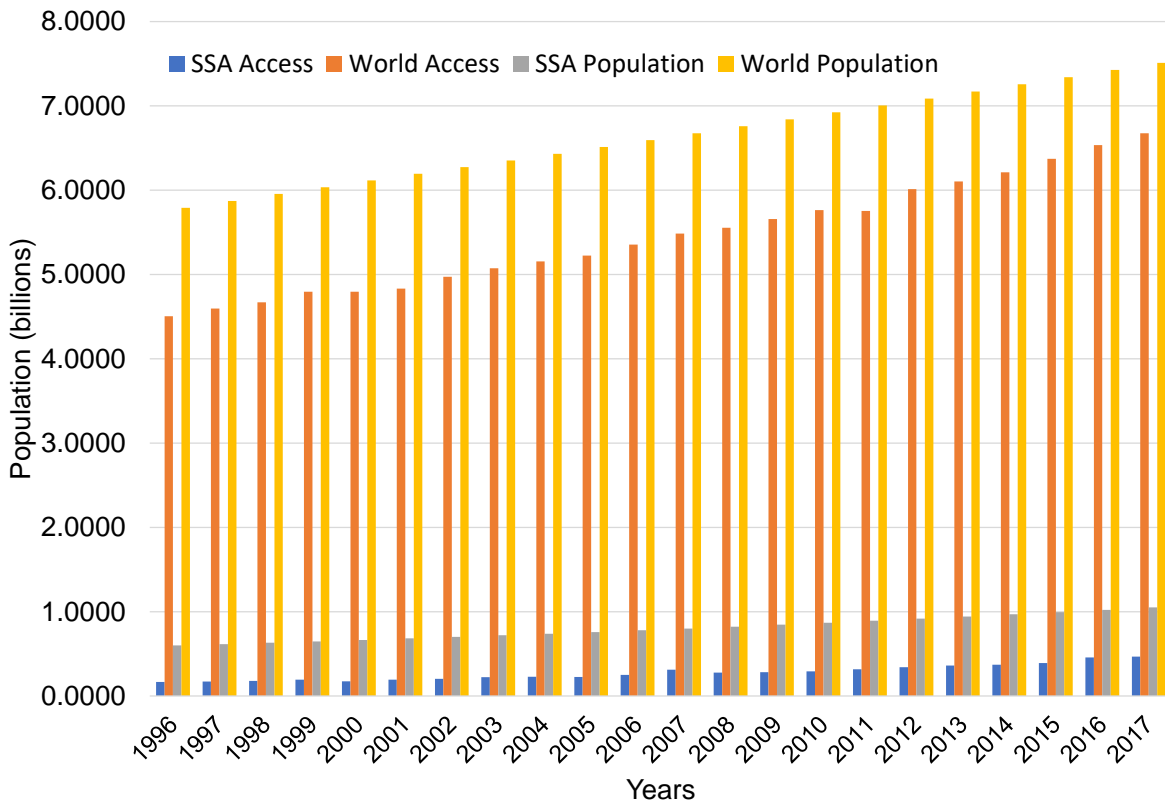


Fig. 2.6 2012 statistics of people without access to electricity by country [81]

gaseous products. The biogas produced has a calorific value range of about $20\sim 25\text{MJ}/\text{Nm}^3$. Kemausuor et. al conducted a review on commercial biogas systems and the implications for Africa [108]. The choice of a conversion technology and the associated processing challenges will depend largely, on the inherent properties of the biomass species and the form in which the energy is required [129, 75]. The wide spectrum of the physio-chemical properties of biomass species is due to the difference in its type and growing conditions, harvesting and storage [8, 45]. Biomass can be classified based on their moisture content, as either wet or dry biomass. The moisture content of wet biomass can exceed 90% and less than 50% for dry biomass. Wet biomass-to-energy conversion is normally achieved by biochemical processes while dry biomass is inclined to thermochemical conversion processes (Fig.). Both conversion paths can yield an intermediate fuel for energy generation purposes. The main conversion technologies involved in the thermochemical process are:

- Combustion
- Gasification
- Pyrolysis

Table 2.1 Electricity access 2014 Regional aggregates [34]

Region	Population without Electrification (Million)	Electrification rate (%)	Urban electrification rate (%)	Rural electrification rate (%)
Developing Countries	1,185	79	92	67
Africa	634	45	71	28
North Africa	1	99	100	99
Sub-Saharan Africa	632	35	63	19
Developing Asia	512	86	96	79
China	0	100	100	100
India	244	81	96	74
Latin America	22	95	98	85
Middle East	18	92	98	78
Transition economies and OECD	1	100	100	100
World	1,186	84	95	71

- Liquefaction

The current standard regulating the classification, terminology and test methods regarding solid biomass fuels, the BS EN ISO 17225-1:2014 Fuel Specification and Classes from the ISO in collaboration with the EU committee for standardization (CEN) is used in this study [165].

Solid biofuels are often classified as primary and secondary. Primary biofuels includes, firewood, wood chips, pellets, animal wastes, forest and crop residues, and landfill gas. Secondary biofuels are subdivided into 1st, 2nd and 3rd generation fuels as follows:

- 1st generation: Bioethanol through fermentation of starch or sugar; and biodiesel through transesterification of plant oils.
- 2nd generation: Bioethanol through enzymic hydrolysis; biodiesel through thermochemical processes; and biomethane through anaerobic digestion.
- 3rd generation: biodiesel from algae; bioethanol from algae and sea weeds; and hydrogen from algae and microbes.

Further, biomass is a heterogeneous mixture of organic, inorganic matter, and several different phases of solid and liquid. The inorganic fraction of biomass is less, to a great extent when compared with the organic content. The complexity and diversity of biomass necessitates a thorough characterisation which is useful for the identification and selection of suitable

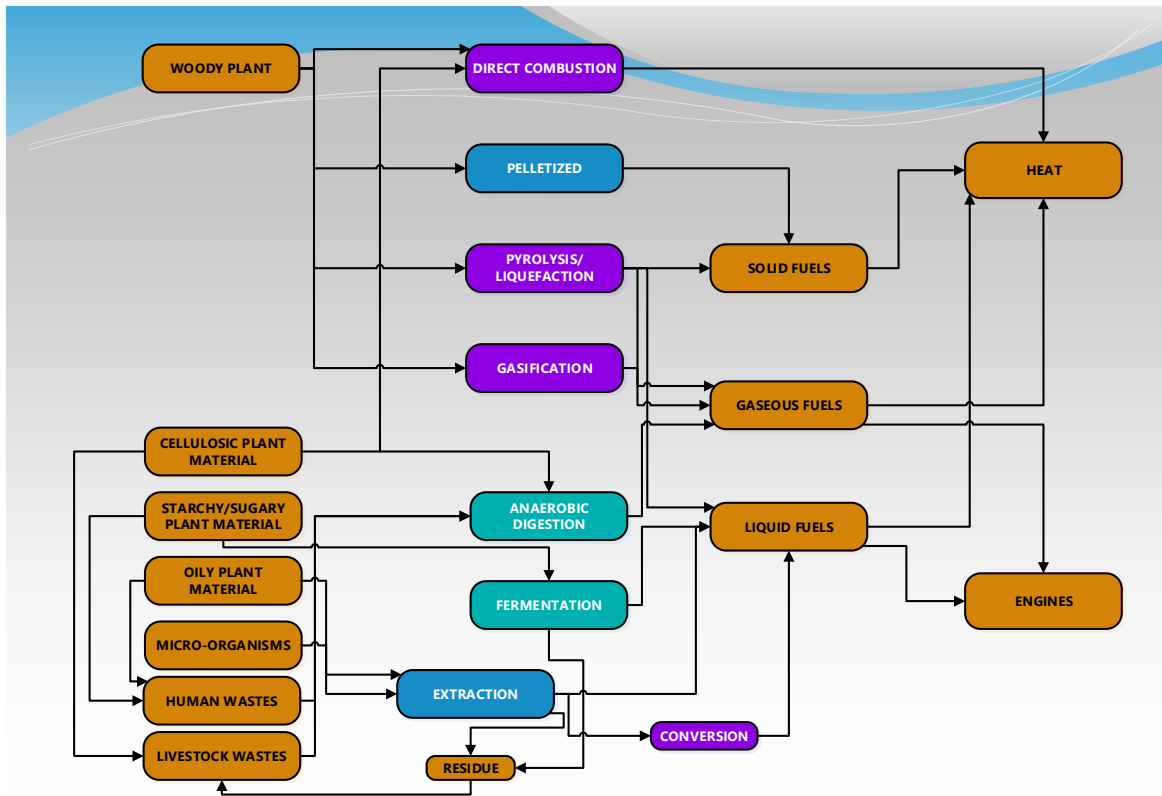


Fig. 2.7 Schematic of biomass conversion technology

species for energy production [156], and for the selection of conversion-to-energy technology [166, 114]. Vaezi et. al. [195] based on the final syngas application, developed numerical algorithm for the selection of appropriate biomass feedstock for downdraft gasification purposes. 80 species are listed in the range suitable for obtaining syngas of desired quality in a moving/fixed bed atmospheric reactor. The direct impact of the constituent of a biomass species on the design and/or choice of the power plant, or conversion technology that will be used, essentially requires that suitability characterisation is done prior to the selection of the process. Consequently, this forms a major consideration in the biomass to energy process. The conversion of biomass to useful energy (heat or electricity) or energy carriers such as charcoal, oil or gas, is achieved by two main conversion technologies - thermochemical and biochemical conversion technologies [121]. Fermentation for the production of alcohol, and anaerobic digestion for the production of methane-enriched gas are the main route for biofuels production in the biochemical technology pathway. There are many feedstock for biofuel production - animal manures, municipal solid wastes, plant-derived starch and sugar feedstock, cereal grain and tubers. Drapcho et. al. [57] discussed the characteristics of feedstock relevant to biofuel production and their availability, as well as the technologies involved in the

production. Lakniemi et. al. and Biosantech et.al. reviewed anaerobic production of methane, hydrogen, ethanol, butanol and electricity from micro-algal biomass [115, 33]. However, the main consideration is thermochemical conversion technologies and solid (woody) biomass (BS EN ISO 17225 - 1:2014) including dedicated energy crops that are subject to thermochemical conversion route to useful energy [165].

Woody biomass is divided in to two major categories - softwoods and hardwoods. Hardwoods are widely distributed, while 92% of softwoods are in North America, Russia and Europe [36]. With regards to energy production, amongst the different types of woody biomass poplar (*Populus*) is of high interest being used as a short rotation coppice crop (SRC) and due to its capacity for fast growth, it is cultivated directly for combustion, gasification (thermochemical conversion processes) and production of briquettes (feedstock). Some annual and perennial (herbaceous) plant species like giant reed *Miscanthus* (*Miscanthus*), Switchgrass (*Panicum virgatum*) Bermuda grass (*Cynodon*) are also cultivated to produce feedstock for bioenergy. They are characterized by high yield potential, high carbon content, and overall positive environmental impact [51, 118, 76].

2.3.1 Biomass Logistics

Biomass logistics is an important consideration in the conversion process. It is a description of all the activities relating to biomass that take place between cultivation and harvesting. The impact of biomass logistic on the overall energy production is a significant one, and can outweigh the economic viability of the process [40, 196]. The cost of the respective supply chain and conversion technology is one of the most important barriers in increased biomass utilization in energy supply [162]. Biomass logistics is therefore attracting attention, with researchers investigation geared towards minimizing the burden of logistics on the overall production and use of bioenergy. Continuous feedstock supply at competitive cost are usually the focal point in addressing bioenergy logistics [176, 164]. Mitchell et.al. investigated the cost of producing short rotation forestry from a spreadsheet model with emphasis on the collection, storage and operation of biomass production [135]. Delivand et. al. used a combination of the Geographical Information System and Multi-Criteria Analysis to develop a model to address the logistics of the production of electricity from biomass in three areas in Southern Italy [53]. An achievement of an optimal cost of logistics was reported. The sequence of the main operations in the supply chain, identified as harvesting, collection, storage, transport and pretreatment, and the associated challenges are highlighted by Gold [72].

2.4 Biomass for Power Generation

The choice of a conversion technology and the associated processing challenge will depend largely on the inherent properties of the biomass species and the form in which the energy is required [75]. The wide range of the physio-chemical properties of biomass species stem from the multi-, and diverse source which significantly influence the production and process technologies [8, 130]. The main influential material properties are:

- moisture content
- calorific value
- fixed carbon and volatile contents
- inorganic content
- ratio of cellulose to lignin content

Whereas the energy content of a species is constant, the energy obtained from it may vary depending on the conversion process. This inclines to an interplay between the form the energy is required and the applicable technology necessary to obtain the energy in the required form.

2.4.1 Thermochemical Conversion Technology

Biofuel production processes can be classed as direct or indirect. In direct production process, the raw feedstock or the preprocessed biofuels can be directly used to release the stored energy. There are, generally, three direct conversion technologies [4] viz, direct firing, co-firing and gasification. On the other hand, there are three major indirect conversion process - physical, thermal and biochemical. It is necessary to consider preprocessing of a biomass species; this may influence the transport and combustion efficiency as quite often, harvested forest derived biomass are of various lengths, sizes and bulk density [122]. Also, preprocessing should address the issues of grit contamination and wood quality. Physical preprocessing can imply comminution - chipping, grinding, cutting or shredding which are size reducing activities to enable it fit in conventional burners or stored in cellars [214]. Comminution is used to produce pellets, wood chips and briquettes of standard size. Woody biomass inclines to several methods of preprocessing options; however, for optimum treatment of the biomass, the characteristic of the material, end-use, and site management requirements are necessary considerations [214]. The annual fuel consumption in relation to the storage capacity would determine the frequency of supply and fuel haulage. For optimum production

cost and to reduce carbon footprint, adequate storage capacity determined by the annual consumption and bulk density is usually considered [178, 161]. Energy density is a function of the calorific value and the bulk density of a biomass fuel species. Bulk density is an intrinsic property of the fuel which changes during conversion process and influences the energy density. This accounts for the difference in energy density between log and pallets of equal volume; with the latter having a higher energy density [197]. Size reduction is accomplished by comminution, the most common being wood chipping. Wood chipping is energy intensive; however, it improves the bulk density with respect to the volume, enhances drying processes, reduces the cost of transportation and generally improves the life cycle of the biomass.

Dewatering is the removal of all or part of the moisture contained in a biomass as a liquid [124]. The difference to drying process is that here the moisture is removed as a vapour. Removal of water from a biomass by dewatering or drying prevents smoky combustion and enhances the efficiency of the conversion process as less energy is required to burn off the excess water content. Reducing the moisture content of a biomass fuel improve may involve significant cost, hence it is important to weigh off the cost vis-à-vis efficiency improvement [181]. Wet biomass needs to undergo dewatering or drying process prior to combustion as flame temperature and combustion efficiency are highly dependent on the moisture content [93, 211, 207]. Wahlund et.al. emphasized that the method of dewatering or drying should be made as energy efficient as possible, so as not to have a significant impact on the total efficiency of the cycle [198]. Biomass drying technologies are considered in Pang & Mujumdar [152]. Bennamoun et.al. looked at drying of alga as a source of bioenergy feedstock [31].

The thermochemical conversion of biomass to energy can be carried out using a number of different processes. The end-user requirement, and the source and nature of the biomass are usually the main factors influencing the choice of one process over the others. Combustion can be used to produce steam and power, gasification for synthetic gas (syngas) that can be used for power and/or heat generation, transport fuels and chemicals, and pyrolysis for liquids used in production of transportation fuels [75].

Combustion (thermal conversion of biomass) is usually carried out in the boiler or stove using stoichiometric amount of oxidants (air) for complete oxidation of the components present in the biomass to release all the stored energy in the fuel. This involves high temperatures, sufficient turbulence and time for ignition, mixing and completion of the oxidation reaction. The entire process entails four basic steps of heating and drying, pyrolysis, flame combustion and char combustion. Drying and heat occurs at 100 °C, at which temperature, the water content of the biomass particles is driven out and no chemical reaction is involved. Usually

time for this process would vary with particle size and ignition temperature of the biomass. For solid fuels, drying and pyrolysis is always the first step; however, the relative importance of the steps would depend on the fuel properties and the combustion process conditions [121].

At the end of the heating and drying process, pyrolysis (chemical decomposition of the biomass in the absence of oxygen) starts with Hemicellulose components at about 225 °C. Other components would decompose at different temperature regimes, with the lignin component at the other extreme of Hemicellulose, degrading at temperatures up to 500 °C. Decomposition rates for various biomass components have been measured using the Thermogravimetric Analyzer (TGA). The major products of pyrolysis are hydrogen, carbon monoxide, carbon dioxide, methane and other hydrocarbons, and various high molecular weight hydrocarbons.

The process leads to the formation of char and volatile gases which continue to react independently. In flame combustion, volatile gases react with the solid fuel in the presence of oxygen to burn with a bright yellow flame appearing on the surface. The product of the complete combustion is usually water and carbon dioxide.

2.5 Biomass Refrigeration

2.5.1 Absorption Refrigeration Cycles

Global demand for cooling and dehumidification of indoor air is growing due to increasing comfort expectation and cooling loads, as well as building and architectural characteristics and trends [38]. Conventional air conditioning systems used in buildings are compression-type air conditioning units with high energy consumption; giving rise to high electricity peaks. Although the vapour-compression refrigeration/cooling cycle was described by Oliver Evans in 1805, it was Jacob Perkins who in 1835 registered the first patent [37]. The machine ran on ethyl ether. Vapour-compression refrigeration/cooling systems are the most widely used. Refrigerant vapour is compressed by a mechanical compressor and enters the condenser where it changes state by evolving heat to the surroundings. High pressure liquid refrigerant then passes through an expansion valve into an evaporator at low pressure where it evaporates, producing useful cooling. Compression systems use CFCs refrigerants. Although these refrigerants have good thermodynamic, heat transfer and chemical properties, they also, are non-flammable and non-toxic which are necessary criteria for the choice of refrigerants. But they have significant negative environmental impact as they are found to be partly responsible for the thinning of the ozone layer. In the stratosphere the refrigerants break up due to

ultraviolet radiation and release their chlorine atoms; this then catalyses the depletion of the ozone layer. Their long resident time in the atmosphere enhances their ability to trap heat more effectively than carbon dioxide resulting in increased global temperatures.

The early development of absorption refrigeration cycle began in the 1700's. However, the principle of absorption cooling was first described by the French scientist Ferdinand Carrié in 1858 [180]. The original design used water and sulphuric acid, but the main set-back of this system was corrosion and leakage of air into the vacuum system. In 1926, Albert Einstein proposed an alternative design, the Einstein refrigerator. This machine is a single-pressure absorption refrigerator using ammonia as a pressure-equalizing liquid, butane as a refrigerant, and water as an absorbing liquid. It has no moving parts and it does not require electricity to operate. Only a heat source is required. Commercial production of absorption refrigeration units began in 1923 by AB Arctic, which was bought by Electrolux in 1925. The first absorption machines that proved to be successful on an industrial scale were developed by James Harrison in Australia. Absorption refrigeration were driven with steam as heat input to provide cooling in the summer in central refrigeration plants because of its availability in most plants where steam is used to provide heating in the winter. In the absorption refrigeration cycle, vapour is generated from a binary solution by the application of heat, cooled and liquefied by giving up heat to the surroundings, and then allowed to evaporate producing cooling. The resultant vapour is reabsorbed into the solution due to its affinity with the absorbent. The binary solution is then returned to the generator to complete the cycle. The thriving market of absorption chillers was curtailed by the price of natural gas and oil used to fuel steam boilers after the energy crisis in the seventies forcing prospective buyers to remain with conventional electric systems with increased control, improved performance and decreased cost of electric cooling. The Montreal protocol, 1987, raised issues surrounding electric cooling including the effect of CFCs refrigerants. These concerns couple with efficient energy utilization and improvement in technology, have re-surged interest in absorption refrigeration systems. In 1992 Swede's Baltzer von Platen and Carl Munters developed and patented an isobaric diffusion absorption cooler [77]. A bubble pump circulates the solution; consequently, no moving parts. Based on Carrié's absorption refrigeration cycle, lithium bromide-water absorption systems were developed in the US in the 1940's with water as refrigerant. They are used in light refrigeration systems (air-conditioning) since water refrigerant cannot function at sub-zero temperatures due to its freezing point. Small capacity powered diffusion absorption refrigerators with COP's between 0.1 and 0.3 have been commercially produced by Electrolux since 1928 [91] The performance of the devices has been assessed during the last half century by various researchers such as Narayankhedka & Maiya [143], and Chen et al. [43]. Lithium Bromide and water (LiBr-water), and Am-

monia and water (NH₃-water) are two commonly used pairs in absorption air-conditioning systems [77, 185, 88]. In the former, water is the refrigerant with higher performance than the latter in which ammonia is the refrigerant. However, several critical limitations exist for the LiBr-H₂O system [141, 98]. A detailed operation of absorption cooling has been explained by various authors including Sun, Srihirin, Kim, Sarbu, and ASHRAE [19, 182, 173, 179, 111]. The low efficiency of absorption cooling systems compared to compression systems, has been a major set-back affecting the cost of manufacturing component parts and market share [48]. The current trend in pursuit of global climate mitigation couple with research and development for system improvement has engaged researchers in activities geared at reversing the trend. The university of Stuttgart carried out a project to develop a single-stage ammonia-water diffusion absorption refrigeration cooling machine with a capacity of 2.5kW. A COP of 0.3 and cooling capacity of 2.0 - 2.4 kW was achieved on the third prototype from a failed machine of a 0.05 - 0.15 COP at a cooling capacity of 0.5 - 1.5kW [89, 90]. Some authors have developed computer models for system simulation and optimization. Alizade et.al. carried out a theoretical study on the design and optimization of the water-lithium bromide and aqua-ammonia absorption refrigeration cycles, and showed that for a fixed initial conditions and cooling capacity, cooling improves with higher generator temperature with smaller heat exchanger surface [12]. On the R22-DEGDME working pair a computer model of a residential gas-fired heat was developed and the pressure-temperature-concentration drawn to make possible the analysis and optimization of the absorption cycle [15]. The optimal relations between the heat transfer areas of the heat exchangers and the coefficient of performance or the specific heat load of a modelled heat-driven absorption heat pump (AHP) was studied by Chen; the COP was the objective function of optimization adopted for the study [42]. The performance of the cycle can be influenced by circulation ratio and the effectiveness of the solution heat exchanger [92, 110, 78]. Grossman developed an interactive computer simulation model for the analysis of absorption refrigeration cycles [73]. Simulation results show good comparison with experimental results from a water-lithium bromide absorption cooling system. Additionally, multi-stage absorption refrigeration cycles have been developed and investigated; they show significant improvement in the overall system performance [179]. Kaushik et al. proposed a two-stage dual fluid absorption cycle. The conceptual computer-aided thermodynamic design uses LiBr-Water and NH₃LiNO₃ as working fluids [104]. Kaushik developed a computer simulation model based on mass and energy conservation, and material balance to carry out a parametric investigation of the multi-component/double effect absorption cycle and found the performance to be nearly twice that of a single-stage [103]. Double effect systems are more commercially available compared to other multi-effect cycles but its operation faces the possibility of crystallization especially in

developing air-cooled absorption systems. Farshi et.al. developed a computational model to study the and compare the effect of parameters on crystallization phenomenon in three double effect configuration of water-lithium bromide cycles [70]. Result shows that the risk of crystallization is slimmer in the parallel and reverse parallel configuration. To further reduce the risk of crystallization a variable effect LiBr-H₂O absorption refrigeration cycle that operates within 85°C and 150°C, with evaporation temperature of 5oc was proposed. Results of the simulation show a COP range of 0.75 - 1.25 [210].

Ammonia-based absorption refrigeration applications have no crystallization issues and can tolerate low freezing temperature [208]. Consequently, ammonia-based working pairs have attracted research attention and application. Sun derived thermodynamic data for the aqua-ammonia pair for absorption refrigeration [182]. Ziegler and Trepp developed a correlation of equilibrium properties for use in design and testing absorption unit, extending the rang the temperature to 500 K and the pressure to 50 bar, and Patek & Klomfar developed correlation functions for the calculation of selected thermodynamic properties of aqua-ammonia systems [153, 213]. A thermodynamic and economic optimization study of the aqua-ammonia vapour absorption refrigeration was carried out by Misra et. al. [134]. A detail thermo-physical properties of aqua-ammonia mixtures was put forward by Conde for use in industrial design of absorption refrigeration equipment [47].

2.5.2 Absorption Refrigeration Working Fluids

The popular CFCs refrigerant was invented by Thomas Midgley, Jr. of General Motors in 1930 for Frigidaire Corporation of Dayton Ohio, USA to solve the problem of toxicity, flammability and horrible smell of previously used refrigerants which were also poisonous especially when they leak at night in an enclosed space. Until the Montreal Protocol when they were banned, CFCs and HCFCs were considered non-toxic, non-flammable and safe refrigerants. The famous ozone depletion hypothesis of Rowland and Molina published in 1974 claims that CFCs diffuse to the stratosphere where the intense energy of the ultraviolet (UV) rays of the solar radiation breaks them down to release Chlorine atoms that catalytically destroys the ozone in a chain reaction which increases the intensity of the UV radiation (0.29 - 0.32 microns) incident upon the earth's surface with harmful effect to humans and other biological systems [18]. For Absorption systems working fluids are combined - refrigerant and absorbent. The performance of an absorption cycle is highly dependent on the thermophysical properties of the working fluids [155]. The mixture of refrigerant-absorbent should basically, be non-explosive, non-toxic and chemically stable. Holmberg & Berntsson listed the requirements of working fluids in ASHRAE Transaction cited by Srikuhirin et.al., gave an exhaustive list of the thermo-physical properties for absorption systems [184, 180].

The most widely used refrigerant-absorbent pairs are ammonia-water and water-lithium bromide. Ammonia is suitable for low temperature applications with a normal boiling point (NBP) of -33°C and a freezing point of -77°C . A rectifier is often required to purge water that evaporates with water during regeneration as a result of the volatility of both substance. Sun carried out the thermodynamic analysis of binary fluids with ammonia as refrigerant to investigate their suitability, compared with ammonia-water [183]. Xu & Goswami presented a method for the computation of the thermodynamic properties of ammonia-water mixtures at elevated temperatures and pressures using Gibbs free energy [209]. The disadvantage of ammonia-water pair include high temperature, toxicity, and corrosive action to copper and copper alloy; however, both are environmentally friendly. Water-Lithium Bromide pair is limited by the freezing point of water to applications below 0°C . The system must be operated in a vacuum condition, but no rectifier is required for regeneration of the refrigerant. Kaita analyzed water-lithium bromide binary solution and developed an equation for the computation of the thermodynamic properties at concentrations of 40 - 65 wt.% and temperatures of $40 - 210^{\circ}\text{C}$ [95]. In addition to aqua-ammonia and lithium bromide-water, Macriss listed 18 other key absorption fluids that have attracted research interest [123]. Lithium chloride salt and water was used as working pair in an absorption cooling prototype designed by Gommed & Grossman, proved successful. A lot of realistic data were obtained from the operation of the main component dehumidifier, regenerator and general quantitative performance data. Sanjuan et.al. in comparison of liquid absorption against salt desiccant (LiCl) reported that salt desiccant can combine absorption process with energy storage and therefore, providing cooling in the absence of solar gains without the use of external storage tank [170]. Bales et.al. applied the LiCl-water pair in the thermochemical accumulator (TCA) in which thermal storage was shown to be sufficient for small scale cooling applications. A commercially produced TCA by ClimateWell uses LiCl-water pair [25].

2.6 Biomass for Cooling and Power

Heat is the main output obtained from a direct conversion process of directly combusting a solid biomass fuel. In the traditional method of biomass utilisation, the heat is used directly for cooking and space heating on open fires, or systems such as cook stoves and traditional fire places. In technological enhanced application, the heat could be used for power generation, heating or refrigeration. The application is usually dependent on whether there is a need for space heating, domestic hot water (DHW) or a combination of both. The application systems are similar to those of conventional fossil fuel used for domestic central heating systems and could vary from ≥ 10 kW for applications such as one room wood stoves

up to 30 kW for family sized housing central heating systems. These single utilisation of generated energy was the mostly known and applied form of energy even in industrial scale prior to industrial revolution when combined energy production from a single source began, though it was not referred to as combined heat and power (CHP). The mechanisation of manufacture across the whole industrial spectrum was driven by energy derived principally from the combustion of coal to generate steam which was converted to mechanical power in the steam engine. The power generated was transmitted via a system of shaft and pulleys to a variety of machines and part of the waste heat (from the heat and power generation) was used to provide heating within the factory in winter. Efficiency achieved reached 66% against < 30% nominal generation efficiencies [112]. Al-Shemmeri showed that a single production does not support high efficiency, usually enhanced by efficient utilisation of energy [6]. Consequently, for an absorption refrigeration and power systems, with low conversion efficiencies, a combined production is preferred.

2.6.1 Combined Dual Systems (CHP/CCH)

Combined dual production systems compared with single generation has the advantages of improving the utilisation of energy production and consumption, and reduction in air pollution [7]. The market holds a variety of combined generation systems ranging from small-scale (200 kWe - 5 MWe) to large-scale (>5MWe) applications, and steam turbines to biomass external combustion systems prime movers. Large-scale CHP covers the widest range of thermal and power output and covers about 90% of global industrial capacity [112]. Small-scale systems predominantly primed by reciprocating gas engines are low-cost and have superior generating efficiency in excess of 40%. However, biomass-driven small-scale combined generation systems apply especially in cases of decentralised systems where they facilitate reduction in transportation cost of the fuel and provide heat and power where they are needed [120]. This is important when considering the fact that there are cases where it has been difficult to find end-user for the great amount of heat produced by large scale systems [65]. In chapter 5, a model for the application of biomass in the production cooling using the waste heat from CCP/CCHP plant has been developed to form an integral part of the combined generation system. Dong et. al. reviewed small-scale biomass CHP systems based on Organic Rankine Cycle and Mertzis et al. developed a small mobile agricultural residue gasification unit for decentralised CHP [56, 133]. These systems still suffer some economic set-backs and technical uncertainties some of which are being addressed. On the economic side, the market share CHP/CCP is on the increase across the globe. For example, Berlin in 2017 acquired \$346m combined heat and power plant (CHPP) to deliver 260MWe and 230MWth [202]. The United States Environmental Protection Agency recognition for CHP

may have contributed to the embracing of the technology and its integration to the energy generation and utilization mix. The university of Maryland and university of Massachusetts Medical Centre and School supplemented their energy supply by integrating CHPP into their energy generation and supply network. An annual saving of \$3 million on the facility cost of energy is estimated [202]. Rural communities in developing countries appeared to highly benefit from decentralised electrification systems. The energy problem in these countries is usually severely felt in the rural area due to losses and cost in transmission, difficult terrain, and sometimes, low population density in settlement to consume supplied energy. Consequently, decentralised, off-grid and micro-generation tend to make sense in these areas [125]. In the Economic Community of West African States region of SSA, Senegal, followed by Nigeria has taken the lead to integrate renewable energy combined generation technology into the energy generation and utilisation system with 21MW and 20MW respectively. Also, development of mini- and micro-grids, and the move towards CHP and Trigeration, with a pilot project in Nigeria has been reported [17].

2.6.2 Trigeration

The gains of combined dual systems could be seasonal with heating and power combination, as heating is hardly required, except for domestic hot water during summer time. However, the current trend in buildings air-conditioning allow other technologies to be added to CHP to facilitate the utilisation of thermal energy for the production of energy required for comfort cooling during the hot season [39]. Absorption refrigeration systems are inclined to thermal energy for operation. Absorption refrigeration is extensively covered in the succeeding chapters. The prime mover in this system (combined cooling, heating and power) produces electricity and waste heat for cooling and/or heating. The benefit of this system stems from the utilisation of waste heat which is, by definition, free with a minimal usage cost. Al-Shemmeri designed a house-hold sized trigeration system based on a small-scale diesel engine generator set, and showed by laboratory performance test, that the system produced electricity, heating and cooling simultaneously from a single fuel source without loss of quality or quantity compared to singular production under the same conditions and system parameters [119]. Puig-Arnavat et. al. presented a model of trigeration system developed for testing and utilisation of different biomass fuels, while Al-Sulaiman et. al. carried out comparison of three trigeration systems based on energetic performances [158, 9]. The three systems are based on fuel type and include, solid oxide fuel cell (SOFC), Biomass and solar trigeration systems. Baghernejad et. al. also carried out a similar investigation on the three fuels considering the exergetic performance and exergoeconomic optimization. According to their result, the SOFC has the maximum trigeration exergy efficiency with

64.5%, followed by biomass with 60% and solar trigeneration integration with 56% [21]. In the literature, the feasibility of trigeneration and its associated efficient energy utilisation and energy efficiency is shown. However, the implementation of a combined generation system and more so, a trigeneration system would require a thorough decision, considering factors pertinent to its efficient operability and sustainability. Such factors may include capital investment, operating cost, availability and reliability and suitability of the technology. Andiapan et.al. highlighted these important uncertainties including consideration for the short term and long term uncertainties that may arise during the course of operation, and developed a systematic approach to synthesize a biomass-based trigeneration system which can handle a variety of raw material depending on energy demand [14].

2.6.3 Prime Movers

In general, combined generation offers a simultaneous multiple useful forms of energy generation and utilisation from a single source. This is usually, thermal and mechanical forms of energy. The advantage of combined generation over single generation is in the extensive use of the energy content of the fuel species. An example of the edge of a combined system over a single generation is the conventional electricity generation where about 35% of the energy potential contained in the fuel is converted to electricity and about 65% is lost as heat. Up to 90% is achieved in combined generation as the lost heat in the former is utilised therefore, increasing the efficiency of the system. In combined generation systems involving electric power generation, prime movers are devices that convert heat and/or chemical energy to mechanical, and drives the generators that convert mechanical energy to electrical [160]. Reciprocating internal combustion (diesel and gas) engines, steam and gas turbines are widely used in large and commercial generating plants and are among the earliest developed [177]. Other prime movers currently used in small and medium scale and combined generation systems include:

- Fuel cells
- External combustion engines (e.g. Stirling engines)
- Combined gas turbine cycles
- Organic Rankine Cycles and
- Steam turbines combined combine cycles

Fuel cell prime movers are mostly chemical to electrical energy converter [41]. They have high efficiency, and are currently being explored. An investigation of the Proton Exchange

Membrane fuel (PEM) cell in a CCHP system was reported to have high efficiency that increases with increase in fuel cell size [150, 41]. Ansarinasab & Mehrpooya investigated a CCHP system driven by a combination of molten carbon fuel cell, gas turbine and Stirling engine. The combination produced high quality energy to drive the system [16]. The performance of PEM as a portable fuel for transportation was investigated by Mert [132]. The choice of a system is influenced by many factors including the fuel type and conversion system. Fuel Cells, Stirling engines and internal combustion (micro gas) engines are readily inclined to micro combined systems for small scale residential or commercial properties. For industrial and commercial applications, Combined systems (CCP/CHP) and CCHP are customized to meet the need.

In this study, electricity generation is not discussed further. The system therefore precludes the aspect electricity generation and prime movers. However, the system can be combined a combine generating plant producing heating and power.

2.7 Summary

In this review, the historical development of energy was presented, and it shows that the global demand for energy has been on the rise following the unyielding quest for improvement in living standards through technological advancement by man of the millennium. The cumulative effect of the fossil-energy driven development is realised to have adversely impacted on the environment with a high chance of jeopardising the future of our environment with the increase of global warming. Consequently efforts are being geared up to forestall the trend by seeking alternative and renewable environmental friendly sources of energy generation and utilisation. The case of Africa on energy demand and impacting factors on the current and future energy sources and utilisation was examined from the literature with particular attention to biomass. The capability of biomass as a reliable and renewable energy source adaptable to diverse technologies that enhances its usability in many applications including refrigeration, was explored.

Chapter 3

Theory of Biomass Refrigeration

3.1 Introduction

Biomass refrigeration as a system can be considered to consist of three major units - the biomass combustion system providing the thermal energy to drive the system, the heat exchanger that provides the platform for efficient distribution and utilisation of the conveyed to the system and within the system and the refrigeration system utilising the thermal energy to produce the desired cooling effect. In this chapter, the theoretical background of biomass-driven refrigeration system is presented. Theories of the three major components are considered in separate section to show their functions in the system. This is followed by the investigation of the combined theoretical relation of the three components. The equations governing mass and energy conservation, and material balance in combination with those for the thermodynamic properties of materials involved apply. All the symbols used are described in the nomenclature, unless otherwise stated.

3.2 Theory of Biomass Combustion

One major concern in the development of biomass combustion systems is efficiency [154]. The composition and structure of biomass materials play a major role in the generation of heat and emissions from the combustion system [8]. Biomass fuels are solid carbonaceous materials and come from sources with widely diverse physiochemical properties. The following properties are considered in the energy application of biomass fuels:

- Bulk density
- Moisture content

- Proximate analysis
- Ultimate analysis
- Ash Content
- Size
- Calorific value

The standard procedure regulating the biomass fuels is the BS EN 14780:2017 which replaced BS EN 14780:2011.

3.2.1 Properties of Biomass fuels

- Bulk density is the mass portion of a solid fuel divided by the volume of the container with which is filled by the portion under specific conditions as obtained in the definitive standard. It is an important parameter of the solid fuel species volume and logistics determinant. Together with the net calorific value, it determines the energy density of the fuel species. ISO 17828:2015 describes the determination of the bulk density of pourable solid biofuels, which can be conveyed in a continuous flow of material. It is affected by moisture content, shape and form of the material.
- Moisture content of a biomass fuel species refers to the free moisture in the fuel. The influence of free water in biomass fuel species makes this property one of high significance. It affects the cost of logistics and combustion efficiency. During Combustion, the free moisture in the biomass fuels absorbs the heat by evaporation of the liquid water and heating of the resulting water vapour, lowering the amount of useful heat available from the biomass, which results in decreased combustion temperatures. For efficient use of biomass fuels, moisture content should be as low as can practicably be. Moisture reduction can be achieved by air-drying species. Percentage loss of moisture for a biomass fuel will depend on the size of the wood, weather conditions and method of storage. The methods for conducting a test analysis of a solid biomass fuel samples to determine the moisture content is described in the standard ISO 18134:2015.

Usually, moisture content is defined on wet or dry basis as shown below.

Percentage moisture content on wet basis:

$$C_m = \frac{M_{wc}}{F_w} * 100 \quad (3.1)$$

where:

C_m is moisture content

M_{wc} is mass of water in fuel

F_w is mass of fuel - wet basis

F_d is mass of fuel - dry basis

Percentage of moisture content on dry basis:

$$C_{md} = \frac{M_{wc}}{F_d} * 100 \quad (3.2)$$

The above equations are related as follows;

$$C_{md} = \frac{100 * C_m}{100 - C_m} \quad (3.3)$$

$$C_m = \frac{100 * C_{md}}{100 + C_{md}} \quad (3.4)$$

- Proximate analysis is used to determine the percentages of volatile matter, fixed carbon and ash in a fuel. It gives an indication of the quality of combustion emanating from the gas phase combustion of the solid char. The ash content provides a measure of the incombustible mineral matter in the fuel. The volatile matter, the fixed carbon, and to a small extent, the ash content depending upon the condition of measurement, constitute the combustible residue. The volatile matter content is determined as the loss in mass, less that due to moisture during the partial pyrolysis of solid biofuels under standardize conditions (ISO 18123:2015).
- Knowledge of the chemical composition of the biofuel is obtained by the ultimate analysis, and is essential for estimating air requirements and flue losses as well as determining the likely emissions of pollutants such as NO_x and SO_x. The chemical composition of fuels are usually in terms of carbon, hydrogen and oxygen.
- Ash content plays an important role in fouling, slagging, clinker formation and corrosion effect in the combustion system. Ash formation occurs in three stages observed in a controlled heating of a standardized cone or cylinder of an ash sample under reducing or oxidizing atmosphere as follows [188]:
 - the initial deformation temperature (IDT) - the temperature at which the first rounding of the tip occurs

- hemispherical temperature (HT) - temperature at which the height of the specimen is half of the base and the shape of the specimen roughly hemispherical and
 - flow temperature (FT) - temperature at which the height of the ash specimen is a third of that for the hemispherical temperature.
- Size of solid biofuel relates to the design of combustion equipment. Fuelwood and many biomass fuel require size reduction and/or preparation depending upon the type and scale of the combustion equipment. The prepared fuel is transported into the combustion equipment by conveying systems, screws, auger or spreader stokers. Larger-scale combustion equipment for hogged or chipped fuel can incorporate various types of grates. Control of the fuel preparation is essential for operation of large systems.
 - Calorific value of a fuel is a measure of the energy content of the fuel and therefore determines the quantity of the fuel which must be burnt to meet a given duty. For biomass fuels, calorific value is measured by determining the gross calorific value (high heating value - HHV) of a solid biofuel at constant volume and at the reference temperature of 15°C in a bomb calorimeter calibrated by the combustion of certified benzoic acid (ISO 18125:2017; CEN/TS 14918:2005). But in practice the net calorific value (lower heating value - LHV), which is a calculated value of the specific energy of combustion for unit mass of fuel burned in oxygen at constant pressure under such condition that all the water of the reaction products remain as water vapour at 0.1MPa and the other products being as for the gross calorific value and at the referenced condition, is recommended. The relation of the net calorific value to the gross if given in (3.5) [190].

$$NCV = GCV - 212H - 0.8(O + N) \quad (\text{measured in MJ/kg}) \quad (3.5)$$

In the absence of calorimetric data from experiment, the GCV of a solid biomass can be estimated by the element composition using proximate and ultimate analysis [131]. Toscano [190] gives a simple correlation for obtaining the GCV presented in equations (3.6) to (3.10)

$$GCV = 971 + 323.6C \quad (3.6)$$

$$GCV = -2494 + 379.3C + 468.8H + 292.6N \quad (3.7)$$

$$GCV = -4311 + 401.1C + 294.3H + 340.7N + 42.3O + 298S \quad (3.8)$$

$$GCV = 297.6 + 389.7C \quad (3.9)$$

$$GCV = -79.5 + 358.7C + 252H + 298.5N + 1201S - 177.1A_c \quad (3.10)$$

3.2.2 Stoichiometric Air and Flue Gas Calculations

Equations (3.11) and (3.12) represent the overall reactions with respect to the starting materials and the end products, and are the bases for the determination of the equipment efficiencies, theoretical flue gas composition and the requirements of combustion air. The oxygen is supplied by air with approximately 79% (by volume) inert nitrogen. The end products (CO_2 and H_2O) and the nitrogen (N_2) as well any excess oxygen are heated by the energy released from the conversion of carbon and hydrogen. The heated gases carry heat out of the system through the flue [188].



The ultimate analysis provides information for the calculation of the stoichiometric air requirements. The stoichiometric air, is given by:

$$A_s = \left\{ \left(\frac{C_C}{M_C} + \frac{C_H}{2M_{H_2}} - \frac{C_O}{M_{O_2}} \right) \left(1 + \frac{79}{21} \right) \right\} * \left\{ \left(1 - \frac{C_m}{100} - \frac{C_a}{100} \right) * \frac{28.84}{100} \right\} \quad (3.13)$$

Where

- A_c is the ash content
- C_C is the carbon content
- C_H is the hydrogen content
- C_m is the moisture content and
- C_O is the oxygen content

The air-fuel ratio (A/F) is defined as the mass of air supplied to combustion system per unit mass of fuel as-fired [188]:

$$\left(\frac{A}{F} \right)_{stio} = \frac{\text{air supplied kg/unit time}}{\text{fuel supplied kg/unit time}} \quad (\text{kg air/kg fuel}) \quad (3.14)$$

The equivalence ratio is defined as the ratio of stoichiometric air to actual air-fuel ratio, and commonly used to quantitatively indicate the quality of the fuel-oxidiser mixture condition - rich, lean or stoichiometric. It is given by:

$$\Phi = \frac{(\frac{A}{F})_{stoi}}{(\frac{A}{F})_{act}} \quad (3.15)$$

The excess air, A_e , is defined as:

$$A_e = \frac{(\frac{A}{F})_{stio}}{A_S} \quad (3.16)$$

The flue gases contain the product of combustion carbon dioxide, water vapour, nitrogen and excess oxygen, and carbon monoxide in the case of lean fuel-oxidiser mixture leading to incomplete combustion. The theoretical composition of the dry flue gases can be calculated from the composition of the fuel and air-fuel ratio thus:

$$n_{CO_2} = \frac{C_C}{12 * 100} (1 - \frac{C_m}{100} - \frac{C_a}{100}) \quad (3.17)$$

$$n_{H_2O} = \frac{C_H}{2 * 100} (1 - \frac{C_m}{100} - \frac{C_a}{100}) \quad (3.18)$$

$$n_{O_2} = \frac{C_O}{32 * 100} (1 - \frac{C_m}{100} - \frac{C_a}{100}) + 0.21 \frac{(\frac{A}{F})}{28.84} - \frac{n_{H_2O}}{2} - n_{CO_2} \quad (3.19)$$

$$n_{N_2} = (0.79) \frac{(\frac{A}{F})}{28.84} \quad (3.20)$$

The molar sum of the dry flue gas per kg of fuel is given by:

$$n_t = n_{CO_2} + n_{O_2} + n_{N_2} \quad (3.21)$$

The theoretical composition by percentage volume of the flue gases is given by:

$$V_{CO_2} = (\frac{n_{CO_2}}{n_t}) * 100 \quad (3.22)$$

$$V_{O_2} = (\frac{n_{O_2}}{n_t}) * 100 \quad (3.23)$$

3.2.3 Adiabatic Flame Temperatures

The equation governing the adiabatic flame temperature is given by:

$$\int_{t_{ref}}^{t_{ad}} m_t C_p dt = LHV \quad (3.24)$$

For a reference temperature of 25 °C, (3.24) reduces to

$$t_{ad} = \frac{LHV}{m_t * C_p} + 298 \quad (3.25)$$

C_p is given by the correlation

$$C_p = a + bt \quad (3.26)$$

The values of the coefficients a and b for species are given by Richard [163]. The adiabatic temperature is never realised in practice due to combustion system heat loss, heat extraction, insufficient residence times in combustor to allow combustion products to reach equilibrium, and unburnt fuels. Consequently, the maximum possible temperature can be calculated thus:

$$t = \frac{LHV - E_h}{m_t C_p} + 298 \quad (3.27)$$

(where E_h is the rate of heat extraction).

3.3 Theory of Heat Exchanger

Heat exchangers are devices deigned to facilitate the exchange of heat between two fluids at different temperatures. It differs from mixing chambers in that the fluids do not mix. They have a wide spectrum of applications and form an essential part of domestic and industrial heating and refrigeration systems. There are numerous type innovative heat exchanger design to match heat transfer hardware and meet heat transfer requirement. The simplest are the double pipe heat exchangers (Fig. 3.1) with parallel flow (Fig. 3.1a) or counter flow (Fig. 3.1b) configuration. However, the most common type used in industrial application is the shell-and-tube heat exchanger [1]. It consist of a large number of tubes packed in a shell with their axes parallel to that of the shell. Heat transfer occurs as one fluid flows inside the tube and the other outside the tube through the shell. Baffles are usually placed inside the shell side to direct fluid flow and to enhance heat transfer surface.

3.3.1 Overall Heat Transfer Coefficient

The overall heat transfer coefficient U accounts for the contribution of both heat transferred by convection from the hot fluid to the wall and cold fluid, and by conduction from the hot

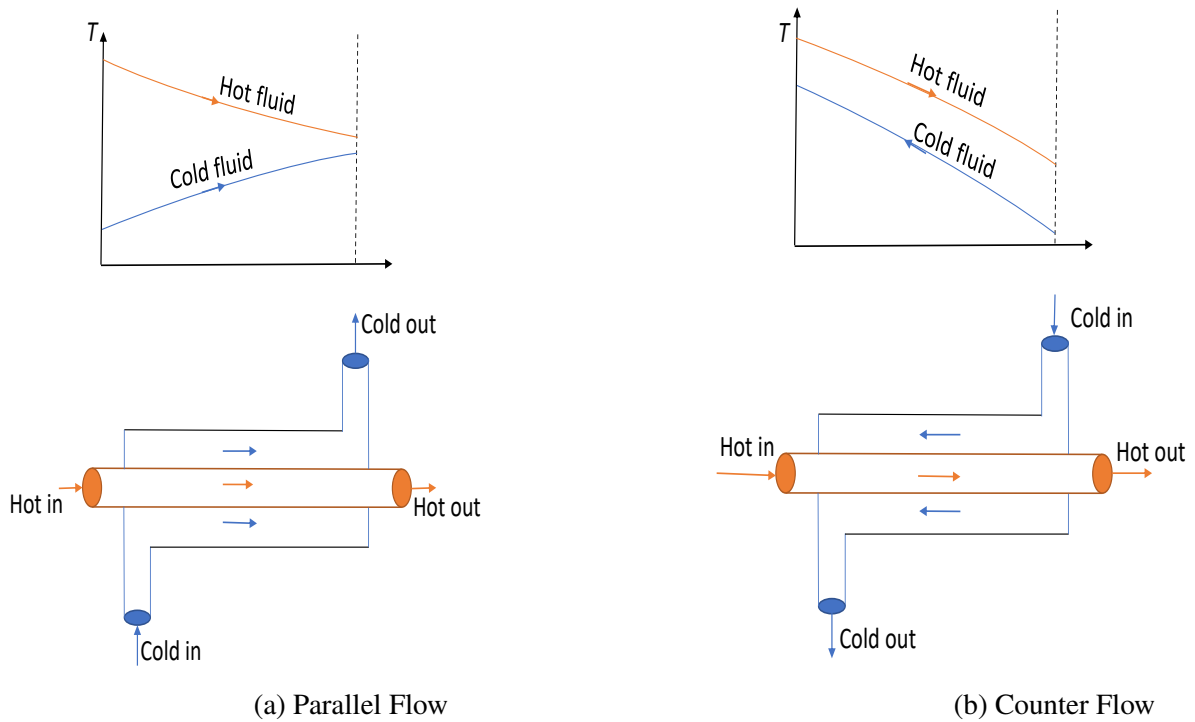


Fig. 3.1 Double pipe heat exchangers

fluid to the wall. Radiation heat transfer effect are usually included in the convection heat transfer coefficients.

Heat lost or gained in a heat exchanger, by the hot and cold fluid, respectively, is given by:

$$Q = \dot{m} C_p \Delta T \tag{3.28}$$

and the heat exchange from hot fluid to cold:

$$Q = A U \Delta T \tag{3.29}$$

In a heat exchanger with a tubular configuration, the overall heat transfer coefficient is dependent on the reference tube side. Two convection and one conduction thermal resistances are associated with the heat transfer process involved. With reference to the inner and outer radius, respectively, of Fig. 3.2 of material conductivity k and length L , the overall heat transfer coefficient can be written as follows:

$$U_i = \frac{1}{\frac{1}{h_i} + R_{fi} + \frac{r_i}{k} \ln\left(\frac{r_o}{r_i}\right) + \frac{r_i}{r_o} R_{fo} + \frac{r_i}{r_o h_o}} \tag{3.30}$$

$$U_o = \frac{1}{\frac{r_o}{r_i h_i} + \frac{r_o}{r_i} R_{fi} + \frac{r_o}{k} \ln\left(\frac{r_o}{r_i}\right) + R_{fo} + \frac{1}{h_o}} \quad (3.31)$$

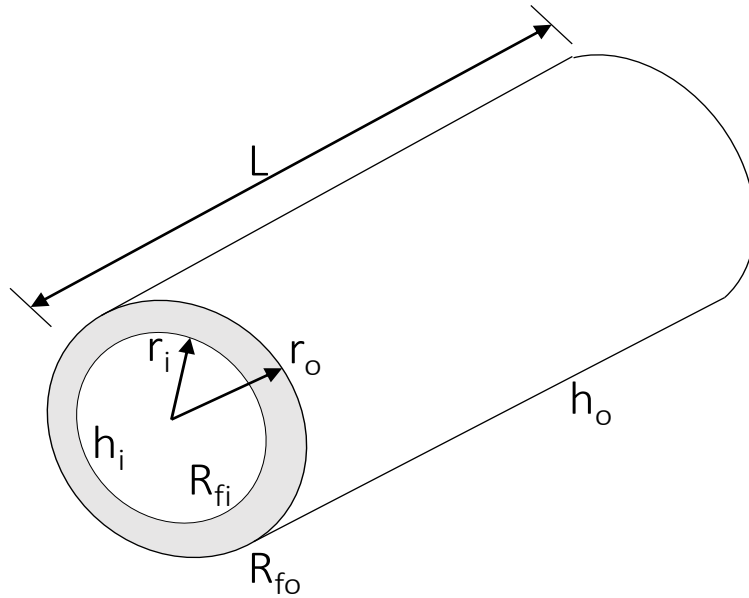


Fig. 3.2 Cross-sectional view of a tube

The parameters in the equations will vary with the type of heat exchanger. Kays & London [106] determined the heat transfer coefficient h by means of scaling parameter. Based on shell and tube type heat exchanger, the hydraulic diameter d_H represents the ratio of the two important size parameters of a heat exchanger - the wetted area and the perimeter.

$$d_H = \frac{4A}{P_x} \quad (3.32)$$

$$Re = \frac{\rho \bar{V} d}{\mu} \quad (3.33)$$

The Reynolds number (3.33) is the ratio of the internal forces to viscous forces, and indicates the nature of the flow, whether it is streamline or turbulent. Friction and heat transfer coefficient are dependent on the on the nature of the flow. There are two methods of presenting the convective heat transfer h . The Stanton (St) number,

$$St = \frac{A_{cs}}{A} * \frac{T_o - T_i}{T_w - T_f} \quad (3.34)$$

and the Nusselt (Nu) number

$$Nu = \frac{hd}{k} \quad (3.35)$$

The Nusselt number on the inside of a tube, in case of forced convection, as obtained in a fan or pump, can be determined as follows ([106]):

- streamline or laminar flow $Re < 2500$ then $Nu = 4.1$
- turbulent flow $Re > 10000$ then $Nu = 0.023Re^{0.8}Pr^n$

where $n = 0.3$ if fluid is being cooled, and $n = 0.4$ if fluid is being heated.

The Prandtl number (Pr) is defined as the ratio of kinematic viscosity to the thermal diffusivity.

$$Pr = \frac{C_p \mu}{k} \quad (3.36)$$

3.3.2 Analysis of Heat Exchanger

For counter flow or parallel flow heat exchanger, figure 3.1 (3.1a & 3.1b), an equation in the form of equation (3.29) can be obtained by applying energy balance to a differential area element dA in the cold and hot fluids. Depending on the heat exchanger configuration, there will be a drop or increase in the temperature difference of the hot fluid dT_h and the temperature difference of the cold fluid dT_c . For adiabatic, steady-state flow the energy balance yields:

$$\delta Q = -(\dot{m}C_p)_h dT_h \quad (3.37)$$

or

$$\delta Q = \pm(\dot{m}C_p)_c dT_c \quad (3.38)$$

From (3.37) and (3.38),

$$\delta Q = -C_h dT_h = \pm C_c dT_c \quad (3.39)$$

C_h and C_c are respectively, the hot and cold fluid heat capacity rates, and the + and - signs indicate heat exchanger flow configuration (parallel or counter). Equation (3.40) is an expression of the rate of heat transfer from the hot fluid to the cold fluid across the elemental heat transfer surface, dA .

$$\delta \dot{Q} = U \delta(T_h - T_c) dA \quad (3.40)$$

Substituting (3.39) in (3.40) and integrating, it can be shown that,

$$Q = UA \frac{(T_{h1} - T_{c2}) - (T_{h2} - T_{c1})}{\ln\left(\frac{T_{h1} - T_{c2}}{T_{h2} - T_{c1}}\right)} \quad (3.41)$$

$$Q = UA \frac{\Delta T_1 - \Delta T_2}{\ln\left(\frac{\Delta T_1}{\Delta T_2}\right)} \quad (3.42)$$

$$Q = UA \Delta T_{lm} \quad (3.43)$$

where

$$\Delta T_{lm} = \frac{\Delta T_1 - \Delta T_2}{\ln\left(\frac{\Delta T_1}{\Delta T_2}\right)} \quad (3.44)$$

ΔT_{lm} is the mean temperature difference between the hot and the cold fluid, and is the average of the temperature which varies along the heat exchanger. The complexities in the flow conditions in multi-pass and cross flow heat exchangers result in a complicated *LMTD* expression. The equivalent temperature difference applies, and it is as follows:

$$Q = UAF \Delta T_{lm,CF} \quad (3.45)$$

where $\Delta T_{lm,CF}$ is the actual mean temperature difference, and a complex function of the state of the fluids at each end of the heat exchanger. Equation (3.45) is used to determine the *LMTD*.

$$\Delta T_{lm,CF} = \frac{(T_{h2} - T_{c1}) - (T_{h1} - T_{c2})}{\ln\left(\frac{T_{h2} - T_{c1}}{T_{h1} - T_{c2}}\right)} \quad (3.46)$$

where F , the correction factor, is dependent on the geometry of the heat exchanger. For cross flow and multi-pass heat exchangers, $F \leq 1$; and $F \geq 1$ respectively. Two dimensionless terms ' P ' and ' R ' which relate to all four temperatures are used to estimate the correction factor as follows:

$$P = \frac{T_{c2} - T_{c1}}{T_{h1} - T_{c1}} = \frac{\Delta T_c}{\Delta T_{max}} \quad (3.47)$$

$$R = \frac{C_c}{C_h} = \frac{T_{h2} - T_{h1}}{T_{c2} - T_{c1}} \quad (3.48)$$

and

$$Q = U A F \Delta T_{lm,CF} \quad (3.49)$$

where

$$F = \psi(P,R, \text{flow arrangement}) \quad (3.50)$$

The correction factor are available in charts [35].

3.4 Theory of Absorption Refrigeration

Heat energy is the main source of energy for driving the absorption refrigeration cycle. In addition, the fluid transport is enhanced by the affinity of the refrigerant pair undergoing phase change at some point of the cyclic process. The phase change is usually, but not restricted to two-phase change of liquid to vapour, solid to vapour or solid to liquid, and vice versa. There are cases where all three material phases are involved - the so-called triple phase operation, as obtained in the thermochemical accumulator [22]. The theory of the thermo-physical principle underlying the operation of absorption refrigeration cycle is presented in this section.

3.4.1 Single Stage Absorption Refrigeration Cycle

Fig. 3.3 is a schematic of vapour absorption refrigeration cycle. Lithium bromide-water and Water-Ammonia (Aqua-Ammonia) are the two commonly used absorbent-refrigerant pair in commercially available VARC systems. The solution is pumped to the generator, which is at (the condenser) high pressure. In the generator evaporates, The refrigerant is desorbed and passes through the condenser where heat is removed due condensation, while the weak solution, with respect to the salt concentration of the solution, flows back to the absorber unsaturated and through a pressure reducing valve. The high pressure liquid refrigerant from the condenser then passes into the evaporator through an expansion valve that reduces the pressure of the refrigerant to the low pressure existing in the evaporator. The liquid refrigerant vaporises in the evaporator by absorbing heat from the environment or space to be cooled, thus generating cooling effect. The resulting low-pressure vapour then goes to the absorber, where it is absorbed by the unsaturated weak solution, completing the cycle. The heat exchanger (HX) - acts a pre-heater and pre-heats the fluid between the absorber and the generator, increasing the efficiency of the system.

The vapour absorption refrigeration cycle model is based on mass continuity, material continuity and energy conservation. These are linked by the equations of the chemical

and thermodynamic properties of the material application. The material considered in this theoretical investigation, is the Lithium Bromide-Water pair ($LiBr - H_2O$). The following conditions are assumed:

- Unintentional pressure drops and heat losses in system components and pipelines are negligible.
- There are no sub-cooling or superheating at the evaporator and condense, respectively. Therefore, the refrigerant at the exit of these components is saturated.
- The processes at all pressure reduction or expansion valves are assumed isentropic.
- Circulating pump is isentropic.

3.4.2 Thermodynamic Properties

Enthalpy

For a reference temperature of 25 °C, concentration X , and specific heat C_x , the enthalpy of $LiBr/H_2O$ solution is given by

$$H_{x,25} = 184.76 - 1910.71 X + 1743.35 X^2 \quad (3.51)$$

and the enthalpy at t (°C) is given by

$$H_{x,25} + C_x (t - 25) \quad (3.52)$$

where

$$C_x = 4.23 - 5.15 X + 3.51 X^2 \quad (3.53)$$

Using the correlation by Lansing [116] of the refrigerant and solution temperatures, t_R and t_m respectively, and the solution concentration X , the concentration is completely defined thus

$$X = \frac{49.04 + 1.125 t_m - t_R}{134.65 + 0.47 t_m} \quad (3.54)$$

3.4.3 Theoretical Performance Evaluation

For a set of input parameters, the system performance is determined by the rate of heat transfer in each component and the flow rates at at different line within the cycle calculated by employing equations (3.51) - (3.54). Thus absorber concentration is given by

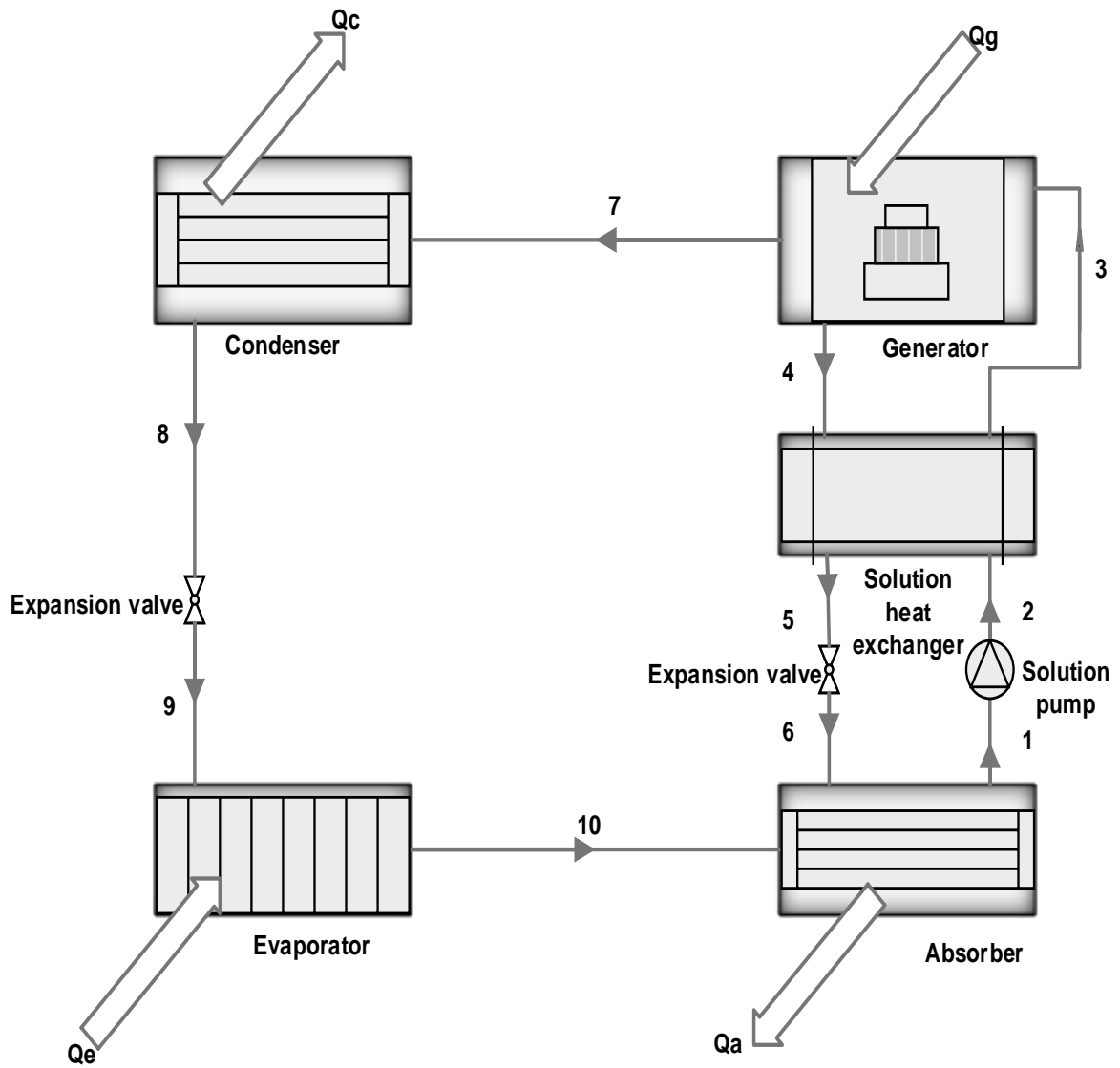


Fig. 3.3 Vapour absorption refrigeration cycle schematic

$$X_1 = X_2 = X_3 = X_{StrongSolution} = \frac{49.04 + 1.125 t_a - t_e}{134.65 + 0.47 t_a} \quad (3.55)$$

where t_a - Absorber temperature, and t_e - Evaporator temperature.

Similarly, the generator concentration is given by

$$X_4 = X_5 = X_6 = X_{WeakSolution} = \frac{49.04 + 1.125 t_g - t_c}{134.65 + 0.47 t_g} \quad (3.56)$$

where t_c - Condenser temperature, and t_g - Generator temperature.

State points (7) to (10) is pure refrigerant. Hence,

$$X_7 = X_8 = X_9 = X_{10} = Zero \quad (3.57)$$

The flow rates of the system is calculated from energy and mass balances; where m_w and m_s are the respective mass rates flow of the strong and weak solutions, m_R the refrigerant flow rate, and Q_E the refrigerant load in kW and H_i is the enthalpy at state point i ($i = 1, 2, 3, \dots$)

$$m_w = \left(\frac{Q_E}{H_{10} - H_8} \right) \left(\frac{X_1}{X_4 - H_1} \right) \quad (3.58)$$

$$m_s = \left(\frac{Q_E}{H_{10} - H_8} \right) \left(\frac{X_4}{X_4 - H_1} \right) \quad (3.59)$$

$$m_R = \frac{Q_E}{H_{10} - H_8} \quad (3.60)$$

$$Q = m \Delta H \quad (3.61)$$

Equation (3.61) will be used in combination of state properties to compute the energy rate of transfer on the refrigerant side, while it will be combined with equations (3.58) to (3.60). Equation (3.62) define the coefficient of performance of the system.

$$COP = \frac{\text{refrigerant effect}}{\text{external heat input}} = \frac{Q_E}{Q_G} \quad (3.62)$$

3.5 Summary

The essential theoretical facets culminating into the operation of a biomass driven refrigeration system was considered in this chapter. This include the theory of biomass combustion, heat exchanger and absorption refrigeration system. Properties for the quantification of the energy content, viability and suitability of a species of biomass solid fuel for an application was theoretically explored in the properties of biofuels. Heat exchangers are essential part of heat transfer systems and play an important part of adapting bioenergy as a source for absorption refrigeration systems. Analysis of heat exchangers preceded the final section on the theory of absorption refrigeration. Theoretical analysis and modelling of a single stage Lithium bromide - Water absorption refrigeration system was used to explore the parametric evaluation of the absorption refrigeration cycle. The model is apt for the study of the system components, components inter-dependability and the their overall effect on system performance, as shown by the coefficient of performance, COP.

Chapter 4

Absorption Cooling and Analytical Modelling

4.1 Introduction

Vapour absorption refrigeration was amongst the early cooling technologies. The stunted development of the technology was predicated by its low efficiency and the limitation of operating only above-zero temperatures due to water which was the popular refrigerant in these systems. As a result of these limitations, vapour compression refrigeration cycles, though costly on energy and lately, realised to be harmful to the environment, was preferred to vapour absorption system because of its efficiency and portability. The high demand for vapour compression systems running on portable fossil source energy led to mass production which makes it more economical both to afford and to run. However, with the issues of global warming and the contribution of HCFC and CFC in ozone depletion, coupled with the discovery of effective vapour absorption refrigerant pair that can operate in the sub-zero cooling temperature spectrum, VARS is gaining consideration. A rise in the demand for the technology could lead to mass productivity, affordability and further improvement. This chapter looks at a special vapour absorption refrigeration cycle - the thermochemical accumulator. The system is a commercially available refrigeration system from ClimateWell and operates in the three phases of matter. Designed to run on solar energy, it has the capacity to accumulate energy for an extended operation in the absence of the intermittent energy. The system is run on biomass and the cooling capacity evaluated. A computer routine was developed to further evaluate its performance by the COP and for system prediction and optimisation.

Another absorption refrigeration system considered in this chapter, is the aqua-ammonia

refrigerant pair system. The importance of this system is its ability to operate in sub-zero temperatures without any issues. A mathematical model was developed and implemented in MATLAB to simplify the evaluation and optimisation of the system. The chapter is sectioned as follows:

- MATLAB Interface
- TCA - Modelling
- TCA - Experimental Evaluation
- $NH_3 - H_2O$ VARC - Modelling

4.2 MATLAB Interface

MATLAB (matrix laboratory) is a software from MathWorks with multi-paradigm for programming, numerical analysis and a platform for technical computing language. It has evolved, from when it was first developed by Steve Moler in the late 1970s to enhance students access to LINPACK and EISPACK without the need to learn Fortran, into a powerful tool for both education and industrial sectors [137]. It is widely used in colleges, universities, industries and research institutions for mathematical computations, modelling and simulations, data analysis and processing, visualisation and graphics, and algorithm development. The software presents a friendly multi-language interface for user interaction and enables matrix manipulations, plotting of functions and data and implementation of algorithms. The MATLAB program provides optional toolboxes that are collections of specialised packages designed to solve specific types of problems [71].

Simulink is a graphical programming environment in MATLAB. It is useful for modelling, simulations and analysis of multi-domain dynamic systems. Component models or subroutines can be graphically modeled using its block diagramming tool and a customisable set of block libraries. Its integration with the MATLAB environment allows it to drive MATLAB or be scripted from MATLAB environment.

The use of MATLAB and Simulink in this work stem from the fact of its acceptance as an apt and standard technical tool, and wide usage in both the academic and industrial worlds, and lends itself as a fit-for-purpose tool to address the modelling and simulations design in this work. All modelling and dynamic simulations were carried out in MATLAB R2019a (9.6.0), 64-bit (win 64) and run on Windows 10 (x64-based processor); Intel(R) Core(TM) i3, CPU @ 1.70GHz; Installed RAM 16.0 GB.

4.3 TCA - Experimental Evaluation/Modelling

4.3.1 Introduction

The ClimateWell Solar Chiller (CWSC) CW10 is a 10 kW TCA (Fig. 4.1). The CW10 is a vapour absorption refrigeration system that utilises refrigerant pair in vapour, liquid and solid phases during operation making it a so-called triple-state operation system. The TCA has an integral energy storage in the form of solid salt crystals and works in a batch mode, intermitting between a charged and a discharged phase. The system's working pair comprises of Lithium Chloride and Water; water is the refrigerant and lithium chloride is the absorbent. Glycol is introduced to act as an antifreeze. The TCA consists of a twin barrel. Each barrel consist of four vessels. At the top is the condenser/evaporator and reactor, and at the bottom is the solution and refrigerant (water) storages. The top vessels contain heat exchanges with which the system communicates with the environment and the internal vessels. At the top of the barrel is the control unit which coordinates the modes and flow sequence (Fig. 4.2).

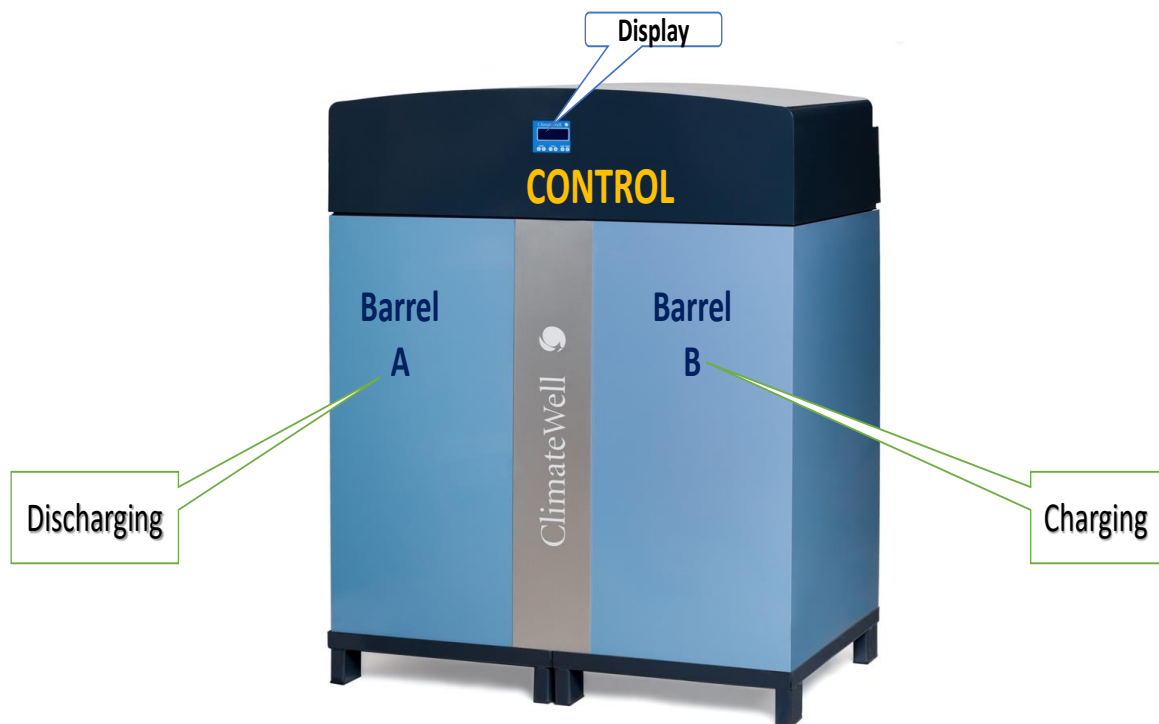


Fig. 4.1 External Features of TCA [24]

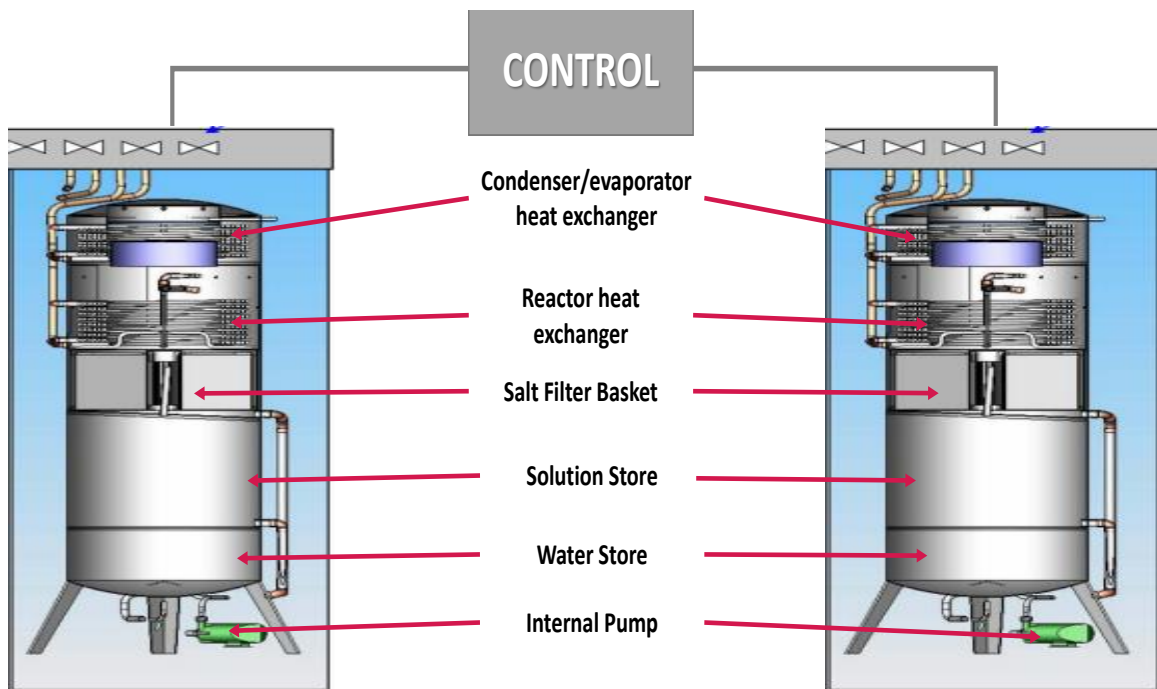


Fig. 4.2 Internal Feature of Complete Unit of TCA ([26])

4.3.2 Theoretical modelling

Fig 4.3 is simplified single unit of the TCA for clarity. The direction of flow and communication between the top vessels and the bottom vessels, and between the top vessels are shown. The condenser and reactor are treated as two separate vessel, with the top used to exchange energy between the vessels and the outside, and the bottom used to store refrigerant and solution. Internal pumps are used for the transportation of refrigerant and solution to the top vessels. The condenser top is the condenser itself and the condenser bottom is the refrigerant store. the reactor top is the reactor itself and the reactor bottom is the solution store.

During the charging phase, solution is pumped over the reactor heat exchanger; the solution comes closer and closer to saturation as a result of desorption. At saturation, further desorption at the reactor heat exchanger results in the formation of solid crystals that fall under gravity into the solution storage. The crystals are prevented from going into the solution by a sieve. They form slurry, holding high energy density with good heat and mass transfer, at the bottom of the solution vessel.

For discharging, the process is reversed. Saturated solution is pumped over the reactor heat exchanger where it absorbs the vapour evaporated in the evaporator. The heat of evaporation is provided by the space to be cooled (cooling mode) or from the heat sink (heating mode). The solution becomes unsaturated as a result of vapour absorption and comes to equilibrium.

But as it passes through the slurry salt crystal, it becomes saturated again as the crystals dissolve in the solution. In this state it is ready to absorb more vapour. The heat of condensation and binding energy released is transferred to the heat sink (cooling mode) and to the space to be heated (heating mode). Consequently, energy flows from the evaporator at a lower temperature to the reactor at moderately higher temperature.

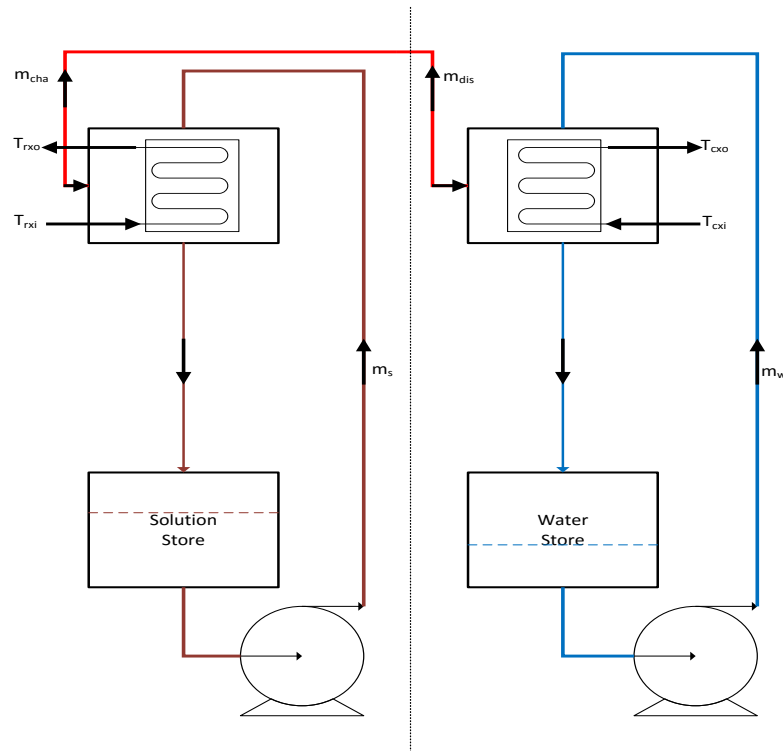


Fig. 4.3 Schematic of a single unit of TCA

The system is assumed to determine its initial conditions and then calculates its corresponding temperature and mass values. This implies that the values on the left hand side of the subsequent equations refer to the adjusted values, while those on the right, refer to the outdated values. At initial conditions, all the salt is dissolved in the reactor, and the concentration (x) of the solution, measured in *kg/kg solution*, is computed by

$$x = \frac{M_{LiCl}}{M_{LiCl} + M_{w0} - M_{wcti} - M_{wcbi}} \quad (4.1)$$

The mass of water and solution in each barrel are computed based on the calculated solution concentration ((4.1)). Thus, equations (4.2) to (4.5) give the mass of water in the system.

$$M_{ssrt} = x \cdot V_{rt0} \cdot \rho_{LiCl} \quad (4.2)$$

$$M_{wsrt} = (1 - x) \cdot V_{rt0} \cdot \rho_{LiCl} \quad (4.3)$$

$$M_{ssrb} = M_{LiCl} - M_{ssrt} \quad (4.4)$$

$$M_{wsrb} = M_{w0} - M_{wsrt} - M_{(wcti)} - M_{wcbi} \quad (4.5)$$

The energy rate of transfer is given by

$$\dot{Q} = \dot{m} C_p \Delta T = UA \Delta T_{LMTD} \quad (4.6)$$

Equation (4.6) is used to compute the reactor and the condenser heat exchangers power, and the energy losses in the system. Thus, the condenser heat exchanger power is given by

$$\dot{Q}_{cx} = \dot{m}_{cx} C_{pcx} (T_{cxi} - T_{cxo}) \quad (4.7)$$

and

$$\dot{Q}_{rx} = \dot{m}_{rx} C_{prx} (T_{rxi} - T_{rxo}) \quad (4.8)$$

for the reactor. The output temperatures of the condenser and reactor heat exchangers are given thus

$$T_{cxo} = T_{cxi} - (T_{cxi} - T_{ct}) \cdot e^{-\left(m_{cx} \frac{C_{pcxf}}{UA_{cx}}\right)} \quad (4.9)$$

$$T_{rxo} = T_{rxi} - (T_{rxi} - T_{rt}) \cdot e^{-\left(m_{rx} \frac{C_{prxf}}{UA_{rx}}\right)} \quad (4.10)$$

The energy due desorption at the reactor is given by

$$Q_{vap,rx} = \frac{-Q_{vap,cx} \cdot (H_{vap} + H_{dil})}{H_{vap}} \quad (4.11)$$

$$Q_{vap,cx} = UA_{cx} (T_{cf} - T_{ct}) \quad (4.12)$$

$$T_{cf} = T_{ct0} + \frac{(T_{rt} - T_{ct0} - \Delta T_f) \cdot UA_{rx}}{UA_{rx} + UA_{cx}} \quad (4.13)$$

Equation (4.13) is used to compute the water film temperature, while ΔT_f gives the temperature difference between the condenser and the reactor when the system reaches equilibrium.

It is a function of the reactor top temperature, salt type and salt mass fraction. For *LiCl*, the expression (4.14) is given in the literature [48].

$$\Delta T_f = T_{rt} - (1.01803 \cdot T_{rt} - 13.3442 \cdot x_{LiCl,r} - 122.667 x_{LiCl,r}^2 - 0.21194 \cdot T_{rt} \cdot x_t) \quad (4.14)$$

The film temperature for the reactor is given by

$$T_{rf} = T_{cf} + \Delta T_f \quad (4.15)$$

The mass of vapour flow between the reactor and the condenser following rate of desorption due to desorption during an internal time step is by equation (4.16)

$$M_{vap} = \frac{\dot{Q}_{cv} \cdot \delta t_i}{H_{vap} + C_{p,vap} \cdot (T_{cf} - T_{rf})} \quad (4.16)$$

The cooling or heating output temperature can be pre-determined using the equations (4.17) and (4.18) respectively, within the limit of the of the full output cooling and heating power \dot{Q}_{cv} and \dot{Q}_{rv} or the set temperature is adjusted to the full power incases where they are larger.

$$\dot{Q}_{cool} = \dot{m}_{cx} \cdot C_{p,cxf} \cdot (T_{cx0set} - T_{cxi}) + (UA_{ct}) \cdot (T_{ct} - T_{amb}) \quad (4.17)$$

$$\dot{Q}_{heat} = \dot{m}_{rx} \cdot C_{p,rx} \cdot (T_{rx0set} - T_{rx}) + (UA_{rt}) \cdot (T_{rt} - T_{amb}) \quad (4.18)$$

To keep the mass of the reactor top constant, certain amount of solution is pumped up to the top vessel from the bottom vessel to compensate for the mass migration due to flow of vapour from the reactor to the condenser during charging and the reverse during discharging. The mass of the reactor top contents is mathematically described as follows

$$M_{wsrt} = M_{wsrt0} - M_{vap} \quad (4.19)$$

The volume is calculated thus

$$V_{rt} = \frac{M_{wsrt} + M_{ssrt}}{\rho_s} \quad (4.20)$$

The mass of solution needed to fill the top reactor is given by

$$M_f = (V_{rt0} - V_{rt}) \cdot \rho_s \quad (4.21)$$

The above equations ((4.19), (4.20), and (4.21)) indicate state of the top content and are therefore used to determine the salt fraction.

$$x_{LiCl,t} = \frac{M_{ssrt}}{M_{ssrb} + M_{wsrt}} \quad (4.22)$$

$$x_{LiCl,b} = \frac{M_{ssrt}}{M_{ssrb} + M_{wsrb}} \quad (4.23)$$

The content of the salt fraction in the reactor top as shown above, holds if $M_{wsrb} + M_{ssrb} \leq 1$ for which $M_f = 0$. If $M_f \geq 0$, then solution is pumped from bottom to top vessel, and the *LiCl* mass fraction, mass of water in the reactor and the temperature of the top reactor is indicated by the following equations.

$$M_{wsrt} = M_{wsrt0} + M_f \cdot (1 - x_b) \quad (4.24)$$

$$M_{wsrb} = M_{wsrb0} + M_f \cdot (1 - x_b) \quad (4.25)$$

$$M_{ssrb} = M_{ssrb0} + M_f \cdot (1 - x_b) \quad (4.26)$$

$$M_{ssrb} = M_{ssrb} - M_f \cdot x_b \quad (4.27)$$

$$T_{rt} = \frac{T_{rt} \cdot M_{rt} + T_{rb} \cdot M_f}{M_{rt} + M_f} \quad (4.28)$$

If $M_f \leq 0$, solution flows down to the bottom from the top, and the mathematical description of *LiCl* mass fraction, mass of water in the reactor, and temperature of the top vessel is given by

$$M_{wsrt} = M_{wsrt0} + M_f \cdot (1 - x_t) \quad (4.29)$$

$$M_{wsrb} = M_{wsrb0} + M_f \cdot (1 - x_t) \quad (4.30)$$

$$M_{ssrt} = M_{ssrt0} + M_f \cdot (1 - x_t) \quad (4.31)$$

$$M_{ssrb} = M_{ssrb} - M_f \cdot x_t \quad (4.32)$$

$$T_{rb} = \frac{T_{rb} \cdot M_{rb} - T_{rt} \cdot M_f}{M_{rb} - M_f} \quad (4.33)$$

Equation (4.34) represent the needed amount of monohydrate crystal.

$$M_{mc} = \frac{(x_e - x_t) \cdot (M_{ssrt} + M_{wsrt} \cdot 42.4 + 18)}{42.4} \quad (4.34)$$

x_e can be obtained from Conde [48] published data.

$$x_e = -4.6427 \cdot 10^{-6} \cdot T_{rt}^2 + 1.9012 \cdot 10^{-3} \cdot T_{rt} + 0.4106 \quad (4.35)$$

The flow of vapour in the top vessels can affect the concentration of the solution. Consequently, to maintain constant concentration, extra salt or water is required. The temperature changes due to the dissolution at the top reactor is expressed by the equation (4.36)

$$T_{rt} = T_{rt} + \frac{M_{mc} \cdot H_{sol}}{M_{rt} \cdot C_{p,r}} \quad (4.36)$$

The adjustment for the masses of salt and water solution, in the case of insufficient water solution for which the mass of monohydrate crystal is set to zero is calculated thus

$$M_{ssrt} = M_{ssrt0} + M_m \left(\frac{42.4 + 18}{42.4} \right) \quad (4.37)$$

$$M_{wsrt} = M_{wsrt0} + M_m \left(\frac{42.4 + 18}{42.4} \right) \quad (4.38)$$

The mass of the condenser bottom depends on the flow of vapour as follows:

$$M_{cb} = M_{cb} + M_{vap} \quad (4.39)$$

$$M_{ct} = M_{ct0} + M_{wcti} \quad (4.40)$$

The temperature of the condenser vessels are dependent on whether the unit is charging or discharging. If the system is charging, the $M_{vap} \leq 0$:

$$T_{cb} = \frac{T_{cb} \cdot (M_{cb} - M_{vap} + T_{ct} \cdot M_{vap})}{M_{cb}} \quad (4.41)$$

$$T_{ct} = \frac{T_{ct} \cdot (M_{ct} + M_{vap} - T_{cb} \cdot M_{vap})}{M_{ct}} \quad (4.42)$$

Table 4.1 System connection for charging and discharging

Status	Heat source (Q_s)	Heat sink (Q_{hs})	Cooling (Q_{ac})
Charging	Reactor	Condenser	
Discharging		Reactor	Condenser

The temperature is also affected by the internal mixing pump. The effect of the internal mixing pump is expressed thus:

$$T_{ct} = T_{ct} + \frac{T_{cb} \cdot m_c \cdot \delta t_i - T_{ct} \cdot m_c \cdot \delta t_i}{M_{ct}} \quad (4.43)$$

$$T_{cb} = T_{cb} + \frac{T_{ct} \cdot m_c \cdot \delta t_i - T_{cb} \cdot m_c \cdot \delta t_i}{M_{cb}} \quad (4.44)$$

Coefficient of Performance (COP)

The output and input energies to the system are determined using equations (4.7) and (4.8). The coefficient of performance for cooling is the ratio of the cooling produced during discharging to the thermal heat input from the heat source. During discharge for heating, the condensation and binding energy released and transferred to the building is used in relation to the heat source energy to obtain the COP heating. Hence,

$$COP_{cool} = \frac{Q_{ac}}{Q_s} \quad (4.45)$$

$$COP_{heat} = \frac{Q_{hs}}{Q_s} \quad (4.46)$$

The COP when the system is operated as a heat pump is given by

$$COP_{heatpump} = \frac{Q_{hs,ch} + Q_{hs,dis}}{Q_s} \quad (4.47)$$

The Computer Model

The model in this performance evaluation is fixed on the number of internal time steps for every output time step to iterate to a solution. The control unit regulates the internal pumps and the swap from one barrel to the other for charging or discharging based on the load - full or empty. The load sensor senses the level of water in the barrel and registers as full or empty and triggers a swap in normal operating mode. During a swap, there is a ninety seconds time

lapse before the a re-initiation of operation. This time lapse is used by the system to redirect flow.

The aim here is to develop a routine for predicting the performance of the system based on input parameters and mathematical calculation. For the purpose of this work, a unit time step was adopted as the emphasis is on the cooling power. Therefore, the swap was not modelled or simulated. The circuitry inlet temperatures for the system is kept constant. The model is interactive, and was implemented in a user friendly software. Fig. 4.4 is the computer flow chart for the model.

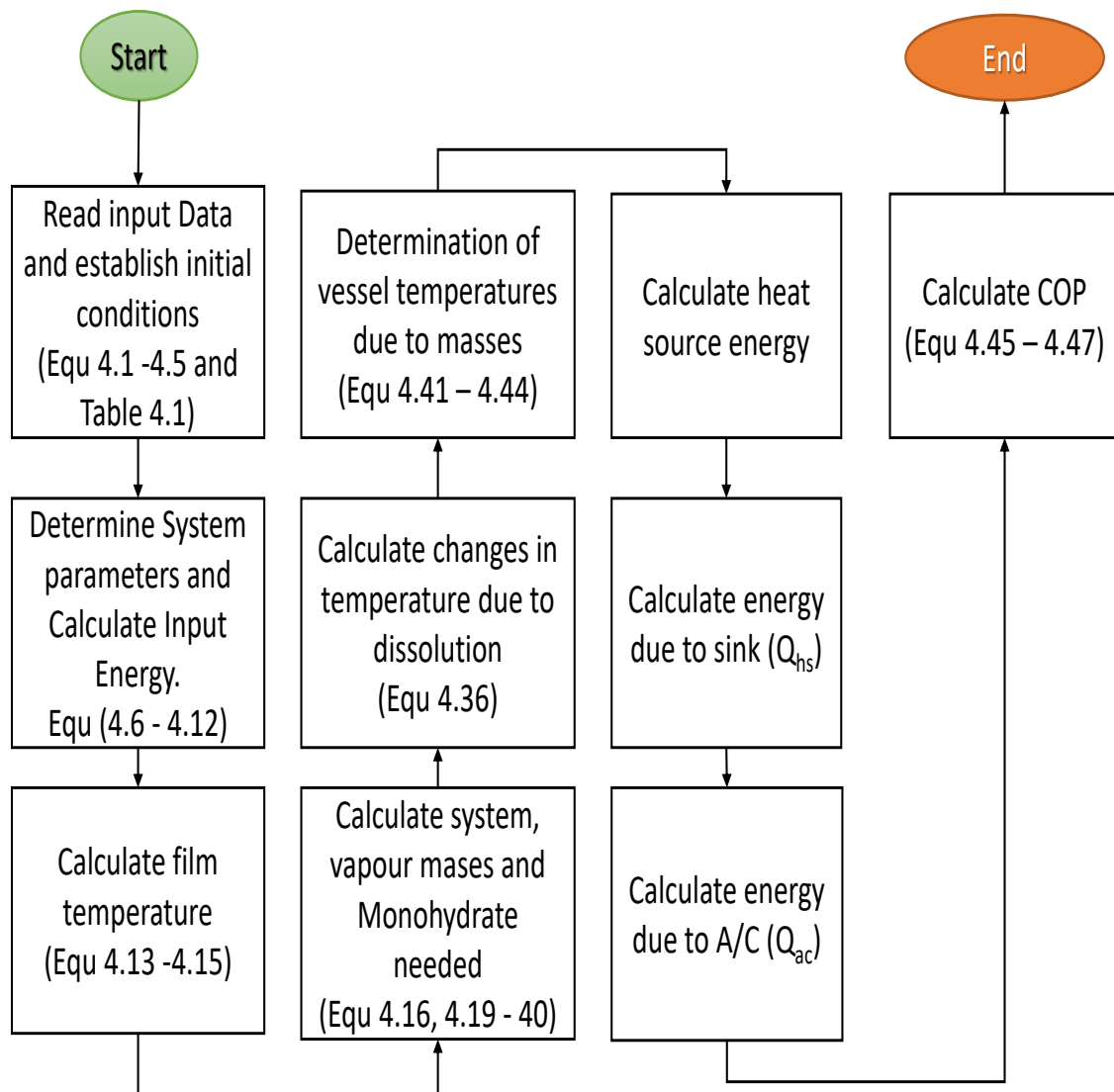


Fig. 4.4 TCA computer model flow chart

4.3.3 Experimental Evaluation

The ClimateWell Solar Chiller (CWSC 10/CW 10) is an absorption refrigeration system designed to obtain its thermal source from solar energy. However in this experiment, the CW 10 was configured to run on source-heat from a biomass boiler. The experiment aims to evaluate the effect of the evaporator inlet temperature (acting as the cooling load), the cooling demand (set cooling temperature) and ambient conditions on the air-condition circuit. Consequently, data extracted from the data acquisition equipment are those necessary for the planned evaluation.

(All the equipment used in this and subsequent experiments carried out in this project are new from the suppliers, and are part of the Arbor Renewable Energy Project at the Centre for Biomass Excellence, Staffordshire University. They were all calibrated and produced reliable measurements at the time of use.)

Data Acquisition System and Software

A P.A.Hilton Limited D102 Data Logger, also known as Hilton Data Logger (HDL), is used in the experiments. P.A.Hilton Limited has been involved with United Nation Industrial Development Organisation to make the change from Ozone depleting CFC refrigerants. The HDL has proved an invaluable tool for showing refrigerant plant performance, before and after conversion.

The HDL is a microprocessor controlled computer interface system, that has multi-channel analogue and digital units with both input and output capability. As the interface has its own microprocessor and independent memory, it is possible to set up the system to return data from most standard transducers in the form required by the data logging software. The interface may be simply configured either as a data logger or a combined data logger and controller, and is operated on a computer serial link responding to simple (ASCII) alphanumeric commands and returning numeric data. Commands and data are transferred via a 5-wire RS232 ribbon serial link using ASCII Character string sent and received by a controlling IBM compatible computer running the HEAT Technology Data Logging software. Once all of the required channels have been set up to return data in the format required by the software, then the whole system configuration maybe stored to disc. The specification includes:

- 15 Differential DC fused (FSD) 20 mV (High gain) or 80 mV channels. These may be configured as thermocouple input channels and on board cold junction compensation is standard for both type T and type K thermocouple.

- 8 Single ended DC voltage channels - FSD 2 V (High gain) or 8 V.
- 1 Internal mains voltage, which detects the voltage supplied to the data logger.
- 3 AC current channels; 2 of FSD 4 mA (High gain) or 16 mA. 1 of FSD 0.4 mA (High gain) or 1.6 mA.
- 8 Logic or frequency counting input channels. Input grounded taken as logic 1 or a pulse.
- 8 Digital output channels. One of which may be set to switch on for a proportion of a second every second until reset or the rate is altered by a further command.

The HDL interface has five on board power supplies giving the following output voltages:

- + 5 V DC
- - 5 V DC
- + 12 V DC (4 connections)
- + 15 V DC
- - 15 V DC

The 5 V and 15 V supplies being regulated to 5%.

Data Acquisition and Instrumentation

The data acquisition and instrumentation for the task is described here; it consists of the following components:

- A data logger for recording of various measurements
- for recording of various measurements
- for recording of various measurements
- Electrical power measured by electrical current

Temperature Measurement

The data acquisition system used provides connections for temperature measurement using K type thermocouples. The K type thermocouple (Nickel – Chromium / Nickel – Aluminium) is extensively used in high temperature and moderate temperature applications. And it provides excellent repeatability (0.1 °C) within the intended temperature range considered. British standard for the output of K type thermocouple is BS EN 60584-1:2013. Maximum continuous working temperature is put around 1100 °C, a grade nominal range of -270 °C to + 1260 °C and accuracy of ± 2.2 °C or ± 0.75 % - whichever is greater. In accordance to BS EN 60584-1:2013, the K type thermocouple offers a high output tolerance value of 1.5 °C (Class 1) between the temperature range of - 40 °C to + 375 °C and 0.004 °C between the temperature range of 375 °C to 1000 °C. The thermocouple used in the test conforms to the above standard.

Flow Rate, Power and Energy Measurements

The CW10 is equipped with a flow meter which measure the flow rate and is displayed on the on the monitor (display) of the control unit. This could be viewed on the computer software if interfaced with the unit via the RS232 connection. The display only shows flow rates above 2.5 litres per minute due to limits. The CW10 uses integrated load cells to calculate the current power and summarises the energy. It is possible to see the performance of the system in kWh of the current day, 7 days summary and the total of last 7 days.

Test Plan & Test Procedure

The experimental plan is to investigate the performance of the heating unit. These experiments include:

- Evaluation of the CW10 cooling capacity
- Investigation of the system's response to change in ambient temperature
- Investigation of the system's response to cooling temperature variation
- To quantify the biomass (energy) demand of the system.

Experiment Plan

A series of tests are designed to study the system characteristics as outlined above. The parameters to be recorded are described in Table 4.2. The tests were carried out as shown

Table 4.2 Recorded Parameters

Parameter	Description	Unit	Remark
T_{cxiset}	Evaporator inlet set temperature	$^{\circ}C$	Fixed
$T_{cxoaset}$	Evaporator outlet set temperature	$^{\circ}C$	Variable
T_{amb}	Ambient Temperature	$^{\circ}C$	Fixed
M_{cx}	A/C Circuit Mass Flow	kg/min	Fixed
Q_{cv}	A/C Cooling Energy	kW	Measured

in Table 4.3. The above readings were recorded regularly at very short intervals (less than 5 seconds) and stored for processing at the end of the session. The data acquisition is spreadsheet friendly, so the data were converted into an excel sheet for analysis.

Table 4.3 TCA test plan

Experiment (i)					
S/N	T_{cxiset} ($^{\circ}C$)	$T_{cxoaset}$ ($^{\circ}C$)	T_{amb} ($^{\circ}C$)	M_{cx} (kg/min)	Q_{cv} (kW)
Test Number	Evaporator Inlet Set Temperature	Evaporator Outlet Set Temperature	Ambient Temperature	A/C Circuit Mass Flow	Cooling Energy

Experimental Rig

The experimental rig installed in Room G-11 at the Centre for Biomass Excellence, Staffordshire University. It consists of a biomass silo containing the biomass fuel sample, a hopper, biomass boiler, heat exchanger and the refrigeration system, as well as a data logging unit - ClimateWell pc interface, data logger and a personal computer (Fig. 4.5). The refrigeration system consists of the TCA unit and a pair of air handling unit (AHU) (Fig. 4.6). The schematic of the test rig is shown in Fig. 4.7.



Fig. 4.5 TCA Experiment Set-up

Test Procedure

In line with the test plan, a series of tests were performed to examine the performance of the refrigeration system, which include a total of 60 tests in 6 experiments.

The following procedure was used for every test:

- A visual inspection of the set up to ensure the integrity of the connections. The flow lines from the plumbing pipe network to the refrigeration system were checked throughout to ensure continuous flow. The flows are set to a predetermined rate and read via a digital flow meter.
- The temperature of the hot water storage is checked to ensure that it is sufficient to drive the system. A temperature of 60 °C and above is desired. However, the boiler is set to deliver hot water at 100 °C.
- The refrigeration system is checked to ensure that it is set to 'Normal'. In this mode, the operation is fully automatic and the overheating protection is activated and the CW10 automatically controls itself to deliver the set temperature to the indoor climate circuit.



Fig. 4.6 TCA Experiment Set-up (AHU)

- The data logging is checked and set to commence data collection.
- The refrigeration system is turned on to commence a cycle. There is a time lapse of 90 seconds between the start up and full operation. During this time, the system checks the barrel's level and starts discharging one and charging the other. This is decided by the barrel's level. The most charged barrel will start discharging.
- The test is allowed to run until there is a swap. This period is indicated on the CWIC display software as the dormant barrel becomes active and the active becomes dormant. Depending on the level of charge of the active barrel and rate of discharge, each experiment could take up to 4 - 8 hours.

The data is retrieved from the logging system for analysis at the end of the experiment and displayed in .csv or .xlsx files for analysis.

(The number of experiments and tests in this work were constrained by weather conditions, breakdown of the refrigeration system and the equipment and laboratory becoming unavailable due to the relocation of the campus from Stafford to Stoke-On-Trent. It was no longer possible to carry out further experiments and tests. Consequently, the reported experiments and tests are those that were repeated and for which the results are reliable.)

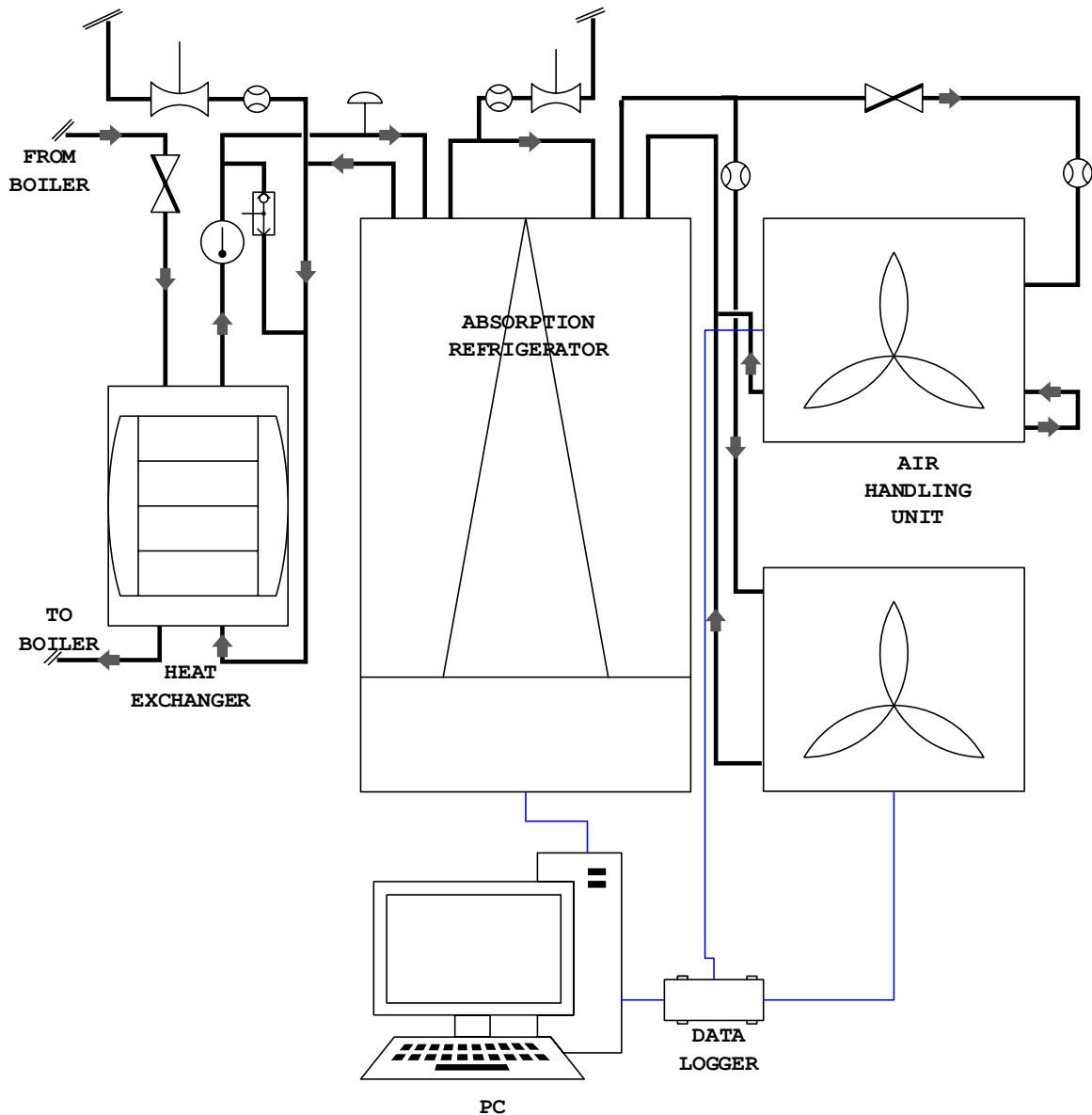


Fig. 4.7 Schematic of TCA test rig

4.4 Aqua-Ammonia VARC - Modelling

Fig. 4.8 is a schematic of the VARC. Refrigerant vapour leaves the evaporator at state 10 at a low temperature and pressure. It is absorbed by a weak solution of ammonia coming from a pressure reduction valve at state point 6 and increases in ammonia concentration, and is referred to as strong solution. The strong solution leaves the absorber at state 1 as a saturated liquid—the enthalpy of condensation being rejected and hence, the heat rejection Q_a in the absorber. A liquid pump increases the pressure of the strong solution from the evaporator

pressure (p_e) to the condenser pressure (p_c) through the solution heat exchanger where it is preheated by the warm weak solution and enters the generator at state 3. The strong solution is heated in the generator to liberate the refrigerant. The weak solution leaves the generator at state 4 through the solution heat exchanger and the solution expansion valve which reduces the pressure of the weak solution as it flows back into the absorber at state point 6. The refrigerant enters the condenser at state 7 at high pressure p_c and the heat of condensation Q_c is rejected to the surroundings. The liquid refrigerant leaves the condenser at state 8 and enters the evaporator at state 9 by an isentropic expansion process. Heat Q_e is added in the evaporator from the space being cooled at low pressure causing the refrigerant to boil, and the vapour leaves to the absorber at state 10, where it is absorbed by the weak solution.

The downside of an aqua-ammonia system is that due to the volatility of ammonia and water, the refrigerant vapour leaving the generator would contain too much water which could freeze in the expansion valve and the evaporator, causing damage to the system. Consequently a rectification column with a dephlegmator is placed between the generator and the condenser to efficiently remove the water vapour from the ammonia. The rectifier removes heat from the dephlegmator section to a temperature that will cause the condensation of water vapour. The condensate drips downward the column, combining with the weak solution and leaves as a vapour from the generator. The ascending refrigerant vapour develops a progressively higher ammonia concentration while the condensate flows back to the generator. The process can produce ammonia vapour concentration close to ideal - nearly 1.0. This model does not consider the rectification column.

4.4.1 Mass and Energy Balance

Based on Fig. 4.8, \dot{m}_1 , \dot{m}_6 and \dot{m}_{10} (kg/s) are respectively, the flow rates of the strong solution, weak solution and the refrigerant; and x_1 , x_6 and x_{10} are ammonia mole fraction in the weak solution, strong solution and the refrigerant. h_i (kJ/kg) is the state point enthalpy $i = 1, 2, \dots, n$ is the state point. Q_i (kW) is the energy rate of change, where $i = a, c, e, g$ for the absorber, condenser, evaporator and generator, respectively. T_{jk} is the flow temperature where j is the component initial and k indicates flow direction—i for inlet and o for outlet. COP_{ref} —the performance coefficient of the refrigeration cycle—is the ratio of the heat supplied in the generator to the rate of heat transfer to the system from the surroundings (refrigeration capacity).

Mass conservation—overall:

$$\dot{m}_1 = \dot{m}_6 + \dot{m}_{10} \quad (4.48)$$

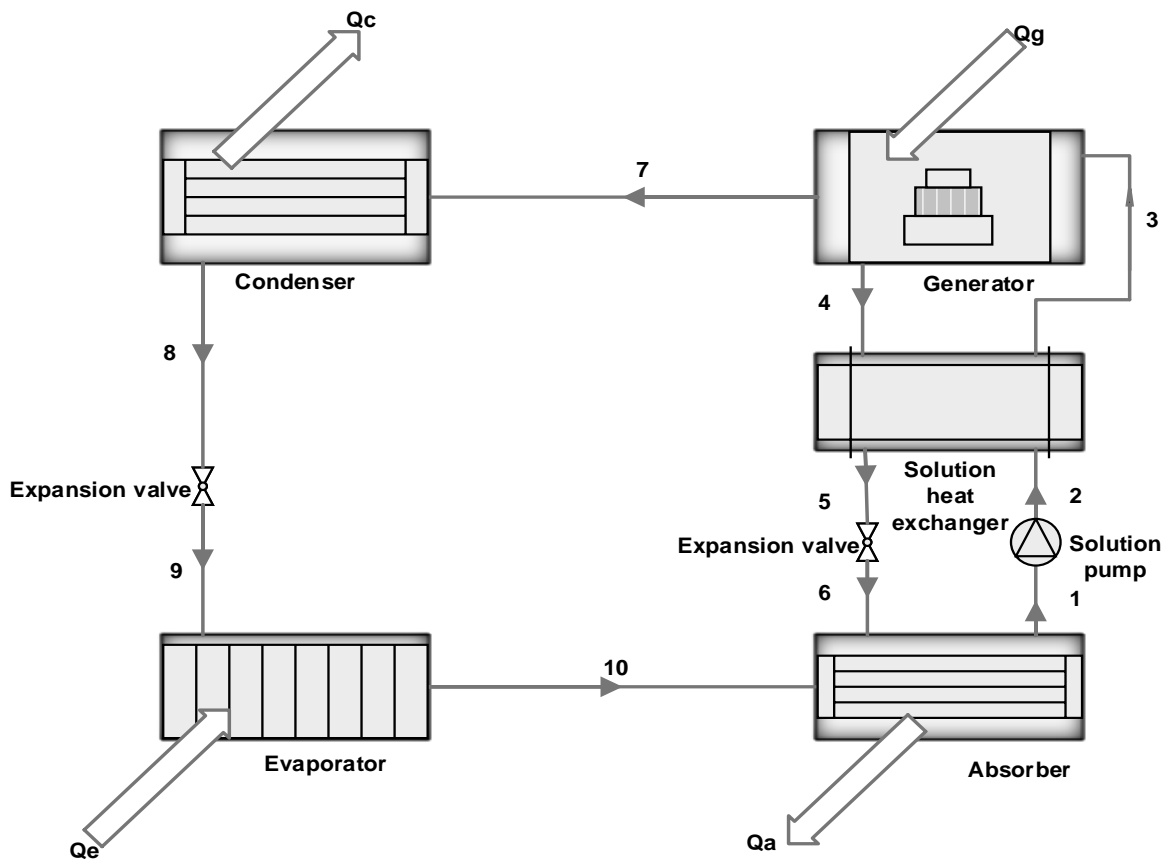


Fig. 4.8 Schematic of VARC

Mass conservation—ammonia:

$$\dot{m}_1 x_1 = \dot{m}_6 x_6 + \dot{m}_{10} x_{10} \quad (4.49)$$

Energy conservation:

$$\dot{m}_1 h_1 = \dot{m}_6 h_6 + \dot{m}_{10} h_{10} \quad (4.50)$$

Combining Equations (2) and (3):

$$x_1 = x_6 + (\dot{m}_{10}/\dot{m}_1)(x_{10} - x_6)$$

Circulation ratio (f):

$$f = \dot{m}_1/\dot{m}_{10} \quad (4.51)$$

$$x_1 = x_6 + (1/f)(x_{10} - x_6)$$

Similarly,

$$h_1 = h_6 + (1/f)(h_{10} - h_6)$$

Energy balance—absorber:

$$Q_A = \dot{m}_{10} h_{10} + \dot{m}_6 h_6 - \dot{m}_1 h_1 \quad (4.52)$$

From Equations (4) and (5),

$$Q_A = \dot{m}_{10}[h_{10} + (f-1)h_6] - \dot{m}_1 h_1 \quad (4.53)$$

Energy balance—heat exchanger:

$$Q_{hx} = \dot{m}_6(h_4 - h_6) = \dot{m}_1(h_3 - h_2) - w_p \quad (4.54)$$

where $\dot{m}_r = \dot{m}_{10} = \dot{m}_7$ —refrigerant mass flow, $x_1 = x_2 = x_3 = X_{ss}$ —strong solution (with respect to the ammonia concentration in solution) and $x_4 = x_5 = x_6 = X_{ws}$ —the weak solution.

Assume pump work $w_p \approx 0$ (negligible), the enthalpy at the generator inlet:

$$h_3 = h_2 + (1/f)(h_4 - h_5) \quad (4.55)$$

Energy balance—generator:

$$Q_G + \dot{m}_1 h_3 = \dot{m}_{10} h_7 + \dot{m}_6 h_4$$

$$Q_G = \dot{m}_{10} [h_7 + (f - 1)h_4] - \dot{m}_1 h_1 \quad (4.56)$$

Energy balance—condenser:

$$Q_C = \dot{m}_{10} (h_7 - h_8) \quad (4.57)$$

Energy balance—evaporator:

$$Q_E = \dot{m}_{10} (h_{10} - h_8) \quad (4.58)$$

Coefficient of performance:

$$COP_{ref} = \frac{Q_E}{Q_G + w_p} = \frac{Q_E}{Q_G} \quad (4.59)$$

4.4.2 Governing Equation

In order to fix the thermodynamic state for a compressible binary solution, the composition is required in addition to the two independent properties—temperature and pressure. The bubble point (T_b) and dew point (T_d) temperatures are calculated from the correlations developed by Patek and Klomfar [153]—Equation (13).

$$T_b(p, x) = T_0 \sum_i a_i (1 - x)^{m_i} \left[\ln \frac{p_0}{p} \right]^{n_i} \quad (4.60)$$

$$T_d(p, y) = T_0 \sum_i a_i (1 - y)^{\frac{m_i}{4}} \left[\ln \frac{p_0}{p} \right]^{n_i} \quad (4.61)$$

$$x = f(T, p) \quad (4.62)$$

$$y = f(T, p) \quad (4.63)$$

where T is temperature (K), T_0 , T_b and T_d are the reference, bubble and dew points temperatures, respectively. The coefficients are shown in Tables 4.4 and 4.5. x and y are the ammonia mole fraction in the liquid and vapour phases, respectively.

Table 4.4 Coefficients for Equation (4.60)

i	m_i	n_i	a_i
1	0	0	+0.322302e+1
2	0	1	-0.384206e0
3	0	2	+0.460965e-1
4	0	3	-0.378945e-2
5	0	4	+0.135610e-3
6	1	0	+0.487755e0
7	1	2	-0.120108e0
8	1	2	+0.106154e-1
9	2	3	-0.533589e-3
10	4	0	+0.785041e+1
11	5	0	-0.115941e+1
12	5	1	-0.523150e+2
13	6	0	+0.489596e-1
14	13	1	0.421059e-1

Where $p_0 = 2$ MPa and $T_0 = 100$ K, the reduced thermodynamic properties are as follows:

$$T_0 = 100 \text{ K}; p_b = 10 \text{ bar}; T_r = \frac{T}{T_0}; p_r = \frac{p}{p_b}; R = 8.314 \text{ J/kmol.}$$

The composition of the solution phase is estimated from Equation (4.62), developed from Equation (4.60). To estimate the composition in the vapour phase, the vapour split, V/F , from Equation (4.65) is numerically computed from the Rachford Rice flash Equation (4.64) using the (fzero) function in MATLAB [159]. Equation (4.66) gives the vapour composition.

$$\sum_{i=1}^S (y_i - x_i) = \sum_{i=1}^S \frac{(K_i - 1)z_i}{((K_i - 1)V + 1)} = 0, \quad 0 \leq \frac{V}{F} \leq 1 \quad (4.64)$$

$$x_i = \frac{z_i}{1 + \frac{V}{F(K_i - 1)}} \quad (4.65)$$

$$y_i = K_i x_i \quad (4.66)$$

K -value defines the ratio of each component:

$$K_i = \frac{y_i}{x_i} \quad (4.67)$$

F in the above Equations represents the feed with composition z_i . V (with composition y_i) is the vapour product and L (with composition x_i) is the liquid product.

The Equations for the enthalpy and the Gibbs free energy equation are as follows [213, 109, 69]:

Table 4.5 Coefficients for Equation (4.61)

i	m_i	n_i	a_i
1	0	0	+0.324004e+1
2	0	1	-0.395920e0
3	0	2	-0.434624e-1
4	0	3	-0.218943e-2
5	1	0	-0.143526e+1
6	1	1	+0.105256e+1
7	1	2	-0.719281e-1
8	2	0	+0.122362e+2
9	2	1	-0.224368e+1
10	3	0	-0.210780e+2
11	3	1	0.110834e+1
12	4	0	+0.145399e+2
13	4	2	+0.644312e0
14	5	2	-0.221264e+1
15	5	2	-0.756266e0
16	6	0	-0.135529e+1
17	7	2	+0.183541e0

$$h = -RT_b T_r^2 \left[\frac{\partial}{\partial T_r} \left(\frac{G_r}{T_r} \right) \right] \quad (4.68)$$

$$G = h_0 - TS_0 + \int_{T_0}^T C_p dT + \int_{p_0}^p v dp - T \int_{T_0}^T \left(\frac{C_p}{T} \right) dT \quad (4.69)$$

The correlation for the heat capacity at constant pressure C_p and specific volumes in the liquid and vapour phases v_l and v_g are given below:

$$C_{pl} = b_1 + b_2 T + b_3 T^2 \quad (4.70)$$

$$C_{pg} = d_1 + d_2 T + d_3 T^2 - T \int_{p_0}^p \left(\frac{\delta^2 V}{\delta T^2} \right) dP \quad (4.71)$$

$$v_l = a_1 + a_2 p + a_3 T^2 + a_4 T^2 \quad (4.72)$$

$$v_g = \frac{RT}{p} + c_1 + \frac{c_2}{T^3} + \frac{c_3}{T^{11}} + \frac{c_4 p^2}{T^{11}} \quad (4.73)$$

Equations (4.68)–(4.69) were solved with MATHCAD using the correlations (4.70)–(4.73) to obtain the liquid (h_{liquid}) and vapour (h_{vapour}) phase enthalpy (4.74) and (4.75). The coefficients are shown in Table 4.6 [213].

Table 4.6 Coefficients for Equations (4.74) and (4.75)

Coefficients	Ammonia	Water
a_1	3.971423e-2	2.748796e-2
a_2	-1.790557e-5	-1.016665e-5
a_3	-1.308905E-2	-4.452025e-3
a_4	3.752836e-3	8.389264e-4
b_1	1.634519e1	1.214557e1
b_2	-6.508119	-1.898065
b_3	1.448937	2.911966e-2
c_1	-1.049377e-2	2.136131e-2
c_2	-8.288224	-3.169291e1
c_3	-6.647257e2	-4.631611e4
c_4	-3.045352e3	0.0
d_1	3.673647	4.019170
d_2	9.989629e-2	-5.175550e-2
d_3	3.617622e-2	1.951939e-2
h_0^l	4.87853	21.821141
h_0^v	26.468879	60.965058
T_{r0}	3.2252	3.0705
p_{r0}	2.0000	3.0000

$$h_{liquid} = -RT_b[-h_0^l + b_1(T_{r0} - T_r) + \frac{b_2}{2}(T_{r0}^2 - T_r^2) + (a_4T_r^2 - a_1)(p_r - p_{r0}) - \frac{a_2}{2}(p_r^2 - p_{r0}^2)] \quad (4.74)$$

$$h_{vapour} = -RT_b[-h_0^v + d_1T_{r0} + \frac{d_2}{2}(T_r^2 - T_{r0}^2) + \frac{d_3}{3}(2T_r^3 - T_{r0}^3) - d_1T_r - d_2T_{r0}^2 - \frac{d_3}{2}(T_r^2 - T_{r0}^2) - c_1(p_r - p_{r0}) + c_2\left(\frac{-4p_r}{T_r^3} + \frac{4p_{r0}}{T_{r0}^3}\right) + c_3\left(\frac{-12p_r}{T_r^{11}} + \frac{12p_{r0}}{T_{r0}^{11}}\right) + \frac{c_4}{3}\left(\frac{-12p_r}{T_r^3} + \frac{12p_{r0}}{T_{r0}^3}\right)] \quad (4.75)$$

Equations (4.76) and (4.78) gives the mixture phase enthalpy. h^E is the energy of mixing as shown in Equation (4.77); the coefficients are given in Table 4.7.

$$h^l = (1 - x)h_{liquid,H_2O} + xh_{liquid,NH_3} + h^E \quad (4.76)$$

$$h^E = e_1 + e_2p + (e_3 + e_4p)T + \frac{e_5}{T} + \frac{e_6}{T^2} + (2x - 1) \\ (e_7 + e_8p + (e_9 + e_{10}p))T + \frac{e_{11}}{T} + 3\frac{e_{12}}{T^2} \\ + (2x - 1)^2 \left(e_{13} + e_{14}p + \frac{e_{15}}{T} + \frac{e_{16}}{T^2} \right) \quad (4.77)$$

Similarly, the vapour phase enthalpy is given as shown in (31) where y' is the ammonia vapour fraction.

$$h^v = (1 - y')h_{vapour,H_2O} + y'h_{vapour,NH_3} \quad (4.78)$$

Table 4.7 Coefficients for Equation (4.77)

Coefficients		Coefficients	
e_1	-41.733398	e_9	0.387983
e_2	0.02414	e_{10}	0.004772
e_3	6.702285	e_{11}	-4.648107
e_4	-0.11475	e_{12}	0.836376
e_5	63.608968	e_{13}	-3.553627
e_6	-62.490768	e_{14}	0.000904
e_7	1.761064	e_{15}	21.361723
e_8	0.008626	e_{16}	-20.736547

The computation procedure for the analysis was implemented in MATLAB. The coefficient of performance (COP), and the rate of energy due to the absorber, condenser, and generator are computed. The refrigeration capacity (Q_e) is calculated from the refrigerant mass flow if it is not given as an input parameter and the refrigerant mass flow is calculated if the Q_e is given instead.

4.4.3 Modelling

For the implementation of the mathematical relations as a software routine it is necessary that the equations and functions are coded in the programme language(s) of the software, as well as ensuring that the organisational format is void of ambiguity and expresses the intent

with precision. Consequently, the code consisting of correlations, subfunctions, functions and logical operations are pre-tested for accuracy before they are called-up as handles in the programme script.

Mass-Pressure-Temperature

Fig. 4.9 shows the saturated liquid and vapour lines defined by dew and bubble points pressure for a given mass fraction (equations (4.60) and (4.61)). The solution at point *B* has a mass concentration of 0.3 at a pressure of 10 bar. The bubble point temperature is approximately 97 °C. This is the temperature at which the solution starts to boil when heat is being added at the specified conditions of pressure and concentration. Similarly, superheated vapour at the concentration of 0.95 and 10 bar will commence condensation at the dew point temperature, point *H*. It was clear that at each mass fraction the solution has a unique bubble point for a given a pressure. This implies that at each temperature and mass fraction, there exist a unique pressure at which the solution is saturated, liquid or vapour. Therefore, a relation of the mass fraction $(x) = f(p, T)$ was further numerically resolved and used to determine the system solution mass fraction. This data, shown in Fig. 4.10, is used to estimate the mass fraction at saturation throughout the system. The area bounded by the saturated liquid and vapour lines is a 2 – *phase* region. The solution at a point such as *E* will be a mixture of liquid and vapour. The quality of the solution in the 2 – *phase* region is determined by equation (4.76) or equation (4.78).

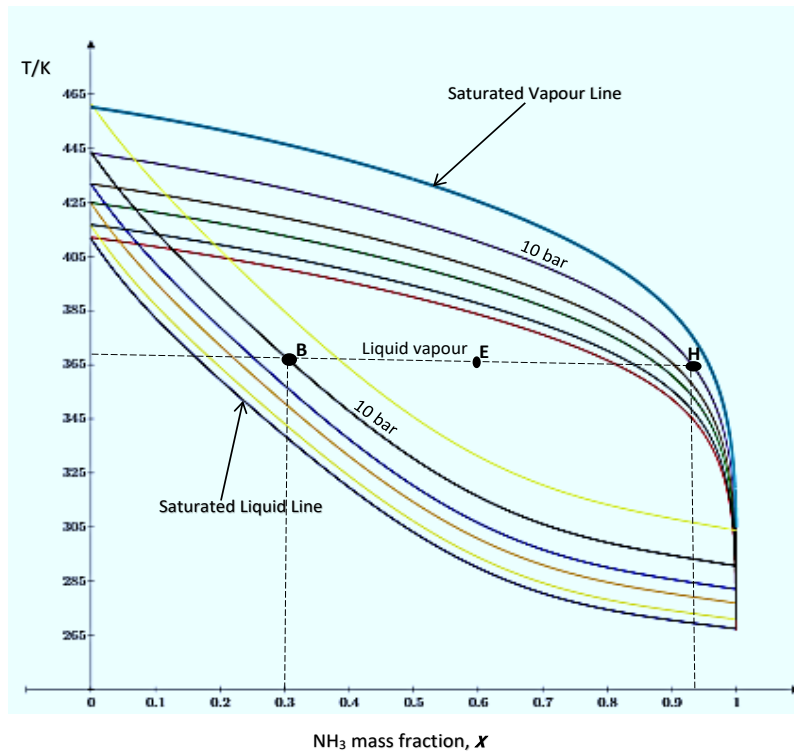


Fig. 4.9 Aqua-ammonia solution temperature-composition diagram

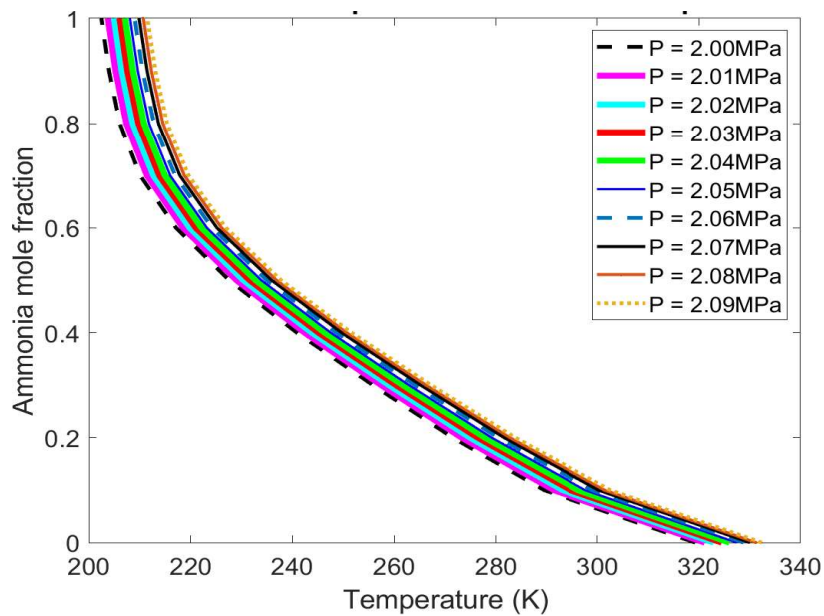


Fig. 4.10 Temperature-concentration (Range: 2.00MPa–2.09MPa)

Thermal Analysis

The thermal analysis of the system requires the evaluation of enthalpy and mass fraction at various state points of the cycle. This is carried out by modelling the mass and energy flows for each major component of the system. In order to evaluate it as a function block, each component is considered as a heat exchanger.

Absorber

The energy flows across the absorber are given by equation (4.52). The subroutines evaluating this component are shown in the Simulink block (MATLAB), Fig. 4.11.

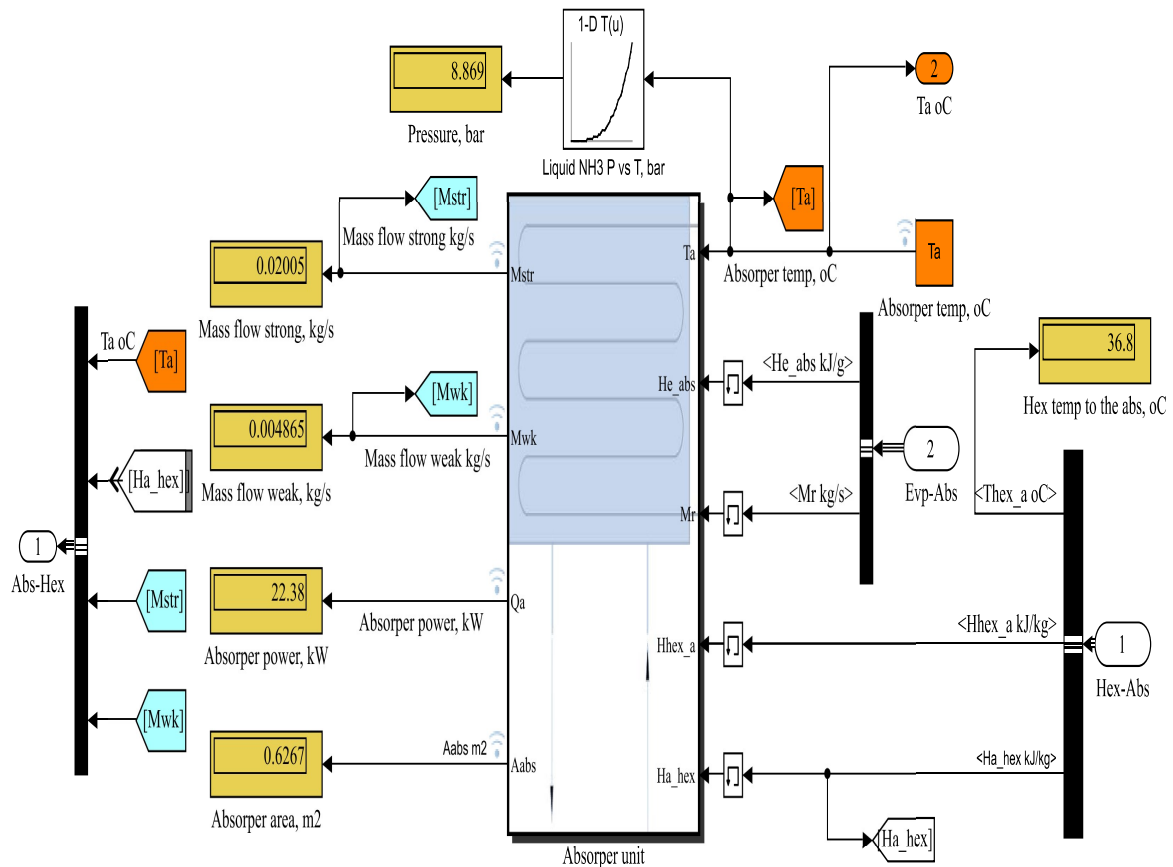


Fig. 4.11 Simulink model block showing absorber input and output parameters

Solution Heat Exchanger

At the solution heat exchanger the temperature at state point 3 & 5 of Fig. 4.8 are determined and combined with the concentration of the solution to obtain the enthalpy. The energy due to solution heat exchanger is give by equation (4.54). The Simulink model is shown in Fig. 4.12.

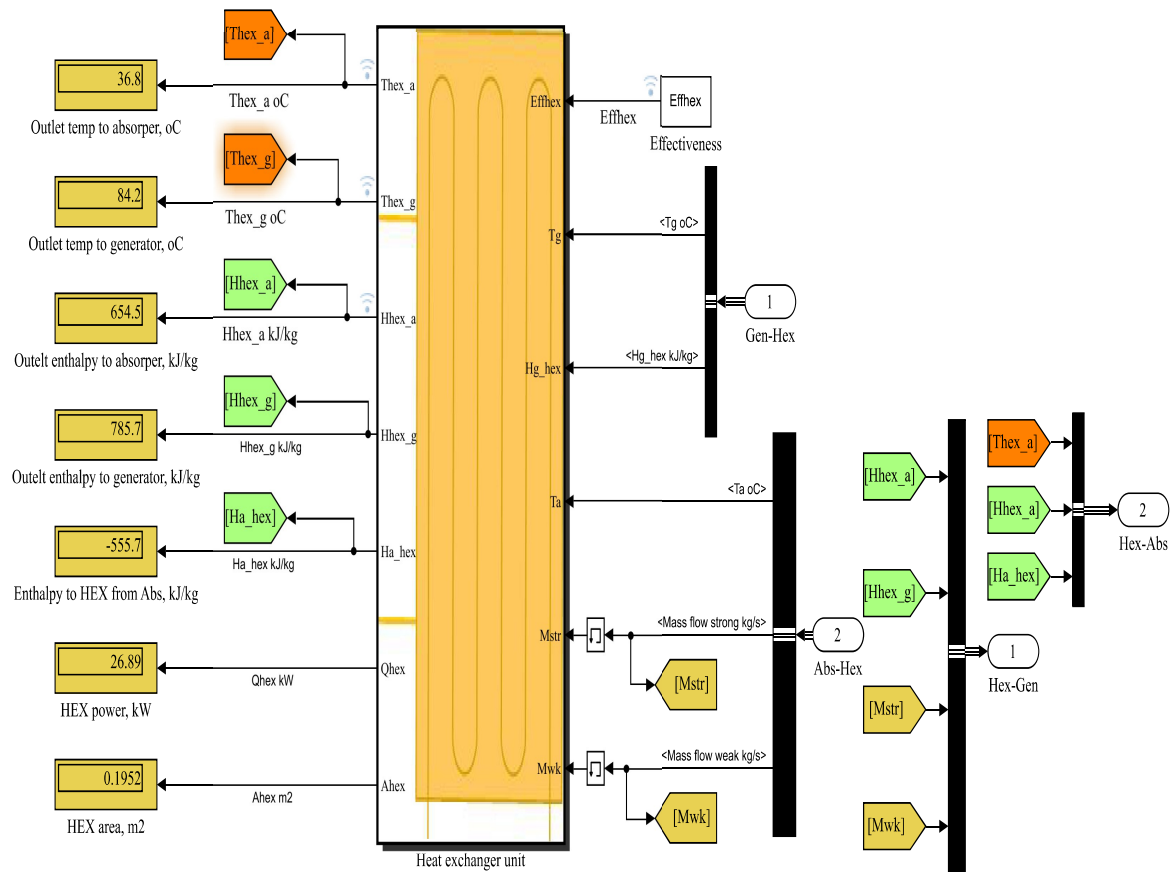


Fig. 4.12 Simulink model block showing solution heat exchanger input and output parameters

Generator

The generator utilises the heat input to desorb ammonia refrigerant from the strong solution by vaporisation, and to simulate pumping effect. The energy rate of flow due to the generator is given by equation (4.56); Fig. 4.13 shows the Simulink model.

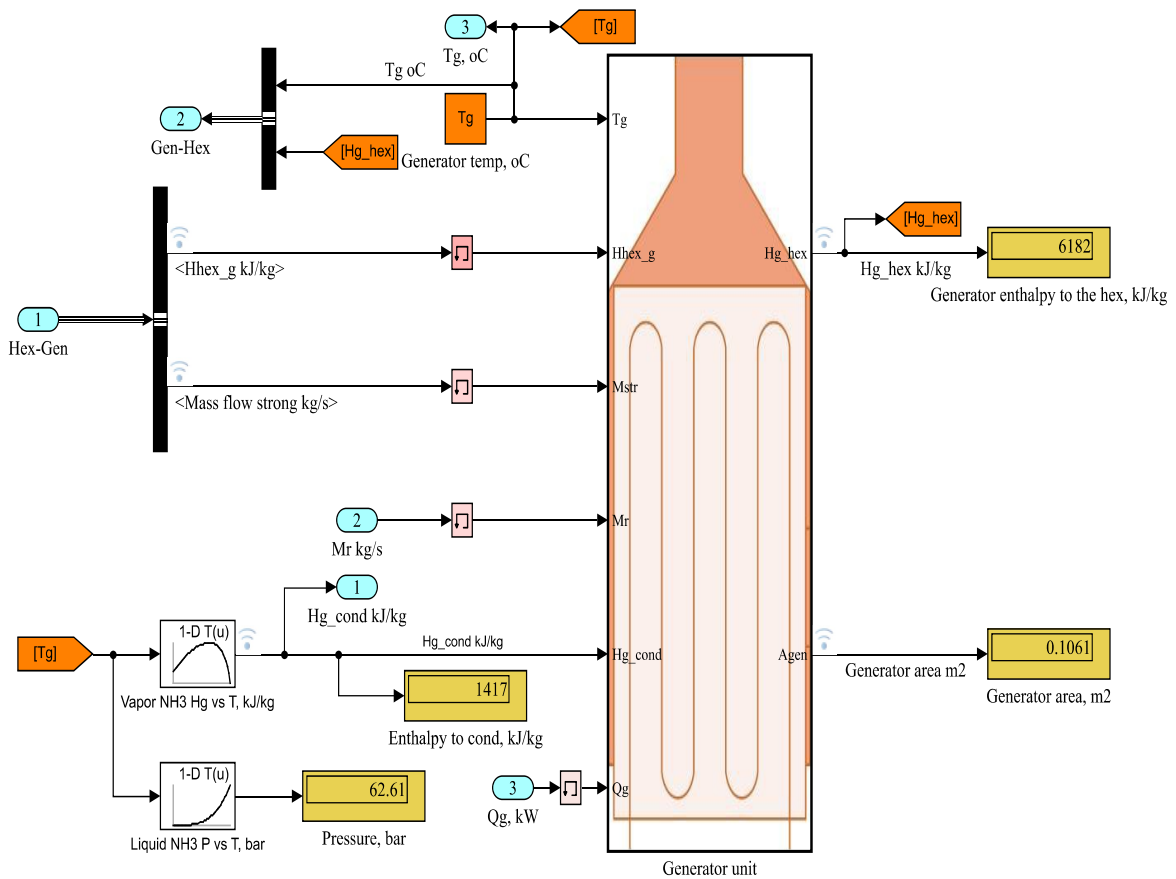


Fig. 4.13 Simulink model block showing generator input and output parameters

Condenser

The refrigerant vapour is cooled at constant pressure at the condenser. The resulting heat of condensation is removed from the system to the surrounding. Equation (4.57) gives the energy balance of the condenser and the Simulink model is presented in Fig. 4.14

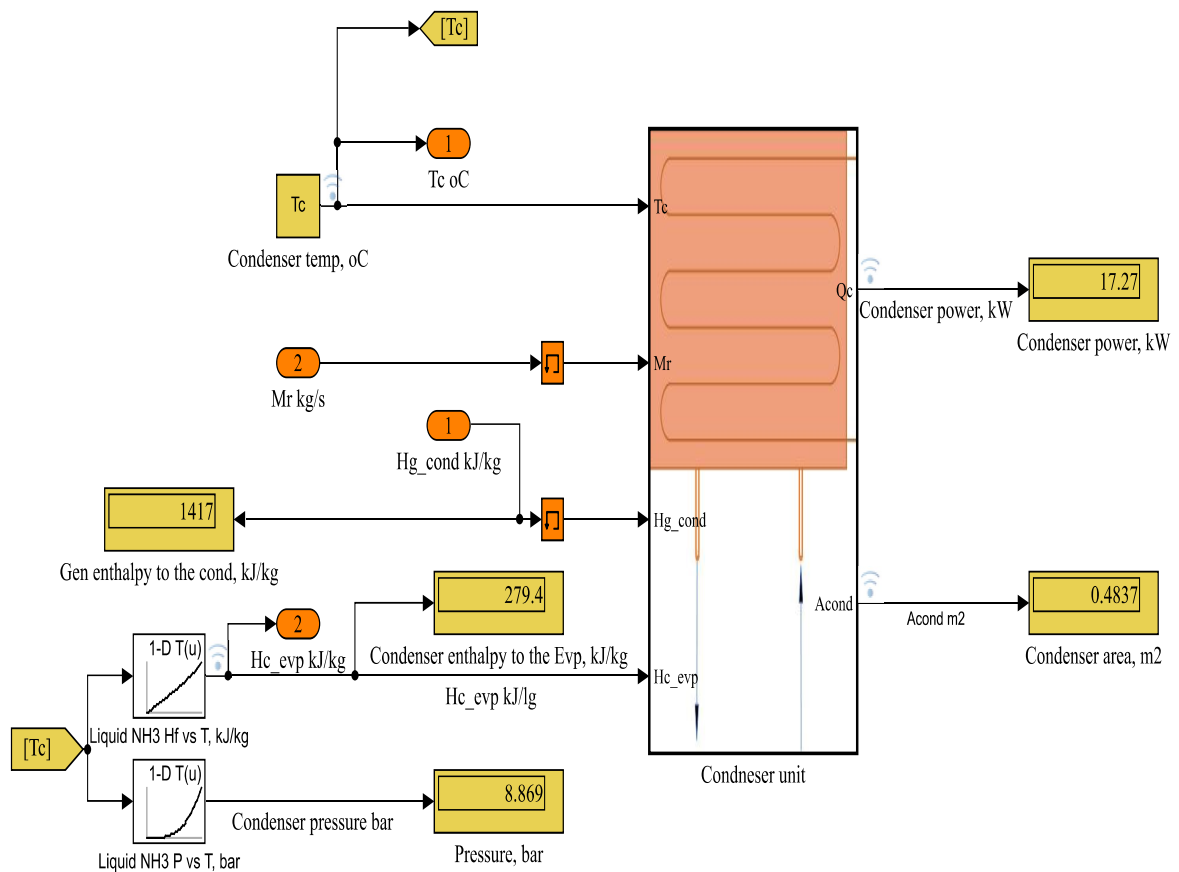


Fig. 4.14 Simulink model block showing condenser input and output parameters

Coefficient of Performance

The performance of the system is evaluated by the coefficient of performance given by equation (4.59). The Simulink model is shown in Fig. 4.16.

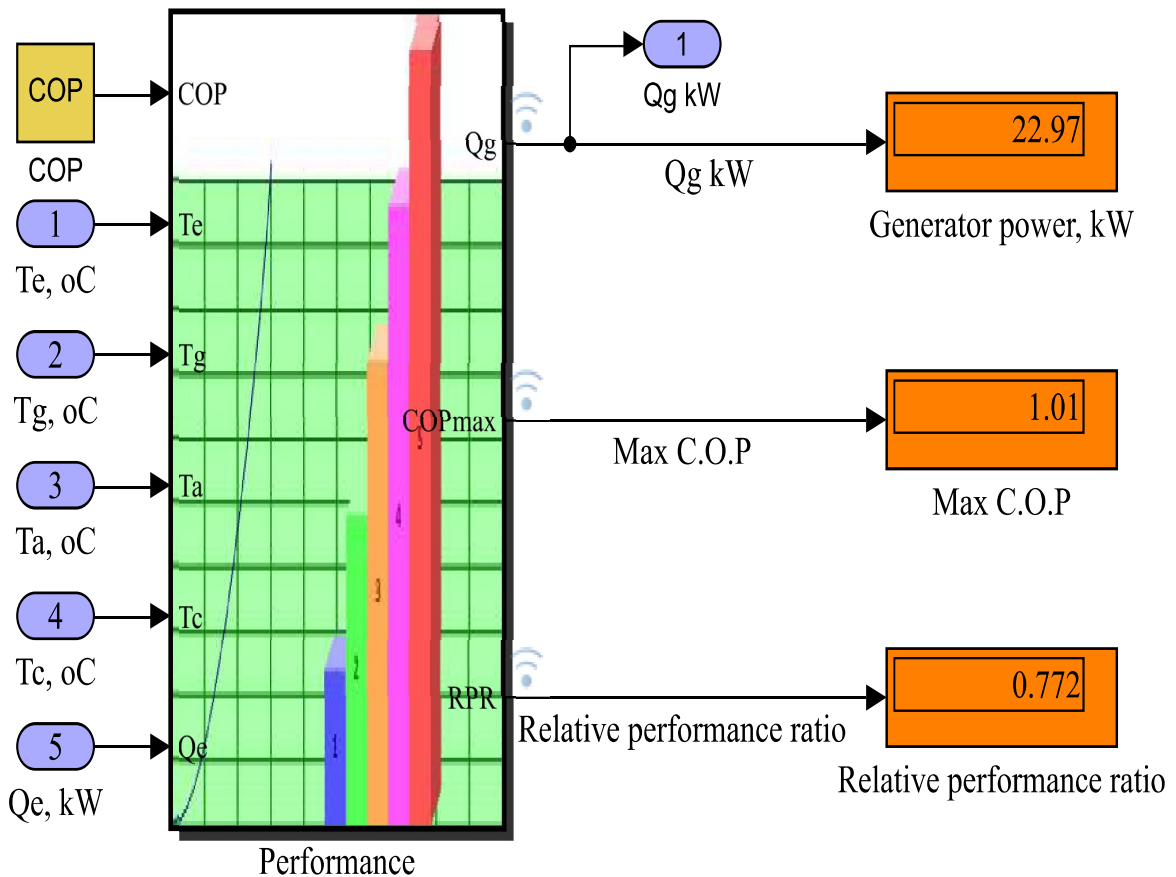


Fig. 4.16 Simulink model block showing system performance parameters

The computational model is shown in Fig. 4.17. The computer routine employs the various equations to compute the energy flows across the components. The programme input are temperatures and refrigerant mass flow rate and/refrigerant capacity. It estimates to a very close approximation, the mass fraction and saturation pressure of the system working temperature range. Also the model can simulate both static and dynamic conditions.

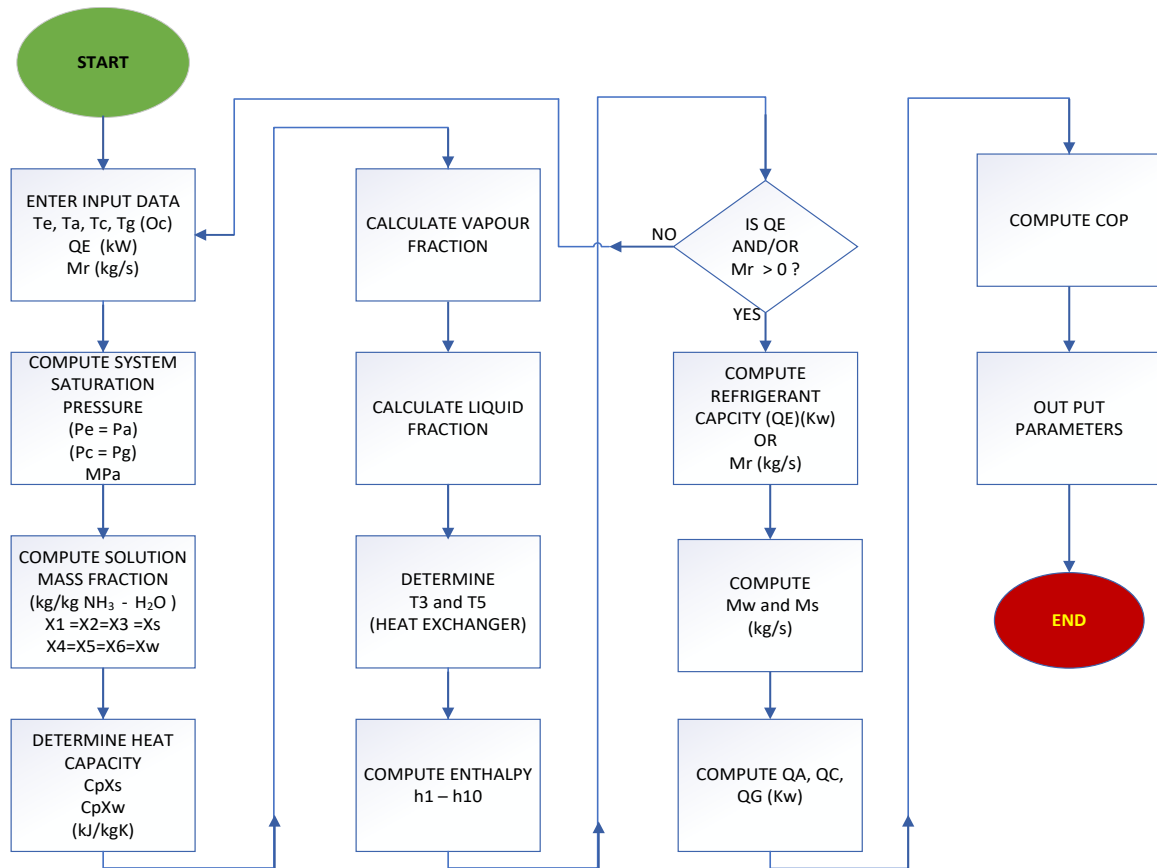


Fig. 4.17 Computational model of aqua-ammonia absorption refrigeration system

4.5 Summary

The thermochemical accumulator was both theoretically and empirically evaluated for performance. The coefficient of performance was the focus of the theoretical evaluation. To achieve this a mathematical model was developed using energy conservation, mass balance and material continuity in addition to the thermodynamic and physical properties of the materials media. The experimental evaluation focussed on the cooling energy or rate of cooling. 60 tests were performed in 6 experiments in which some parameters were varied to examine the system's response.

A simplified model was developed to aid the parametric study of the inter-components relationship and performance of the aqua-ammonia vapour absorption refrigeration system. The mathematical model was implemented in MATLAB and only requires temperature input and the refrigerant mass flow or the refrigerant capacity to return the values of the desired evaluated parameters.

Chapter 5

Biomass Performance Evaluation

5.1 Introduction

This chapter describes the tests and theoretical analysis of biomass carried out in the course of this study. This includes the evaluation of some key energy influencing properties of solid biomass fuels, descriptive evaluation of the biomass boiler as a stand alone water boiler and heat source for the absorption unit with the capability of providing heat to drive a combined cooling and heating (CCH) system such as the TCA. The assessment and quantification of biomass as a sustainable fuel source to provide energy for cooling will be described.

The consideration of biomass as a reliable feedstock to produce energy for power would depend on the availability, accessibility and sustainability of the resource, as well as the readiness of the conversion technologies and the rate of demand. Consequently, these factors underlie the investigation on the feasibility of biomass as a sustainable energy source for rural Nigeria in this chapter. The results of these measurements and assessments shall be included in the chapter on results and discussion.

(All the equipment used in this and subsequent experiments carried out in this project are new from the suppliers, and are part of the Arbor Renewable Energy Project at the Centre for Biomass Excellence, Staffordshire University. They were all calibrated the equipment supplier and produced reliable measurements at the time of use.)

5.2 Solid Biomass Fuel Properties

In section 3.2 the theoretical principles of the key properties of biomass fuel were considered in details. Two of these properties were empirically evaluated in this study. The two properties evaluated are:

- Moisture Content
- Calorific value

5.2.1 Moisture content

The electric oven method was used to determine the moisture content of different biomass fuel. 1g of the fuel sample is crush and weighed in a crucible and heated in an oven. The sample is heated evenly at 105 °C for two hours. The sample weighed and replaced in the oven for another hour. The procedure is repeated till a constant weight is obtained. The value of the moisture content are obtained using equation (3.1) or equation (3.2) in combination with the physical measurement as follows.

$$C_m = \frac{M_{wc}}{F_w} * 100$$

$$M_{wc} = m_1 - m_2 \quad (5.1)$$

$$F_w = m_1 - m \quad (5.2)$$

where:

m₁ is the weight of the sample before heating

m₂ is the weight of the sample after heating procedure and

m is the weight of the empty crucible.

Other solid fuel properties such as ash content, volatile matter and fixed carbon content are determined from the moisture content. The analysis is conducted in accord with the test analysis for a solid biomass fuel samples to determine the moisture content described in the standard ISO 18134:2015. Five biomass fuel sample were tested in this study. Each test was repeated at least three times.

5.2.2 Energy content

The energy content of biomass solid was determined by burning a unit mass of the fuel sample in an oxygen bomb calorimeter. The PARR 1341 bomb calorimeter was used. The calorimeter

was calibrated with 1.0g sulphur in combustible solid in line with ISO 18125:2017. The test sample is placed in the oxygen combustion chamber. The calorimeter bucket is then filled with 2000 (+/- 0.5) grams of distilled water of about 15 °C. The temperature of the water is recorded. The oxygen combustion chamber is placed in the bucket and set in the calorimeter jacket. The stir is turned on and allowed to run for five minutes to reach equilibrium. The temperature is read off a digital thermometer and recorded in one-minute intervals for five minutes before the bomb is fired. The bucket temperature is recorded as it rises and drops to a constant. The knurled knob on the head of the bomb head is opened to release the gas pressure before the cap is removed. After every experiment, the interior of the bomb is inspected for soot and or other evidence of incomplete combustion. Tests with evidence of incomplete combustion are discarded and repeated. Unburnt wire is removed and measured. This is followed by washing the interior of the bomb with a jet of distil water. Titration is conduction on the washings using methyl orange indicator and standard sodium carbonate solution The test was carried out for five samples of biomass solid fuel. The experiment set-up is shown in Fig. 5.1. The experiment is analysed using the following equations.

The gross heat of combustion is given by:

$$H_g = \frac{t * W - e_1 - e_2 - e_3}{m} \quad (5.3)$$

Where t , the net corrected temperature rise is given by:

$$t = t_c - t_a - r_1(b - a) - r_2(c - b) \quad (5.4)$$

Where

a = time of firing

b = time (to nearest 0.1 min.) when the temperature reaches 60 per cent of the total rise

c = time at beginning of period (after the temperature rise) in which the rate of temperature change has become constant

e_1 = correction in calories for heat of formation of nitric acid (HNO_3) = c_1 if 0.0709N alkali was used for the titration

e_2 = correction in calories for heat of formation of sulfuric acid (H_2SO_4)

e_3 = correction in calories for heat of combustion of fuse wire.

t_a = temperature at time of firing

t_c = temperature at time c

r_1 = rate (temperature units per minute) at which the temperature was rising during the 5-min. period before firing

r_2 = rate (temperature units per minute) at which the temperature was rising during the 5-min. period after time c.

W (cal/°C) is the energy equivalent of the calorimeter.

$$W = \frac{H * m + e_1 + e_3}{t} \quad (5.5)$$

Where

H = heat of combustion of the standard benzoic acid sample in calories per gram

m = mass of the standard benzoic acid sample in grams.

The equivalent energy W in equation (5.5) is obtained by conducting the procedure with a standard sample (standardisation). this value is unique to the bomb and it is used to obtain the net calorific value of each sample.

The experimental is given in the Parr documentation 204M.



Fig. 5.1 PARR bomb calorimeter set up

5.3 Biomass Combustion for Energy

This section describes the boiler for the combustion of biomass and outline prime movers

The heat source for the operation of the TCA was from the combustion of biomass solid fuel. The biomass fuel was stored in a storage tank fitted with suction probes and connected to the biomass boiler through an automated fuel feed system which uses a vacuum blowing technology to transfer the solid fuel to the boiler in-storage of about 135 kg capacity. Fuel feed unit is fitted with sensory probes by which it checks the level of the boiler in-storage, roughly every 6 hours, and/or determines when the tank is just about empty, and refills it. The system can be set to operate at a regular or set time. At full load heating hours equivalent(FLHE), it takes about 14.4 hours to empty. This is dependent on the solid fuel species. The boiler unit is a 45 kW Windhager Biomass Boiler. it is linked to the buffer vessel via a mixing valve. The buffer vessels are fitted with internal heating coils and temperature sensor to enhance sustained set temperature of the system. It feeds the refrigeration unit heat source circuitry through a heat exchanger, and the heating panel for space heating as providing domestic hot water (DHW).

5.3.1 Biomass Combustion System

The biomass solid fuel storage is a 1000 kg tank made from plastic material. It is placed in the laboratory close to the goods entrance for easy access of solid fuel delivery trucks during refilling. The storage tank is fitted with suction probes and connected to the fuel feed unit. The fuel feed unit is automated and has a vacuum blowing system. It feeds the boiler with solid fuel from the solid fuel storage tank by means of the vacuum blowing system; it is also fitted with probes and can determine the level of solid fuel in the boiler-feed store. It can be programmed to check the level of the feed storage at a predetermined time - 6 hourly, for instance.

The boiler unit is a 45 kW Windhager biomass boiler, with a 135 kg solid fuel feed-store. It is designed to combust wood pellets of all sizes, but it can combust shredded shrubs and wood, sawdust and grasses. The boiler consists of a combustion chamber, a feed-store and a control unit. During operation, the combustion chamber is fed from the feed-storage within the boiler unit by an auger mechanism. At full working load the fuel the feed-store can be used up in 10 to 12 hours. However, this can be influenced by the size and other prevailing operating conditions. The flue from the combustion process is thrown to the atmosphere through the flue pipe. The water circuitry of the boiler is connected to the external plumbing unit and a buffer tank. The combustion chamber is routinely checked and cleaned to maintain the efficiency of the boiler. Fig. 5.2 shows the boiler unit connected to the feed unit and the buffer vessel. The inside of the unit is split into two vertical halves. On the top left is the boiler in-storage with a built-in silo. At the bottom left is the auger which links the combustion chamber in the right half of the unit. At the top right is the logic control unit. The boiler requires a scheduled maintenance but sometimes maintenance can be done off-schedule and it is mainly emptying the ash tank, hovering and brushing off dust as shown in Figs. 5.4 and 5.5



Fig. 5.2 Windhager biomass boiler, feed unit and buffer tank



Fig. 5.3 Windhager biomass boiler: inside view



Fig. 5.4 Boiler Maintenance



Fig. 5.5 Boiler Maintenance - scooping up ash remains

The hot water storage tank is a Windhager 860 litres capacity buffer vessel. It has internal heating coils and temperature sensor. The temperature is displayed on a temperature dial attached to the lagged wall. These devices enhances the maintenance of the set water temperature from the boiler in the storage. The vessel is connected to the boiler by a mixing valve. Both the boiler and the hot buffer vessel are connected to the external plumbing unit. They feed the TCA refrigeration unit, the heating panel for space heating and provide domestic hot water.

5.3.2 Biomass Source to Drive Absorption Refrigeration

The Quantity of biomass fuel required to provide source-energy to drive any system will vary for different end user but will generally depend on:

- The properties and condition of the fuel
- Boiler capacity
- Boiler efficiency
- Operating hours
- Type and availability of biomass.

To provide thermal energy to drive the refrigeration system for a given load, the quantity of biomass solid fuel needed is estimated based on the above factors and the heating value of the solid fuel species. The heat generated in the boiler from combusting the biomass solid fuel is used to raise the temperature of the water flowing in the heating circuitry of the system and provides energy that is transferred to the generator or reactor (for TCA) circuit through the heat exchanger. A counterflow heat exchanger configuration was used to enhance the heat transfer from the boiler unit to the refrigerating unit through the flow of water in the circuit (Fig. 5.6). T_{h1} is the hot water exit from the boiler unit (hot inlet of the heat exchanger) and T_{h0} is the return water to the boiler unit from the heat exchanger. T_{c1} is the temperature of the cold inlet to the heat exchanger from the refrigeration generator. This fluid leaves as T_{c0} , temperature of the cold outlet, after gaining heat and returns to the generator. The theory of heat exchangers was extensively discussed in *section 3.3*.

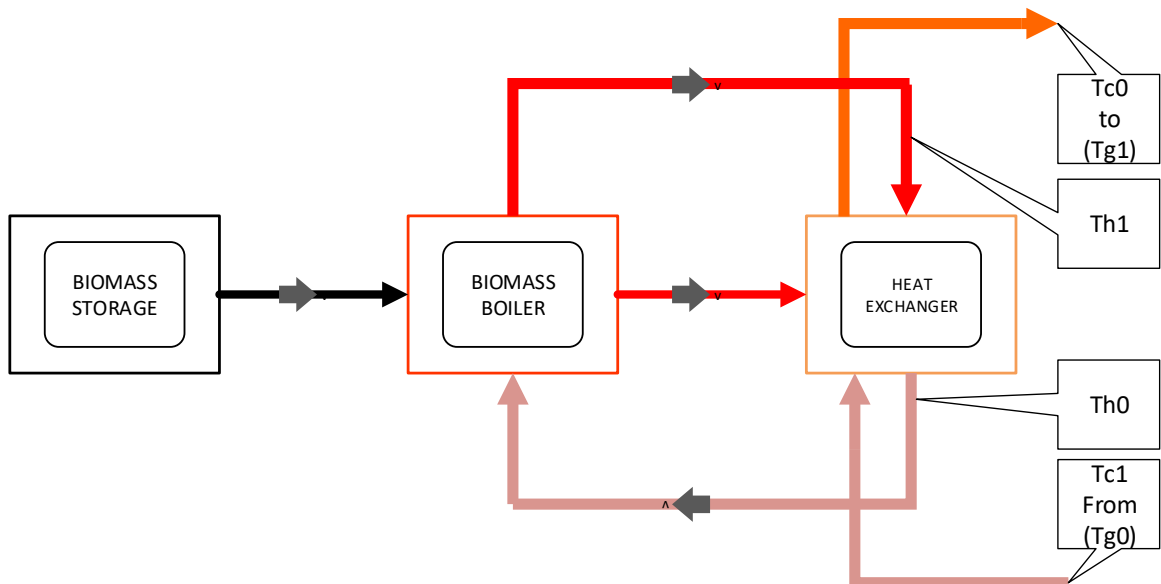


Fig. 5.6 Schematic of system heat transfer

The amount of required to raise the temperature of the of a substance is given as:

$$q = mC_p dT \quad (5.6)$$

For a continuous flow rate of change,

$$q = \dot{m}C_p dT \quad (5.7)$$

For a set temperature of (hot) water from the boiler unit and assuming that for the heat exchanger:

- Steady operating conditions apply;
- The heat exchanger is well insulated so that the heat loss to the surroundings is negligible;
- The kinetic and potential energy changes of the fluid are very small and negligible;
- No fouling conditions apply;
- The properties of the fluid remain the same throughout the process, and
- No pressure drop across the lines (pipe work).

The rate of heat required for the generator of the aqua-ammonia refrigeration system or the reactor heat exchanger of the TCA , for a set inlet and exit temperature, is estimated, and hence, the biomass quantity required for the load and operating duration as follows:

$$\dot{Q}_{hx} = \dot{m}C_p(T_{hi} - T_{ho}) \quad (5.8)$$

and

$$\dot{Q}_G = \dot{m}C_p(T_{co} - T_{ci}) \quad (5.9)$$

For a heat exchanger effectiveness of ε ,

$$\dot{Q}_{hx} = \dot{m}C_p\varepsilon(T_{hi} - T_{ho}) \quad (5.10)$$

the rate of heat for Equations (5.8) – (5.10) is assumed to be same.

For a boiler efficiency of η_B and full load heating hours' equivalent (FLHE), the energy required E_R and the biomass fuel quantity required B_Q , is estimated thus:

$$E_R = \frac{Q_{hx} * FLHE}{\eta_B} \quad (5.11)$$

where Q_{hx} is the rate of heat transfer from the heat exchanger.

$$B_Q = Q_{hx} * F_d * E_R \quad (5.12)$$

F_d is the fuel density of the biomass species.

$$Q_G = \dot{m}_c C_{pc} (T_{ci} - T_{co}) \quad (5.13)$$

$$Q_{hx} = \dot{m}_h C_{ph} (T_{ho} - T_{hi}) \quad (5.14)$$

$$\dot{q}_{loss} = UA_{hx} * (T_{hx} - T_{amb}) + UA_G * (T_G - T_{amb}) \quad (5.15)$$

where $T_{hx} = T_{hi} - T_{ci}$.

$$Q_{hx} = Q_G + \dot{q}_{loss} \quad (5.16)$$

$$B_Q = Q_G + \dot{q}_{loss} * \left(\frac{FLHE}{F_d * \eta_B} \right) \quad (5.17)$$

The quality of combustion in the boiler depends on several factors including design, air velocity, air temperature, etc. The influence of the design factor which can be evaluated by Computational Fluid Dynamics (CFD) analysis [46] , is not directly considered but assumed to be built into the boiler efficiency and the effectiveness of the heat exchanger.

5.3.3 Biomass Quantity Estimation

Computation for the estimation of biomass fuel quantity that would be need to supply thermal energy to drive the refrigeration system was carried out on a user friendly software based on the following input parameters for some biomass fuels. Table 5.1 shows the fixed and variable parameters used in combination with the equations set out in the previous section. The results and analyses are contained in the chapter 'Results and Discussions'.

Table 5.1 Parameters for estimating biomass fuel

Fixed & Variable Input				
Input	Type	Description	Magnitude	Unit
T_{c0}	Temperature	Generator Inlet temperature from boiler heat exchanger	100	°C
T_{c1}	Temperature	Generator Outlet temperature to boiler heat exchanger	40	°C
T_{h1}	Temperature	Heat exchanger inlet temperature from boiler unit	120	°C
T_{h0}	Temperature	Heat exchanger outlet temperature to boiler unit	90	°C
C_c	Thermal capacity	Specific heat capacity for cold water	4.2	$kJ/kg K$
C_h	Thermal capacity	Specific heat capacity for hot water	4.2	$kJ/kg K$
Woodchips (30% MC)	Fuel	Average energy density	3000	kJ/Tonne
Wood pellets	Fuel	Average energy density	5000	kJ/Tonne
Log Wood (staked-air dried; 20% MC)	Fuel	Average energy density	4200	kJ/Tonne
Wood	Fuel	Average energy density	5400	kJ/Tonne
Miscanthus (bale)	Fuel	Average energy density	4700	kJ/Tonne
\dot{m}_h	Mass flow rate	Mass flow rate of hot water	variable	kg/s
\dot{m}_c	Mass flow rate	Mass flow rate of cold water	variable	kg/s
FLHE	Time	duration of system operation	variable	hours
v_B	Ratio	Boiler efficiency	percentage	

5.4 Feasibility of Nigeria's Reliance on Biomass

In Nigeria with a population of about 180 million, the proportion of the population with access to electricity is less than 60% as at 2017 [205, 206]. The potential of biomass to sustainably improve Nigeria's energy consumption through the improvement of the energy situation in the rural communities is investigated.

Biomass, as a major source of energy, accounts for about 80% of the primary energy consumed in Nigeria; however, the application has been mainly traditional.

The potential energy recoverable from fuelwood, agro-waste, sawdust and municipal solid waste is estimated as 7,104,333,000 MJ [169]. Aquatic biomass and grasses, both of which are available, hold substantial prospect in the production of energy [36], [108]. But access to clean energy is still a challenge as Currently, biomass like other renewable resources in Nigeria, contribute very little to the energy mix [11, 174]. In 2010 the demand for energy in the industrial, transport, service and household sectors amounted to 58.87 (mtoe) based on 10% GDP growth rate. A demand of about 251 (mtoe) is predicted by 2030 [18].

In 2016, the gross energy supply by source in Nigeria was 136 mtoe. Biomass accounted for about 84% [82]. Ironically, it is richly distributed in the rural areas and provide energy as open fires for cooking and heating. This form of usage is inefficient and unsustainable. The unreadiness, unavailability and/or insufficient biomass to energy conversion technologies on a large scale, may have contributed to the sustenance of this form of usage. Some biomass to energy projects are currently in place, but mostly in the area of bio-ethanol production [146]. The investigation employs secondary data and time series analysis on a select biomass species to assess the potential contribution to clean and efficient energy access and utilisation in the country. The biomass-select criteria is based on:

- Potential available quantity
- Possible feedstock for direct combustion and/or thermochemical conversion processes and technologies.

5.4.1 Biomass Energy Potential

The energy potential of the biomass fuel is estimated from available data [147, 32, 68, 13]. Time-series analysis ANOVA model and linear regression was performed to predict the production of species in the near-future and to estimate lost or non-existing data based on the trend. Equations (5.18) to (5.22) were used to obtain the energy potential of the species. The total potential energy, $E_T(PJ)$ is obtained by the summation of the annual energy potential ϵ_p . This is a function of the calorific value and annual rate of generation/production as shown

below. A loss factor 2% of the energy content is set across all species. Tables 5.3 and 5.4 shows the annual production of some energy crops and forest biomass between 2009 and 2017, and between 1990 and 2010, respectively.

$$E_T = \sum \varepsilon_{pi} \quad (5.18)$$

$$\varepsilon_{pi} = h_{va} * \gamma_i \quad (5.19)$$

$$\gamma = r_{dp} * p_{ai} \quad (5.20)$$

$$h_{va} = \psi * h_v \quad (5.21)$$

Where:

E_T – total annual energy potential of all species

ε_{pi} – annual energy potential of species i

γ – annual feedstock or feedstock generation

p_{ai} – annual crop production

r_{dp} – ratio of feedstock to crop production

ψ – lost factor

h_v – calorific value

h_{va} – adjusted calorific value

A correlation for the estimation of the high heating value is given by reference [144]:

$$h_v = \mu_1 - \mu_2 * \frac{VM}{FC} + \mu_3 * \left(\frac{VM}{FC}\right)^2 - \mu_4 * \frac{ASH}{VM} + \mu_5 * \left(\frac{ASH}{VM}\right)^2 - \mu_6 * \left(\frac{ASH}{VM}\right)^3 + \mu_7 * \left(\frac{ASH}{VM}\right)^4 + \mu_8 * \frac{ASH}{VM} \quad (5.22)$$

Where

μ_i – coefficients

FC – fixed carbon content

ASH – Ash content

The coefficient μ_i is given in Table 5.2.

Table 5.2 μ_i values for equation (5.22)

i	μ
1	20.7999
2	0.3214
3	0.0051
4	11.2277
5	4.4953
6	0.7223
7	0.0383
8	0.0076

To estimate, for example, the total annual energy available from cassava, the crop thermal characteristics such as the volatile matter (VM), fixed carbon content (FC) and Ash content (ASH) are obtained. The data from Nhuchhen & Salam is used in this study [144]. They are given as $VM = 84.50$, $FC = 9.56$ and $ASH = 6.29$. The energy content h_v is obtained from the equation (5.22) as $17.57 MJ/kg$ and hence, h_{va} from equation (5.21) as $17.22 MJ/kg$. From Table 5.3, the annual production of cassava is $36.822 * 10^6$ ($tons$) and residue to crop ration rdp is 1.0835 which gives an annual feedstock generation of $39.896 * 10^6$ ($tons$). The energy potential is obtained from equation (5.19) as $70.10 PJ$. This procedure is carried out for each species to obtain its annual energy potential which is used in equation (5.18) to obtain the annual total for all species.

Table 5.3 Yearly production of some energy crops in Nigeria - excerpt from reference [68]

Crops (x1000 tons)	Year				
	2009	2011	2013	2015	2017
Cassava	36822	46190	40470	57643	59486
Coffee Green	2.040	2.525	2.100	1.979	1.556
Cotton lint	130.00	130.00	75.00	-	-
Cottonseed	225.00	175.00	130.00	-	-
Groundnut	2977.62	2962.63	2474.53	3467.45	2420.00
Maize	7358.26	8878.46	8422.67	10562.05	10420.00
Millet	4929.95	1271.37	909.56	1485.39	1500.00
Rice Paddy	3546.25	4612.61	4823.33	6256.23	9864.28
Sorghum	5279.17	5690.15	5300.27	7005.03	6939.00
Soybean	426.59	492.85	517.96	588.52	730.00
sugarcane	1401.68	755.81	1272.03	1449.96	1497.76
Taro (Cocoyam)	3033.34	3011.66	2932.53	3276.70	3250.86
Wheat	80.00	165.00	80.00	60.00	66.58

Table 5.4 Nigeria Forest and wood stock (courtesy: Global Forest Resources - Country Report, Nigeria [13])

Category	Forest Biomass (million metric tons)			
	1990	2000	2005	2010
Above-ground biomass	3459	2660	2261	1861
Below-ground biomass	830	638	543	447
Dead wood	601	462	392	323
Total	4890	3760	3196	2631

5.5 Summary

Two important properties, moisture content and calorific value, influencing the energy performance of a biomass solid fuel species were tested for five biomass samples. The measurement is useful in the determination of energy performance and fuel utilisation. A

mathematical model for the prediction of the quantity of biomass that will be needed for specified conditions of operation for an absorption refrigeration system such as proposed in this study was developed. This could serve as selection information tool. Lastly, the credibility of proposing biomass as a sustainable source of energy was explored in the investigation on the feasibility of Nigeria's reliance on biomass.

Chapter 6

Result and Discussion

6.1 Introduction

The analyses of the simulations and experimental work carried out in this study will be presented in this chapter. The simulation results from the models developed and those from the empirical tests will be discussed. A sample computation of the aqua-ammonia absorption refrigeration cycle will be manually performed to further ascertain the validity of the model. The computation procedure and the parameters will be shown and the results will be compared with the results obtained from the computer model. This will precede the validation of the model by comparison with experimental and theoretical data from the literature. The moisture content and calorific value of biomass species are two important factors with significant impact on the energy obtained from the solid fuel and the economic value. The results of laboratory experiment conducted on some biomass species in the study will be presented and discussed. The feasibility of Nigeria's reliance on Biomass will be analysed and discussed as well as other system considerations affecting biomass refrigeration potential and influencing the uptake of biomass solid fuels and absorption refrigeration systems.

(The number of experiments and tests in this work were constrained by weather conditions, breakdown of the refrigeration system and the equipment and laboratory becoming unavailable due to the relocation of the campus from Stafford to Stoke-On-Trent. It was no longer possible to carry out further experiments and tests. Consequently, the reported experiments and tests are those that were repeated and for which the results are reliable.)

6.2 TCA – Results and Analyses

A mathematical model was developed to investigate, predict the performance of the TCA, and the optimisation feasibilities of the system. An experiment was designed and carried out to evaluate the effect of the cooling load, the cooling demand and the ambient conditions on the air-condition circuit. The suitability of the system for rural communities, based on the considerations of operation, maintenance and cost vis-à-vis the availability and/or accessibility of human and material resources, was also examined. The results and analyses are presented in this section.

6.2.1 Results - Modelling

The system parameters used for the model and simulation were those defined by ClimateWell - Product Information Manual' Bales [24].

At a flow rate of 0.25 kg/s of the condenser, ambient temperature of 22 °C and inlet temperature of 30 °C to the reactor (at discharging for cooling), the simulation results gives an energy to the condenser circuit (Q_S) of 48.1 kWh and 28.9 kWh from the air-conditioning circuit (Q_{ac}) The system's average coefficient of performance for cooling is calculated from heat source circuit and the air-condition circuit (equation (4.45)). Table 6.1 is a comparison of the COP obtained from the simulation with reference [22]. The manufacturer stated COP 0.68, but varies between 0.52 and 0.57 on installed systems [145]. Heat losses and pressure drops may affect the system energy flow and could lead to reduced performance. As cooling load varies with energy demand, depending on the designed capacity of the system, the performance may drop below designed level. The present estimate is both close to experimental and published data.

Figs. 6.1 - 6.4 show how the rate at which cooling vary with evaporator inlet temperature, for a fixed power and inlet temperature to the reactor (during discharge for cooling). The data shows a similar trend compared with reference [24]. The increase in the cooling load would require greater cooling power to maintain the set cooling temperature within the system designed cooling power. Normally the system will deliver the set cooling or heating power, but will increase power with demand to the designed limit.

In Figs. 6.5 and 6.6 , the cooling capacity is shown to vary with the cooling load for a given reactor heat exchanger inlet temperature (during discharge for cooling). From both cases, it could be seen that the rate at which cooling is obtained for a set cooling temperature would be influenced by the reactor inlet temperature.

Table 6.1 Comparison of COP and Cooling Power

Work	COP_{cool}	$Q_{ac}(kWh)$	$Q_s(kWh)$
Present	0.6008	28.9	48.1
Bales & Ayadi [22]	0.6025	28.2	48.1
Error (%)	0.28	-2.48	-2.77

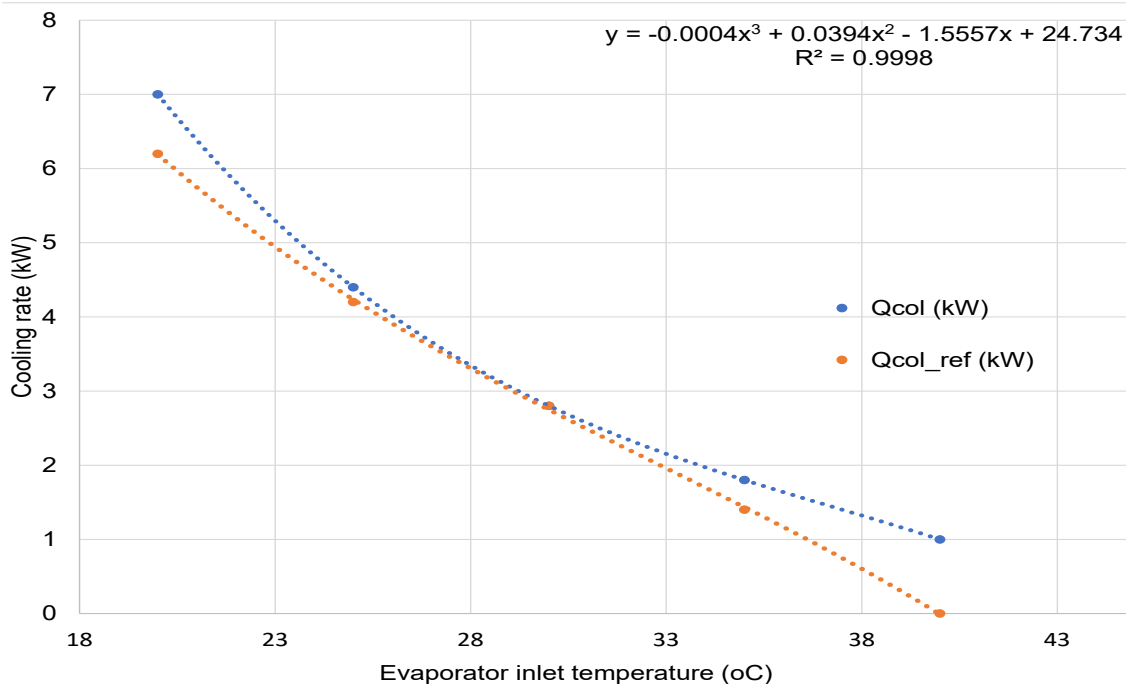


Fig. 6.1 Variation of cooling rate with evaporator inlet temperature at 7 kW discharge power for cooling

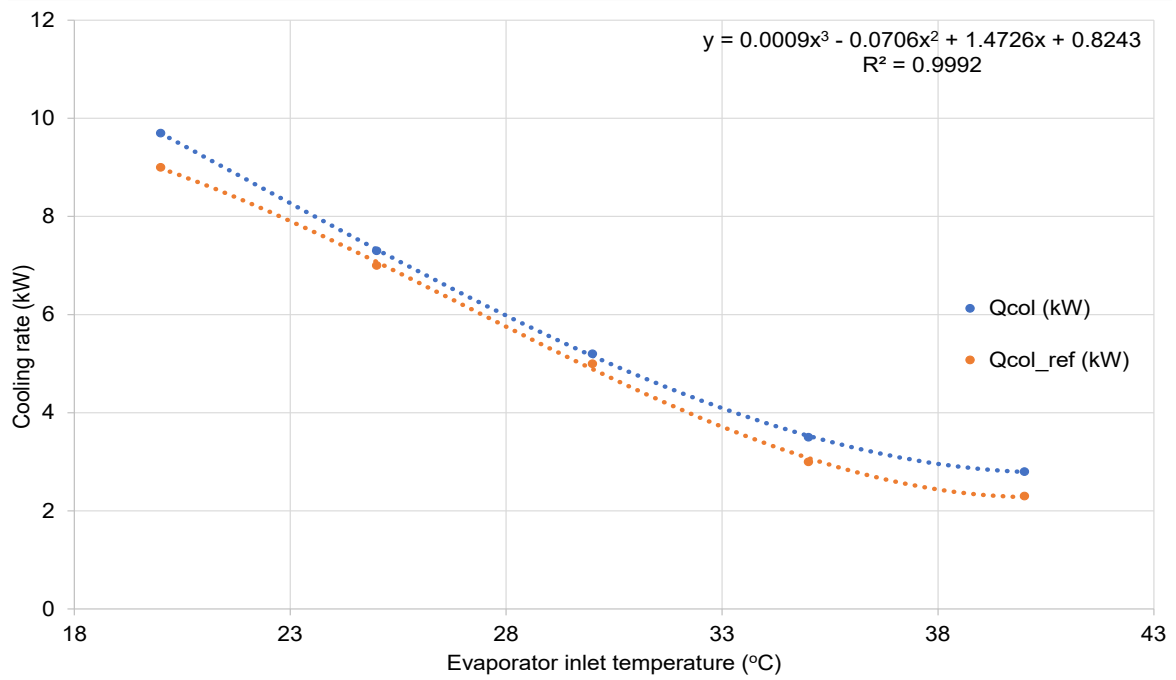


Fig. 6.2 Variation of cooling rate with evaporator inlet temperature at 12 kW discharge power for cooling

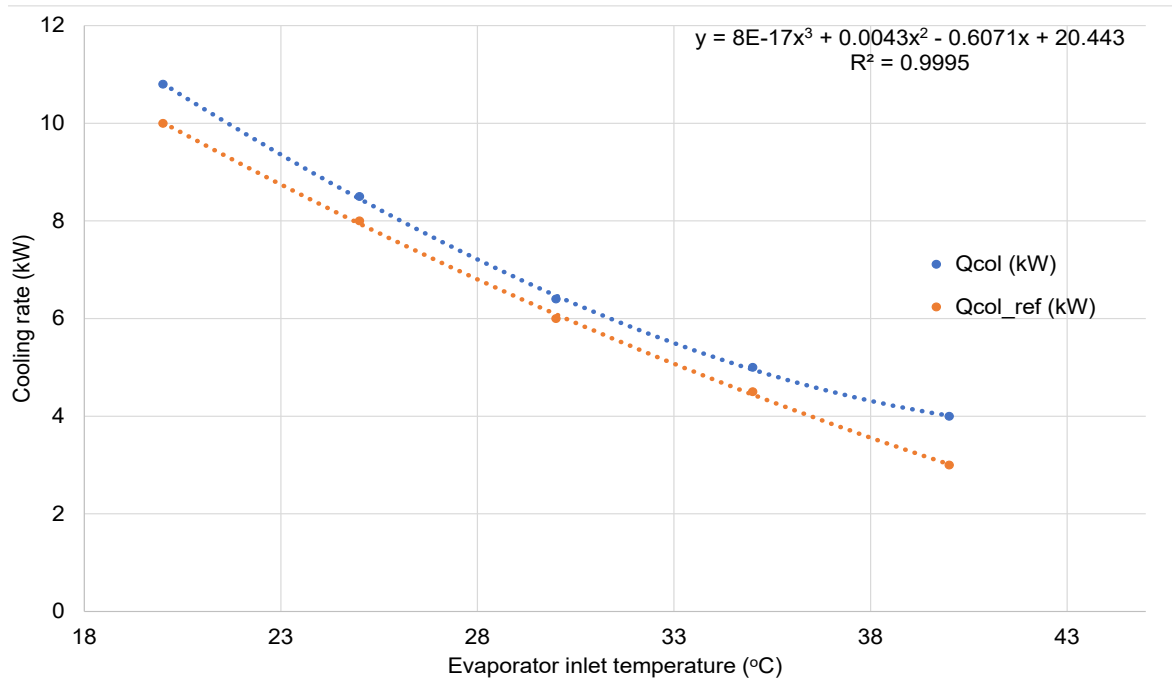


Fig. 6.3 Variation of cooling rate with evaporator inlet temperature at 15 kW discharge power for cooling

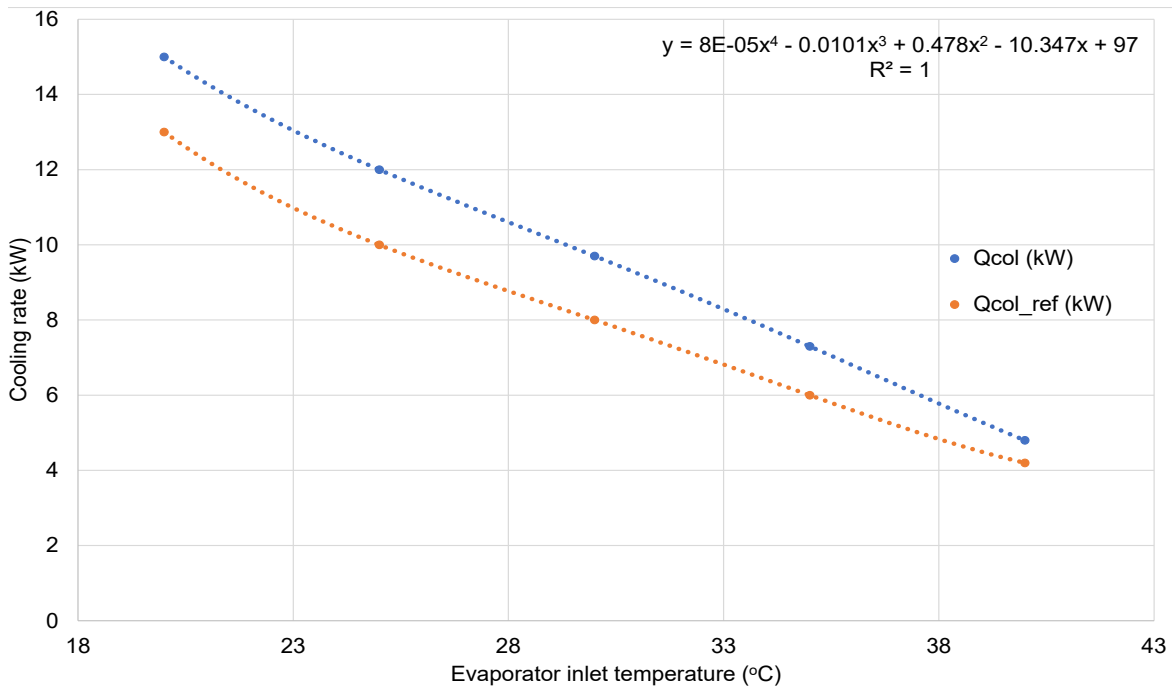


Fig. 6.4 Variation of cooling rate with evaporator inlet temperature at 18 kW discharge power for cooling

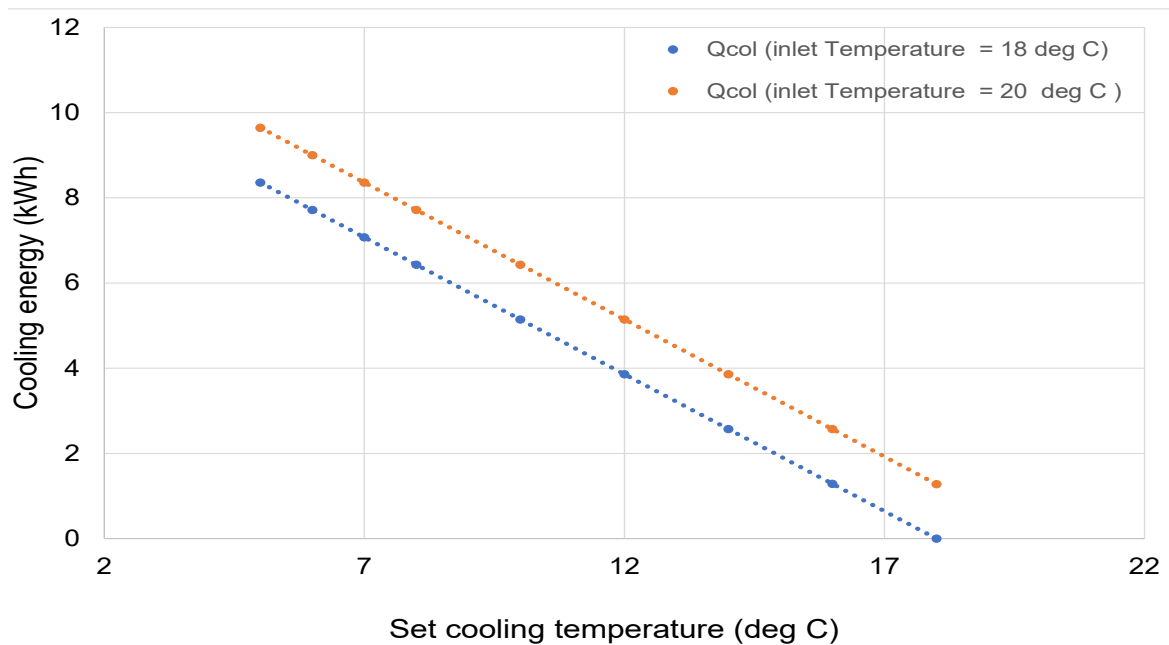


Fig. 6.5 Variation of cooling energy with set cooling temperature at 18 & 20 °C inlet temperature

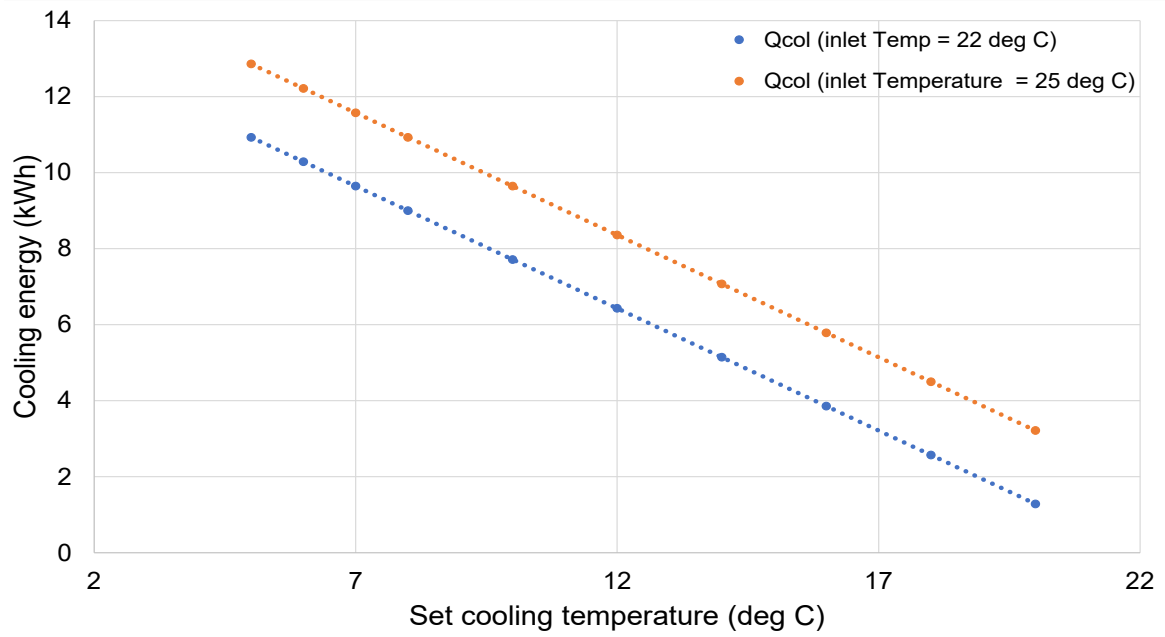


Fig. 6.6 Variation of cooling energy with set cooling temperature at 22 & 25 °C inlet temperature

6.2.2 Results - Experimental

In line with the experimental plan, 60 tests were carried out in 6 experiments. The extracted data for analyses are presented in Tables 6.2 – 6.7. The evaporator inlet temperature was varied from 18 °C, 20 °C, 22 °C, 25 °C, 30 °C and 35 °C for the respective experiment, while the set cooling temperature was varied from 5 °C - 20 °C. The flow rate and the source heat temperature from the boiler were kept constant throughout the experiment.

The result shows that for a set ambient temperature and load (simulated by the inlet temperature), the heavy cooling demand (low cooling temperature) requires higher cooling energy. This relationship was observed throughout the experiments (Figs 6.7 - 6.12).

The effect of the ambient temperature is also observed. The system reacts sharply to the ambient conditions. It tends to increase energy demand to overcome the temperature gradient contributed by the external environmental conditions. However, this effect can be overridden by high inlet temperatures. This is the case shown in Fig. 6.12 where the ambient temperature was very low but the high inlet temperature is responsible for the high cooling energy. Fig. 6.13 shows the effect of the set inlet temperature on the cooling energy.

Table 6.2 TCA experiment 1

Experiment (1)					
S/N	T_{cxiset} (°C)	T_{cxoset} (°C)	T_{amb} (°C)	M_{cx} (kg/min)	Q_{cv} (kW)
1	18	5	25	17.1	8.3
2	18	6	25	17.1	7.72
3	18	7	25	17.1	7.07
4	18	8	25	17.1	6.43
5	18	10	25	17.1	5.14
6	18	12	25	17.1	3.86
7	18	14	25	17.1	2.57
8	18	16	25	17.1	1.29
9	18	18	25	17.1	0.00
10	18	20	25	17.1	-1.29

Table 6.3 TCA experiment 2

Experiment (2)					
S/N	T_{cxiset} (°C)	T_{cxoset} (°C)	T_{amb} (°C)	M_{cx} (kg/min)	Q_{cv} (kW)
1	20	5	25	17.1	9.6
2	20	6	25	17.1	9.00
3	20	7	25	17.1	8.36
4	20	8	25	17.1	7.72
5	20	10	25	17.1	6.43
6	20	12	25	17.1	5.14
7	20	14	25	17.1	3.86
8	20	16	25	17.1	2.57
9	20	18	25	17.1	1.28
10	20	20	25	17.1	0.00

Table 6.4 TCA experiment 3

Experiment (3)					
S/N	T_{cxiset} (°C)	T_{cxoset} (°C)	T_{amb} (°C)	M_{cx} (kg/min)	Q_{cv} (kW)
1	22	5	25	17.1	10.93
2	22	6	25	17.1	10.29
3	22	7	25	17.1	9.65
4	22	8	25	17.1	9.00
5	22	10	25	17.1	7.72
6	22	12	25	17.1	6.43
7	22	14	25	17.1	5.14
8	22	16	25	17.1	3.86
9	22	18	25	17.1	2.57
10	22	20	25	17.1	1.29

Table 6.5 TCA experiment 4

Experiment (4)					
S/N	T_{cxiset} (°C)	T_{cxoset} (°C)	T_{amb} (°C)	M_{cx} (kg/min)	Q_{cv} (kW)
1	25	5	25	17.1	12.86
2	25	6	25	17.1	12.22
3	25	7	25	17.1	11.57
4	25	8	25	17.1	10.93
5	25	10	25	17.1	9.65
6	25	12	25	17.1	8.36
7	25	14	25	17.1	7.07
8	25	16	25	17.1	5.79
9	25	18	25	17.1	4.50
10	25	20	25	17.1	3.22

Table 6.6 TCA experiment 5

Experiment (5)					
S/N	T_{cxiset} (°C)	T_{cxoset} (°C)	T_{amb} (°C)	M_{cx} (kg/min)	Q_{cv} (kW)
1	30	5	10	17.1	16.07
2	30	6	10	17.1	15.43
3	30	7	10	17.1	14.79
4	30	8	10	17.1	14.14
5	30	10	10	17.1	12.86
6	30	12	10	17.1	11.57
7	30	14	10	17.1	10.29
8	30	16	10	17.1	09.00
9	30	18	10	17.1	07.71
10	30	20	10	17.1	06.43

Table 6.7 TCA experiment 6

Experiment (6)					
S/N	T_{cxiset} (°C)	T_{cxoset} (°C)	T_{amb} (°C)	M_{cx} (kg/min)	Q_{cv} (kW)
1	35	5	10	17.1	19.29
2	35	6	10	17.1	18.65
3	35	7	10	17.1	18.00
4	35	8	10	17.1	17.36
5	35	10	10	17.1	16.07
6	35	12	10	17.1	14.79
7	35	14	10	17.1	13.50
8	35	16	10	17.1	12.22
9	35	18	10	17.1	10.93
10	35	20	10	17.1	09.64

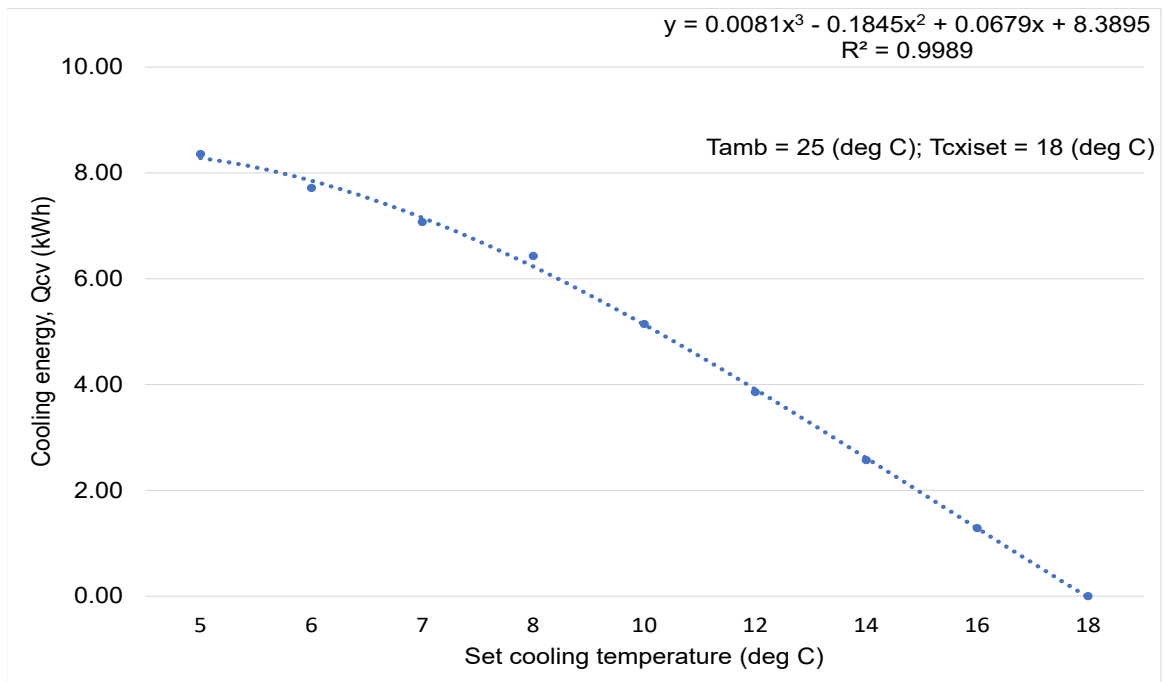


Fig. 6.7 Variation of cooling energy set cooling temperature (Exp1)

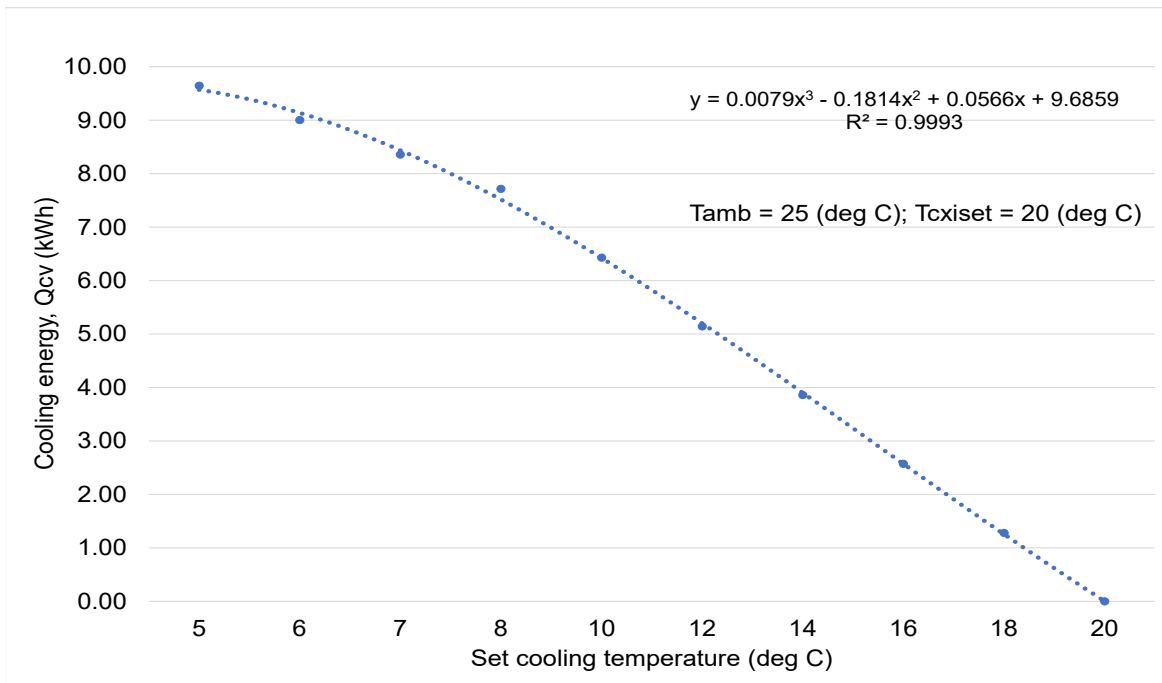


Fig. 6.8 Variation of cooling energy set cooling temperature (Exp2)

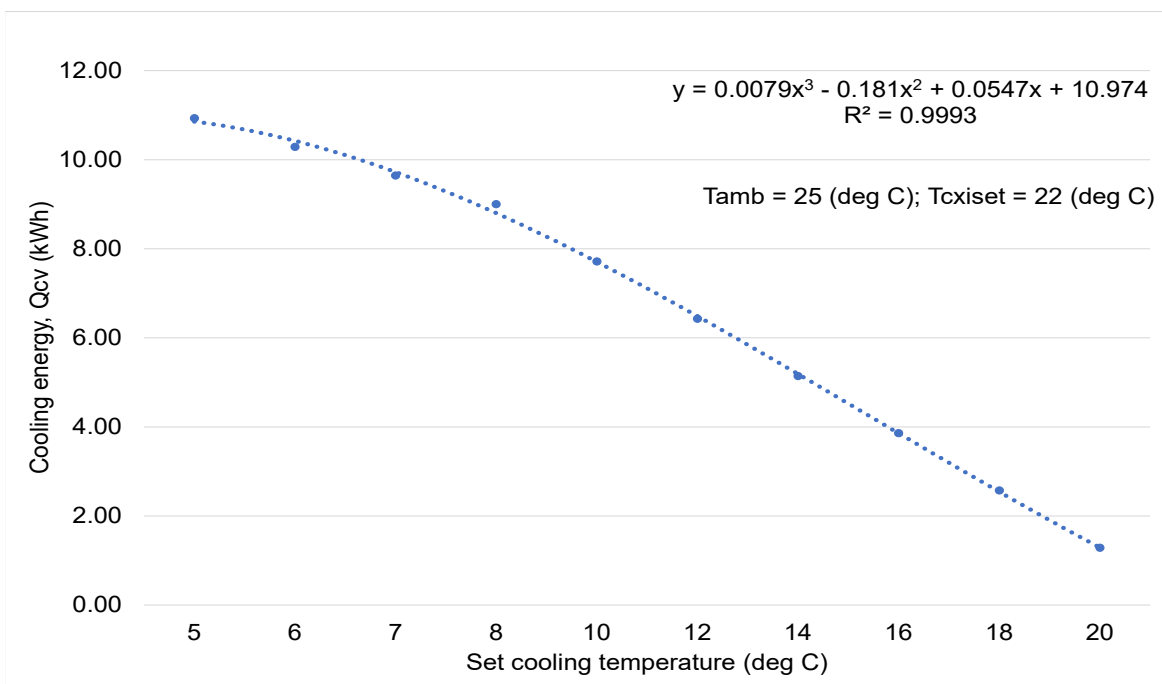


Fig. 6.9 Variation of cooling energy set cooling temperature (Exp3)

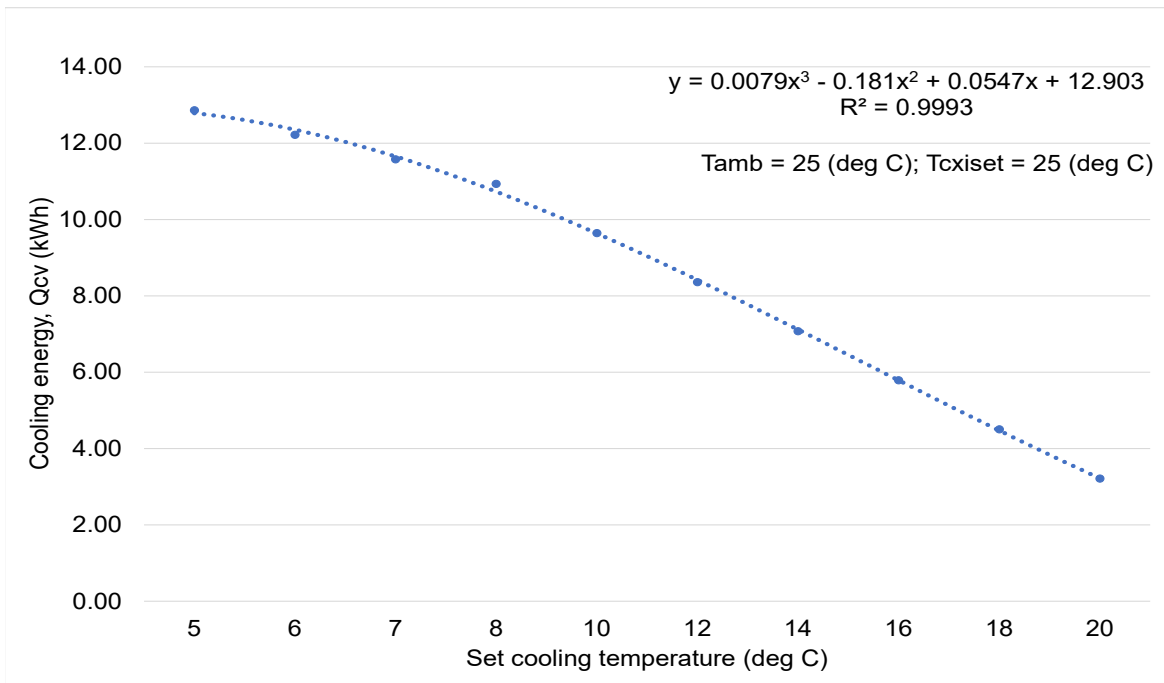


Fig. 6.10 Variation of cooling energy set cooling temperature (Exp4)

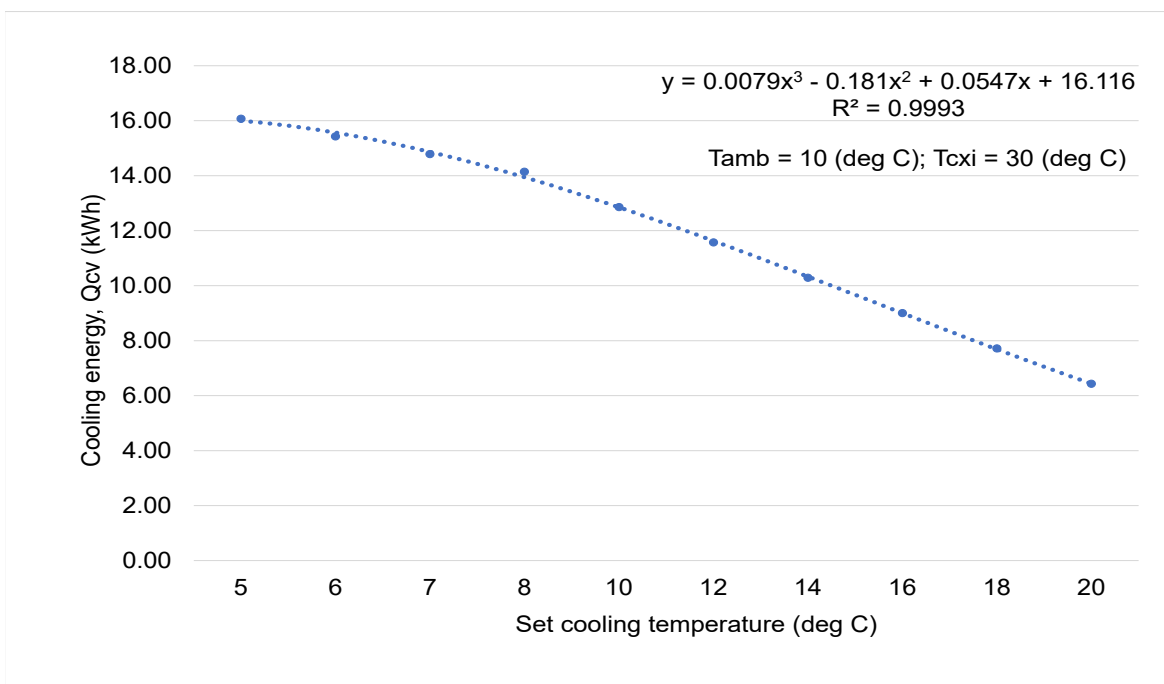


Fig. 6.11 Variation of cooling energy set cooling temperature (Exp5)

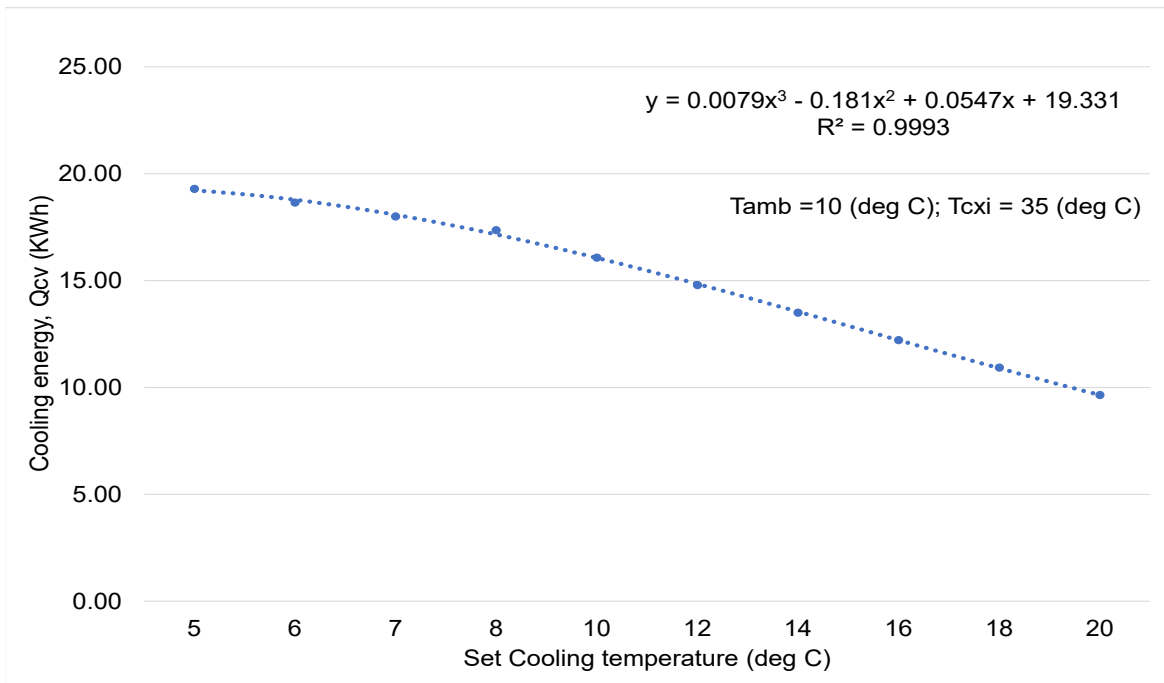


Fig. 6.12 Variation of cooling energy set cooling temperature (Exp6)

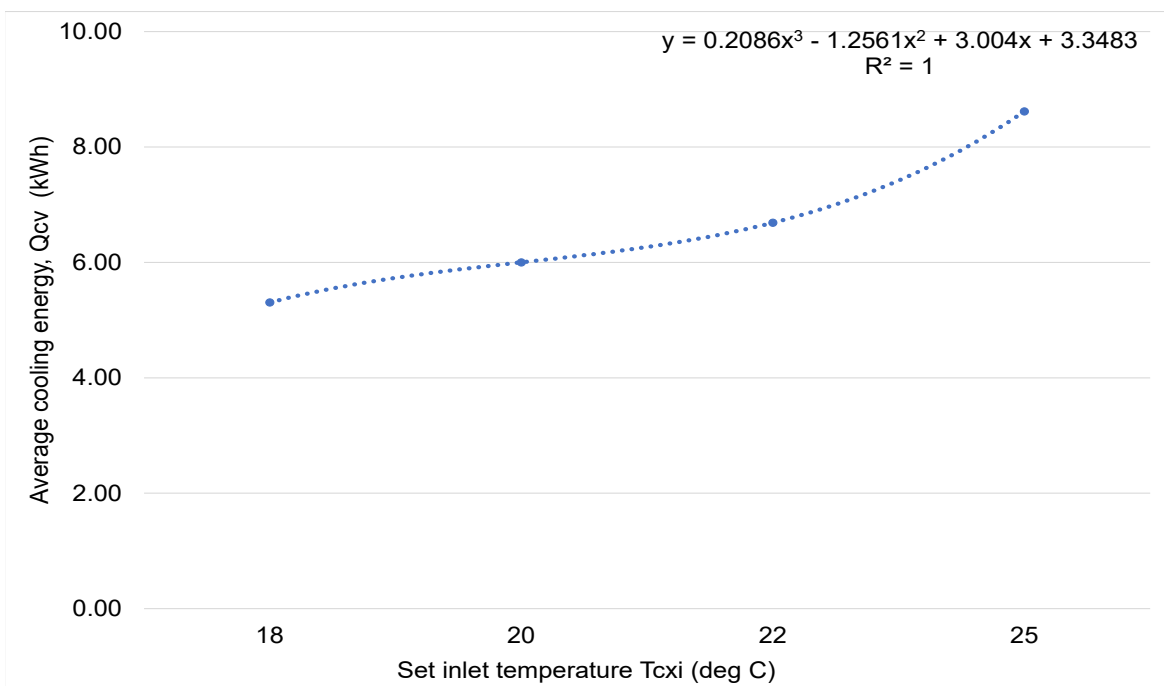


Fig. 6.13 Variation of cooling energy set cooling temperature (Exp1)

6.3 Aqua-Ammonia VARC - Model Validation

The tests for the validation of the aqua-ammonia is presented in this section. Firstly, results from a sample calculation of the system parameters from given state-point conditions are manually calculated and compared with those computed using the mathematical model for the specified conditions and parameters of the system. The output parameters are calculated from the input.

6.3.1 Sample Calculation Compared with Simulation

A sample computation was manually performed for an aqua-ammonia absorption refrigeration cycle operating on the state points conditions as shown in Table 6.8 and compared with that from the computer model. The mass flow rate through the evaporator and those for the weak and strong solutions for a 1 *TR* (refrigerant ton) cooling capacity were determined. The heat transfer rates through the absorber, generator and condenser were determined and finally, the system's COP was also computed. A comparison of both computations were made. The calculation is based on the assumption that:

- The state points are based on Fig. 4.8
- At state points the solution is either saturated vapour or liquid
- No heat loss
- Fluid is incompressible
- No pressure drop across components

Table 6.8 Operating condition

State Point	Pressure (bar)	Temperature (°C)
1	1.75	25
3	13.5	100
7	13.5	100
8	13.5	40
10	1.75	0

6.3.2 Manual Solution Procedure

It is assumed that the evaporator pressure p_e is same as the absorber pressure p_a and the generator pressure p_g is same as the condenser pressure p_c . That is,

$$p_e = p_a = p_1$$

$$p_g = p_c = p_8$$

State 1 (absorber exit): from $h-x$ diagram, at 1.5 bar and 25 °C, $x_1 = 0.393$ and $h_1 = -115$ kJ/kg.

States 3 and 7: In the generator boiling occurs resulting in liquid-vapour equilibrium. Consequently, state 3 is saturated liquid and state 7 is saturated vapour. State 3 coincides with the isobar 13.5 bar and 100 °C in the liquid region.

$$x_3 = 0.37 \text{ and } h_3 = 220.0 \text{ kJ/kg; } x_7 = 0.94 \text{ and } h_7 = 1530 \text{ kJ/kg.}$$

State 8: In the condenser the concentration of ammonia does not change, and remains the same through the expansion valve and the evaporator, as no mass of water or ammonia is added in these components.

Therefore, $x_8 = x_9 = \text{constant}$. $x_8 = 0.94$, $h_8 = h_9 = 125.0$ kJ/kg and $t_8 = 40$ °C.

x_{10} is worked from table as 0.995 and $h_{10} = 1460$ kJ/kg

The mass and energy rate of flow are obtained from the refrigeration capacity information, mass and energy conservation equations and energy balance (equations (4.48) - (4.58)) as follows:

Cooling capacity ($Q_e = 1TR = 3.5167$ kW).

From equation (4.58), refrigerant mass flow rate,

$$\begin{aligned} \dot{m}_{10} &= 3.5167 / (h_{10} - h_8) \\ &= 3.5167 / (1460 - 125) \\ &= 2.6342 * 10^{-3} \text{ kg/s} \end{aligned}$$

The mass flow rates of the weak and strong solutions are obtained from equations (4.48) - (4.52).

$$\begin{aligned} \dot{m}_6 &= \dot{m}_{10}(x_{10} - x_1) / (x_1 - x_6) \\ &= 2.634 * 10^{-3} * (0.94 - 0.393) / (0.393 - 0.37) \\ &= 6.26433 * 10^{-2} \text{ kg/s} \end{aligned}$$

Similarly, $\dot{m}_1 = 6.52825 * 10^{-2}$ kg/s.

The energy balance equation is used to calculate the energy rate of flow due to the components, and the performance ratio.

$$Q_A = 11.3534 \text{ kW}$$

$$Q_C = 3.70106 \text{ kW}$$

$$Q_G = 11.5378 \text{ kW}$$

$$Q_E = 3.5167 \text{ kW}$$

$$\text{COP} = Q_E/Q_G = 3.5167/11.5378 = 0.3048$$

6.3.3 Results of sample calculation from model

Inputs

Evaporator temperature (T_e) °C

Absorber temperature (T_a) °C

Condenser temperature (T_c) °C

Generator temperature (T_g) °C

Refrigeration capacity – 3.1567 kW – (set to zero when information is not available)

Refrigerant mass flow rate kg/s – (set to zero when information is not available)

Outputs

Saturation pressure at condenser (pc) MPa Saturation pressure at the evaporator (pe) MPa

Refrigerant mass flow rate (mR) – (\dot{m}_{10})

Mass flow rate of Weak solution (mw) – (\dot{m}_6)

Mass flow rate of strong solution (ms) – (\dot{m}_1)

NH_3 mass fraction of weak solution (X4) – kg/kg of solution

NH_3 mass fraction of strong solution (X1) – kg/kg of solution

Absorber energy rate of flow (Qa)

Condenser energy rate of flow (Qc)

Generator energy rate of flow (Qg)

Evaporator energy rate of flow (Qe)

Table 6.9 Comparison of results

Parameter	Unit	Manual result	Model result	% difference
Evaporator pressure (pe)	bar	1.75	1.743	0.40
Condenser pressure (pc)	bar	13.5	13.69	1.398
Mass fraction (Xs)	(-)	0.393	0.390	0.766
Mass fraction (Xw)	(-)	0.37	0.367	0.814
mass flow rate - refrigerant (Mr)	kg/s	0.0026342	0.0026544	0.764
mass flow rate - weak solution (Mw)	kg/s	0.0626483	0.062375	0.437
mass flow rate - weak solution (Ms)	kg/s	0.0652825	0.0649421	0.523
Generator energy rate of flow (Qg)	kW	11.5378	11.4854	0.455
Absorber energy rate of flow (Qa)	kW	11.3534	11.211	1.262
Generator energy rate of flow (Qc)	kW	3.70106	3.6538	1.285
Evaporator energy rate of flow (Qe)	kW	3.5167	3.5167	0.000
Performance ratio (COP)	(-)	0.3048	0.3062	0.455

6.4 Model Validation

The single stage aqua-ammonia refrigeration system proposed, to provide cooling, in the preceding section is validated in this section. The outputs and performance ratio are compared with theoretical and empirical data from the literature to ascertain the efficacy of the system and reliability of the output data as well as the predictions from the system. Therefore, relevant data with respect to the outputs of the proposed model are extracted from the literature. The opted outputs for the validation are those closely related to the parametric and overall system optimisation.

The validation procedure is carried as follows:

- Examine and selection of data
- Examine system conditions/parameters that apply to the data generation.
- Simulate the conditions/parameter in current work. Therefore, the comparison was not grouped based on the measured parameters but on related individual work.
- Compare results

The output parameters are:

- Coefficient of performance
- Energy rate of flow due to the evaporator and/or evaporator temperature
- Energy rate of flow due to the generator and/or generator temperature

- Energy rate of flow due to the absorber and/or absorber temperature
- Energy rate of flow due to the condenser and/or condenser temperature

The validation process is split in to two categories - experimental and theoretical categories. The former being the major.

6.4.1 Comparison with empirical results and analysis

The comparison relies on the published experimental data and the specified parametric conditions by which the results were obtained. The defined conditions are used as input variable and/or fixed parameters in the current work. Where information are unclear or lost, assumptions are made and iterated to match the data set. For example, where information about the refrigeration capacity is not found, a refrigeration capacity of 1 *TR* is initially assumed. This could be further readjusted to closely match data.

A. Comparison with Du et. al [58].

The experiment was carried using a prototype absorption refrigeration system with ammonia and water - the refrigerant and absorbent, respectively. Waste heat from a diesel engine exhaust, with temperatures up to 500 °C, was the source of thermal energy driving the system. It is assumed that the quality of heat from the exhaust was less for an ammonia-water absorption refrigeration system. Consequently, a maximum temperature of 150 °C was used for the simulation. A comparison of the COP and cooling energy form the model and the experiment were made for varying cooling temperature.

Fig. 6.14 shows the variation of COP with evaporator temperature. At high evaporator temperature (low cooling demand) the COP is as expected for a constant generator energy and other parameters. The COP reduces as the cooling temperature falls well below 0 °C. This could also be the case if the cooling load is increased for a set cooling temperature. The simulated result showed good comparison with - but in most part of the simulation, slightly higher than - the experimental. A fluctuating difference was observed in the case of the cooling capacity. This significantly narrowed between 45 minutes and 150 minutes and diverged slight at the 165 minutes going forward. However, the trend is quite similar and the average difference was 8% (Fig. 6.15).

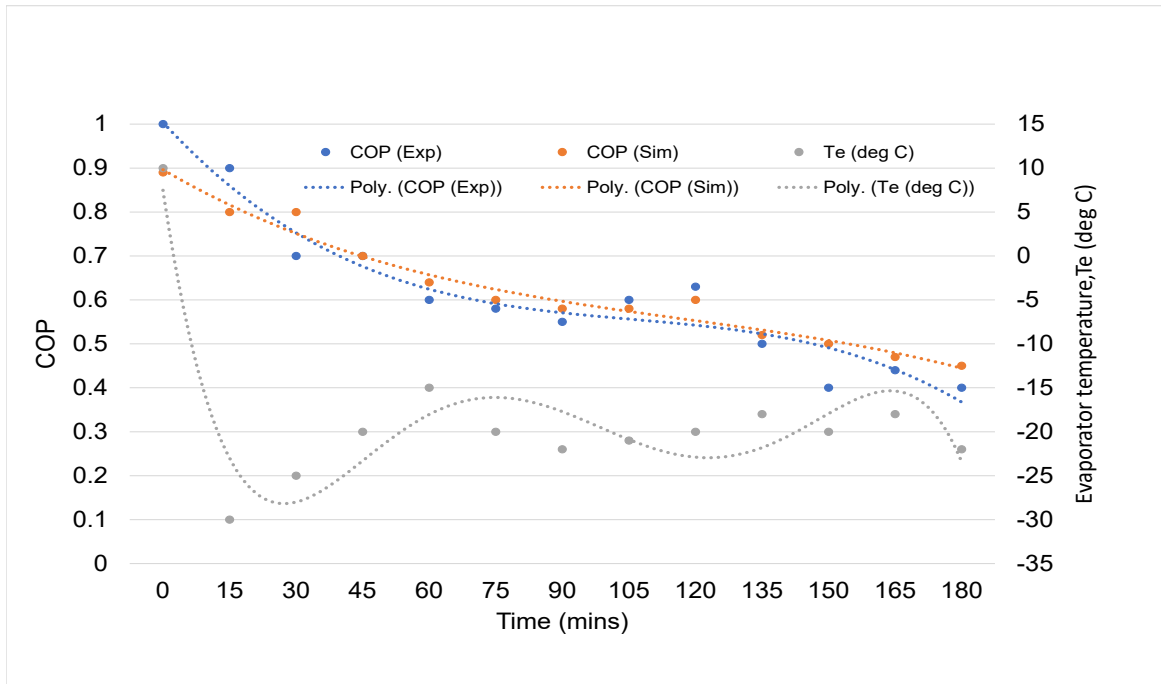


Fig. 6.14 Variation of COP with evaporator temperature

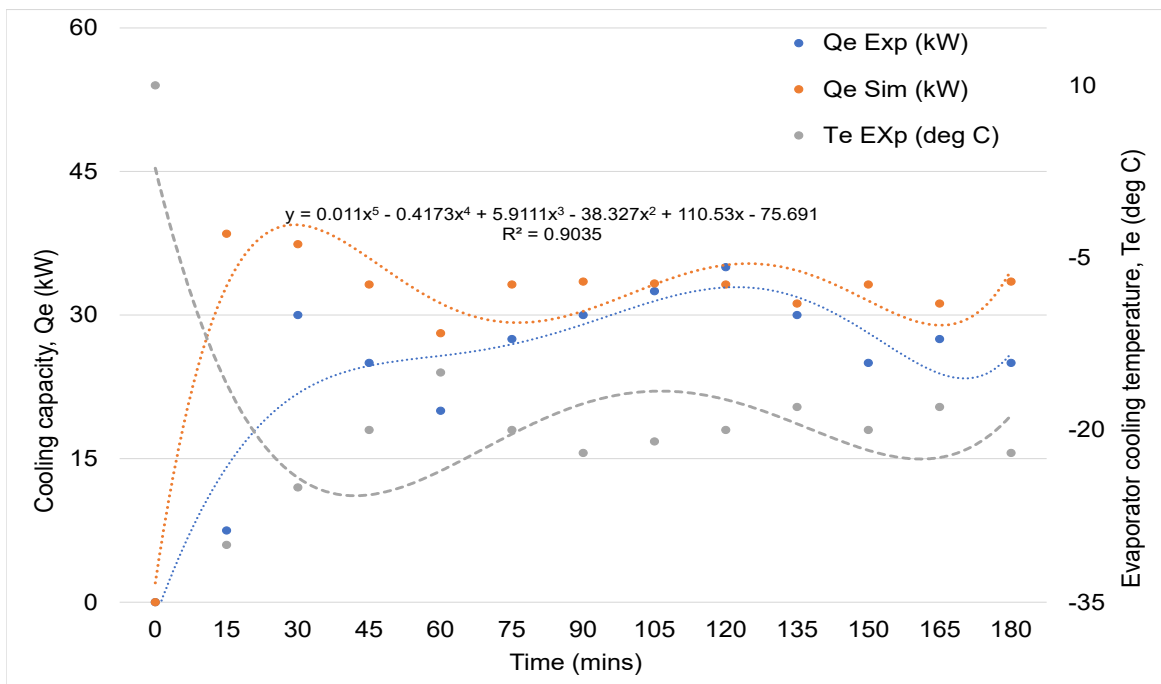


Fig. 6.15 Variation of Cooling capacity with evaporator temperature

B. Comparison with El-Shaarawi et. al. [64]

The COP and the heating capacities of the absorber, condenser and generator were compared. The system is 5 kW solar-driven ammonia-water absorption refrigeration cycle. The simulation time was 480 minutes and the generator temperature varied between 100 to 110 °C for a cooling temperature of -5 °C.

The simulated results showed a good comparison with the experimental. The COP and energy of the heat transfer components showed similar trends. The absorber, condenser, and generator heat capacities are closely matched with the model showing a slightly higher value of about 6% (Figs.6.16 - 6.18).

A wide difference was observed for the COP (Fig. 6.19). The simulated value was four times greater than the experimental. This may be due to assumptions and computing methods as well as sets of equation used by the model to arrive at a solution. In this case, the refrigerant mass flow and saturation pressures were automatically estimated by the model.

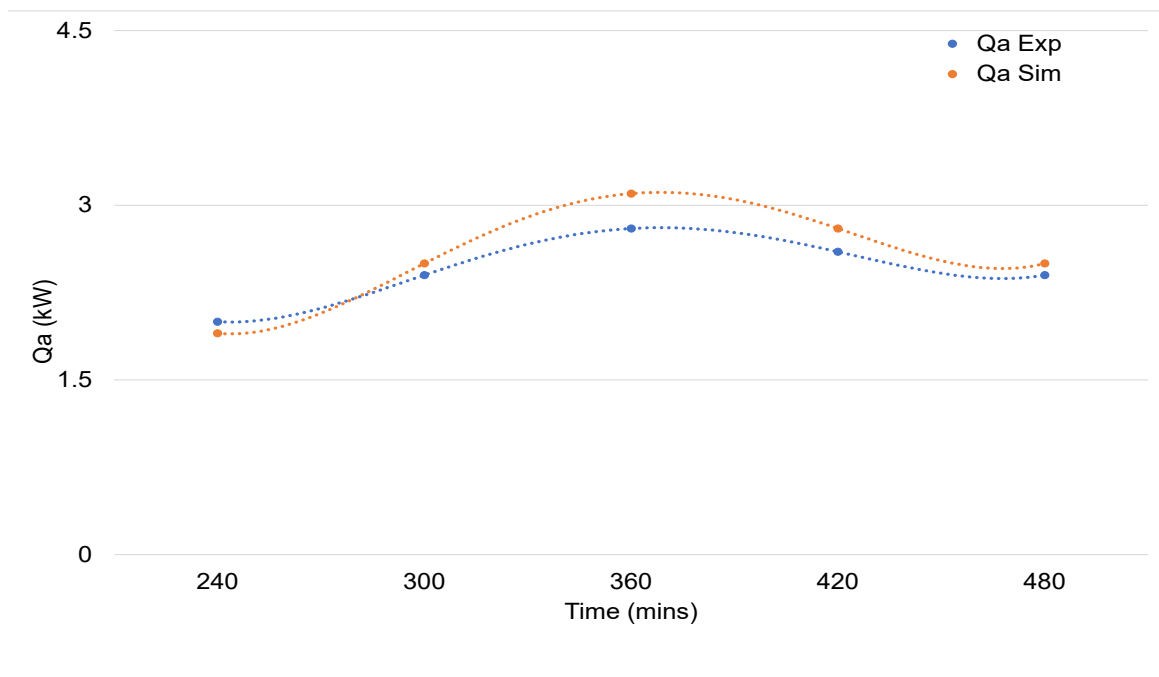


Fig. 6.16 Comparison of absorber heat capacity

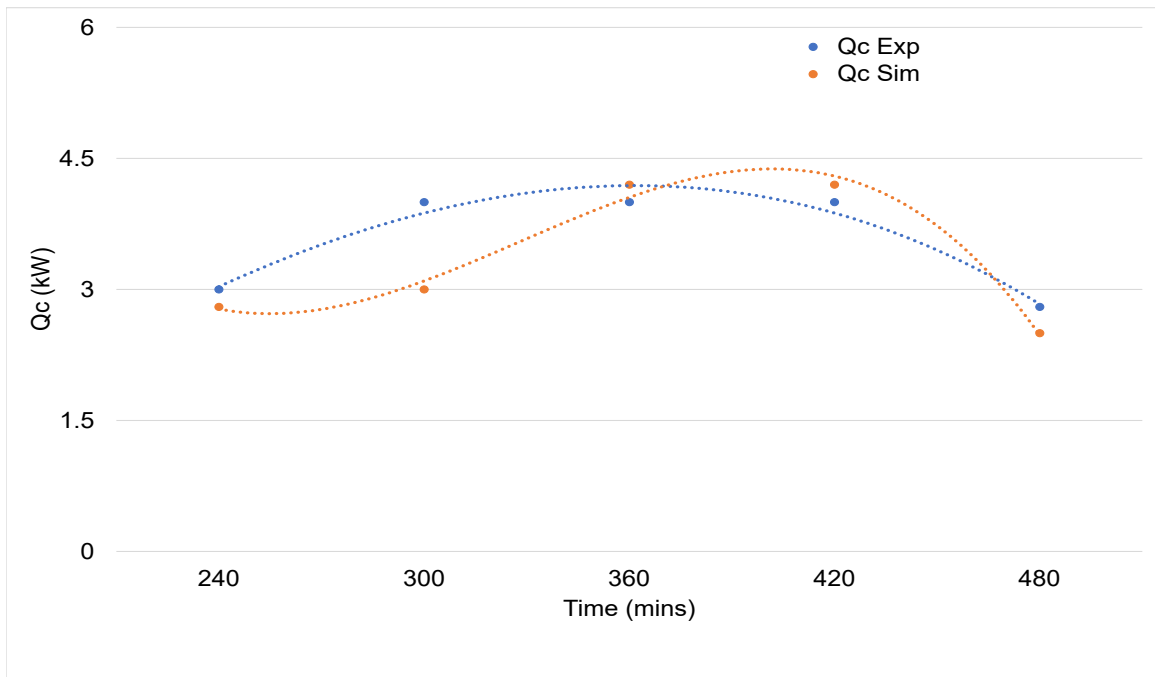


Fig. 6.17 Comparison of condenser heat capacity

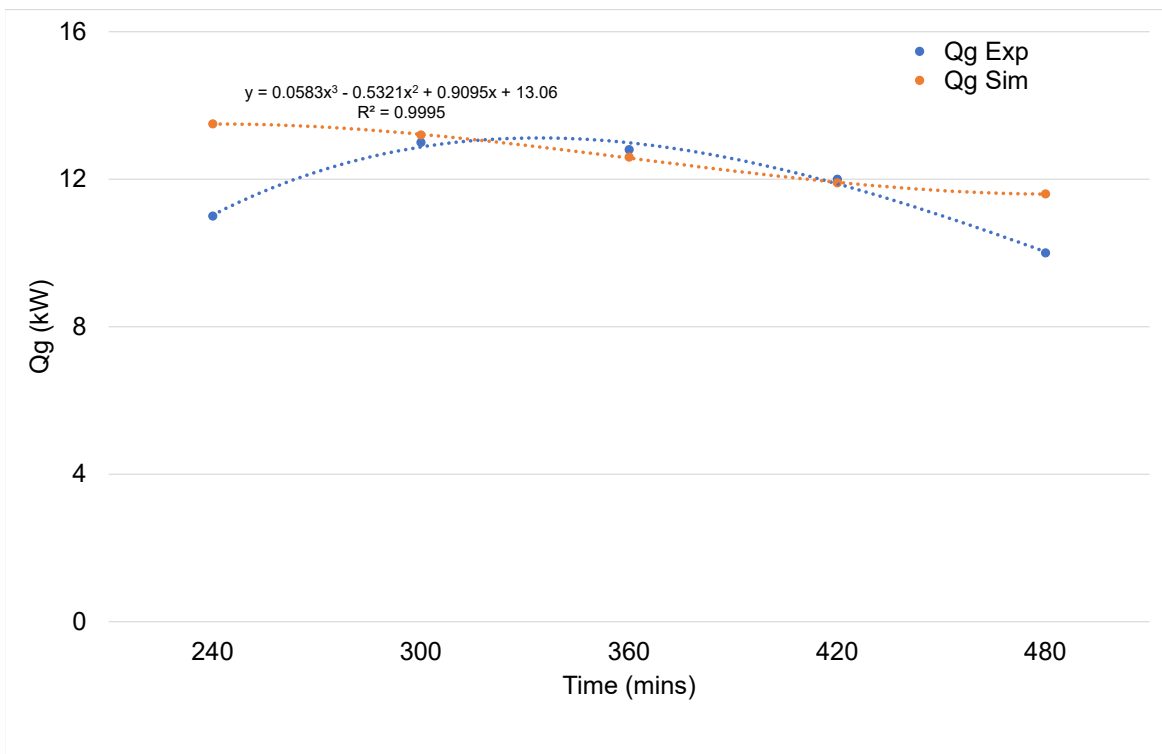


Fig. 6.18 Comparison of generator heat capacity

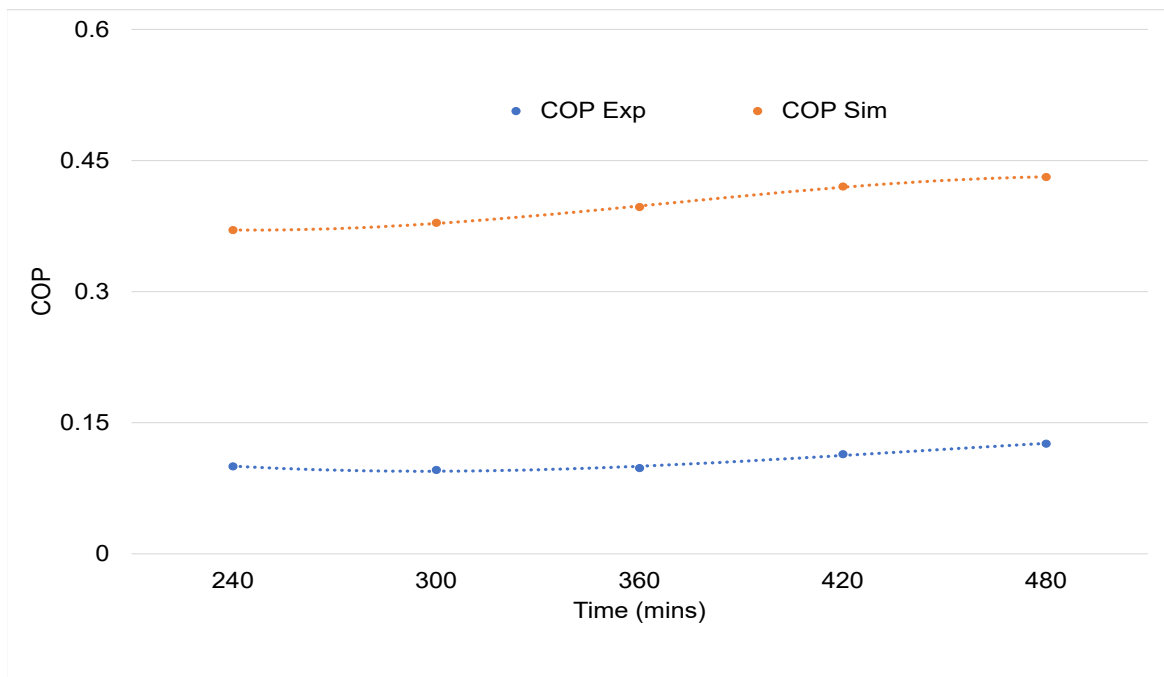


Fig. 6.19 Comparison of COP

C. Comparison with Du et. al [59]

The two main energy input component of an absorption refrigeration system are the generator and the evaporator. Data of the variation of the components energy variation with the system performance are compared with simulation results from the model. The generator temperature is kept constant. The variable input parameters are the condenser, absorber and evaporator temperatures. The results are presented in Tables 6.10 to 6.15. The difference between the simulated and experimental results are within 5 to 8% as the shown in the tables.

Table 6.10 Comparison of input energies variation with COP (1) (reference [59])

Comparison (1)			
Parameter (unit)	Reference	Current Simulation	% difference
Cooling capacity (kW)	29.9	29.7	0.67
Evaporator temperature (°C)	-18.8	-18.8	-
Condenser temperature (°C)	28.9	28.9	-
Generator temperature (°C)	100	100	-
Absorber temperature (°C)	27.5	27.5	-
Generator energy rate (kW)	55.4	58.62	5.65
COP (-)	0.54	0.51	6.37

Table 6.11 Comparison of input energies variation with COP (2) (reference [59])

Comparison (2)			
Parameter (unit)	Reference	Current Simulation	% difference
Cooling capacity (kW)	24.8	24.2	2.45
Evaporator temperature (°C)	-19.2	-19.2	-
Condenser temperature (°C)	29.2	29.2	-
Generator temperature (°C)	100	100	-
Absorber temperature (°C)	28.3	28.3	-
Generator energy rate (kW)	53.9	57.35	6.20
COP (-)	0.54	0.51	8.62

Table 6.12 Comparison of input energies variation with COP (3) (reference [59])

Comparison (3)			
Parameter (unit)	Reference	Current Simulation	% difference
Cooling capacity (kW)	29.1	29.1	0.00
Evaporator temperature (°C)	-18.9	-18.9	-
Condenser temperature (°C)	29.4	29.4	-
Generator temperature (°C)	100	100	-
Absorber temperature (°C)	27.2	27.2	-
Generator energy rate (kW)	56.11	61.03	8.55
COP (-)	0.52	0.48	8.62

Table 6.13 Comparison of input energies variation with COP (4) (reference [59])

Comparison (4)			
Parameter (unit)	Reference	Current Simulation	% difference
Cooling capacity (kW)	25.8	25.8	0.00
Evaporator temperature (°C)	-18.9	-18.9	-
Condenser temperature (°C)	28.6	28.6	-
Generator temperature (°C)	100	100	-
Absorber temperature (°C)	28.2	28.2	-
Generator energy rate (kW)	54.9	56.91	3.60
COP (-)	0.54	0.51	3.61

Table 6.14 Comparison of input energies variation with COP (5) (reference [59])

Comparison (5)			
Parameter (unit)	Reference	Current Simulation	% difference
Cooling capacity (kW)	27.4	27.1	1.10
Evaporator temperature (°C)	-18.6	-18.6	-
Condenser temperature (°C)	29.1	29.1	-
Generator temperature (°C)	100	100	-
Absorber temperature (°C)	28.5	28.5	-
Generator energy rate (kW)	53.7	56.22	4.59
COP (-)	0.51	0.48	5.64

Table 6.15 Comparison of input energies variation with COP (6) (reference [59])

Comparison (6)			
Parameter (unit)	Reference	Current Simulation	% difference
Cooling capacity (kW)	32.2	32.3	2.45
Evaporator temperature (°C)	-19.3	-19.3	-
Condenser temperature (°C)	29.3	29.3	-
Generator temperature (°C)	100	100	-
Absorber temperature (°C)	27.6	27.6	-
Generator energy rate (kW)	57.7	60.81	5.25
COP (-)	0.54	0.51	5.29

D. Comparison with Abdulateef et. al. (reference [2])

An actual compact aqua-ammonia absorption refrigeration unit operated under real conditions for Malaysia (tropical) climate is tested for performance. The authors investigated the influence of generator, evaporator and condenser temperatures on the system performance. The heat energy to drive the system was provided by solar system via solar collectors. The system produced a refrigeration capacity of 1.5 ton. The system parameters were simulated and resulted compared.

The comparison of the variation of the evaporator temperature with COP was observed to closely match and in a linear relation (Fig. 6.20). The experimental result was higher at the lower temperature range. The experimental result was lower compared to the simulation at lower temperature of the condenser (Fig: 6.21). But the trend indicates the tendency of it increasing with temperatures higher than 40 °C. Fig. 6.22 shows a diverged result at 60 °C to 75 °C of the generator temperature variation with COP, with a COP of 0.25 and 0.75 for the experiment and simulation, respectively. From equation (4.59), it can be deduce that at constant energy to the evaporator, an increase in the generator temperature will lead to an increase in the energy rate due to the generator and consequently, as the quotient of the relation, the COP will be reduced.

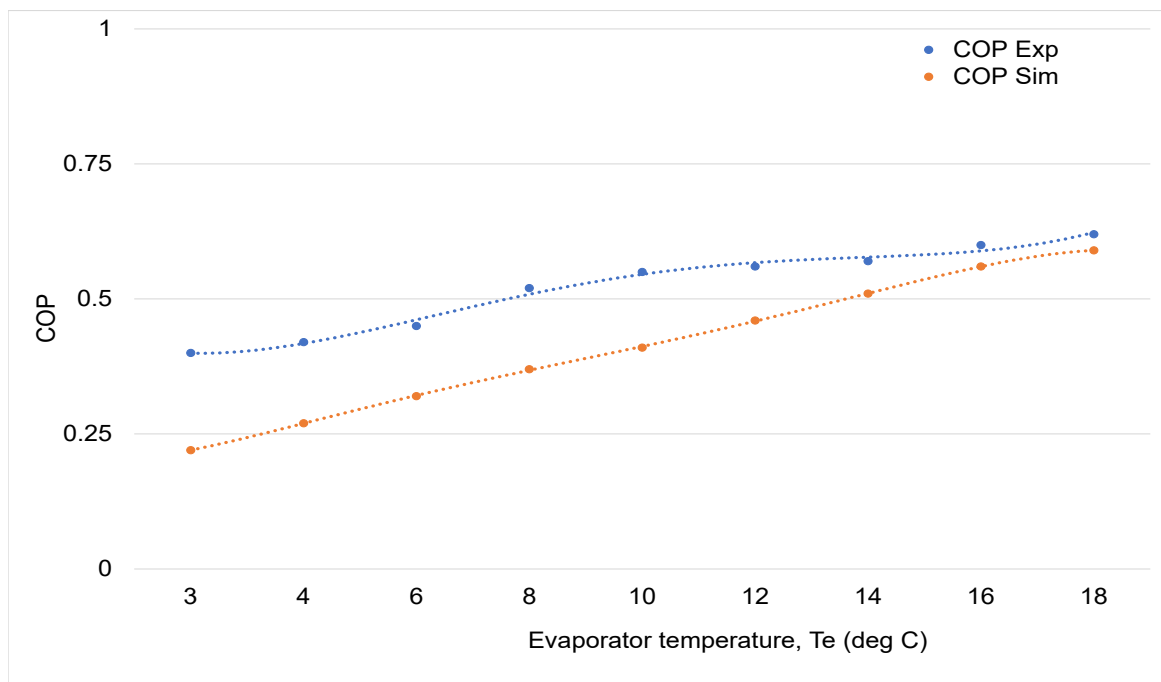


Fig. 6.20 Comparison of the variation of COP with evaporator temperature

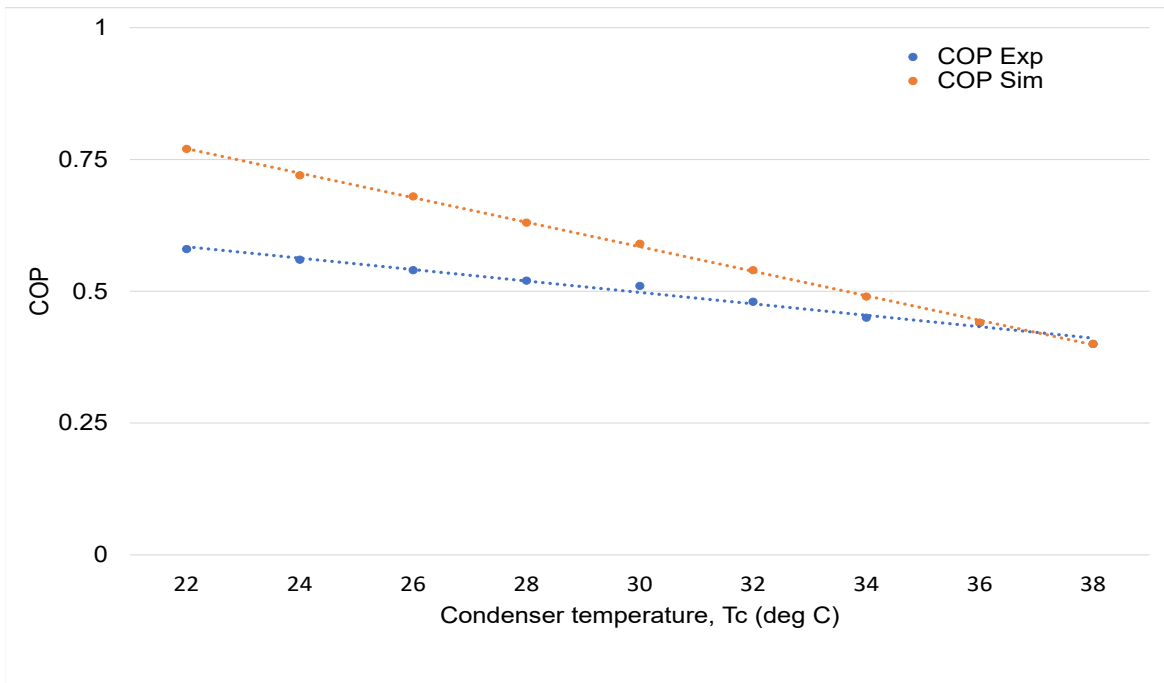


Fig. 6.21 Comparison of the variation of COP with condenser temperature

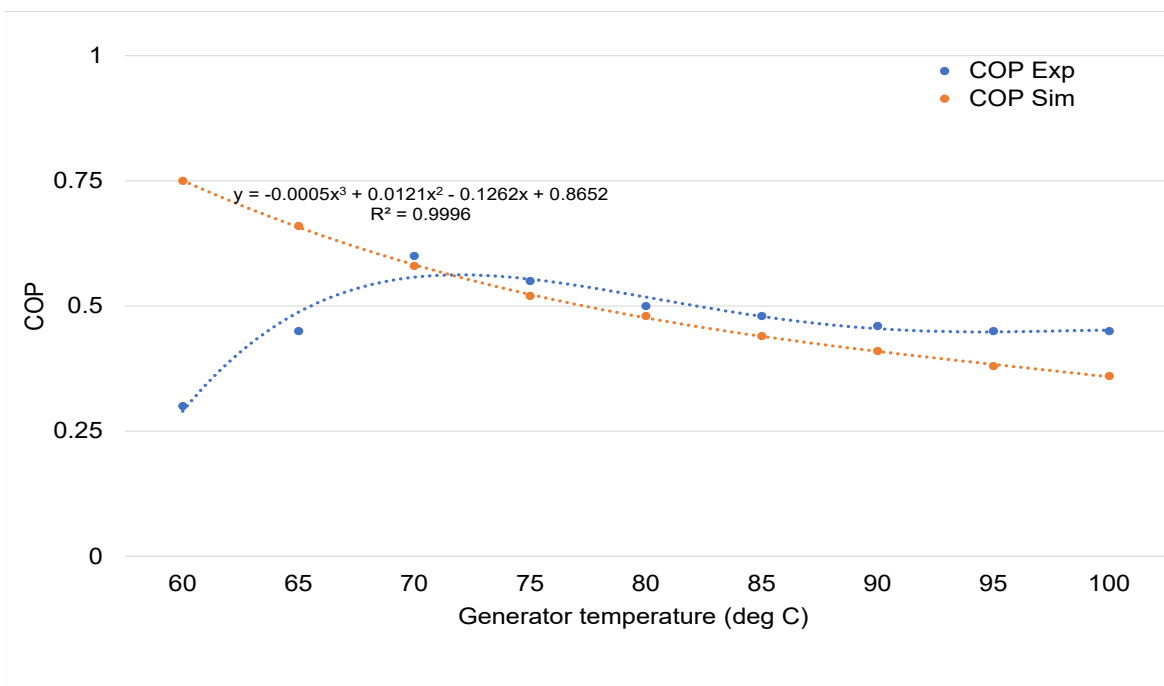


Fig. 6.22 Comparison of the variation of COP with generator temperature

E. Comparison with Horuz and Callander (reference [80])

This is an experimental investigation of the performance of a commercially available vapour absorption refrigeration system. The thermal energy driving the system is provided by natural gas and the refrigerant pair is aqua-ammonia. Ammonia is the refrigerant and water is the absorbent. the system has a cooling capacity of 10 kW. The experiment measures the mass flow rate of the refrigerant and those of the weak and strong solutions. The response and or performance of the refrigeration system to the variation of the input temperatures and energy flows are compared and presented.

The results of the comparisons are in good agreement in all five simulations (Figs 6.23 - 6.27). The percentage difference is less than 0.5.

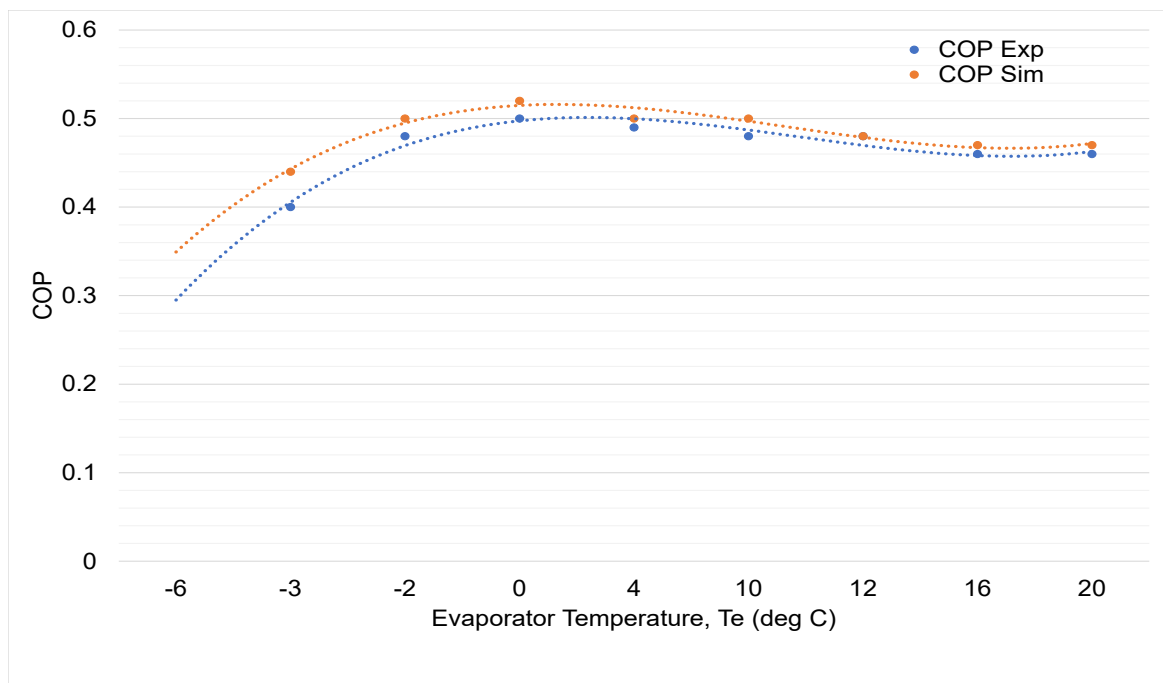


Fig. 6.23 Comparison of the variation of COP with evaporator temperature

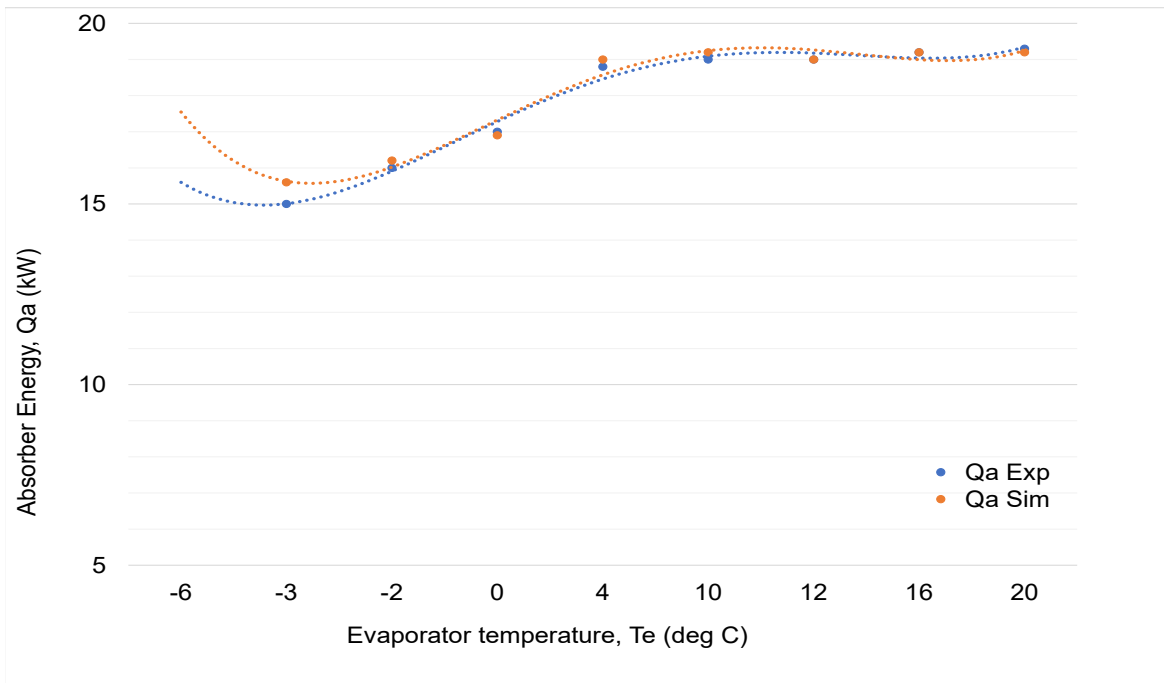


Fig. 6.24 Comparison of the variation of absorber energy with evaporator temperature

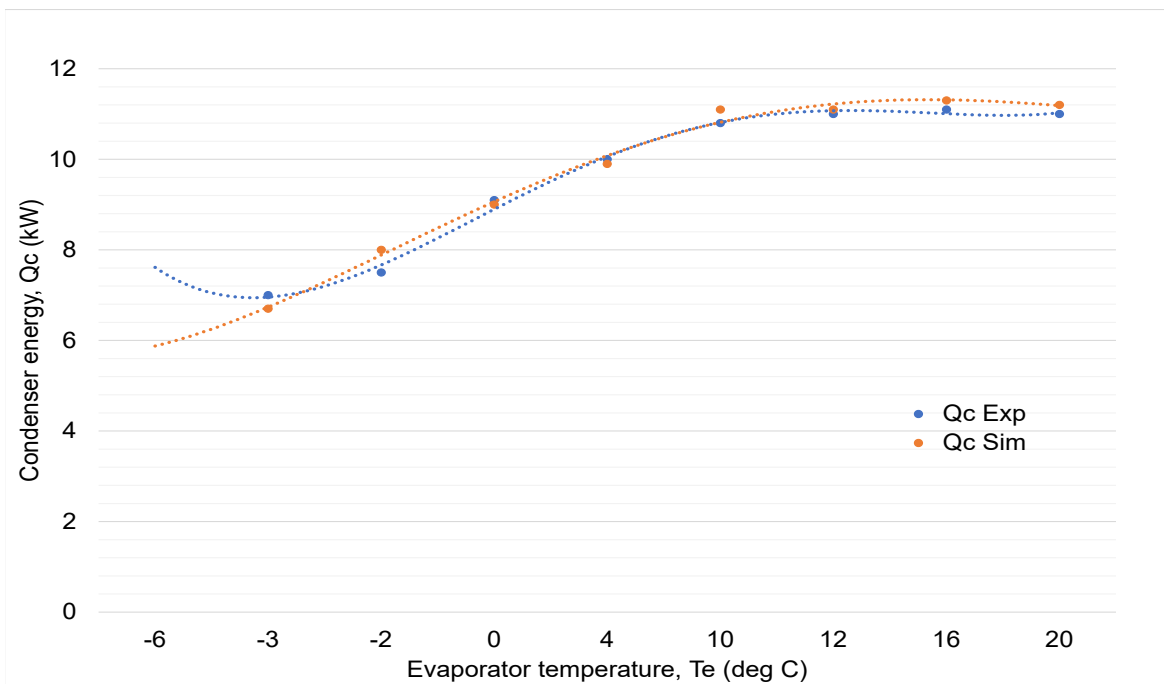


Fig. 6.25 Comparison of the variation of condenser energy with evaporator temperature

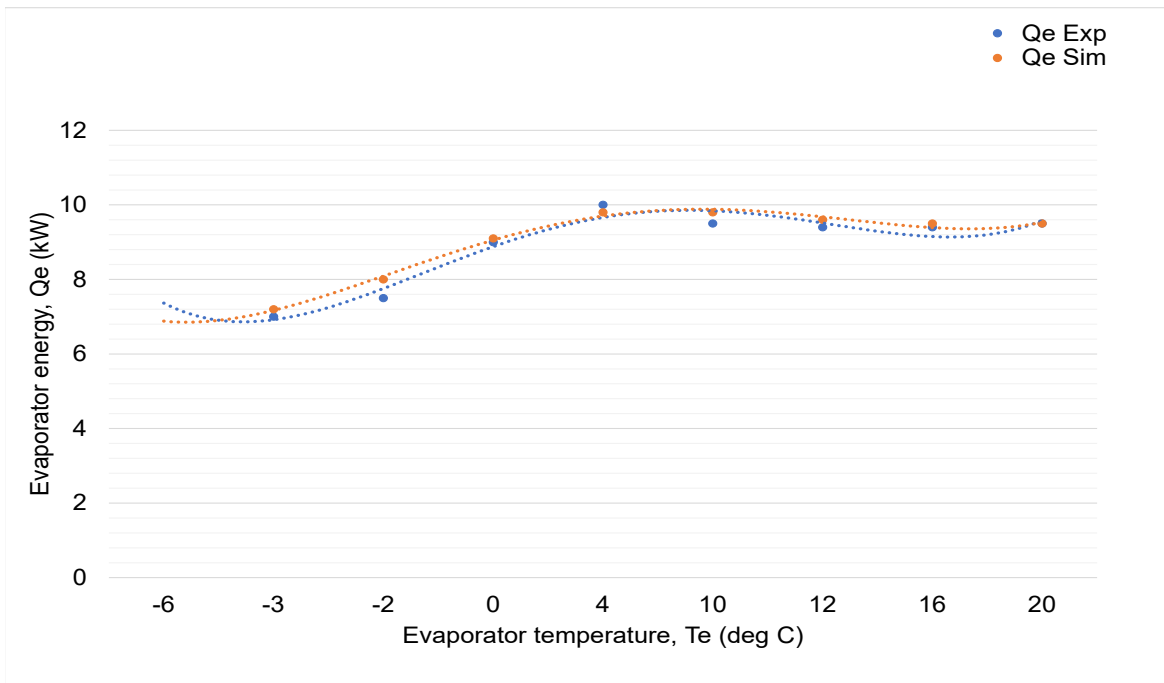


Fig. 6.26 Comparison of the variation of evaporator energy with evaporator temperature

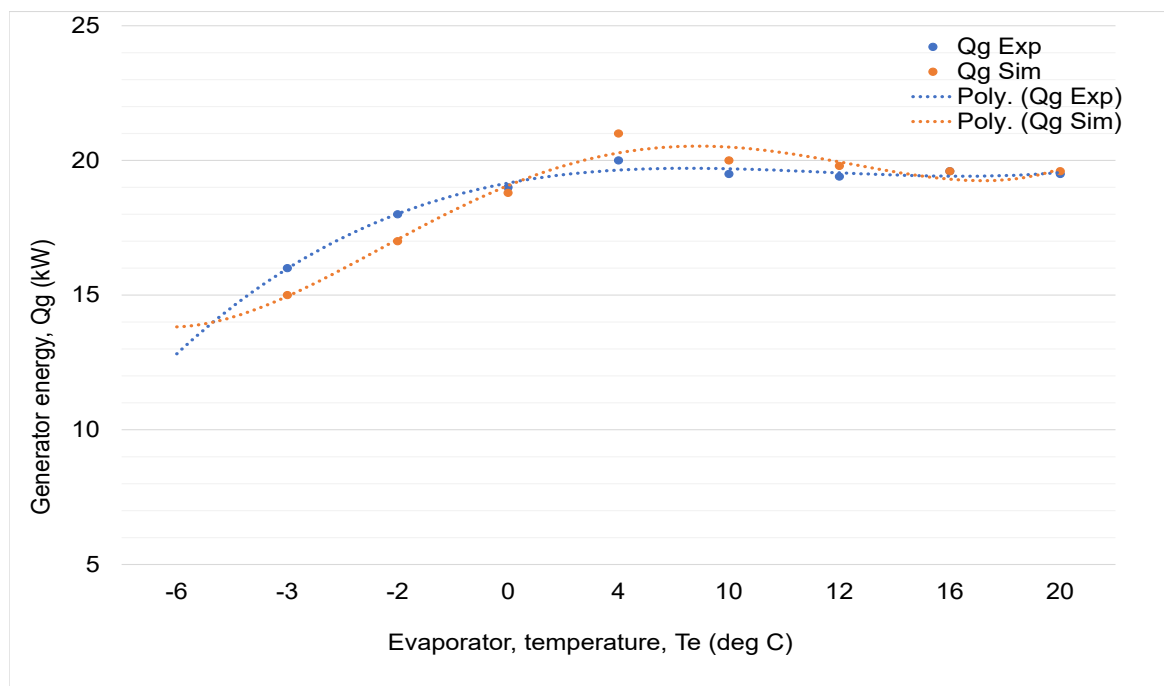


Fig. 6.27 Comparison of the variation of generator energy with evaporator temperature

F. Comparison with Lazzarin et. al. (reference [117])

The ammonia-water absorption refrigeration system is air cooled. A cooling temperature of 8 °C which is outside the range of the cooling media of the simulation model (15 °C to 50 °C). Data sets with higher cooling temperatures were used, although the system could be scaled and/or adjusted to accommodate lower cooling temperatures. However, in reality such cooling temperature would not be necessary for the location of intended use.

The results of the comparisons are shown in Figs: 6.28 to 6.31. The trends are quite similar with the exception of the variation of the rate of energy due to the condense with the set cooling temperature (Fig. 6.29). Although the simulation showed higher condenser energy, both showed a decrease in the energy with increasing cooling temperature. However, the trend suggest an increasing condenser energy beyond 7 °C of the cooling water for the experiment, while the opposite can be said of the said of the simulation.

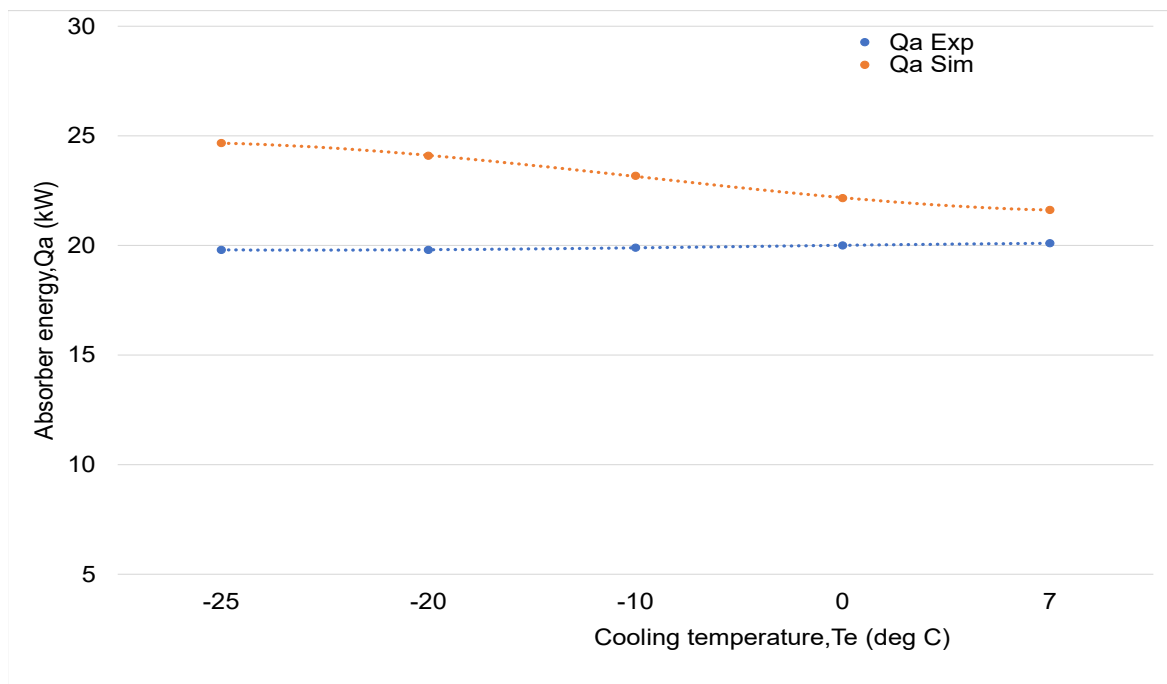


Fig. 6.28 Comparison of the variation of absorber energy with cooling temperature

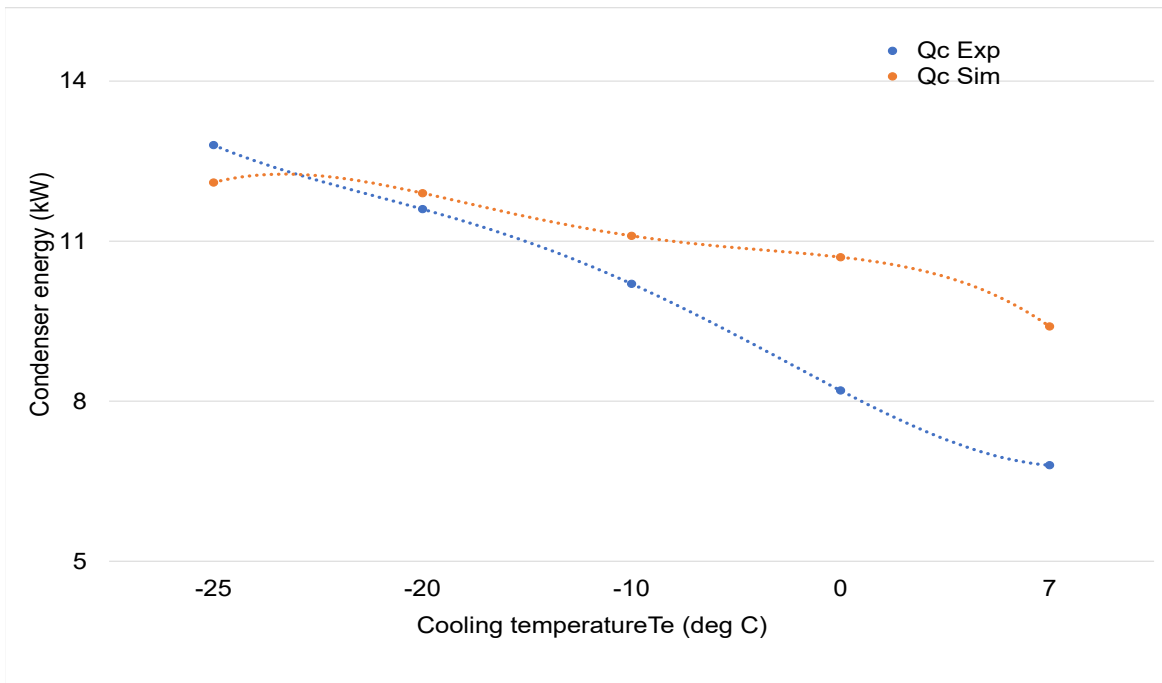


Fig. 6.29 Comparison of the variation of condenser energy with cooling temperature

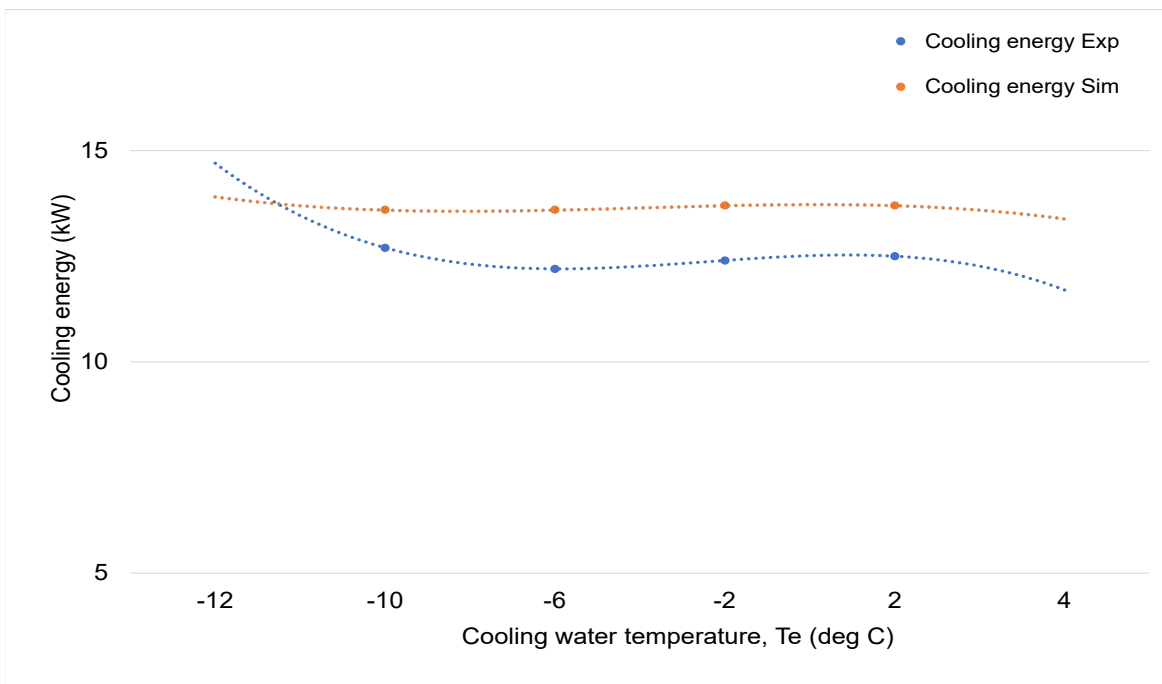


Fig. 6.30 Comparison of the variation of cooling energy with cooling temperature

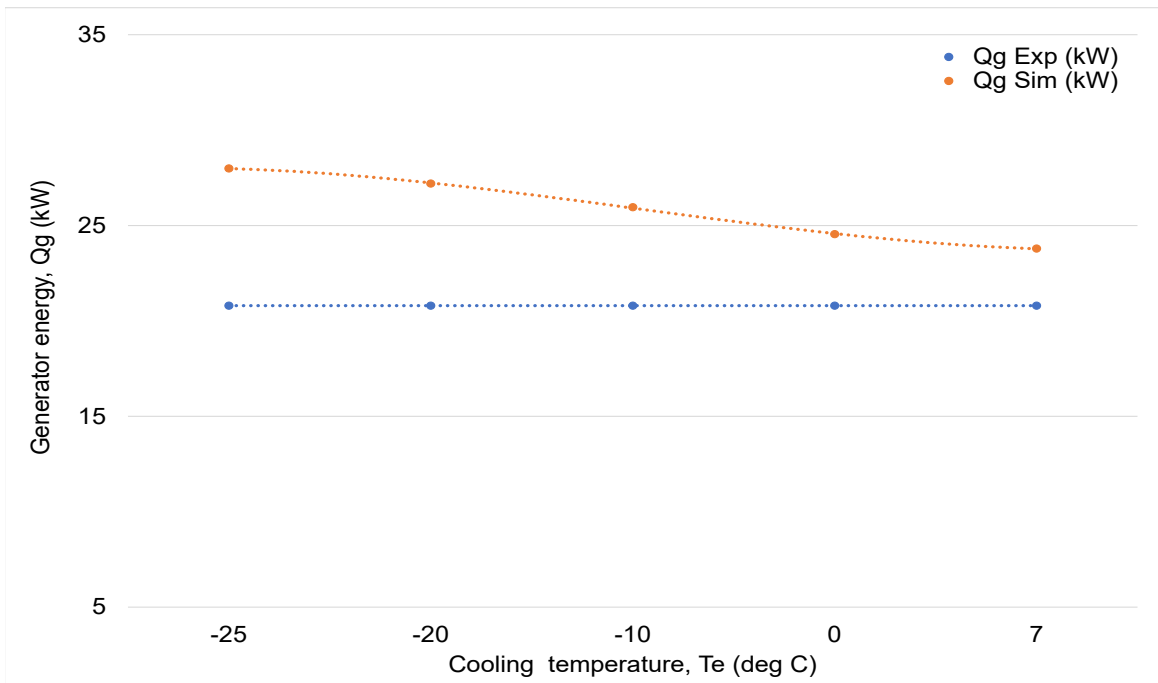


Fig. 6.31 Comparison of the variation of cooling energy with cooling temperature

6.4.2 Comparison with theoretical results

A comparison of results from theoretical ammonia-water absorption refrigeration models is considered in this section.

G. Comparison with Karamangil et. al. (reference [97])

This is a simulation study of the performance of single-stage absorption refrigeration system using conventional working fluids and alternatives. Data for the ammonia-water alternative was used for the comparison.

The results from the variation of the coefficient of performance with the heat exchanger effectiveness showed good comparison in both trend and performance ratio (Fig. 6.32). Also the trend is similar for the variation of the flow ratio with the generator temperature. However, the range of difference between the flows is more than 300% (Fig. 6.33). The flow circulation is the ratio of the strong solution mass flow rate to the mass flow rate of the refrigerant. Flow rate may affect the rate of heat transfer within the system and the components interaction with the surroundings. The COP for the referenced simulation tend to increase linearly with the generator temperature. This is true to the extent of the variation of other system input parameters. But if they are held constant, the reverse holds (Fig. 6.34

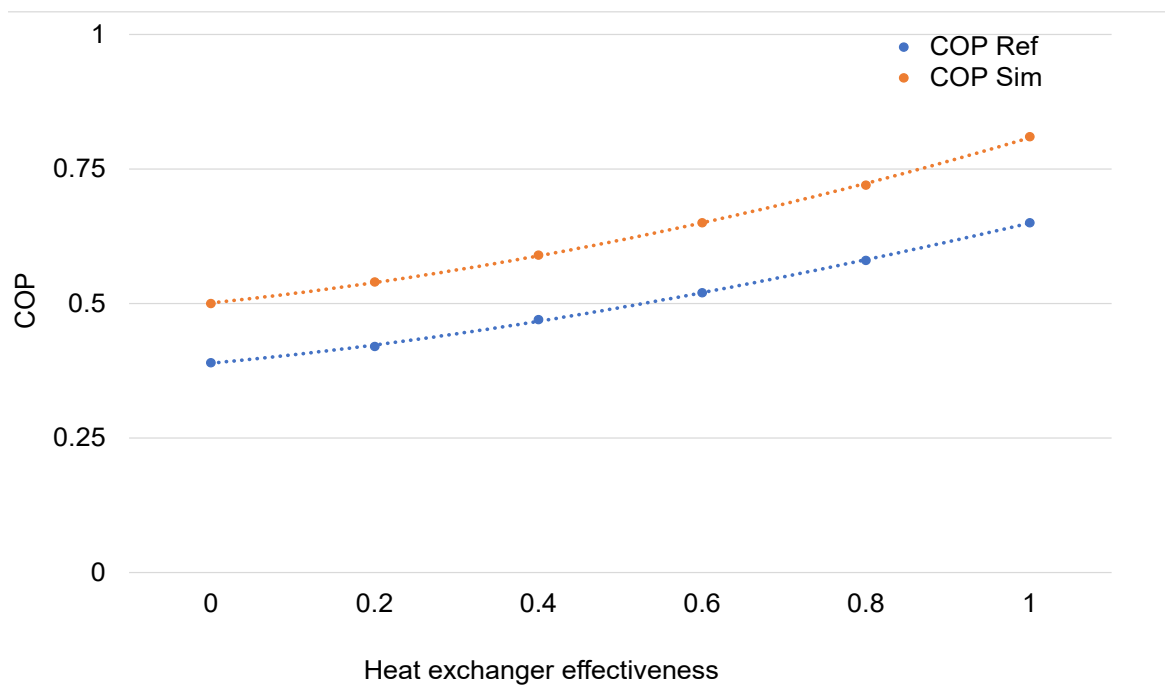


Fig. 6.32 Comparison of the variation of the COP with heat exchanger effectiveness

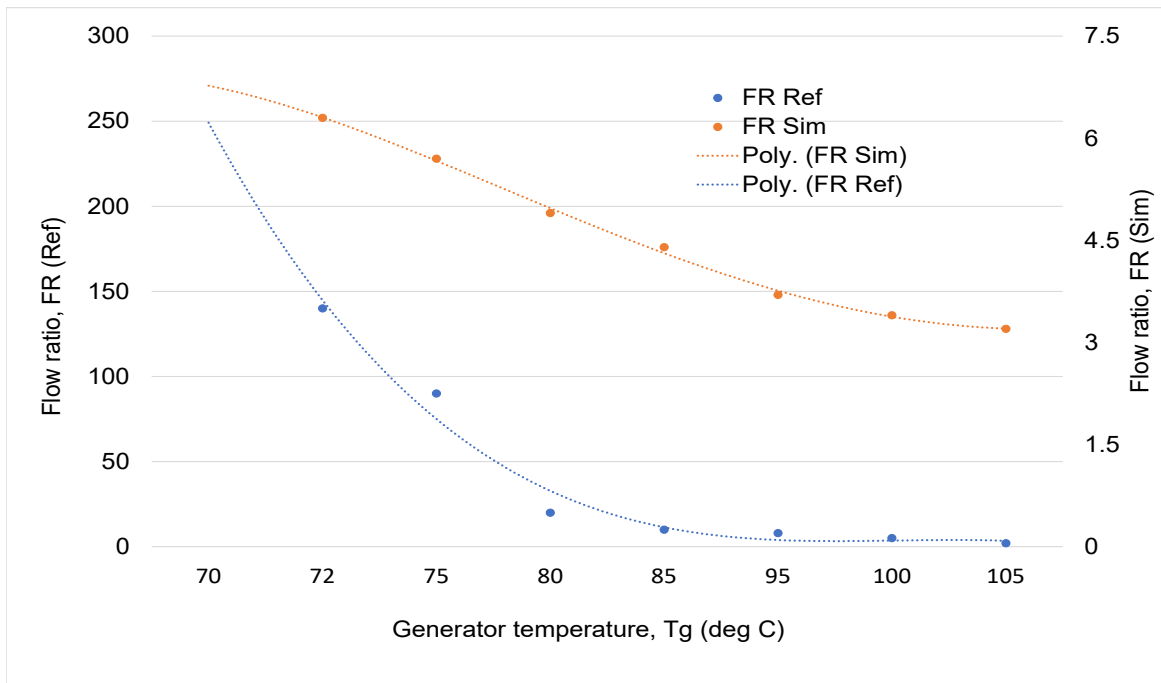


Fig. 6.33 Comparison of the variation of the flow ratio with generator temperature

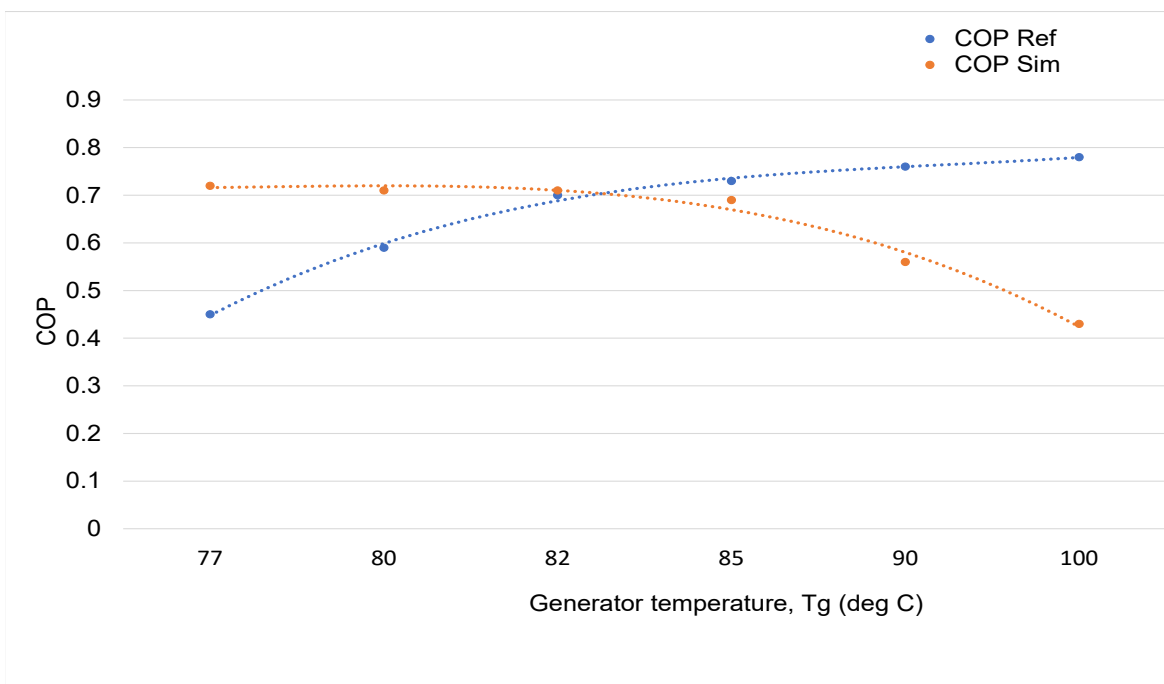


Fig. 6.34 Comparison of the variation of the COP with generator temperature

H. Comparison with Da-Wen Sun (reference [183])

The model is an aqua-ammonia absorption system proposed as an alternative refrigeration system for the food industry. The study enables the analysis of the performance characteristics of the system, and its optimization. Some of the parametric analyses include the variation of COP with generator temperature for various ammonia concentration and condenser temperature on COP for various solution heat exchanger effectiveness. The current simulation is carried out with the application of the parameters defined in the referenced work.

The results are compared and shown in Figs. 6.35 and 6.36. Both simulation results show good comparison with the referenced work.

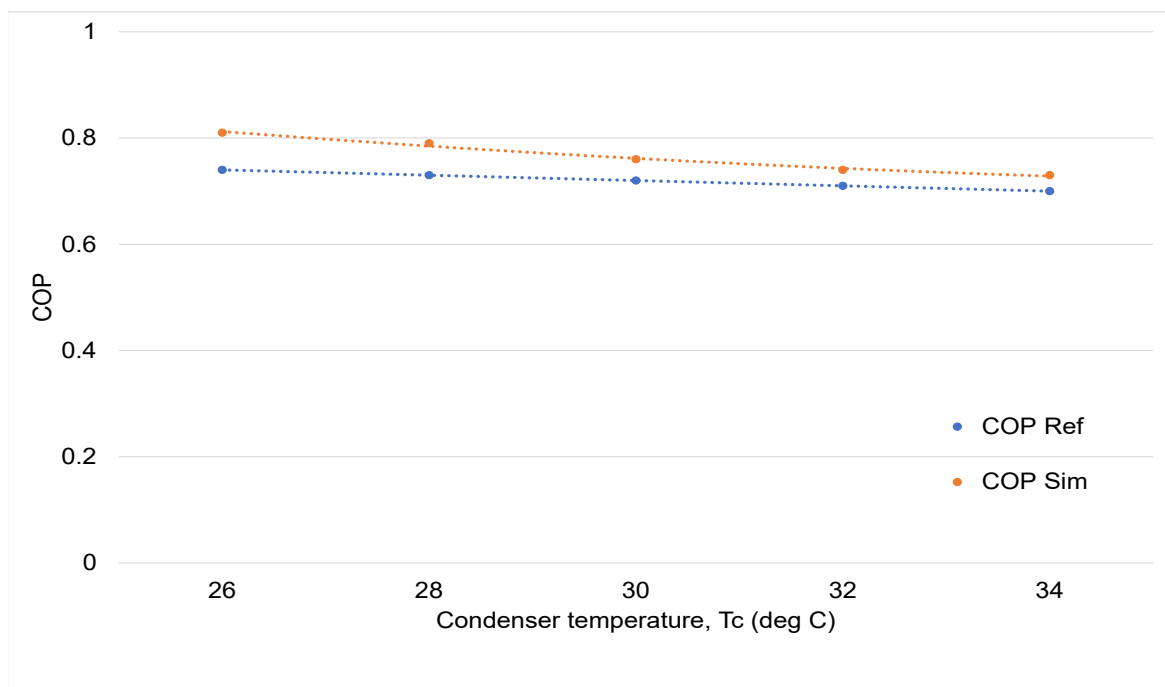


Fig. 6.35 Comparison of the variation of the COP with condenser temperature

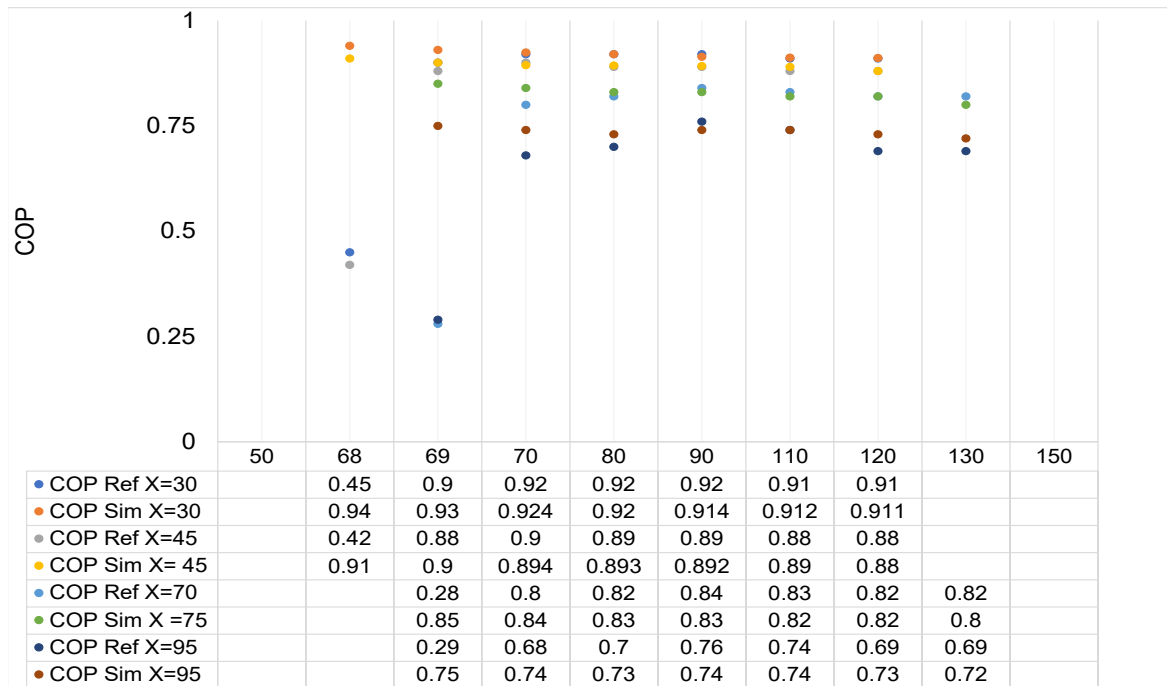


Fig. 6.36 Comparison of the variation of the COP with condenser temperature

I. Comparison with Kaushik and Bhardwaj (reference [102])

Results from the current model is compared with those from aqua-ammonia absorption refrigeration cycle for solar refrigeration and air-conditioning for space heating designed by the authors. The system consist of a solar-driven generation, rectifier, condenser, evaporator, absorber and heat exchangers. The result of the steady state simulation shows the variation of the coefficient of performance for cooling with varying input parameters.

The results from the current work shows good comparison with the referenced work. The results from the current simulation is however, about 8% higher in both cases considered.

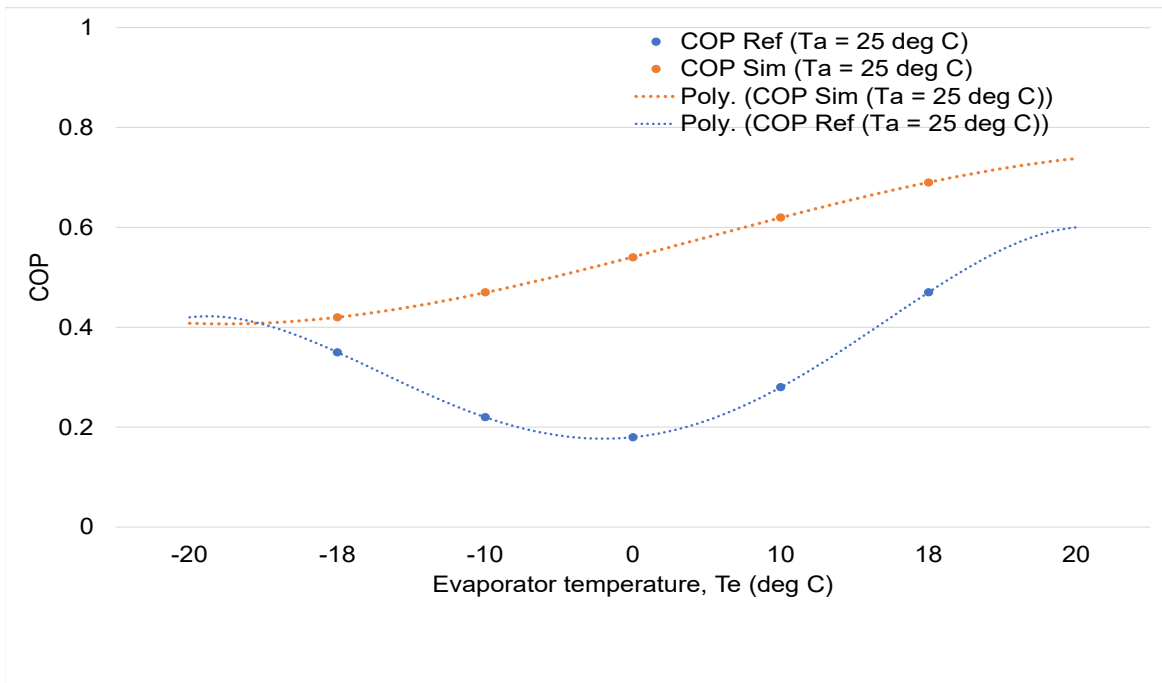


Fig. 6.37 Comparison of the variation of the COP with evaporator temperature

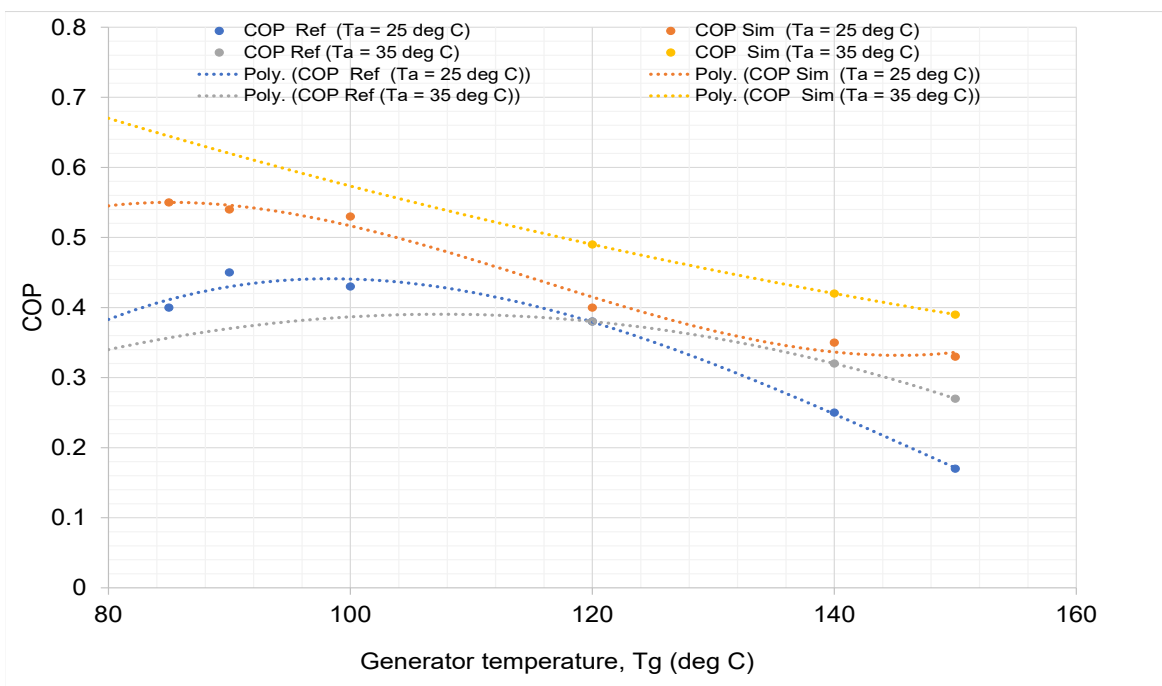


Fig. 6.38 Comparison of the variation of the COP with generator temperature for set absorber temperature

6.5 Solid Biomass Fuel Properties

This section looks at the results of the moisture content and calorific value test conducted in the course of this study.

6.5.1 Moisture Content

An overview of the fuel samples tested in the course of this study is presented in the Table 6.16. The tests comply standard ISO 18134:2015. Table 6.17 contain the results of the moisture content tests. The results show that the moisture content of all the tests samples are less than 12 %. This is an indication that they comply with the DIN plus 51731 and satisfy the ÖNorm M7135 standards which are generally accepted as high quality commercial solid biomass fuels for domestic and industrial applications. miscanthus, rice husk and straw exhibit lower moisture content than sawdust (9.7%). The moisture contents of wood is the highest (11.9%). However, the moisture content of the fuels reduces with further heating. This implies that the decrease in moisture content is a function of the drying energy used and the bulk density of the fuel. The value of the moisture content of the fuels test are typical of those reported in the literature [201, 8].

Table 6.16 Sold fuels samples tested

Fuel	Description	Country
Miscanthus	log (60 mm x 60 mm)	UK
Rice Husk	Pellets	UK
Sawdust	Shredded	UK
Straw	Pallets	Uk
Wood	Chipped	UK

Table 6.17 Sold fuels moisture content tests results

Fuel	Moisture content (%)	Description
Miscanthus	8.9	Dry basis
Rice Husk	8.8	Dry basis
Saw dust	9.7	Dry basis
Straw	8.6	Dry basis
Wood	11.7	Dry basis

6.5.2 Calorific Value

The gross heat of combustion obtained from the experiment and using the equations (5.3) to (5.5) is the calorific value of the sample with the moisture as it existed when the sample was weighed. This was converted to a moisture free value using the formula published by in ASTM method D3180 and given by:

$$H_n = 1.8Hg - 91.23H$$

Where

H is the percentage of hydrogen in the sample.

It is observed that the ambient temperature of the water was not constant and therefore, inconsistent from test to test. Consequently, to normalise the results and enhance comparison, the temperature at the start of each experiment, is considered the datum. The temperature profile of the bomb experiment for the fuel samples is shown in Fig. 6.39. The system takes about ten minutes to reach steady state condition. The figure shows a sudden rise in temperature for all the fuels just after ignition. However, the magnitude of the temperature rise differs for each fuel. Miscanthus shows the highest temperature while straw compared with the miscanthus, did not attain high temperature. Fig. 6.40 shows the heating values as determined by the experiment. The values lies approximately between 18 MJ/kg and 20 MJ/kg . The tests results are in line with the DIN and ÖNorm standards recommendations. The rice husks has the lowest heating value followed by straw. This is to be expected as the heating value is a function of the energy density. Woodchip has the highest calorific value, 21.58 MJ/kg .

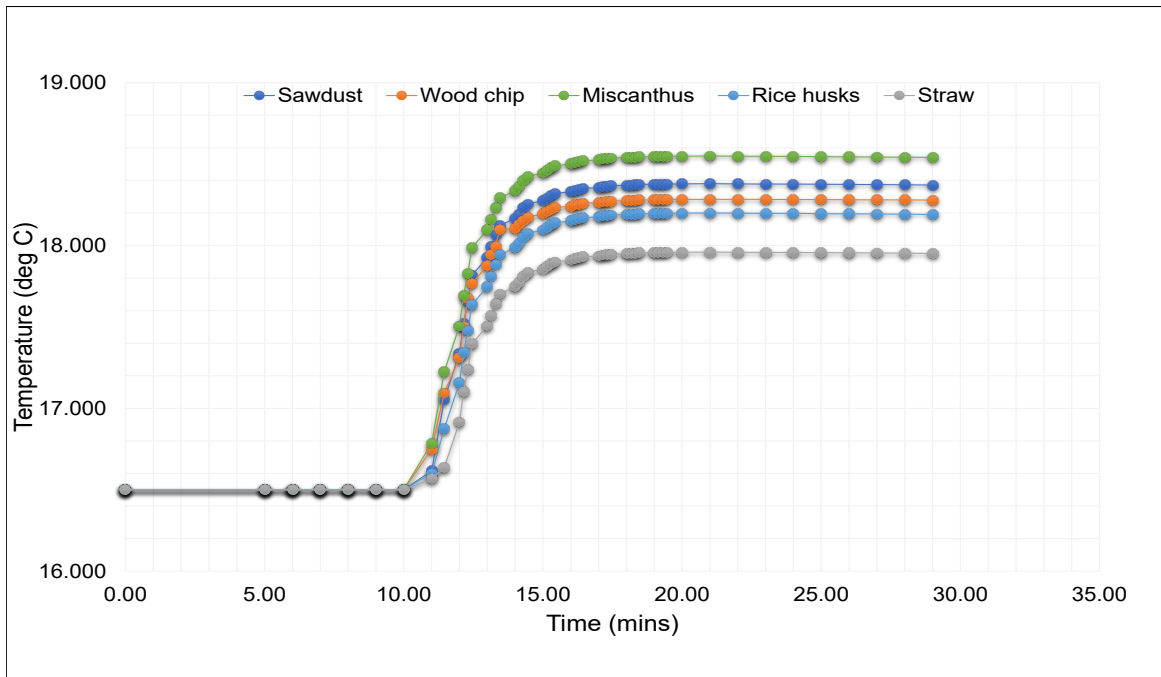


Fig. 6.39 Bomb calorimeter experiment temperature profile of biomass fuels

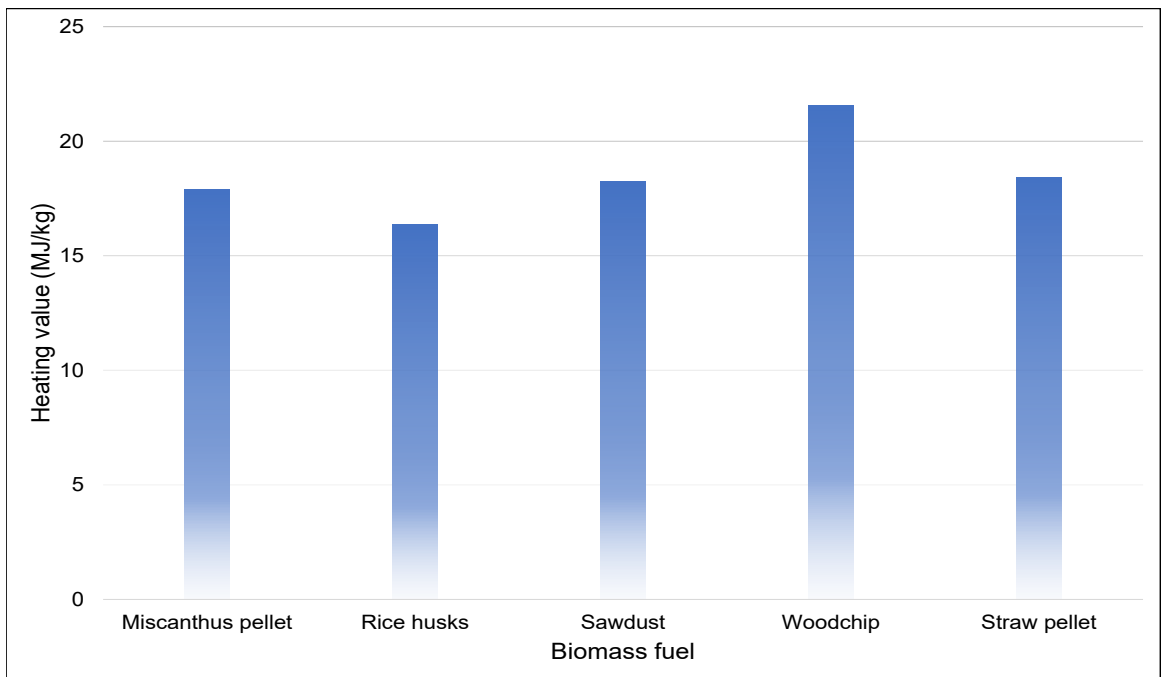


Fig. 6.40 Calorific value for the different fuel samples

6.6 Biomass to Drive Absorption Refrigeration

According to the planned study, the aim was to quantify the biomass fuel that will be required for a specified operating condition including the energy produced, and to study such parameters that impacts on the efficiency, and hence can influence cost, selection of equipment and design. The following biomass fuels were considered (the properties of the fuels are stated in Table 5.1):

- Woodchip
- Wood pellet
- Log wood
- Wood
- Miscanthus

It was observed that there is a linear relationship between the quantity of a biomass fuel required for a specified energy output and its fuel density. Figs. 6.41 and 6.42 It can be seen that for a set output energy, less of the biomass with higher fuel density will be needed. Consequently, for a full load operating hours equivalent of 24 hours at a difference of 20 °C between the hot and cold sides of the heat exchanger ($\Delta T = 20$), nearly twice as much woodchip at 20% moisture content will be required than wood. The figures also show the influence of the temperature difference at the heat exchanger on the energy output. Although an increase in the difference may increase energy output, this may require more fuel consumption. A mean difference is desired for optimum performance.

The input temperature to the generator of the absorption refrigeration system goes from the boiler heat exchanger outlet. The increase in the generator temperature to meet set or varying cooling demand results in the variation of the energy output. Further ΔT will adjust subject to the return water temperature (T_{c1} or T_{g0}). Figs. 6.43 and 6.42 shows a linear relation between the output energy and the generator temperature, as well as between ΔT and the generator input temperature.

The efficiency of the boiler is a very important paramant that influences or affects the energy utilisation of the system, as well as the operational cost and to a great extent, payback time of the installation. It can be seen from Fig. 6.45 the energy output or the energy required to meet a demand increases with a decrease in the efficiency of the system. The efficiency of the Windhager biomass boiler is put between 80% and 90%.

Result and Discussion

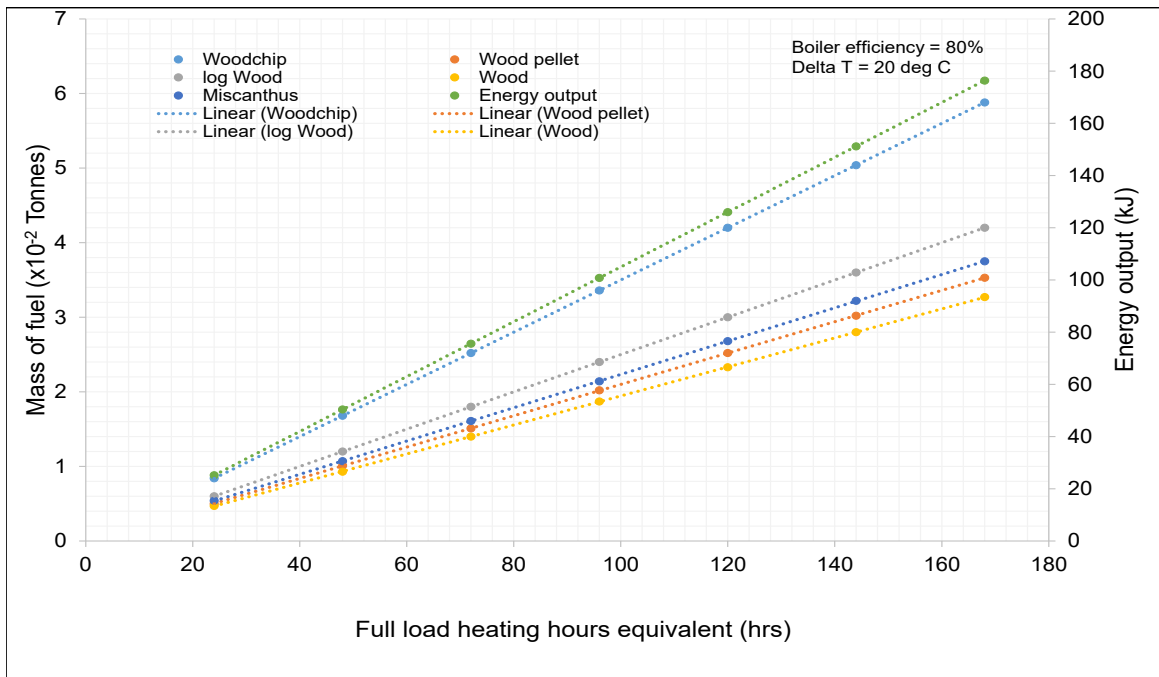


Fig. 6.41 Variation of mass of fuel and energy output with FLHE (at $\Delta T = 20\text{ }^{\circ}\text{C}$)

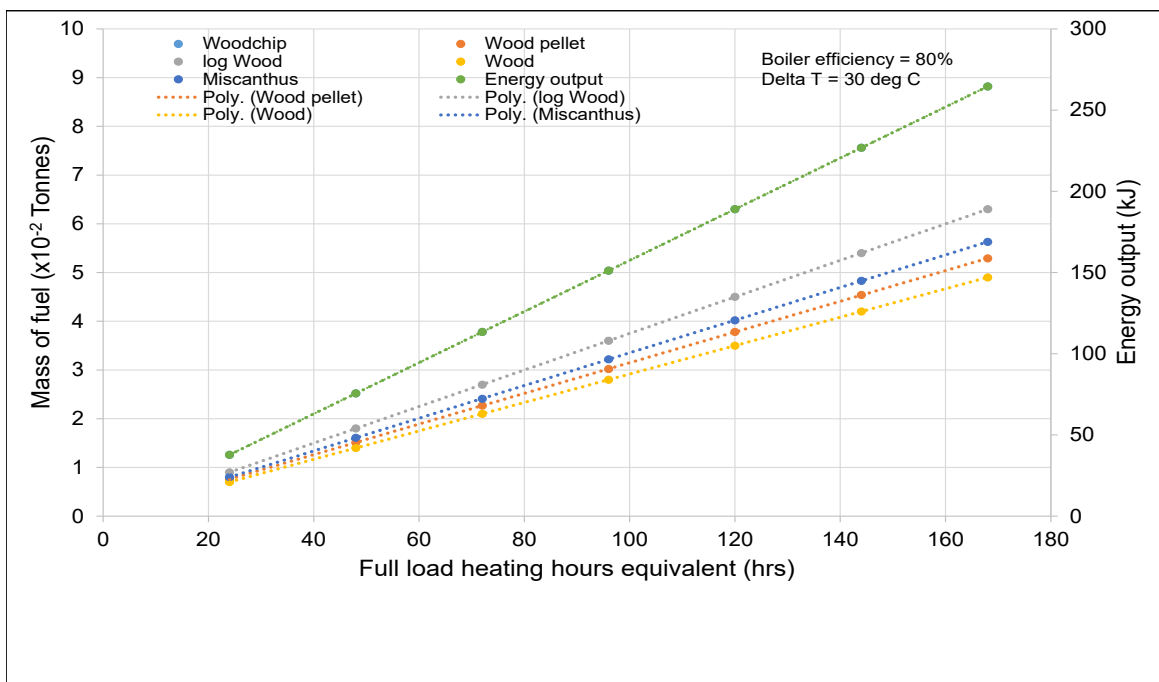


Fig. 6.42 Variation of mass of fuel and energy output with FLHE (at $\Delta T = 30\text{ }^{\circ}\text{C}$)

Result and Discussion

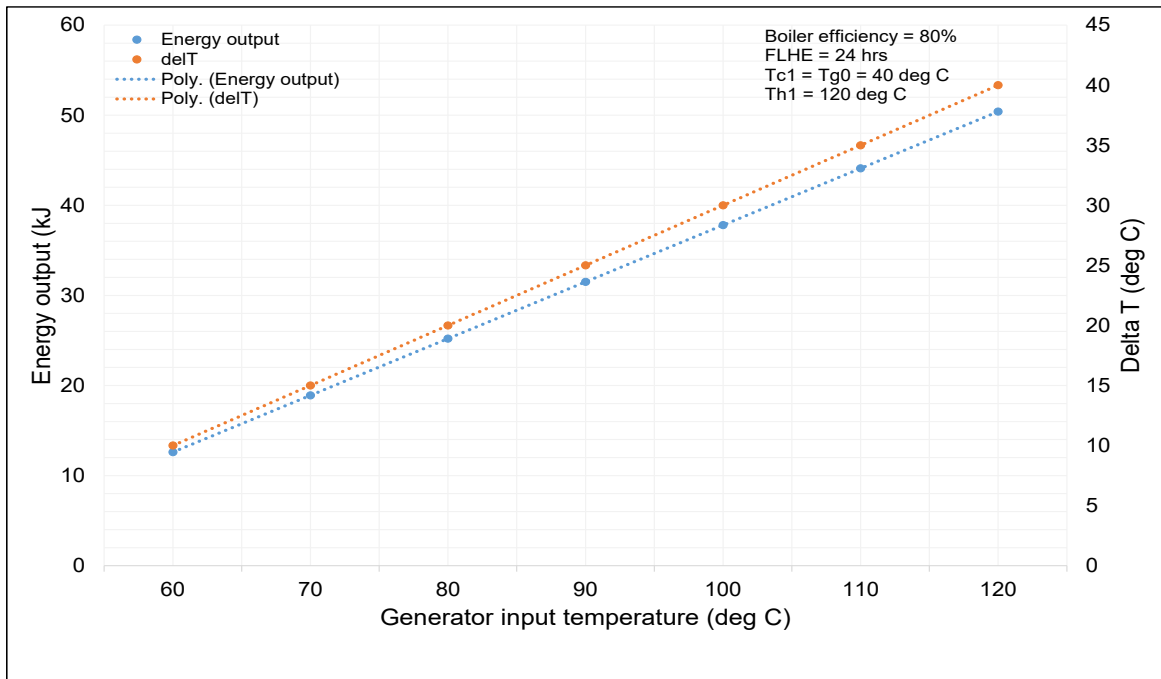


Fig. 6.43 Relation between energy output and ΔT on generator input temperature at $T_{c1} = 40\text{ }^{\circ}\text{C}$

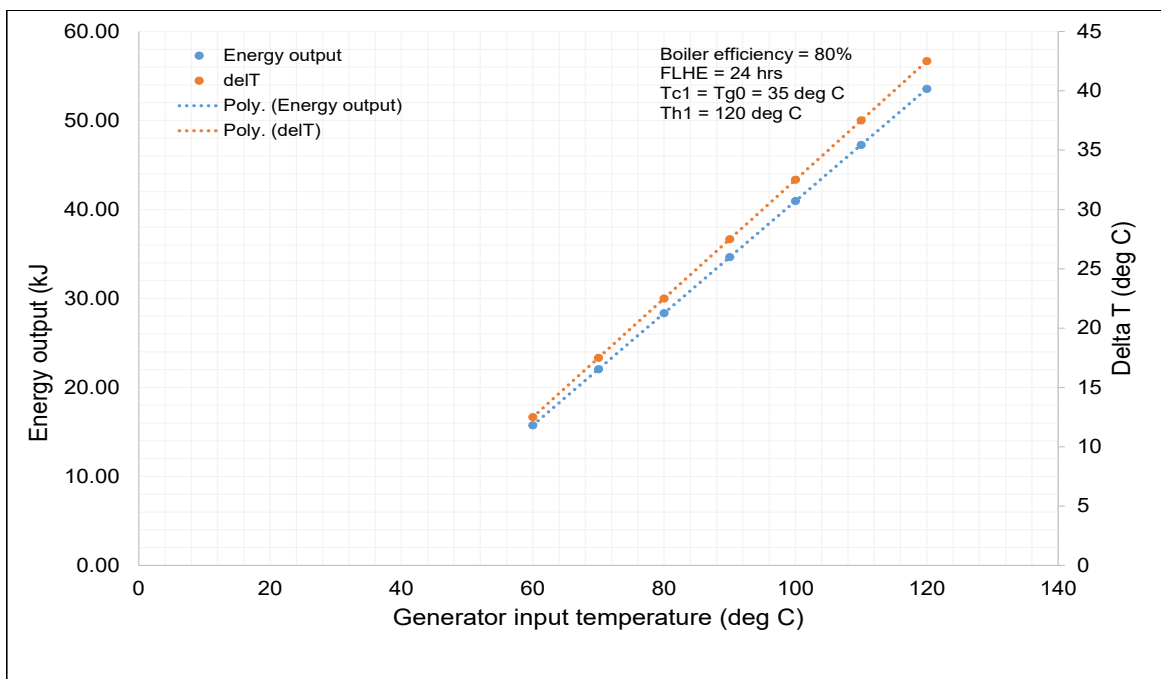


Fig. 6.44 Relation between energy output and ΔT on generator input temperature at $T_{c1} = 35\text{ }^{\circ}\text{C}$

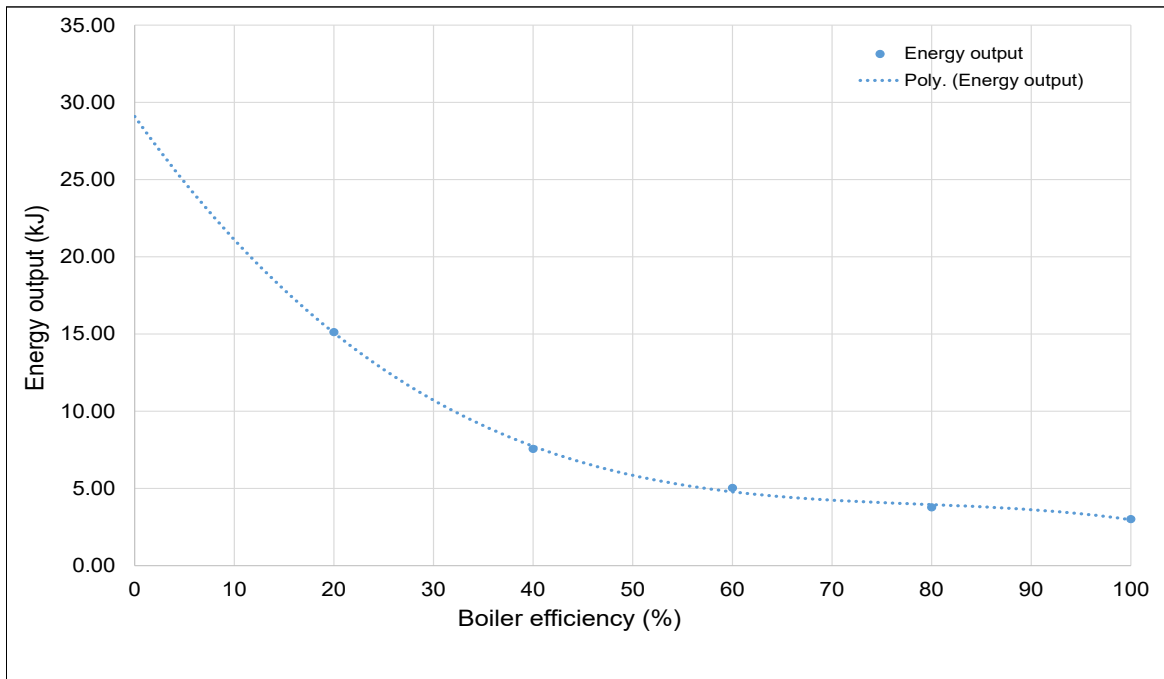


Fig. 6.45 Energy utilisation with boiler efficiency

6.7 Feasibility of Nigeria's reliance on Biomass

The energy potential from biomass annually available was estimated to ascertain its viability as a sustainable energy source amidst a dynamic population, changing social needs and lifestyle. A five-yearly estimate of energy available from potential energy crops including woodfuel was made from historic data to year 2050. The estimated energy was expressed in electric energy and projected in the short term to year 2030 to examine the impact on overall energy consumption.

The thermal characteristics of the biomass fuel was used to estimate the energy content of the fuel. Table 6.18 shows the computed energy content estimated from the thermal characteristics of each species and Table 6.19 contains energy potential and the adjusted energy potential computed from the energy content and the annual production. The estimates are in agreement with published data in the literature [87, 144, 147]. Table 6.20 shows a comparison with reference [147]. Although there is a ratio difference of about 0.06 which may have resulted from methods adopted and assumptions made coupled with the loss factor of 2% in the present work to moderate exaggeration where data was estimated or assumed as well as for the fact that the equation for the estimation of the energy content was not derived from a direct measurement of crops within the geographical region of the area under investigation, the results are similar and the trend is conserved. The projection of the energy potential from agro-residue, forest-residue and woodfuel is presented in Table 6.21. The result from the estimation shows a steady increase in the agro- and forest-residues but a decline in the woodfuel category. This is generally due to the growing population, the high dependency on traditional biomass, though inefficiently, and the slow growth in energy consumption. Time series forecast from this shows that the population will reach about 260 million by 2030 (Fig. 6.46). A comparison of energy consumption of Nigeria and some other nations across the globe shows the level of energy impoverishment in the nation (Fig. 6.47). The natural habitat hosting a greater percentage of potential energy from biomass are the rural areas. However, statistics shows that these areas need more access to clean energy than the urban areas (Fig. 6.48). The energy projection from the table shows that an average of 10819 PJ of energy could have been generated from biomass within thirty years period from 2020 to 2050 equivalent to the availability or access of extra 385 kWh/capita/year. A significant improvement compared to the status quo (Fig. 6.49). The feasibility is based on the assumption that the increases in the annual production of agricultural produce equals the generation of agro-residues, and energy conversion technologies in the region is developed and ready or developing. The latter is true of the Nigeria situation, from the study.

Table 6.18 Estimation of biomass energy content from thermal characteristics

Crop	<i>VM</i>	<i>FC</i>	<i>VM/FC</i>	<i>ASH</i>	<i>ASH/VM</i>	<i>FC/ASH</i>	$h_v(MJ/kg)$
Rice husks	61.81	16.95	3.6466	21.24	0.3436	0.7980	16.35
Cassava	84.50	9.56	8.8389	6.29	0.0744	1.5199	17.57
Cotton lint	75.80	19.60	3.8673	4.6	0.0607	4.2609	19.01
Groundnut	72.70	21.60	3.3657	5.7	0.0784	3.7895	18.96
Maize	74.40	18.50	4.0216	1.36	0.0183	13.6029	19.50
Millet	78.20	16.45	4.7538	5.27	0.0674	3.1214	18.68
Rice Paddy	65.70	13.91	4.7232	20.38	0.3102	0.6825	16.34
Sorghum	82.60	14.70	5.6190	2.7	0.0327	5.4444	18.84
Soybean	76.86	16.00	4.8038	7.14	0.0929	2.2409	18.39
Sugarcane	81.50	13.30	6.1278	5.2	0.0638	2.5577	18.35
Cocoyam	84.15	9.56	8.8023	6.29	0.0747	1.5199	17.58
Wheat	82.12	10.98	7.4791	6.9	0.0840	1.5913	17.79

Table 6.19 Estimation of biomass energy potential

Crop	Residue to crop ratio	Annual crop production (x1000 Tonnes)	Annual residue production (x1000 Tonnes)	Annual Energy potential (PJ)	Adjusted annual energy potential (PJ)
Rice husks	0.20	3713.9	742.78	12.15	11.92
Cassava	1.08	36822	39896.64	70.10	68.70
Cotton lint	4.25	130	552.50	10.50	10.30
Groundnut	2.30	2977.6	6848.48	12.98	12.72
Maize	0.27	7358.26	1986.73	38.73	37.96
Millet	2.00	4929.95	9859.90	18.42	18.05
Rice Paddy	0.26	3546.25	922.03	15.06	14.76
Sorghum	2.00	5279.17	10558.34	19.89	19.50
Soybean	2.10	426.59	895.84	16.48	16.15
Sugarcane	0.10	1401.68	140.17	25.72	25.20
Cocoyam	0.06	3033.34	182.00	31.98	31.34
Wheat	1.20	80	96.00	17.08	16.74
TOTAL		65984.84	71938.62	1302.2	1276.2

Table 6.20 Comparison of 5-yearly estimate: energy potential of agro-residue in Nigeria

Energy potential	2010	2015	2020	2025	2030	2035	2040	2045	2050
Reference [147]	2575	3445.9	4611.5	6171.17	8258.4	11051.6	14789.6	19791.8	26485.9
Present	2734.7	3656.1	4892.8	6542.0	8762.2	11714.7	15677.0	21009.0	28084.9
% difference	6.2	6.1	6.1	6.0	6.0	6.0	6.0	6.2	5.9

Table 6.21 Projection of 5-yearly energy potential to 2050

Biomass energy Source (PJ)	2010	2015	2020	2025	2030	2035	2040	2045	2050	Total
Agro-Residue	2735	3656	4893	6542	8762	11715	15677	21009	28085	103082
Forest Residue	7	9.4	12.3	16.1	21.1	25.9	29.8	32.5	38.2	193
Woodfuel	2631	2079	1527	974	422	250	160	95	52	7883
Total (PJ)	5382	5745	6432	7532	9205	11991	15867	21137	28175	111158

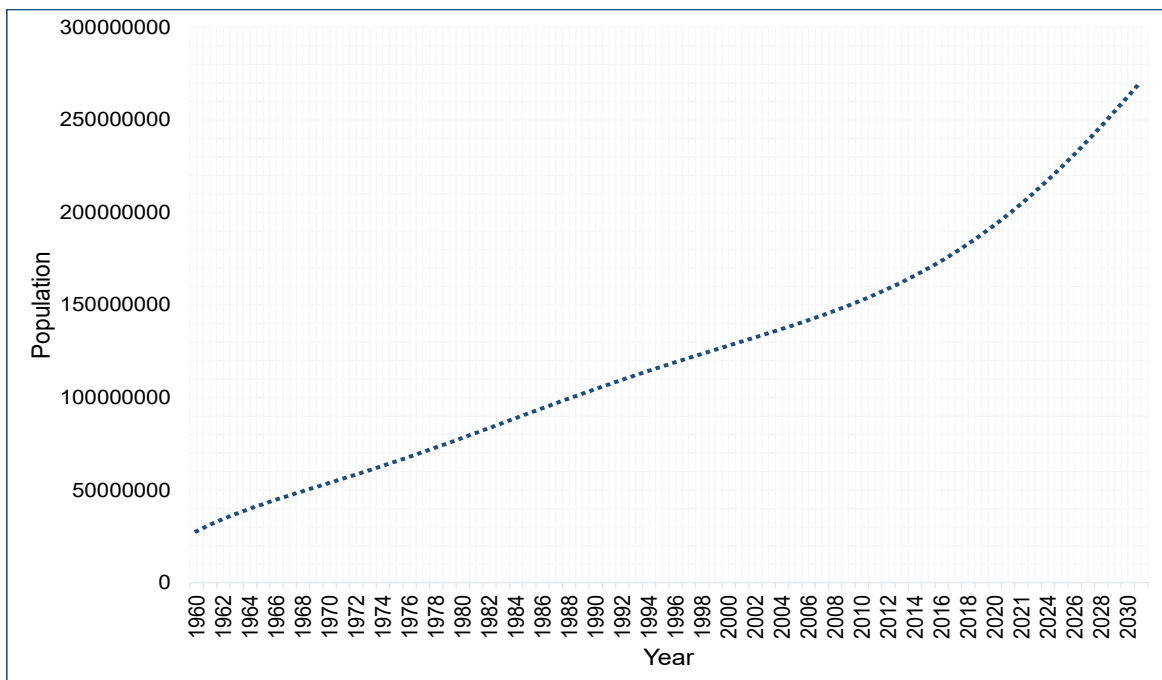


Fig. 6.46 Nigeria population projected

Result and Discussion

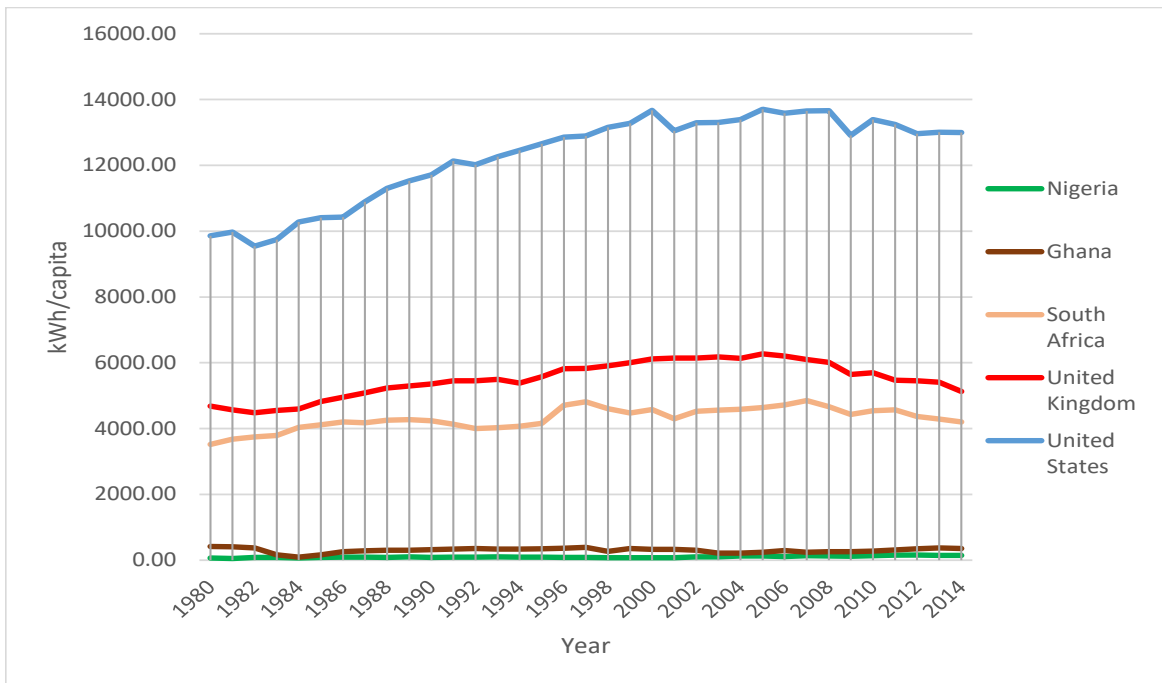


Fig. 6.47 Comparison of energy consumption (Excerpt from Wold Bank [205])

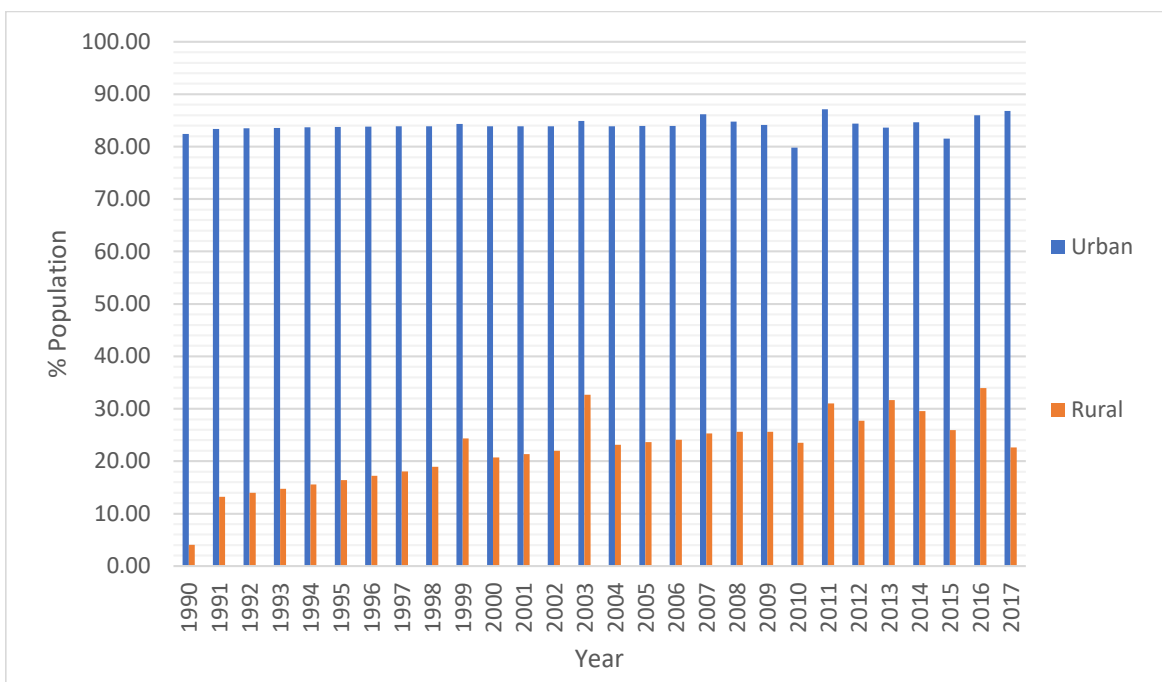


Fig. 6.48 Nigeria population projected (Data source: World Bank [206])

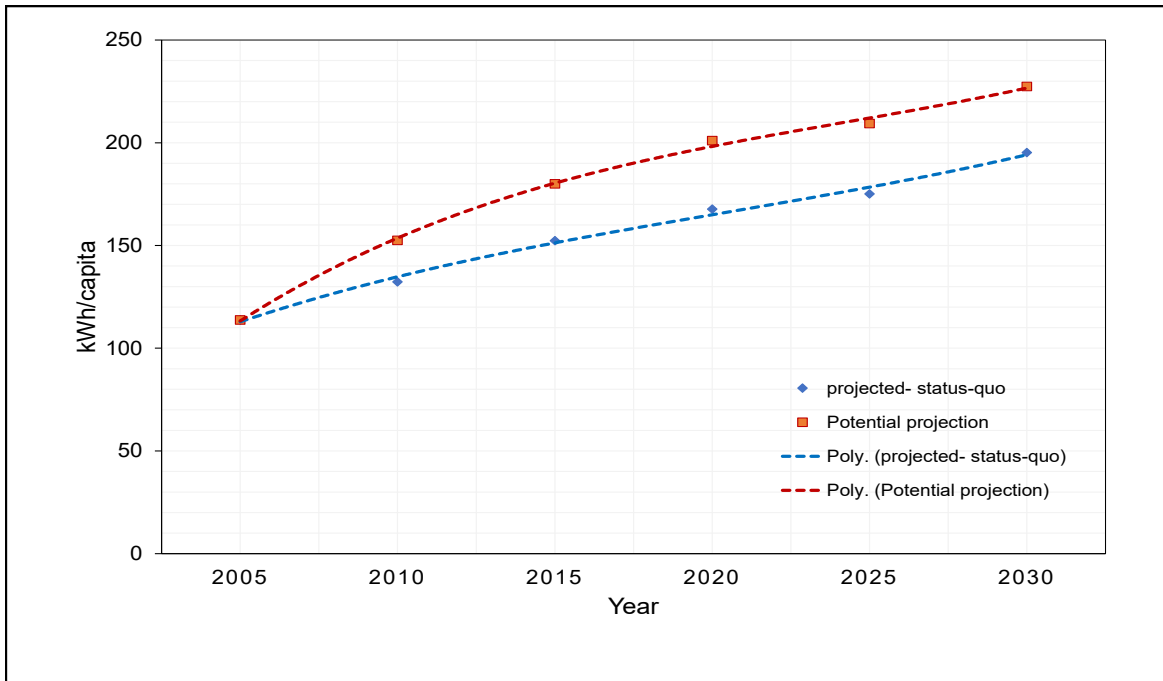


Fig. 6.49 Comparison of consumption based on study with current trend

6.8 Other System Considerations

Absorption refrigeration systems are cheap to run as they require a far less significant power to drive the solution pump than the power needed to drive the compressor in vapour compression refrigeration systems. They are also noiseless as there are no moving parts and require little or no maintenance. The refrigerants are cheap, environmental friendly and are readily available. These systems operate in vacuum conditions and there are normally no risk of leakages. The running cost of the vapour absorption refrigeration system is therefore, relatively very low compared to the vapour compression system and may be insignificant when integrated in a combined generation system such as combined cooling and power (CCP) or trigeneration system such as combined cooling heating and power systems (CCHP) since they add no extra burden on the system but use the heat that would be otherwise disposed and hence, increase utilisation and overall system efficiency. As a stand alone, the cost may be considered as the cost of the biomass solid fuel and logistics. However the initial capital cost is significantly high.

The performance ratio (COP) of these systems depends on the refrigerant pair but are generally low compared to vapour compression systems - usually less than 7.0. In cases where the absorption system is not very efficient and the refrigerant entering the evaporator is not pure ammonia (aqua-ammonia system), the evaporation will not be an isothermal process and the temperature in the evaporator will increase. This will inhibit the achievement of low temperature at saturation pressure. Other consequences include reduced refrigeration effect, decreased COP, variation of evaporator temperature and forced reduced evaporator pressured to achieve a set temperature. A rectification column is usually installed to improve the quality of refrigerant entering the evaporator. This will affect the initial capital cost of the system. The rectification column was not modelled in this study.

Generally, compared to other renewable energy options, biomass offers the advantage of being controlled and available when needed. The challenges associated with biomass fuel include handling, pre-processing, logistics and storage as well as low energy density and combustion emissions.

- Transportation of fuel accounts for a significant amount of its cost, so resources should ideally be available from local sources to reduce logistic expenses and carbon footprint. In most cases the rural areas are the natural habitat of biomass resources especially in the Africa region. Consequently, where the terrain is not a challenge, transportation cost will be reduced.
- Biomass has a relatively low energy density, implying a lot more biomass is needed to supply the same amount of energy as a traditional hydrocarbon fuel and twice the

amount of coal. However, the impact of this issue can be reduced by preprocessing the fuel to reduce both moisture and water content. Drying biomass fuel improves the overall efficiency of the system but this may affect the operating cost. Preprocessing can also be used to address the issue of length, size, quality and bulk density which influences the transport combustion efficiencies as well as contamination. Physical processing such as comminution - chipping, grinding, cutting and shredding may be used to reduce size and enhance use in conventional burners or storing in cellars.

- Ample space is usually required and depending on the magnitude and capacity of installation a manual or automated feed and/or handling system may be required.
- Flue from biomass combustion convey by-products to the environment. Biomass fuel emissions depend on the system design and fuel characteristics. Emission control of unburned hydrocarbons, oxides of nitrogen (NO_x) and sulphur (SO_x) may be put in place. Cyclones and multi-cyclones can be used as pre-collectors to remove large particles. Electrostatic precipitation (ESP) modules that are scalable devices employed to capture flue particulate content, preventing them from being flared into the atmosphere are in use in power stations such as Drax Power Station in the United Kingdom. ESP captures up to 99% of particulate including ozone.
- Currently, the issue of low yield, corrosion and atmospheric air contamination of biomass solid fuels have being drastically reduced and adequately managed. Drax Power Station for instance, have successfully converted six of their coal power plants to biomass. These plants operate on the application of the above mentioned measures. Similarly, some of these measures can be implemented with a project like this directly or with modification to meet the need.

Determining the optimal size of a particular application involves an iterative process but generally, system cost intensity tends to vary inversely with size. Stand alone systems in the range of 5 *MWth* - 25 *MWth* may cost between £2400.00 and £4000.00. The operation and maintenance costs of biomass systems are predominately the costs of labour and fuel. Operation is continual and should be assessed alongside purchase and storage needs. The estimation of capital and operation costs can be made by using the combination of exergy and economic analysis (exergoeconomic model) [94].

6.9 Summary

The chapter presented results of mathematical analysis and experimental evaluation of the performance of the thermochemical accumulator. The commercial available model of ClimateWell Solar Chiller (CWSC - CW10) at the Centre for Biomass Excellence - Arbor Project, Staffordshire University was used. The mathematical model was used to theoretically predict the coefficient of performance, while the rate of cooling was evaluated experimentally. The computer model was executed in a user friendly computer program. The parameters used are published system parameters from the literature and manufacturer's technical information manual, as well as data collected from experimental rig via data logger. The average COP showed good comparison and differed by 0.2% from published results. The cooling rate variation with evaporator inlet temperature for a fixed reactor temperature and system power, was found to be consistent as is the case of set cooling temperature with cooling capacity. The rate of cooling was observed to vary with load and set cooling temperature. However, average cooling power was about 10 kW.

The test for aqua-ammonia VARS was used to validate the model. It was tested in comparison to 6 experimental results and 3 theoretical. The results showed good comparison in trend and similarity with over 90% of the entire tests. The results from the model in most cases were better in terms of performance ratio. However, there were a few cases where the disparity was huge. In such case results from the model were double checked against the underlying governing equations of thermodynamics, material and mass continuity. The few disagreements are also reported.

Lastly, the issues surrounding the uptake of biomass energy and absorption cooling and the technologies to overcome the challenges were considered and discussed.

Chapter 7

Conclusions and Recommendations

This chapter gives an answer to the questions raised in the introductory chapter in the light of the experimental and theoretical findings of this study. It also proposes some recommendations for future studies to further enhance the use of biomass and vapour absorption refrigeration systems.

7.1 Conclusions

The following conclusions can be drawn from the present study:

A predictive model for the thermochemical accumulator was realised. Simulation results from the model showed good comparison with manufacturer's published data and data from similar studies. A COP of 0.6 was reached. The simulation was run for a variety of evaporator inlet and set cooling temperatures at different discharge power for cooling. The result shows that as the load increases, as simulated by increase in the evaporator inlet temperature, increase in discharge power for cooling would be needed to maintain the set cooling temperature. The experimental results collaborates the system response to high cooling demand obtained by simulation. It also shows that the system is sensitive to environmental changes. Overall, biomass solid fuel was the source energy to drive the refrigeration system. The experiment shows the potential of biomass as a reliable source of energy for the provision of cooling. The ClimateWell Solar Chiller can be adapted to run biomass or on biomass and solar energy simultaneously. This is an added advantage to the self-energy storage of the system. However, the following issues are noted with the CWSC:

- High sensitivity to slight system and environmental changes
- Requires trained and highly skilled personnel for installation and maintenance

- Installation and running costs are comparatively high and
- Regular reliance on OEM for service parts and call-outs.

The above issues may constitute a significant economic and operational setback in the use of the CWSC in a typical rural community considered in the study and may not be advised.

Vapour absorption refrigeration systems benefit from the ability to run on low quality thermal energy. The capability to handle heavy cooling and refrigeration duties would depend on the refrigeration working fluid-pair arrangement. Aqua-ammonia absorption refrigeration cycle has ammonia as the refrigerant and water the absorbent. Therefore, the system can provide or handle cooling temperatures at sub-zero levels without the issues of freeing as obtained with water refrigerant systems. Simulation and experimental results shows that aqua-ammonia absorption refrigeration system can run conveniently on a generator temperature from about 70 °C with COP reaching 0.7. Parametric evaluation from the model shows that at constant evaporator, condenser and absorber temperatures, the COP decreases with increase in generator temperature. The COP ranges between 0.84 for generator temperature of 60 °C and 0.76 for 90 °C, beyond which the variation is insignificant. The concentration of the refrigerant exiting the generator is dependent on the solution mass flow and temperature, and varies between 0.9 to 0.98 for the simulated data. This quantity is usually assumed to be 100%. Direct combustion of biomass is apt to provide the thermal energy required to drive absorption refrigeration system. The results from the model agrees with experimental and theoretical results.

Although the energy content of a biomass species is constant, the technology employed in the extraction of this energy, which is highly influenced by the form and end user requirement, influences and determines the useful energy derivable. The quantity of biomass fuel that will be required for a specified operation will be mainly influenced by the energy density of the fuel, all other characterisation properties being constant. But the effectiveness in cost and efficient energy production would rest mainly on the efficiency on the biomass combustion unit (boiler efficiency) and the heat exchanger effectiveness as depicted by the effect of temperature difference between the hot and the cold sides (ΔT).

The sustainability of biomass as an effective renewable energy source would depend on the following key factors:

- Availability of the resource (biomass)
- Proximity of the resource to the location of the generating plant
- Availability of effective conversion technologies

- Demand for the energy produced

From the feasibility study, Nigeria is endowed with a substantial amount of renewable energy resources. The biomass resource in the country is significant and sufficient to support the energy needs. The time series analysis predicts growth of the resource and indicates its sustainability amidst a growing population.

The issues associated with biomass energy technologies as pointed out, can be effectively managed and reduced by the technologies discussed. Some of these measures are already being implemented by some energy generating firms using biomass as the source fuel. An example is the Drax Power Station in the United Kingdom. Although it could be argued that Drax benefits from external economic support, and the importation of part of its biomass resources from outside the continent may impact its carbon footprint, it has shown that all other technical issues associated with biomass energy generation have been significantly reduced or completely eliminated. The profitability can be increased and carbon footprint reduced significantly, if the biomass resources are source or produced locally.

With proper utilisation of biomass, Nigeria's energy consumption can grow by up to a third in the short term. The natural distribution of the resource occurs mostly in the rural communities. This means that it can be source locally and processed in situ reducing cost and improving savings on carbon footprint.

The study proves that biomass can contribute to the energy share for the requirement of Nigeria. The use of biomass for refrigeration is straightforward and can replace the use of electricity to produce refrigeration.

The study shows that it is possible for Nigeria to use its own resources to reduce its global warming and carbon production.

This present study can be easily applied to another country of similar climate, topology and situation as Nigeria.

7.2 Recommendation

The present study has explored the use of biomass for the production of energy to drive vapour absorption refrigeration for cooling. Useful data on biomass energy potential was realised. To further this study and the efficient energy utilisation, the data could be used as a preliminary source to study the feasibility and impact of electricity production from biomass using available technologies such as steam turbines, indirect gas turbines, thermoelectricity, etc.

References

- [1] A. Cengel, Y. and J. Ghajar, A. (2015). *Heat and Mass Transfer, Fundamentals and Application, Fifth Edition in SI Units*, volume 5th.
- [2] Abdulateef, J., Alghoul, M., Zaharim, A., and Sopian, K. (2009). Experimental investigation on solar absorption refrigeration system in Malaysia. In *Proceedings of the 3rd WSEAS International Conference on Energy Planning, Energy Saving, Environment and Education EPESE 2009. Renewable Energy Sources.*, Malaysia.
- [3] Adeyeye, J. (2012). Africa In Fact. *The Journal of Good Governance Africa*, (4):21–24.
- [4] Aggarwal, S. K. (2013). Simulations of combustion and emissions characteristics of biomass-driven fuels. In Bundschuh, J., editor, *Technologies for Converting Biomass to Useful Energy*, chapter Two, pages 5 – 33. CRC Press, London, volume 4 edition.
- [5] Akinlo, A. E. (2008). Energy consumption and economic growth: Evidence from 11 Sub-Sahara African countries. *Energy Economics*, 30(5):2391–2400.
- [6] Al-Shemmeri, T., Lin, L., Wang, Y., Zeng, S., Huang, X., Li, S., and Yang, J. (2006). Characteristics of a diffusion absorption refrigerator driven by waste heat from engine-exhaust. *Proceedings of the Institution of mechanical Engineering, Part E: Journal of Process Mechanical Engineering*, 220:139 – 149.
- [7] Al-Shemmeri, T. T. (2011). Thermodynamics, performance analysis and computational modelling heat and power (CHP) systems. In Robert Beith, editor, *Small and micro combined heat and power (CHP) systems*, chapter Three, pages 43–69. Woodhead Publishing, London.
- [8] Al-Shemmeri, T. T., Yedla, R., and Wardle, D. (2015). Thermal characteristics of various biomass fuels in a small-scale biomass combustor. *Applied Thermal Engineering*, 85:243–251.
- [9] Al-Sulaiman, F. a., Hamdullahpur, F., and Dincer, I. (2011). Performance comparison of three trigeneration systems using organic rankine cycles. *Energy*, 36(9):5741–5754.
- [10] Alfaro, J. and Miller, S. (2014). Satisfying the rural residential demand in Liberia with decentralized renewable energy schemes. *Renewable and Sustainable Energy Reviews*, 30:903–911.
- [11] Aliyu, A. S., Dada, J. O., and Adam, I. K. (2015). Current status and future prospects of renewable energy in Nigeria. *Renew. Sustain. Energy Rev.*, 48:336–346.

REFERENCES

- [12] Alizadeh, S., Bahar, F., and Geoola, F. (1979). Design and optimisation of an absorption refrigeration system operated by solar energy. *Solar Energy*, 22(2):149–154.
- [13] Amosun, O. O. and Adedoyin, O. S. (2010). Global forest resources assessment 2010 country report, Nigeria: The Forest Resources Assessment Programme. pages 1–47.
- [14] Andiappan, V., Ng, D. K., and Bandyopadhyay, S. (2014). Synthesis of biomass-based trigeneration systems with uncertainties. *Industrial and Engineering Chemistry Research*, 53(46):18016–18028.
- [15] Ando, E. and Takeshita, I. (1984). Residential gas-fired absorption heat pump based on R 22-DEGDME pair. Part 1 thermodynamic properties of the R 22-DEGDME pair. *International Journal of Refrigeration*, 7(3):181–185.
- [16] Ansarinassab, H. and Mehrpooya, M. (2018). Investigation of a combined molten carbonate fuel cell, gas turbine and Stirling engine combined cooling heating and power (CCHP) process by exergy cost sensitivity analysis. *Energy Convers. Manag.*, 165(January):291–303.
- [17] Appleyard, D. (2016). Powering Africa’s Economic Growth with Decentralized Energy.
- [18] Arora, R. C. (2012). *Refrigeration and Air Conditioning*. PHI Learning Private Limited, New Delhi.
- [19] ASHRAE (2009). Thermodynamics and refrigeration cycles. *ASHRAE Handbook Fundamentals*, pages 21.1–21.67.
- [20] Avila, N., Carvallo, J. P., Shaw, B., and Kammen, D. M. (2017). The energy challenge in sub-Saharan Africa : A guide for advocates and policy makers Part 1 : Generating energy for sustainable and equitable development. *oxfam Researcher Background*, Part 1.
- [21] Baghernejad, A., Yaghoubi, M., and Jafarpur, K. (2016). Exergoeconomic comparison of three novel trigeneration systems using SOFC, biomass and solar energies. *Applied Thermal Engineering*, 104:534–555.
- [22] Bales, C. and Ayadi, O. (2009a). Modelling of a Commercial Absorption Heat Pump with Integral Storage. In *Effstock 2009 - The 11th International Conference on Energy Storage*, page Stockholm.
- [23] Bales, C. and Ayadi, O. (2009b). Modelling of commercial absorption heat pump with integral storage. In *Proceedings Effstock*.
- [24] Bales, C. and Gantenbein, P. (2007). Laboratory prototypes of thermo-chemical and sorption storage units ,Report B3—IEA SHC Task 32. *Report B3—IEA SHC Task 32*.
- [25] Bales, C., Jaehnig, D., Kerskes, H., and Zondag, H. (2008). Store Models for Chemical and Sorption Storage Units. *International Energy Agency - Solar Heating and Cooling Programme*.
- [26] Bales, C. and Norlander, S. (2005). TCA Evaluation:Lab measurements, modelling and system simulations. *Solar Energy Research Centre*, (Task 32).

REFERENCES

- [27] Banks, D. (2012). *An Introduction to Thermogeology: Ground Source Heating and Cooling*. Wiley-Blackwell, Oxford, UK, 2nd editio edition.
- [28] Barnes, D. F. and Floor, W. M. (1996). Rural energy in developing countries: A challenge for economic development. *Annual Review of Energy and the Environment*, 21(1):497–530.
- [29] Barry, M. L., Steyn, H., and Brent, A. (2011). Selection of renewable energy technologies for Africa: Eight case studies in Rwanda, Tanzania and Malawi. *Renewable Energy*, 36(11):2845–2852.
- [30] Bazilian, M., Nussbaumer, P., Rogner, H. H., Brew-Hammond, A., Foster, V., Pachauri, S., Williams, E., Howells, M., Niyongabo, P., Musaba, L., Gallach??ir, B. ., Radka, M., and Kammen, D. M. (2012). Energy access scenarios to 2030 for the power sector in sub-Saharan Africa. *Utilities Policy*, 20(1):1–16.
- [31] Bennamoun, L., Afzal, M. T., and Léonard, A. (2015). Drying of alga as a source of bioenergy feedstock and food supplement - A review.
- [32] Bhattacharya, S. C., Abdul Salam, P., Runqing, H., Somashekar, H. I., Racelis, D. A., Rathnasiri, P. G., and Yingyuad, R. (2005). An assessment of the potential for non-plantation biomass resources in selected Asian countries for 2010. *Biomass and Bioenergy*, 29(3):153–166.
- [33] Biosantech, T. A. S., Rutz, D., Janssen, R., and Drosch, B. (2013). *Biomass resources for biogas production*.
- [34] Birol, F., Cozzi, L., Gould, T., Bromhead, A., and Priddle, R. (2015). World Outlook Energy. *World Energy Outlook 2015*, pages 1–12.
- [35] Bowman, R. A., Mueller, A. C., and Nagle, W. (1940). Mean Temperature Difference in Design. *Transactions of the ASME*, 62(4):283–294.
- [36] Bowyer, J. L. (2001). Environmental implications of wood production in intensively managed plantations. *Wood fiber Sci.*, 33(3):318–333.
- [37] Briley, G. C. (2004). A History of Refrigeration. *ASHRAE Journal*.
- [38] Bvumbe, T. J. and Inambao, F. L. (2013). Operational evaluation of the performance of a solar powered absorption system in Pretoria. 24(3):26–32.
- [39] Cabeza, L. and de Gracia, A. (2015). *Thermal energy storage (TES) systems for cooling in residential buildings*.
- [40] Caputo, A. C., Palumbo, M., Pelagagge, P. M., and Scacchia, F. (2005). Economics of biomass energy utilization in combustion and gasification plants: Effects of logistic variables. *Biomass and Bioenergy*, 28(1):35–51.
- [41] Chahartaghi, M. and Kharkeshi, B. A. (2018). Performance analysis of a combined cooling, heating and power system with PEM fuel cell as a prime mover. *Appl. Therm. Eng.*, 128:805–817.

REFERENCES

- [42] Chen, J. and Andresen, B. (1995). Optimal analysis of primary performance parameters for an endoreversible absorption heat pump. *Heat Recovery Systems and CHP*, 15(8):723–731.
- [43] Chen, J., Kim, K. J., and Herold, K. E. (1996). Performance enhancement of a diffusion - Absorption refrigerator. *International Journal of Refrigeration*, 19(3):208–218.
- [44] Chiou-Wei, S. Z., Chen, C.-F., and Zhu, Z. (2008). Economic growth and energy consumption revisited — Evidence from linear and nonlinear Granger causality. *Energy Economics*, 30(6):3063–3076.
- [45] Chiumenti, A., Boscaro, D., Da Borso, F., Sartori, L., and Pezzuolo, A. (2018). Biogas from fresh spring and summer grass: Effect of the harvesting period. *Energies*, 11(6).
- [46] Collazo, J., Porteiro, J., Míguez, J. L., Granada, E., and Gómez, M. A. (2012). Numerical simulation of a small-scale biomass boiler. In *Energy Conversion and Management*, volume 64, pages 87–96.
- [47] Conde, M. (2006). Thermophysical Properties of {NH₃ + H₂O} Mixtures for the Industrial Design of Absorption Refrigeration Equipment. *Update*.
- [48] Conde, M. R. (2004). Properties of aqueous solutions of lithium and calcium chlorides: formulations for use in air conditioning equipment design. *International Journal of Thermal Sciences*, 43(4):367–382.
- [49] Cook, E. (1971). The Flow of Energy in an Industrial Society. *Scientific American*, 225(3):134–144.
- [50] Cook, P. (2011). Infrastructure, rural electrification and development. *Energy for Sustainable Development*, 15(3):304–313.
- [51] DEFRA (2007). Planting and Growing Miscanthus. *DEFRA. Crops for Energy Branch*, (July):1–19.
- [52] Deichmann, U., Meisner, C., Murray, S., and Wheeler, D. (2011). The economics of renewable energy expansion in rural Sub-Saharan Africa. *Energy Policy*, 39(1):215–227.
- [53] Delivand, M. K., Cammerino, A. R. B., Garofalo, P., and Monteleone, M. (2015). Optimal locations of bioenergy facilities, biomass spatial availability, logistics costs and GHG (greenhouse gas) emissions: A case study on electricity productions in South Italy. *Journal of Cleaner Production*, 99:129–139.
- [54] Dequaire, X. (2012). Passivhaus as a low-energy building standard: Contribution to a typology. *Energy Effic.*
- [55] Desideri, U., Proietti, S., and Sdringola, P. (2009). Solar-powered cooling systems: Technical and economic analysis on industrial refrigeration and air-conditioning applications. *Applied Energy*, 86(9):1376–1386.
- [56] Dong, L., Liu, H., and Riffat, S. (2009). Development of small-scale and micro-scale biomass-fuelled CHP systems - A literature review.

REFERENCES

- [57] Drapcho, C. M., Nhuan, N. P., and Walker, T. H. (2008). *Biofuels Feedstocks*.
- [58] Du, S., Wang, R. Z., and Chen, X. (2017). Development and experimental study of an ammonia water absorption refrigeration prototype driven by diesel engine exhaust heat. *Energy*, 130:420–432.
- [59] Du, S., Wang, R. Z., Lin, P., Xu, Z. Z., Pan, Q. W., and Xu, S. C. (2012). Experimental studies on an air-cooled two-stage NH₃-H₂O solar absorption air-conditioning prototype. *Energy*, 45(1):581–587.
- [60] Ebohon, O. J. (1996). Energy, economic growth and causality in developing countries: a case study of Tanzania and Nigeria. *Energy Policy*, 24(5):447–453.
- [61] Eggoh, J. C., Bangake, C., and Rault, C. (2011). Energy consumption and economic growth revisited in African countries. *Energy Policy*, 39(11):7408–7421.
- [62] EIA (2016a). Annual Energy Outlook 2016 with projections to 2040 .
- [63] EIA (2016b). *International Energy Outlook 2016*, volume 0484(2016).
- [64] El-Shaarawi, M. A., Said, S. A., and Siddiqui, F. R. (2014). Unsteady thermodynamic analysis for a solar driven dual storage absorption refrigeration cycle in Saudi Arabia. *Sol. Energy*, 110:286–302.
- [65] Eriksson, O., Finnveden, G., Ekvall, T., and Björklund, A. (2007). Life cycle assessment of fuels for district heating: A comparison of waste incineration, biomass- and natural gas combustion. *Energy Policy*, 35(2):1346–1362.
- [66] Fan, Y., Luo, L., and Souyri, B. (2007). Review of solar sorption refrigeration technologies: Development and applications. *Renewable and Sustainable Energy Reviews*, 11(8):1758–1775.
- [67] Florides, G., Kalogirou, S., Tassou, S., and Wrobel, L. (2002). Modelling and simulation of an absorption solar cooling system for Cyprus. *Solar Energy*, 72(1):43–51.
- [68] Food and Agricultural Organisation of the United Nations (2014). Food and Agricultural Organisation of the United Nations.
- [69] Ganesh, N. S. and Srinivas, T. (2011). Evaluation of thermodynamic properties of ammonia- water mixture up to 100 bar for power application systems. *Journal of Mechanical Engineering Research*, 3(1):25–39.
- [70] Garousi Farshi, L., Seyed Mahmoudi, S. M., and Rosen, M. A. (2011). Analysis of crystallization risk in double effect absorption refrigeration systems. *Applied Thermal Engineering*, 31(10):1712–1717.
- [71] Gilat, A. (2016). *Matlab an Introduction With Applications*, volume 53. John Wiley & Sons, Colubus, Ohio, 6th edition.
- [72] Gold, S. and Seuring, S. (2011). Supply chain and logistics issues of bio-energy production. *Journal of Cleaner Production*, 19(1):32–42.

REFERENCES

- [73] Grossman, G., Gommed, K., and Gadoth, D. (1991). Computer Model for Simulation of Absorption Systems in Flexible and Modular Form. *Oak Ridge National Laboratory*.
- [74] Hartmann, D. L., Tank, A. M. G. K., and Rusticucci, M. (2013). IPCC Fifth Assessment Report, Climate Change 2013: The Physical Science Basis. *IPCC*, AR5:31 – 39.
- [75] Hasan, J., Keshwani, D. R., Carter, S. F., and Treasure, T. H. (2010). Thermochemical Conversion of Biomass to Power and Fuels. In Cheng, J., editor, *Biomass to Renewable Energy Processes*, chapter Ten, pages 437 – 489. CRC Press, London.
- [76] Heaton, E. A., Dohleman, F. G., Miguez, A. F., Juvik, J. A., Lozovaya, V., Widholm, J., Zabolina, O. A., McIsaac, G. F., David, M. B., Voigt, T. B., Boersma, N. N., and Long, S. P. (2010). Miscanthus. A Promising Biomass Crop. *Advances in Botanical Research*, 56(C):76–137.
- [77] Herold, K. E., Radermacher, R., and Klein, S. A. (1996). *Absorption Chillers and Heat Pumps*.
- [78] Hong, D., Chen, G., Tang, L., and He, Y. (2011). Simulation research on an EAX (Evaporator-Absorber-Exchange) absorption refrigeration cycle. *Energy*, 36(1):94–98.
- [79] Höök, M. and Tang, X. (2013). Depletion of fossil fuels and anthropogenic climate change-A review. *Energy Policy*, 52:797–809.
- [80] Horuz, I. and Callander, T. M. S. (2004). Experimental investigation of a vapor absorption refrigeration system. *Int. J. Refrig.*, 27(1):10–16.
- [81] IEA (2014). Africa Energy Outlook: A focus on Energy Prospect in Sub-Saharan Africa (World Energy Outlook Special Report). Technical report.
- [82] IEA (2017). Key world energy statistics. Technical report.
- [83] IEA (2018). Sustainable Development Scenarios - A cleaner and more inclusive energy future.
- [84] IPCC (2001). Intergovernmental Panel on Climate Change.
- [85] IPCC (2006). Intergovernmental Panel on Climate Change. In *Guidelines for National Greenhouse Gas Inventories*, volume 4.
- [86] IRENA (2015). Africa 2030: Roadmap for a Renewable Energy Future. *International Renewable energy Agency REmap 2030: A renewable Energy Roadmap*, page 72.
- [87] Iye, E. L. and Bilsborrow, P. E. (2013). Assessment of the availability of agricultural residues on a zonal basis for medium- to large-scale bioenergy production in Nigeria. *Biomass and Bioenergy*, 48:66–74.
- [88] Izquierdo, M., Venegas, M., Rodríguez, P., and Lecuona, A. (2004). Crystallization as a limit to develop solar air-cooled LiBr-H₂O absorption systems using low-grade heat. *Solar Energy Materials and Solar Cells*, 81(2):205–216.

REFERENCES

- [89] Jakob, U. and Eicker, U. (2006). Simulation and performance of diffusion absorption cooling machines for solar cooling. *Published in the Proceedings of the 9th World Renewable Energy Congress. Florence, (August):*pages 21–25.
- [90] Jakob, U., Eicker, U., Schneider, D., and Teuber, A. (2007). Heat transfer in Components and Systems for Sustainable Energy Technologies. In *Heat-SET 2007*, France. Editions-GRETh.
- [91] Jakob, U., Eicker, U., Taki, A. H., and Cook, M. J. (2003). Development of an optimised solar driven diffusion-absorption cooling machine. In *Proceedings of the ISES Solar World Congress*.
- [92] Jeng, C. Y., Yo, Y. Y., Chuah, Y. K., and Chu, P. H. (1989). A simple analysis on the performance of absorption heat pump system. In *Proceedings of the 24th Intersociety Energy Conversion Engineering Conference*.
- [93] Jindal, V. K. and Siebenmorgen, T. J. (1987). Effects of Oven Drying Temperature and Drying Time on Rough Rice Moisture Content Determination. *Transactions of the ASABE*, 30(4)(4):1185–1192.
- [94] Jing, Y., Li, Z., Liu, L., and Lu, S. (2018). Exergoeconomic assessment of solar absorption and absorption-compression hybrid refrigeration in building cooling. *Entropy*, 20(2).
- [95] Kaita, Y. (2001). Thermodynamic properties of lithium bromide–water solutions at high temperatures. *International Journal of Refrigeration*, 24(5):374–390.
- [96] Kalinowski, P., Hwang, Y., Radermacher, R., Al Hashimi, S., and Rodgers, P. (2009). Application of waste heat powered absorption refrigeration system to the LNG recovery process. *International Journal of Refrigeration*, 32(4):687–694.
- [97] Karamangil, M., Coskun, S., Kaynakli, O., and Yamankaradeniz, N. (2010a). A simulation study of performance evaluation of single-stage absorption refrigeration system using conventional working fluids and alternatives. *Renewable and Sustainable Energy Reviews*, 14(7):1969–1978.
- [98] Karamangil, M. I., Coskun, S., Kaynakli, O., and Yamankaradeniz, N. (2010b). A simulation study of performance evaluation of single-stage absorption refrigeration system using conventional working fluids and alternatives.
- [99] Karekezi, S. (2002). Poverty and energy in Africa—A brief review.
- [100] Karlsson, M. (2004). The Energy Challenge for Achieving the Millennium Development Goals:Energy and the MDGs. *UN Energy*.
- [101] Kauffmann, C. (2008). Energy and Poverty in Africa. *OECD Development Center Policy Insights*, (8):1–2.
- [102] Kaushik, S. C. and Bhardwaji, S. C. (1982). Theoretical Analysis of Ammonia-Water Absorption Cycles for Refrigeration and. *Energy Reserach*, 6(March 1982):205–225.

REFERENCES

- [103] Kaushik, S. C., Gadhi, S. M. B., Agarwal, R. S., and Kumari, R. (1988). Modeling and simulation studies on single/double-effect absorption cycle using water-multicomponent salt (MCS) mixture. *Solar Energy*, 40(5):431–441.
- [104] Kaushik, S. C. and Kumar, R. (1989). Conceptual thermodynamic design of a dual mode absorption cycle with an auxiliary heat exchanger. *Heat Recovery Systems and CHP*, 9(4):335–341.
- [105] Kaygusuz, K. (2011). Energy services and energy poverty for sustainable rural development. *Renewable and Sustainable Energy Reviews*, 15(2):936–947.
- [106] Kays, W. M. and London, A. L. (1984). *Compact Heat Exchangers*; McGraw-Hill, New York, USA.
- [107] Kebede, E., Kagochi, J., and Jolly, C. M. (2010). Energy consumption and economic development in Sub-Sahara Africa. *Energy Economics*, 32(3):532–537.
- [108] Kemausuor, F., Adaramola, M. S., and Morken, J. (2018). A Review of Commercial Biogas Systems and Lessons for Africa. *Energies*, 11(11):1–21.
- [109] Kherris, S., Makhlof, M., Zebbar, D., and Sebbane, O. (2013). Contribution study of the thermodynamics properties of the ammonia-water mixtures. *Thermal Science*, 17(3):891–902.
- [110] Kilic, M. and Kaynakli, O. (2007). Second law-based thermodynamic analysis of water-lithium bromide absorption refrigeration system. *Energy*, 32(8):1505–1512.
- [111] Kim, D. S. and Infante Ferreira, C. A. (2008). Solar refrigeration options - a state-of-the-art review. *International Journal of Refrigeration*, 31(1):3–15.
- [112] Knowles, J. (2011). Overview of small and micro combined heat and power (CHP) systems. In Beith, R., editor, *Small and micro combined heat and power (CHP) systems*, chapter One, pages 3 – 16. London.
- [113] Kraft, J. and Kraft, A. (1978). On the relationship between energy and GNP. *Journal of Energy and Development*, 3:401–403.
- [114] Kruse, A., Funke, A., and Titirici, M.-M. (2013). Hydrothermal conversion of biomass to fuels and energetic materials. *Current opinion in chemical biology*, 17(3):515–21.
- [115] Lakaniemi, A.-M., Tuovinen, O. H., and Puhakka, J. A. (2013). Anaerobic conversion of microalgal biomass to sustainable energy carriers—a review. *Bioresource technology*, 135:222–31.
- [116] Lansing, F. L. (1978). Computer Modeling of Lithium Bromide/Water Absorption Refrigeration Unit. Technical report, Jet Propulsion Laboratory, NASA Deep Space Network, California Institute of Technology, California.
- [117] Lazzarin, R. M. (1996). Ammonia-water absorption machines for refrigeration: theoretical and real performances. *International Journal of Refrigeration*, 19(4):239–246.
- [118] Lewandowski, I., Clifton-Brown, J., Scurlock, J., and Huisman, W. (2000). Miscanthus: European experience with a novel energy crop. *Biomass and Bioenergy*, 19(4):209–227.

REFERENCES

- [119] Lin, L., Wang, Y., Al-Shemmeri, T., Ruxton, T., Turner, S., Zeng, S., Huang, J., He, Y., and Huang, X. (2007). An experimental investigation of a household size trigeneration. *Applied Thermal Engineering*, 27(2-3):576–585.
- [120] Liu, H. (2011). Biomass fuels for small and micro combined heat and power (CHP) systems. In *Small and micro combined heat and power (CHP) systems*, chapter Five, pages 88 – 122. Woodhead Publishing, London.
- [121] Loo, S. V. and Koppejan, J. (2008). *The handbook of biomass combustion and co-firing*; Earthscan, United Kingdom.
- [122] Lope Tabil, P. A. and Kashaninejad, M. (2011). Biomass Feedstock Pre-Processing – Part 1: Pre- Treatment, Biofuel’s Engineering Process Technology. *Biofuel’s Engineering Process Technology*, pages 978–953–307–480–1.
- [123] Macriss, R. A., Gutraj, J. M., and Zawacki, T. S. (1987). Printed in the United States of America . Available from National Technical Information Service U . S . Department of Commerce 5285 Port Royal Road , Springfield , Virginia 22161 NTIS price codes-Printed Copy : A08 Microfiche A01. Technical report, Institute of Gas Technology, Chicago, Illinois.
- [124] Mahmoud, A., Arlabosse, P., and Fernandez, A. (2011). Application of a thermally assisted mechanical dewatering process to biomass. *Biomass and Bioenergy*, 35(1):288–297.
- [125] Mandelli, S., Barbieri, J., Mereu, R., and Colombo, E. (2016). Off-grid systems for rural electrification in developing countries: Definitions, classification and a comprehensive literature review.
- [126] Manzela, A. A., Hanriot, S. M., Cabezas-Gómez, L., and Sodr e, J. R. (2010). Using engine exhaust gas as energy source for an absorption refrigeration system. *Applied Energy*, 87(4):1141–1148.
- [127] Marchetti, C. (1977). Primary energy substitution models: On the interaction between energy and society. *Technological Forecasting and Social Change*, 10(4):345–356.
- [128] Mathkor, R. Z., Agnew, B., Al-Weshahi, M. A., and Latrsh, F. (2015). Exergetic analysis of an integrated tri-generation organic rankine cycle. *Energies*, 8(8):8835–8856.
- [129] Mbikan, M. and Al-Shemmeri, T. (2017). Computational model of a biomass driven absorption refrigeration system. *Energies*.
- [130] McKendry, P. (2002). Energy production from biomass (Part 1): Overview of biomass. *Bioresour Technol*, 83:37–46.
- [131] Meraz, L., Dom nguez, A., Kornhauser, I., and Rojas, F. (2003). A thermochemical concept-based equation to estimate waste combustion enthalpy from elemental composition. *Fuel*, 82(12):1499–1507.
- [132] Mert, S. O., Dincer, I., and Ozcelik, Z. (2012). Performance investigation of a transportation PEM fuel cell system. *Int. J. Hydrogen Energy*, 37(1):623–633.

REFERENCES

- [133] Mertzis, D., Mitsakis, P., Tsiakmakis, S., Manara, P., Zabaniotou, A., and Samaras, Z. (2014). Performance analysis of a small-scale combined heat and power system using agricultural biomass residues: The smart CHP demonstration project. *Energy*, 64:367–374.
- [134] Misra, R., Sahoo, P., and Gupta, A. (2006). Thermoeconomic evaluation and optimization of an aqua-ammonia vapour-absorption refrigeration system. *International Journal of Refrigeration*, 29(1):47–59.
- [135] Mitchell, C. P., Stevens, E. A., and Watters, M. P. (1999). Short-rotation forestry - Operations, productivity and costs based on experience gained in the UK. *Forest Ecology and Management*, 121(1-2):123–136.
- [136] Mohammed, Y., Mokhtar, A., Bashir, N., and Saidur, R. (2013). An overview of agricultural biomass for decentralized rural energy in Ghana. *Renewable and Sustainable Energy Reviews*, 20(0):15–25.
- [137] Moler, C. and Little, J. (2020). A history of MATLAB. *Proc. ACM Program. Lang.*
- [138] Moner-Girona, M., Ghanadan, R., Jacobson, A., and Kammen, D. M. (2006). Decreasing PV costs in Africa. *Refocus*, 7(1):40–45.
- [139] Morrissey, J. (2017). The energy challenge in sub-Saharan Africa : A guide for advocates and policy makers Part 2: Addressing energy poverty. (September).
- [140] Mukasa, A. D., Mutambatsere, E., Arvanitis, Y., and Triki, T. (2015). Wind energy in sub-Saharan Africa: Financial and political causes for the sector’s under-development. *Energy Research and Social Science*, 5:90–104.
- [141] Muthu, V., Saravanan, R., and Renganarayanan, S. (2008). Experimental studies on R134a-DMAC hot water based vapour absorption refrigeration systems. *International Journal of Thermal Sciences*, 47(2):175–181.
- [142] Nanka-Bruce, O. (2010). *The socio economic drivers of rural electrification in Sub-Saharan Africa*. Number August.
- [143] Narayankhedkar, K. G. and Maiya, M. P. (1985). Investigations on triple fluid vapour absorption refrigerator. *International Journal of Refrigeration*, 8(6):335–342.
- [144] Nhuchhen, D. R. and Abdul Salam, P. (2012). Estimation of higher heating value of biomass from proximate analysis: A new approach. *Fuel*, 99:55–63.
- [145] Oberweis, S. and Al-Shemmeri, T. (2012). Performance Evaluation of a Lithium-Chloride Absorption Refrigeration and an Assessment of Its Suitability for Biomass Waste Heat. *Applied Sciences*, 2(4):709–725.
- [146] Ohimain, E. I. (2015). First generation bioethanol projects in Nigeria: Benefits and barriers. *Energy Sources, Part B Econ. Plan. Policy*, 10(3):306–313.
- [147] Ojolo, S., Orisaleye, J., Ismail, S., and Abolarin, S. (2012). Technical potential of biomass energy in Nigeria. *Ife J. Technol.*, 21(2):60–65.
- [148] Onyeji, I., Bazilian, M., and Nussbaumer, P. (2012). Contextualizing electricity access in sub-Saharan Africa. *Energy for Sustainable Development*, 16(4):520–527.

REFERENCES

- [149] Ouedraogo, N. S. (2013). Energy consumption and economic growth: Evidence from the economic community of West African States (ECOWAS). *Energy Economics*, 36:637–637.
- [150] Özgür, T. and Yakaryılmaz, A. C. (2018). A review: Exergy analysis of PEM and PEM fuel cell based CHP systems. *Int. J. Hydrogen Energy*, 43(38):17993–18000.
- [151] Ozturk, I., Aslan, A., and Kalyoncu, H. (2010). Energy consumption and economic growth relationship: Evidence from panel data for low and middle income countries. *Energy Policy*, 38(8):4422–4428.
- [152] Pang, S. and Mujumdar, A. S. (2010). Drying of Woody Biomass for Bioenergy: Drying Technologies and Optimization for an Integrated Bioenergy Plant. *Drying Technology*, 28(5):690–701.
- [153] Pátek, J. and Klomfar, J. (1995). Simple functions for fast calculations of selected thermodynamic properties of the ammonia-water system. *International Journal of Refrigeration*, 18(4):228–234.
- [154] Payne, F. A. (1984). Energy and mass Flow Computation in Biomass Combustion Systems. In *Transactions of the American Society of Agricultural Engineers*, pages 1532 – 1541. American Society of Agricultural Engineers.
- [155] Perez-Blanco, H. (1984). Absorption heat pump performance for different types of solutions. *International Journal of Refrigeration*, 7(2):115–122.
- [156] Plis, P. and Wilk, R. K. (2011). Theoretical and experimental investigation of biomass gasification process in a fixed bed gasifier. *Energy*, 36(6):3838–3845.
- [157] Prasad, G. (2011). Improving access to energy in sub-Saharan Africa. *Current Opinion in Environmental Sustainability*, 3(4):248–253.
- [158] Puig-Arnavat, M., Bruno, J. C., and Coronas, A. (2014). Modeling of trigeneration configurations based on biomass gasification and comparison of performance. *Applied Energy*, 114:845–856.
- [159] Rachford, H.H. Rice, J.D. (1952). Procedure for Use of Electrical Digital Computers in Calculating Flash Vaporization Hydrocarbon Equilibrium. *Trans AIME*, 4:19–20.
- [160] Reddy, a. S., Ahmed, I., Kumar, T. S., Reddy, a. V. K., and Bharathi, V. V. P. (2014). Analysis Of Steam Turbines 1. *Int. Ref. J. Eng. Sci.*
- [161] Rentizelas, A. A. (2016). Biomass storage. In *Biomass Supply Chains for Bioenergy and Biorefining*, pages 127–146.
- [162] Rentizelas, A. A., Tolis, A. J., and Tatsiopoulou, I. P. (2009). Logistics issues of biomass: The storage problem and the multi-biomass supply chain.
- [163] Richard c., F. and Jhon H., S. (1988). Fundamentals of air pollution engineering.
- [164] Richard Hess, J., Wright, C. T., and Kenney, K. L. (2007). Cellulosic biomass feedstocks and logistics for ethanol production. *Biofuels, Bioproducts and Biorefining*, 1(3):181–190.

REFERENCES

- [165] Richardson, W. (2015). *Woodfuel Standards and Waste Wood; Forestry Commission, Scotland*.
- [166] Ruiz, J., Juárez, M., Morales, M., Muñoz, P., and Mendivil, M. (2013). Biomass gasification for electricity generation: Review of current technology barriers. *Renewable and Sustainable Energy Reviews*, 18:174–183.
- [167] Sahay, A., Sethi, V. K., Tiwari, A. C., and Pandey, M. (2015). A review of solar photovoltaic panel cooling systems with special reference to Ground coupled central panel cooling system (GC-CPCS). *Renewable and Sustainable Energy Reviews*, 42:306–312.
- [168] Said, S. A. M., El-Shaarawi, M. A. I., and Siddiqui, M. U. (2012). Alternative designs for a 24-h operating solar-powered absorption refrigeration technology. *International Journal of Refrigeration*, 35(7):1967–1977.
- [169] Sambo, A. S. (2009). Strategic Developments In Renewable Energy In Nigeria. *Int. Assoc. Energy Economics*, pages 15–19.
- [170] Sanjuan, C., Soutullo, S., and Heras, M. (2010). Optimization of a solar cooling system with interior energy storage. *Solar Energy*, 84(7):1244–1254.
- [171] SANTAMOURIS, M. and ARGIRIOU, A. (1994). Renewable Energies and Energy Conservation Technologies for Buildings in Southern Europe. *International Journal of Solar Energy*, 15(1-4):69–79.
- [172] Santamouris, M., Papanikolaou, N., Livada, I., Koronakis, I., Georgakis, C., Argiriou, A., and Assimakopoulos, D. (2001). On the impact of urban climate on the energy consumption of buildings. *Solar Energy*, 70(3):201–216.
- [173] Sarbu, I. and Sebarchievici, C. (2015). General review of solar-powered closed sorption refrigeration systems. *Energy Conversion and Management*, 105:403–422.
- [174] Shaaban, M. and Petinrin, J. O. (2014). Renewable energy potentials in Nigeria: Meeting rural energy needs. *Renewable and Sustainable Energy Reviews*, 29:72–84.
- [175] Siddiqui, M. U. and Said, S. A. M. (2015). A review of solar powered absorption systems. *Renewable and Sustainable Energy Reviews*, 42:93–115.
- [176] Sims, R. E. H. and Venturi, P. (2004). All-year-round harvesting of short rotation coppice eucalyptus compared with the delivered costs of biomass from more conventional short season, harvesting systems. *Biomass and Bioenergy*, 26(1):27–37.
- [177] Smil, V. (2007). The two prime movers of globalization: History and impact of diesel engines and gas turbines.
- [178] Sokhansanj, S., Kumar, A., and Turhollow, A. F. (2006). Development and implementation of integrated biomass supply analysis and logistics model (IBSAL). *Biomass and Bioenergy*, 30(10):838–847.
- [179] Srihirin, P., Aphornratana, S., and Chungpaibulpatana, S. (2000). A review of absorption refrigeration technologies. *Renewable and Sustainable Energy Reviews*, 5(4):343–372.

REFERENCES

- [180] Srihirin, P., Aphornratana, S., and Chungpaibulpatana, S. (2001). A review of absorption refrigeration technologies. *Renewable and Sustainable Energy Reviews*, 5(4):343–372.
- [181] Ståhl, M., Granström, K., Berghel, J., and Renström, R. (2004). Industrial processes for biomass drying and their effects on the quality properties of wood pellets. *Biomass and Bioenergy*, 27(6):621–628.
- [182] Sun, D.-w. (1997). Thermodynamic design data and optimum design maps for absorption refrigeration systems. 17(3).
- [183] Sun, D.-w. (1998). Comparison of the performances of NH₃-H₂O, NH₃-LiNO₃ and NH₃-NaSCN absorption refrigeration systems. *Energy Conversion and Management*, 39(5-6):357–368.
- [184] Sun, J., Fu, L., Sun, F., and Zhang, S. (2014). Experimental study on a project with CHP system basing on absorption cycles. *Applied Thermal Engineering*, 73(1):732–738.
- [185] Taha Al-Zubaydi, A. Y. (2011). Solar Air Conditioning and Refrigeration with Absorption Chillers Technology in Australia – An Overview on Researches and Applications. *Journal of Advanced Science and Engineering Research*, 1:23–41.
- [186] Tanaka, N. (2010). World Energy Outlook.
- [187] Tanaka, N. I. e. A. P., Development, K. O. U. N., and Yumkella, k. K. U. N. I. D. O. (2010). Energy Poverty: How to make modern energy access universal? *World Energy Outlook*, (September):52.
- [188] Tariq, A. S., Reupke, P., and Sarwar, G. (1994). *Biomass combustion systems: a guide for monitoring and efficient operation*.
- [189] Taylor, P. and Kostic, M. M. (2008). Energy : Global and Historical Background Energy : Global and Historical Background. *Encyclopedia of Energy Engeneering*, pages 1–15.
- [190] Toscano, G. and Foppa Pedretti, E. (2009). Calorific Value Determination of Solid Biomass Fuel By Simplified Method. *Journal of Agricultural Engineering*, 40(3):1–6.
- [191] Turkson, J. and Wohlgemuth, N. (2001). Power sector reform and distributed generation in sub-Saharan Africa. *Energy Policy*, 29(2):135–145.
- [192] Ullah, K., Saidur, R., Ping, H., Akikur, R., and Shuvo, N. (2013). A review of solar thermal refrigeration and cooling methods. *Renewable and Sustainable Energy Reviews*, 24:499–513.
- [193] UN (2017). Transforming our world: The 2030 agenda for sustainable development – 17 Goals To Transform Our World. *United Nations Sustainable Development Goals*, (A/RES/70/1).
- [194] UNEP (2005). Working group 3 report: Mitigation of climate change. *Intergovernmental Panel on Climate Change*, 3(09):52–57.

REFERENCES

- [195] Vaezi, M., Passandideh-Fard, M., Moghiman, M., and Charmchi, M. (2012). On a methodology for selecting biomass materials for gasification purposes. *Fuel Processing Technology*, 98:74–81.
- [196] Veal, M. W. (2010). Biomass Logistics. In Cheng, J., editor, *Biomass to Renewable Energy Processes*, chapter Four, pages 71–133. CRC Press.
- [197] Vinterback, J. (2004). Pellets 2002: The first world conference on pellets. In *Biomass and Bioenergy*, volume 27, pages 513–520.
- [198] Wahlund, B., Yan, J., and Westermarck, M. (2002). A total energy system of fuel upgrading by drying biomass feedstock for cogeneration: A case study of Skellefte?? bioenergy combine. *Biomass and Bioenergy*, 23(4):271–281.
- [199] Welsch, M., Bazilian, M., Howells, M., Divan, D., Elzinga, D., Strbac, G., Jones, L., Keane, A., Gielen, D., Balijepalli, V. S. K. M., Brew-Hammond, A., and Yumkella, K. (2013). Smart and Just Grids for sub-Saharan Africa: Exploring options. *Renewable and Sustainable Energy Reviews*, 20:336–352.
- [200] WEO (2016). International Energy Agency.
- [201] Williams, A., Jones, J. M., Ma, L., and Pourkashanian, M. (2012). Pollutants from the combustion of solid biomass fuels.
- [202] Williams, D. (2017). US EPA recognition for Combined Heat and Power Plants.
- [203] Wolde-Rufael, Y. (2004). Disaggregated industrial energy consumption and GDP: The case of Shanghai, 1952-1999. *Energy Economics*, 26(1):69–75.
- [204] Wolde-Rufael, Y. (2005). Energy demand and economic growth: The African experience. *Journal of Policy Modeling*, 27(8):891–903.
- [205] World Bank (2017). Sub-Saharan Africa Data - World Bank Group.
- [206] World Bank (2019). Population, total | Data.
- [207] Wotton, B. M., Gould, J. S., McCaw, W. L., Cheney, N. P., and Taylor, S. W. (2012). Flame temperature and residence time of fires in dry eucalypt forest. *International Journal of Wildland Fire*, 21(3):270–281.
- [208] Wu, W., Zhang, X., Li, X., Shi, W., and Wang, B. (2012). Comparisons of different working pairs and cycles on the performance of absorption heat pump for heating and domestic hot water in cold regions. *Applied Thermal Engineering*, 48:349–358.
- [209] Xu, F. and Goswami, D. Y. (1999). Thermodynamic properties of ammonia-water mixtures for power-cycle applications. *Energy*, 24(6):525–536.
- [210] Xu, Z. Y., Wang, R. Z., and Xia, Z. Z. (2013). A novel variable effect LiBr-water absorption refrigeration cycle. *Energy*, 60:457–463.
- [211] Yashwanth, B. L., Shotorban, B., Mahalingam, S., Lautenberger, C. W., and Weise, D. R. (2016). A numerical investigation of the influence of radiation and moisture content on pyrolysis and ignition of a leaf-like fuel element. *Combustion and Flame*, 163:301–316.

REFERENCES

- [212] Yoo, S. H. (2006). The causal relationship between electricity consumption and economic growth in the ASEAN countries. *Energy Policy*, 34(18):3573–3582.
- [213] Ziegler, B. and Trepp, C. (1984). Equation of state for ammonia-water mixtures. *International Journal of Refrigeration*, 7(2):101–106.
- [214] Zugenmaier, P. (2008). *Springer Series in Wood Science*.

Appendix A

Absorption Cooling and Analytical Modelling

A.1 TCA Evaluation

Specification and routine for the analysis of the thermochemical accumulator.

A.1.1 Technical Data

Technical Data		ClimateWell Solar Chiller
Average Power Consumption	Electrical	18 W
COP	(Thermal)	Triple state absorption process COP 0.68. Implemented COP will depend on installation characteristics, typically 0,52-0,57.
The Maximum Temperature to ClimateWell	From Heat Source	120°C
Maximum Pressure	From Heat Source	10 bar
Pressure Drop	Heat Source Circuit	30 kPa at 25l/min
	Heat Rejection Circuit	38 kPa at 50l/min
	Distribution Circuit	45 kPa at 25l/min
Energy Storage Capacity	Cooling	56 kWh
Weight		990 kg
Fluid Volume	Operational	74,5 l
Salt Solution	Lithium chloride	LiCl

Fig. A.1 ClimateWell Solar Chiller Technical Data

A.1.2 Operational Data

Operational Data		ClimateWell Solar Chiller	
Heat Source Circuit	Flow	25 - 30 l/min	
	Typical Power Range	15 - 20 kW	
	Operational Temperature	Out	75 °C – 100 °C
		In	85 °C – 110 °C
	Operational Pressure	3 bars	
	Maximum Pressures	6 bars	
Type of Fluid	Propylene Glycol 1,2 L ≥ 15 % concentration		
Distribution Circuit	Flow	25 - 30 l/min	
	Nominal Power	See Power Curves	
	Operational Temperature	Out	10 °C – 16 °C
		In	15 °C – 21 °C
Type of Fluid	Propylene Glycol 1,2 L ≥ 15 % concentration		
Heat Rejection Circuit	Flow	50 - 60 l/min	
	Operational Temperature	Out	30 °C to 45 °C
		In	< 30 °C
Type of Fluid	Propylene Glycol 1,2 L ≥ 15 % concentration		

Fig. A.2 ClimateWell Solar Chiller Operational Data

A.1.3 MATLAB Code: TCA Evaluation

MATLAB Version: *R2019a*

HARDWARE: Windows 10 (x64-based processor); Intel(R) Core(TM) i3, CPU @ 1.70GHz;

Installed RAM 16.0 GB

Contents

- Inputs/Parameters
- Charging
- Discharging
- Performance

```
clc  
clear all
```

Inputs/Parameters

```
Ms = input('enter mass flow of source circuit ');  
%Cps = input('enter specific heat capacity of source circuit ');  
TR1 = input('enter thermal source tempeature to CWSC ');  
TR0 = input('enter thermal source temperature from CWSC ');  
Tsr = input('enter saturation temperature of reactor ');  
Tr = input('enter intial temperature of reactor ');  
Tct = input('enter condenser temperature ');  
Tcf = input('enter condenser film temperature ');  
TC1 = input('enter heat sink circuit temperature to CWSC ');  
TC0 = input('enter hear sink circuit temperature from CWSC ');  
Te1 = input('enter a\c circuit temp to CWSC ');  
Te0 = input('enter a\c circuit temp from CWSC ');  
Mhs = input('enter mass flow of heat sink circuit ');  
Mr = input('enter mass of reactor ');  
Mex = input('enter a\c circuit mass flow ');  
dti = input('time duration in seconds ');  
Cps = 3.76;  
Cphs = 3.76;  
Hvap = 2477;  
Mwcti = 50;
```

```
Error using input
Cannot call INPUT from EVALC.
```

```
Error in TCA2_3 (line 4)
Ms = input('enter mass flow of source circuit      ');
```

Charging

```
%Qsource = EnTrn(Ms,Cps,TR1,TR0);
% TR1 - thermal source temp to CWSC
% TR0 - thermal source temp from CWSC

Qsen = EnTrn(Mr,Cps,Tsr,Tr);
% Mr - mass of reactor; Cpr - heat Capacity of reactor; Tsr - Sat temp of
% reactor; Tr - initial temp of reactor
Mvap = MVapour(Tct,Tcf,Tsr,dti);
Qvap = Hvap * Mvap;
% Qvap - energy rate due to vapour; Hvap - specific heat cap of
% vaporisation; Mvap - mass of vapour.

Qcharge = Qsen + Qvap;
% Qsen - sensible heat energy rate
% Qcon - condensation heat energy rate; deltaHs -

Qhs_ch = EnTrn(Mhs,Cphs,TC1,TC0); % Heat sink (hs) for during charging
% Mhs - mass flow of hs circuit; Cphs - heat cap of hs circuit; TC1 - hs
% circuit temp to CWSC; TC0 - hs circuit temp from CWSC
```

Discharging

```
Qcool = EnTrn(Mex,Cphs,Te1,Te0); % + Hvap*Mwcti; % ex - evaporator exchanger
% Mex - mass flow of condenser circuit @discharge; Tex1 - A/C circuit temp to
% CWSC; Tex0 - A/C circuit temp from CWSC
```

Performance

```
COPcool = Qcool/Qsource;
```

```
COP_heat = abs(Qhs_ch)/Qsource;
```

```
%COP_heatpump = (Abs(Qhs_ch)+abs(Qhs_dis))/Qsource;
```

A.2 MATLAB Code: NH_3-H_2O VARC

MATLAB Version: R2019a

HARDWARE: Windows 10 (x64-based processor); Intel(R) Core(TM) i3, CPU @ 1.70GHz;
Installed RAM 16.0 GB

Contents

- Calculating the liquid and vapour mole fractions of ammonia and water. Flash type calculation is used

```
function [QA, QC, QG, mR, ms, mw, T3] = NAquaA(Te, Ta, Tc, Tg)

%UNTITLED2 Summary of this function goes here
% Detailed explanation goes here
%Pc = input('Enter the condenser pressure in Mega Pascal (MPa)
%Pe = input('Enter the evaporator pressure in Mega Pascal (MPa)
%Qe1 = input('Enter refrigeration capacity in Kw )
%M101 = input('Enter refrigerant mass flow in Kg/s
E = input('Enter heat exchanger effectiveness

% The above are properties of the solution at saturation point.
% Xss (strong solution) is the ammonia concentration of the
% solution at the exit of the absorber.
% This concentration is assumed to be same throughout the pipe
% flow to the inlet of the generator. Similarly, Xws (weak solution)
% is the concentration from the exit of the generator to the inlet of
% the absorber.

Pe = Antoine1(Te+273.15)*0.1; Peo= sprintf('Pe = %d',Pe); disp(Peo);
Pc = Antoine1(Tc+273.15)*0.1; Pco= sprintf('Pc = %d',Pc); disp(Pco);

Xss = TpxSE(Ta + 273, Pe); Xsso= sprintf('Xss = %d',Xss); disp(Xsso);

Xws = TpxSE(Tg + 273, Pc); Xwso= sprintf('Xws = %d',Xws); disp(Xwso);
[~,~,Xam,~] = TP_Flash(Xws,Te); % Te must be in degrees celcius
%Xam = 0.70;
```

Error using input

Cannot call INPUT from EVALC.

Error in NAquaA (line 6)

```
Qe1 = input('Enter refrigeration capacity in Kw ');
```

Calculating the liquid and vapour mole fractions of ammonia and water. Flash type calculation is used

X1 = ammonia mole fraction and X2 = (1 - X1) = water mole fraction.

```
[H1,~,~,~] = H_liquid(Ta,Pe,Xss); H1o= sprintf('H1= %d',H1); disp(H1o);
```

```
H2 = H1;
```

```
[H4,~,~,~,~] = H_liquid(Tg,Pc,Xws); H4o= sprintf('H4 = %d',H4); disp(H4o);
```

```
%[H6,~,~,~] = H_liquid(Ta,Pe,[],Xws);
```

```
[H7,~,~] = Hvapour(Tg+273,Pc,Xam); H7o= sprintf('H7= %d',H7); disp(H7o);
```

```
[H8,~,~,~,~] = H_liquid(Tc,Pc,Xam); H8o= sprintf('H8= %d',H8); disp(H8o);
```

```
H9 = H8;
```

```
[H10,~,~] = Hvapour(Te+273,Pe,Xam);H10o= sprintf('H10= %d',H10); disp(H10o);
```

Flow Rates

```
if Qe1 == 0
```

```
    QE = M101*(H10 - H8); QEo= sprintf('QE= %d',QE); disp(QEo);
```

```
    mR = M101; mRo= sprintf('mR= %d',mR); disp(mRo);
```

```
elseif Qe1 > 0
```

```
    QE = Qe1;
```


A.2.1 Sub-routine: NH_3-H_2O VARS

The followings are the sub-routines stringed to the NH_3-H_2O VARC code.

A. Saturation Pressure

```
function [ P ] = Antoine1( T )
%Antoine calculates the saturated pressure of ammonia (bar) for a given
%temperature using the Antoine correlation which could be found on the NIST
%webpage
%(https://webbook.nist.gov/cgi/cbook.cgi?ID=C7664417&Mask=4&Type...
% =ANTOINE&Plot=on)
% Detailed explanation goes here

%A = 6.67956; B = 1002.711; C = 25.215;
A = 3.18757; B = 506.713; C = -80.78;
A1 = 4.86886; B1 = 1113.928; C1 = -10.409;

if T ==164.0 || T < 239.599
    P = exp(A - (B/(T+C)));
elseif T >= 239.599 || T == 371.5
    P = exp(A1 - (B1/(T+C1)));
end
```

B. Ammonia Concentration

```
function [X] = TpxSE(T,p)
if p == 0.010 || p < 0.011
    A1 = -0.06034;
    A2 = 0.1883;
    A3 = -0.3248;
    A4 = 0.3695;
    um = 240.4;
    sig = 39.25;
elseif p == 0.011 || p < 0.012
    A1 = -0.06056;
    A2 = 0.1883;
    A3 = -0.3243;
```

```
A4 = 0.3695;
um = 241.9;
sig = 39.48;
elseif p == 0.012 || p < 0.013
    A1 = -0.06076;
    A2 = 0.1883;
    A3 = -0.3239;
    A4 = 0.3695;
    um = 243.3;
    sig = 39.68;
elseif p == 0.013 || p < 0.014
    A1 = -0.06093;
    A2 = 0.1883;
    A3 = -0.3235;
    A4 = 0.3696;
    um = 244.6;
    sig = 39.88;
elseif p == 0.014 || p < 0.015
    A1 = -0.06109;
    A2 = 0.1882;
    A3 = -0.3232;
    A4 = 0.3696;
    um = 245.9;
    sig = 40.06;
elseif p == 0.015 || p < 0.016
    A1 = -0.06123;
    A2 = 0.1881;
    A3 = -0.3228;
    A4 = 0.3697;
    um = 247;
    sig = 40.22;
elseif p == 0.016 || p < 0.017
    A1 = -0.06135;
    A2 = 0.1881;
    A3 = -0.3225;
    A4 = 0.3698;
```

```
    um = 248.1;
    sig = 40.38;
elseif p == 0.017 || p < 0.018
    A1 = -0.06146;
    A2 = 0.1880;
    A3 = -0.3222;
    A4 = 0.3698;
    um = 249.1;
    sig = 40.53;
elseif p == 0.018 || p < 0.019
    A1 = -0.06157;
    A2 = 0.1879;
    A3 = -0.3219;
    A4 = 0.3699;
    um = 250.1;
    sig = 40.67;
elseif p == 0.019 || p < 0.020
    A1 = -0.06166;
    A2 = 0.1878;
    A3 = -0.3216;
    A4 = 0.3700;
    um = 251.1;
    sig = 40.80;
elseif p == 0.020 || p < 0.021
    A1 = -0.06174;
    A2 = 0.1877;
    A3 = -0.3214;
    A4 = 0.3700;
    um = 252.0;
    sig = 40.93;
elseif p == 0.021 || p < 0.022
    A1 = -0.06182;
    A2 = 0.1876;
    A3 = -0.3211;
    A4 = 0.3701;
    um = 252.8;
```

```
    sig = 41.05;
elseif p == 0.022 || p < 0.023
    A1 = -0.06190;
    A2 = 0.1875;
    A3 = -0.3209;
    A4 = 0.3702;
    um = 253.7;
    sig = 41.17;
elseif p == 0.023 || p < 0.024
    A1 = -0.06196;
    A2 = 0.1874;
    A3 = -0.3207;
    A4 = 0.3703;
    um = 254.5;
    sig = 41.28;
elseif p == 0.024 || p < 0.025
    A1 = -0.06202;
    A2 = 0.1873;
    A3 = -0.3205;
    A4 = 0.3703;
    um = 255.2;
    sig = 41.38;
elseif p == 0.025 || p < 0.026
    A1 = -0.06208;
    A2 = 0.1872;
    A3 = -0.3203;
    A4 = 0.3704;
    um = 256.0;
    sig = 41.49;
elseif p == 0.026 || p < 0.027
    A1 = -0.06213;
    A2 = 0.1871;
    A3 = -0.3201;
    A4 = 0.3705;
    um = 256.7;
    sig = 41.58;
```

```
elseif p == 0.027 || p < 0.028
    A1 = -0.06218;
    A2 = 0.1870;
    A3 = -0.3199;
    A4 = 0.3706;
    um = 257.4;
    sig = 41.68;
elseif p == 0.028 || p < 0.029
    A1 = -0.06223;
    A2 = 0.1869;
    A3 = -0.3197;
    A4 = 0.3706;
    um = 258.1;
    sig = 41.77;
elseif p == 0.029 || p < 0.030
    A1 = -0.06227;
    A2 = 0.1868;
    A3 = -0.3195;
    A4 = 0.3707;
    um = 258.7;
    sig = 41.86;
elseif p == 0.030 || p < 0.031
    A1 = -0.06231;
    A2 = 0.1867;
    A3 = -0.3193;
    A4 = 0.3708;
    um = 259.4;
    sig = 41.95;
elseif p == 0.031 || p < 0.032
    A1 = -0.06235;
    A2 = 0.1865;
    A3 = -0.3192;
    A4 = 0.3709;
    um = 260.0;
    sig = 42.03;
elseif p == 0.032 || p < 0.033
```

```
A1 = -0.06239;
A2 = 0.1864;
A3 = -0.3190;
A4 = 0.3709;
um = 260.6;
sig = 42.11;
elseif p == 0.033 || p < 0.034
  A1 = -0.06242;
  A2 = 0.1863;
  A3 = -0.3189;
  A4 = 0.3710;
  um = 261.2;
  sig = 42.19;
elseif p == 0.034 || p < 0.035
  A1 = -0.06245;
  A2 = 0.1862;
  A3 = -0.3187;
  A4 = 0.3711;
  um = 261.7;
  sig = 42.27;
elseif p == 0.035 || p < 0.036
  A1 = -0.06248;
  A2 = 0.1861;
  A3 = -0.3186;
  A4 = 0.3712;
  um = 262.3;
  sig = 42.34;
elseif p == 0.036 || p < 0.037
  A1 = -0.06251;
  A2 = 0.1860;
  A3 = -0.3184;
  A4 = 0.3712;
  um = 262.8;
  sig = 42.42;
elseif p == 0.037 || p < 0.038
  A1 = -0.06253;
```

```
A2 = 0.1859;
A3 = -0.3183;
A4 = 0.3713;
um = 263.4;
sig = 42.49;
elseif p == 0.038 || p < 0.039
    A1 = -0.06256;
    A2 = 0.1858;
    A3 = -0.3182;
    A4 = 0.3714;
    um = 263.9;
    sig = 42.56;
elseif p == 0.039 || p < 0.040
    A1 = -0.06258;
    A2 = 0.1857;
    A3 = -0.3180;
    A4 = 0.3714;
    um = 264.4;
    sig = 42.62;
elseif p == 0.040 || p < 0.041
    A1 = -0.06260;
    A2 = 0.1856;
    A3 = -0.3179;
    A4 = 0.3715;
    um = 264.9;
    sig = 42.69;
elseif p == 0.041 || p < 0.042
    A1 = -0.06262;
    A2 = 0.1855;
    A3 = -0.3178;
    A4 = 0.3716;
    um = 265.4;
    sig = 42.76;
elseif p == 0.042 || p < 0.043
    A1 = -0.06265;
    A2 = 0.1854;
```

```
A3 = -0.3177;
A4 = 0.3716;
um = 265.9;
sig = 42.82;
elseif p == 0.043 || p < 0.044
  A1 = -0.06267;
  A2 = 0.1853;
  A3 = -0.3175;
  A4 = 0.3717;
  um = 266.3;
  sig = 42.88;
elseif p == 0.044 || p < 0.045
  A1 = -0.06268;
  A2 = 0.1852;
  A3 = -0.3174;
  A4 = 0.3718;
  um = 266.8;
  sig = 42.94;
elseif p == 0.045 || p < 0.046
  A1 = -0.06270;
  A2 = 0.1851;
  A3 = -0.3173;
  A4 = 0.3718;
  um = 267.3;
  sig = 43.00;
elseif p == 0.046 || p < 0.047
  A1 = -0.06272;
  A2 = 0.1850;
  A3 = -0.3172;
  A4 = 0.3719;
  um = 267.7;
  sig = 43.06;
elseif p == 0.047 || p < 0.048
  A1 = -0.06273;
  A2 = 0.1849;
  A3 = -0.3171;
```

```
A4 = 0.3720;
um = 268.1;
sig = 43.12;
elseif p == 0.048 || p < 0.049
    A1 = -0.06275;
    A2 = 0.1848;
    A3 = -0.3170;
    A4 = 0.3720;
    um = 268.6;
    sig = 43.17;
elseif p == 0.049 || p < 0.050
    A1 = -0.06276;
    A2 = 0.1847;
    A3 = -0.3169;
    A4 = 0.3721;
    um = 269.0;
    sig = 43.23;
elseif p == 0.050 || p < 0.051
    A1 = -0.06278;
    A2 = 0.1847;
    A3 = -0.3168;
    A4 = 0.3721;
    um = 269.4;
    sig = 43.28;
elseif p == 0.051 || p < 0.052
    A1 = -0.06279;
    A2 = 0.1846;
    A3 = -0.3167;
    A4 = 0.3722;
    um = 269.8;
    sig = 43.34;
elseif p == 0.052 || p < 0.053
    A1 = -0.06280;
    A2 = 0.1845;
    A3 = -0.3166;
    A4 = 0.3723;
```

```
    um = 270.2;
    sig = 43.39;
elseif p == 0.053 || p < 0.054
    A1 = -0.06281;
    A2 = 0.1844;
    A3 = -0.3165;
    A4 = 0.3723;
    um = 270.6;
    sig = 43.44;
elseif p == 0.054 || p < 0.055
    A1 = -0.06282;
    A2 = 0.1843;
    A3 = -0.3164;
    A4 = 0.3724;
    um = 271.0;
    sig = 43.49;
elseif p == 0.055 || p < 0.056
    A1 = -0.06283;
    A2 = 0.1842;
    A3 = -0.3163;
    A4 = 0.3724;
    um = 271.4;
    sig = 43.54;
elseif p == 0.056 || p < 0.057
    A1 = -0.06284;
    A2 = 0.1841;
    A3 = -0.3162;
    A4 = 0.3725;
    um = 271.8;
    sig = 43.59;
elseif p == 0.057 || p < 0.058
    A1 = -0.06285;
    A2 = 0.1840;
    A3 = -0.3162;
    A4 = 0.3726;
    um = 272.1;
```

```
    sig = 43.64;
elseif p == 0.058 || p < 0.059
    A1 = -0.06286;
    A2 = 0.1839;
    A3 = -0.3161;
    A4 = 0.3726;
    um = 272.5;
    sig = 43.68;
elseif p == 0.059 || p < 0.060
    A1 = -0.06287;
    A2 = 0.1838;
    A3 = -0.3160;
    A4 = 0.3727;
    um = 272.9;
    sig = 43.73;
elseif p == 0.060 || p < 0.061
    A1 = -0.06287;
    A2 = 0.1838;
    A3 = -0.3159;
    A4 = 0.3727;
    um = 273.2;
    sig = 43.77;
elseif p == 0.061 || p < 0.062
    A1 = -0.06288;
    A2 = 0.1837;
    A3 = -0.3158;
    A4 = 0.3728;
    um = 273.6;
    sig = 43.82;
elseif p == 0.062 || p < 0.063
    A1 = -0.06289;
    A2 = 0.1836;
    A3 = -0.3157;
    A4 = 0.3728;
    um = 273.9;
    sig = 43.86;
```

```
elseif p == 0.063 || p < 0.064
    A1 = -0.06289;
    A2 = 0.1835;
    A3 = -0.3157;
    A4 = 0.3729;
    um = 274.3;
    sig = 43.91;
elseif p == 0.064 || p < 0.065
    A1 = -0.06290;
    A2 = 0.1834;
    A3 = -0.3156;
    A4 = 0.3729;
    um = 274.6;
    sig = 43.95;
elseif p == 0.065 || p < 0.066
    A1 = -0.06290;
    A2 = 0.1833;
    A3 = -0.3155;
    A4 = 0.3730;
    um = 274.9;
    sig = 43.99;
elseif p == 0.066 || p < 0.067
    A1 = -0.06291;
    A2 = 0.1833;
    A3 = -0.3154;
    A4 = 0.3731;
    um = 275.3;
    sig = 44.04;
elseif p == 0.067 || p < 0.068
    A1 = -0.06291;
    A2 = 0.1832;
    A3 = -0.3154;
    A4 = 0.3731;
    um = 275.6;
    sig = 44.08;
elseif p == 0.068 || p < 0.069
```

```
A1 = -0.06292;
A2 = 0.1831;
A3 = -0.3153;
A4 = 0.3732;
um = 275.9;
sig = 44.12;
elseif p == 0.069 || p < 0.070
  A1 = -0.06292;
  A2 = 0.1830;
  A3 = -0.3152;
  A4 = 0.3732;
  um = 276.2;
  sig = 44.16;
elseif p == 0.070 || p < 0.071
  A1 = -0.06293;
  A2 = 0.1829;
  A3 = -0.3152;
  A4 = 0.3733;
  um = 276.5;
  sig = 44.20;
elseif p == 0.071 || p < 0.072
  A1 = -0.06293;
  A2 = 0.1829;
  A3 = -0.3151;
  A4 = 0.3733;
  um = 276.8;
  sig = 44.24;
elseif p == 0.072 || p < 0.073
  A1 = -0.06293;
  A2 = 0.1828;
  A3 = -0.3150;
  A4 = 0.3734;
  um = 277.1;
  sig = 44.28;
elseif p == 0.073 || p < 0.074
  A1 = -0.06294;
```

```
A2 = 0.1827;
A3 = -0.3149;
A4 = 0.3734;
um = 277.5;
sig = 44.32;
elseif p == 0.074 || p < 0.075
    A1 = -0.06294;
    A2 = 0.1826;
    A3 = -0.3149;
    A4 = 0.3735;
    um = 277.8;
    sig = 44.35;
elseif p == 0.075 || p < 0.076
    A1 = -0.06294;
    A2 = 0.1825;
    A3 = -0.3148;
    A4 = 0.3735;
    um = 278.1;
    sig = 44.39;
elseif p == 0.076 || p < 0.077
    A1 = -0.06294;
    A2 = 0.1825;
    A3 = -0.3148;
    A4 = 0.3736;
    um = 278.3;
    sig = 44.43;
elseif p == 0.077 || p < 0.078
    A1 = -0.06294;
    A2 = 0.1824;
    A3 = -0.3147;
    A4 = 0.3736;
    um = 278.6;
    sig = 44.47;
elseif p == 0.078 || p < 0.079
    A1 = -0.06295;
    A2 = 0.1823;
```

```
A3 = -0.3146;
A4 = 0.3737;
um = 278.9;
sig = 44.50;
elseif p == 0.079 || p < 0.080
  A1 = -0.06295;
  A2 = 0.1822;
  A3 = -0.3146;
  A4 = 0.3737;
  um = 279.2;
  sig = 44.54;
elseif p == 0.080 || p < 0.081
  A1 = -0.06295;
  A2 = 0.1822;
  A3 = -0.3145;
  A4 = 0.3738;
  um = 279.5;
  sig = 44.57;
elseif p == 0.081 || p < 0.082
  A1 = -0.06295;
  A2 = 0.1821;
  A3 = -0.3144;
  A4 = 0.3738;
  um = 279.8;
  sig = 44.61;
elseif p == 0.082 || p < 0.083
  A1 = -0.06295;
  A2 = 0.1820;
  A3 = -0.3144;
  A4 = 0.3739;
  um = 280.0;
  sig = 44.64;
elseif p == 0.083 || p < 0.084
  A1 = -0.06295;
  A2 = 0.1819;
  A3 = -0.3143;
```

```
A4 = 0.33739;
um = 280.3;
sig = 44.68;
elseif p == 0.084 || p < 0.085
    A1 = -0.06295;
    A2 = 0.1819;
    A3 = -0.3143;
    A4 = 0.3739;
    um = 280.6;
    sig = 44.71;
elseif p == 0.085 || p < 0.086
    A1 = -0.06295;
    A2 = 0.1818;
    A3 = -0.3142;
    A4 = 0.3740;
    um = 280.9;
    sig = 44.74;
elseif p == 0.086 || p < 0.087
    A1 = -0.06295;
    A2 = 0.1817;
    A3 = -0.3142;
    A4 = 0.3740;
    um = 281.1;
    sig = 44.78;
elseif p == 0.087 || p < 0.088
    A1 = -0.06295;
    A2 = 0.1817;
    A3 = -0.3141;
    A4 = 0.3696;
    um = 281.4;
    sig = 44.81;
elseif p == 0.088 || p < 0.089
    A1 = -0.06295;
    A2 = 0.1816;
    A3 = -0.3140;
    A4 = 0.3741;
```

```
    um = 281.6;
    sig = 44.84;
elseif p == 0.089 || p < 0.090
    A1 = -0.06295;
    A2 = 0.1815;
    A3 = -0.3140;
    A4 = 0.3742;
    um = 281.9;
    sig = 44.88;
elseif p == 0.090 || p < 0.091
    A1 = -0.06295;
    A2 = 0.1814;
    A3 = -0.3139;
    A4 = 0.3742;
    um = 282.2;
    sig = 44.91;
elseif p == 0.091 || p < 0.092
    A1 = -0.06295;
    A2 = 0.1814;
    A3 = -0.3139;
    A4 = 0.3743;
    um = 282.4;
    sig = 44.49;
elseif p == 0.092 || p < 0.093
    A1 = -0.06295;
    A2 = 0.1813;
    A3 = -0.3138;
    A4 = 0.3743;
    um = 282.7;
    sig = 44.97;
elseif p == 0.093 || p < 0.094
    A1 = -0.06295;
    A2 = 0.1812;
    A3 = -0.3138;
    A4 = 0.3744;
    um = 282.9;
```

```
    sig = 45.00;
elseif p == 0.094 || p < 0.055
    A1 = -0.06294;
    A2 = 0.1812;
    A3 = -0.3137;
    A4 = 0.3744;
    um = 283.2;
    sig = 45.03;
elseif p == 0.095 || p < 0.096
    A1 = -0.06294;
    A2 = 0.1811;
    A3 = -0.3137;
    A4 = 0.3744;
    um = 283.4;
    sig = 445.06;
elseif p == 0.096 || p < 0.097
    A1 = -0.06294;
    A2 = 0.1810;
    A3 = -0.3136;
    A4 = 0.3745;
    um = 283.7;
    sig = 45.09;
elseif p == 0.097 || p < 0.098
    A1 = -0.06294;
    A2 = 0.1810;
    A3 = -0.3136;
    A4 = 0.3745;
    um = 283.9;
    sig = 45.12;
elseif p == 0.098 || p < 0.099
    A1 = -0.06294;
    A2 = 0.1809;
    A3 = -0.3135;
    A4 = 0.3746;
    um = 284.1;
    sig = 45.15;
```

```
elseif p == 0.099 || p < 0.10
    A1 = -0.06293;
    A2 = 0.1808;
    A3 = -0.3135;
    A4 = 0.3746;
    um = 284.4;
    sig = 45.18;
elseif p == 0.10 || p < 0.11
    A1 = -0.06293;
    A2 = 0.1808;
    A3 = -0.3134;
    A4 = 0.3747;
    um = 284.6;
    sig = 45.12;
elseif p == 0.11 || p < 0.12
    A1 = -0.06290;
    A2 = 0.1801;
    A3 = -0.3130;
    A4 = 0.3751;
    um = 286.9;
    sig = 45.49;
elseif p == 0.12 || p < 0.13
    A1 = -0.06287;
    A2 = 0.1795;
    A3 = -0.3126;
    A4 = 0.3755;
    um = 289.0;
    sig = 45.47;
elseif p == 0.13 || p < 0.14
    A1 = -0.06283;
    A2 = 0.1789;
    A3 = -0.3122;
    A4 = 0.3758;
    um = 290.9;
    sig = 45.98;
elseif p == 0.14 || p < 0.15
```

```
A1 = -0.06278;  
A2 = 0.1783;  
A3 = -0.3119;  
A4 = 0.3762;  
um = 292.8;  
sig = 46.21;  
elseif p == 0.15 || p < 0.16  
  A1 = -0.06273;  
  A2 = 0.1778;  
  A3 = -0.3116;  
  A4 = 0.3765;  
  um = 294.5;  
  sig = 46.42;  
elseif p == 0.16 || p < 0.17  
  A1 = -0.06267;  
  A2 = 0.1773;  
  A3 = -0.3113;  
  A4 = 0.3768;  
  um = 296.1;  
  sig = 46.61;  
elseif p == 0.17 || p < 0.18  
  A1 = -0.06262;  
  A2 = 0.1768;  
  A3 = -0.3110;  
  A4 = 0.3771;  
  um = 297.7;  
  sig = 46.80;  
elseif p == 0.018 || p < 0.19  
  A1 = -0.06256;  
  A2 = 0.1763;  
  A3 = -0.3108;  
  A4 = 0.3774;  
  um = 299.2;  
  sig = 46.98;  
elseif p == 0.19 || p < 0.20  
  A1 = -0.06250;
```

```
A2 = 0.1758;
A3 = -0.3105;
A4 = 0.3777;
um = 300.6;
sig = 47.15;
elseif p == 0.20 || p < 0.21
    A1 = -0.06245;
    A2 = 0.1754;
    A3 = -0.3103;
    A4 = 0.3780;
    um = 302.0;
    sig = 47.31;
elseif p == 0.21 || p < 0.22
    A1 = -0.06239;
    A2 = 0.1749;
    A3 = -0.3101;
    A4 = 0.3783;
    um = 303.3;
    sig = 47.46;
elseif p == 0.22 || p < 0.23
    A1 = -0.06233;
    A2 = 0.1745;
    A3 = -0.3099;
    A4 = 0.3785;
    um = 304.6;
    sig = 47.61;
elseif p == 0.23 || p < 0.24
    A1 = -0.06227;
    A2 = 0.1741;
    A3 = -0.3097;
    A4 = 0.3788;
    um = 305.8;
    sig = 47.76;
elseif p == 0.24 || p < 0.25
    A1 = -0.06221;
    A2 = 0.1737;
```

```
A3 = -0.3095;
A4 = 0.3790;
um = 307.0;
sig = 47.89;
elseif p == 0.25 || p < 0.26
  A1 = -0.06215;
  A2 = 0.1734;
  A3 = -0.3094;
  A4 = 0.3793;
  um = 308.2;
  sig = 48.03;
elseif p == 0.26 || p < 0.27
  A1 = -0.06209;
  A2 = 0.1730;
  A3 = -0.3092;
  A4 = 0.3795;
  um = 309.3;
  sig = 48.16;
elseif p == 0.27 || p < 0.28
  A1 = -0.06203;
  A2 = 0.1726;
  A3 = -0.3090;
  A4 = 0.3797;
  um = 310.4;
  sig = 48.28;
elseif p == 0.28 || p < 0.29
  A1 = -0.06197;
  A2 = 0.1723;
  A3 = -0.3089;
  A4 = 0.3799;
  um = 311.4;
  sig = 48.40;
elseif p == 0.29 || p < 0.30
  A1 = -0.06191;
  A2 = 0.1719;
  A3 = -0.3087;
```

```
A4 = 0.3801;
um = 312.4;
sig = 48.52;
elseif p == 0.30 || p < 0.31
    A1 = -0.06185;
    A2 = 0.1716;
    A3 = -0.3086;
    A4 = 0.3803;
    um = 313.4;
    sig = 48.63;
elseif p == 0.31 || p < 0.32
    A1 = -0.06179;
    A2 = 0.1713;
    A3 = -0.3085;
    A4 = 0.3805;
    um = 314.4;
    sig = 48.74;
elseif p == 0.32 || p < 0.33
    A1 = -0.06174;
    A2 = 0.1709;
    A3 = -0.3084;
    A4 = 0.3807;
    um = 315.3;
    sig = 48.85;
elseif p == 0.33 || p < 0.34
    A1 = -0.06168;
    A2 = 0.1706;
    A3 = -0.3082;
    A4 = 0.3809;
    um = 316.3;
    sig = 48.95;
elseif p == 0.34 || p < 0.35
    A1 = -0.06162;
    A2 = 0.1703;
    A3 = -0.3081;
    A4 = 0.3811;
```

```
    um = 317.2;
    sig = 49.06;
elseif p == 0.35 || p < 0.36
    A1 = -0.06157;
    A2 = 0.1700;
    A3 = -0.3080;
    A4 = 0.3813;
    um = 318.0;
    sig = 49.15;
elseif p == 0.36 || p < 0.37
    A1 = -0.06151;
    A2 = 0.1697;
    A3 = -0.3079;
    A4 = 0.3815;
    um = 318.9;
    sig = 49.25;
elseif p == 0.37 || p < 0.38
    A1 = -0.06146;
    A2 = 0.1695;
    A3 = -0.3078;
    A4 = 0.3816;
    um = 319.7;
    sig = 49.35;
elseif p == 0.38 || p < 0.39
    A1 = -0.06140;
    A2 = 0.1692;
    A3 = -0.3077;
    A4 = 0.3818;
    um = 320.6;
    sig = 49.44;
elseif p == 0.39 || p < 0.40
    A1 = -0.06135;
    A2 = 0.1689;
    A3 = -0.3076;
    A4 = 0.3820;
    um = 321.4;
```

```
    sig = 49.53;
elseif p == 0.40 || p < 0.41
    A1 = -0.06129;
    A2 = 0.1686;
    A3 = -0.3075;
    A4 = 0.3821;
    um = 322.2;
    sig = 49.62;
elseif p == 0.41 || p < 0.42
    A1 = -0.06124;
    A2 = 0.16842;
    A3 = -0.33074;
    A4 = 0.3823;
    um = 322.9;
    sig = 49.70;
elseif p == 0.42 || p < 0.43
    A1 = -0.06119;
    A2 = 0.1681;
    A3 = -0.3073;
    A4 = 0.3825;
    um = 323.7;
    sig = 49.79;
elseif p == 0.43 || p < 0.44
    A1 = -0.06114;
    A2 = 0.1679;
    A3 = -0.3072;
    A4 = 0.3826;
    um = 324.4;
    sig = 49.87;
elseif p == 0.44 || p < 0.45
    A1 = -0.06109;
    A2 = 0.1676;
    A3 = -0.3071;
    A4 = 0.3828;
    um = 325.2;
    sig = 49.95;
```

```
elseif p == 0.45 || p < 0.46
    A1 = -0.06103;
    A2 = 0.1674;
    A3 = -0.3071;
    A4 = 0.3829;
    um = 325.9;
    sig = 50.03;
elseif p == 0.46 || p < 0.47
    A1 = -0.06098;
    A2 = 0.1671;
    A3 = -0.3070;
    A4 = 0.3831;
    um = 326.6;
    sig = 50.11;
elseif p == 0.47 || p < 0.48
    A1 = -0.06093;
    A2 = 0.1669;
    A3 = -0.3069;
    A4 = 0.3832;
    um = 327.3;
    sig = 50.19;
elseif p == 0.48 || p < 0.49
    A1 = -0.06088;
    A2 = 0.1667;
    A3 = -0.3068;
    A4 = 0.3834;
    um = 328;
    sig = 50.26;
elseif p == 0.49 || p < 0.50
    A1 = -0.06084;
    A2 = 0.1664;
    A3 = -0.3068;
    A4 = 0.3835;
    um = 328.7;
    sig = 50.34;
elseif p == 0.50 || p < 0.51
```

```
A1 = -0.06079;
A2 = 0.1662;
A3 = -0.3067;
A4 = 0.3836;
um = 329.3;
sig = 50.41;
elseif p == 0.51 || p < 0.52
  A1 = -0.06074;
  A2 = 0.1660;
  A3 = -0.3066;
  A4 = 0.3838;
  um = 330.0;
  sig = 50.48;
elseif p == 0.52 || p < 0.53
  A1 = -0.06069;
  A2 = 0.1658;
  A3 = -0.3066;
  A4 = 0.3839;
  um = 330.6;
  sig = 50.55;
elseif p == 0.53 || p < 0.54
  A1 = -0.06064;
  A2 = 0.1656;
  A3 = -0.3065;
  A4 = 0.3840;
  um = 331.2;
  sig = 50.62;
elseif p == 0.54 || p < 0.55
  A1 = -0.06060;
  A2 = 0.1653;
  A3 = -0.3064;
  A4 = 0.3842;
  um = 331.9;
  sig = 50.69;
elseif p == 0.55 || p < 0.56
  A1 = -0.06055;
```

```
A2 = 0.1651;
A3 = -0.3064;
A4 = 0.3843;
um = 332.5;
sig = 50.76;
elseif p == 0.56 || p < 0.57
    A1 = -0.06051;
    A2 = 0.1649;
    A3 = -0.3063;
    A4 = 0.3844;
    um = 333.1;
    sig = 50.82;
elseif p == 0.57 || p < 0.58
    A1 = -0.06064;
    A2 = 0.1647;
    A3 = -0.3062;
    A4 = 0.3845;
    um = 333.7;
    sig = 50.89;
elseif p == 0.58 || p < 0.59
    A1 = -0.06042;
    A2 = 0.1645;
    A3 = -0.3062;
    A4 = 0.3846;
    um = 334.3;
    sig = 50.95;
elseif p == 0.59 || p < 0.60
    A1 = -0.06037;
    A2 = 0.1643;
    A3 = -0.3061;
    A4 = 0.3848;
    um = 334.9;
    sig = 51.02;
elseif p == 0.60 || p < 0.61
    A1 = -0.06033;
    A2 = 0.1641;
```

```
A3 = -0.3061;
A4 = 0.3849;
um = 335.4;
sig = 51.08;
elseif p == 0.61 || p < 0.62
  A1 = -0.06028;
  A2 = 0.1640;
  A3 = -0.3060;
  A4 = 0.3850;
  um = 336.0;
  sig = 51.4;
elseif p == 0.62 || p < 0.63
  A1 = -0.06024;
  A2 = 0.1638;
  A3 = -0.3060;
  A4 = 0.3851;
  um = 336.6;
  sig = 51.2;
elseif p == 0.63 || p < 0.64
  A1 = -0.06020;
  A2 = 0.1636;
  A3 = -0.3059;
  A4 = 0.3852;
  um = 337.1;
  sig = 51.26;
elseif p == 0.64 || p < 0.65
  A1 = -0.06015;
  A2 = 0.1634;
  A3 = -0.3058;
  A4 = 0.3853;
  um = 337.7;
  sig = 51.32;
elseif p == 0.65 || p < 0.66
  A1 = -0.06011;
  A2 = 0.1632;
  A3 = -0.3058;
```

```
A4 = 0.3855;
um = 338.2;
sig = 51.38;
elseif p == 0.66 || p < 0.67
    A1 = -0.06007;
    A2 = 0.1630;
    A3 = -0.3057;
    A4 = 0.3856;
    um = 338.7;
    sig = 51.44;
elseif p == 0.67 || p < 0.68
    A1 = -0.06003;
    A2 = 0.1629;
    A3 = -0.3057;
    A4 = 0.3857;
    um = 339.3;
    sig = 51.49;
elseif p == 0.68 || p < 0.69
    A1 = -0.05999;
    A2 = 0.1627;
    A3 = -0.3057;
    A4 = 0.3858;
    um = 339.8;
    sig = 51.55;
elseif p == 0.69 || p < 0.70
    A1 = -0.05995;
    A2 = 0.1625;
    A3 = -0.3056;
    A4 = 0.3859;
    um = 340.3;
    sig = 51.61;
elseif p == 0.70 || p < 0.71
    A1 = -0.05990;
    A2 = 0.1623;
    A3 = -0.3056;
    A4 = 0.3860;
```

```
    um = 340.8;
    sig = 51.66;
elseif p == 0.71 || p < 0.72
    A1 = -0.005986;
    A2 = 0.1622;
    A3 = -0.3055;
    A4 = 0.3861;
    um = 341.3;
    sig = 51.71;
elseif p == 0.072 || p < 0.73
    A1 = -0.05982;
    A2 = 0.1620;
    A3 = -0.3055;
    A4 = 0.3862;
    um = 341.8;
    sig = 51.77;
elseif p == 0.73 || p < 0.74
    A1 = -0.05979;
    A2 = 0.1618;
    A3 = -0.3054;
    A4 = 0.3863;
    um = 342.3;
    sig = 51.82;
elseif p == 0.74 || p < 0.75
    A1 = -0.05975;
    A2 = 0.1617;
    A3 = -0.3054;
    A4 = 0.3864;
    um = 342.8;
    sig = 51.87;
elseif p == 0.75 || p < 0.76
    A1 = -0.05971;
    A2 = 0.1615;
    A3 = -0.3055;
    A4 = 0.3865;
    um = 343.3;
```

```
    sig = 51.92;
elseif p == 0.76 || p < 0.77
    A1 = -0.05967;
    A2 = 0.1614;
    A3 = -0.3053;
    A4 = 0.3866;
    um = 343.7;
    sig = 51.97;
elseif p == 0.77 || p < 0.78
    A1 = -0.05963;
    A2 = 0.1612;
    A3 = -0.3053;
    A4 = 0.3867;
    um = 344.2;
    sig = 52.03;
elseif p == 0.78 || p < 0.79
    A1 = -0.05959;
    A2 = 0.1611;
    A3 = -0.3052;
    A4 = 0.3868;
    um = 344.7;
    sig = 52.07;
elseif p == 0.79 || p < 0.80
    A1 = -0.05955;
    A2 = 0.1609;
    A3 = -0.3052;
    A4 = 0.3869;
    um = 345.1;
    sig = 52.12;
elseif p == 0.80 || p < 0.81
    A1 = -0.05952;
    A2 = 0.1607;
    A3 = -0.3051;
    A4 = 0.3870;
    um = 345.6;
    sig = 52.17;
```

```
elseif p == 0.81 || p < 0.82
    A1 = -0.05948;
    A2 = 0.1606;
    A3 = -0.3051;
    A4 = 0.3870;
    um = 346.1;
    sig = 52.22;
elseif p == 0.82 || p < 0.83
    A1 = -0.05944;
    A2 = 0.1604;
    A3 = -0.3051;
    A4 = 0.3871;
    um = 346.5;
    sig = 52.27;
elseif p == 0.83 || p < 0.84
    A1 = -0.05941;
    A2 = 0.1603;
    A3 = -0.3050;
    A4 = 0.3872;
    um = 347.0;
    sig = 52.32;
elseif p == 0.84 || p < 0.85
    A1 = -0.05937;
    A2 = 0.1602;
    A3 = -0.3050;
    A4 = 0.3873;
    um = 347.4;
    sig = 52.36;
elseif p == 0.85 || p < 0.86
    A1 = -0.05933;
    A2 = 0.1600;
    A3 = -0.3050;
    A4 = 0.3874;
    um = 347.8;
    sig = 52.41;
elseif p == 0.86 || p < 0.87
```

```
A1 = -0.05930;
A2 = 0.1599;
A3 = -0.3049;
A4 = 0.3875;
um = 348.3;
sig = 52.46;
elseif p == 0.87 || p < 0.88
  A1 = -0.05926;
  A2 = 0.1597;
  A3 = -0.3049;
  A4 = 0.3876;
  um = 348.7;
  sig = 52.50;
elseif p == 0.88 || p < 0.89
  A1 = -0.05923;
  A2 = 0.1596;
  A3 = -0.3049;
  A4 = 0.3877;
  um = 349.1;
  sig = 52.55;
elseif p == 0.89 || p < 0.90
  A1 = -0.05919;
  A2 = 0.1594;
  A3 = -0.3048;
  A4 = 0.3877;
  um = 349.5;
  sig = 52.59;
elseif p == 0.90 || p < 0.91
  A1 = -0.05916;
  A2 = 0.1593;
  A3 = -0.3048;
  A4 = 0.3878;
  um = 350.0;
  sig = 52.63;
elseif p == 0.91 || p < 0.92
  A1 = -0.05912;
```

```
A2 = 0.1592;
A3 = -0.3048;
A4 = 0.3879;
um = 350.4;
sig = 52.68;
elseif p == 0.92 || p < 0.93
    A1 = -0.05909;
    A2 = 0.1590;
    A3 = -0.3047;
    A4 = 0.3880;
    um = 350.8;
    sig = 52.72;
elseif p == 0.93 || p < 0.94
    A1 = -0.05906;
    A2 = 0.1589;
    A3 = -0.3047;
    A4 = 0.3880;
    um = 351.2;
    sig = 52.76;
elseif p == 0.94 || p < 0.95
    A1 = -0.05902;
    A2 = 0.1588;
    A3 = -0.3047;
    A4 = 0.3881;
    um = 351.6;
    sig = 52.81;
elseif p == 0.95 || p < 0.96
    A1 = -0.05899;
    A2 = 0.1586;
    A3 = -0.3046;
    A4 = 0.3882;
    um = 352.0;
    sig = 52.85;
elseif p == 0.96 || p < 0.97
    A1 = -0.05896;
    A2 = 0.1585;
```

```
A3 = -0.3046;
A4 = 0.3883;
um = 352.4;
sig = 52.89;
elseif p == 0.97 || p < 0.98
  A1 = -0.05892;
  A2 = 0.1584;
  A3 = -0.3046;
  A4 = 0.3884;
  um = 352.8;
  sig = 52.93;
elseif p == 0.98 || p < 0.99
  A1 = -0.05889;
  A2 = 0.1583;
  A3 = -0.3046;
  A4 = 0.3885;
  um = 353.2;
  sig = 52.97;
elseif p == 0.99 || p < 1.00
  A1 = -0.05886;
  A2 = 0.1581;
  A3 = -0.3045;
  A4 = 0.3885;
  um = 353.6;
  sig = 53.01;
elseif p == 1.00 || p < 1.01
  A1 = -0.05883;
  A2 = 0.1580;
  A3 = -0.3045;
  A4 = 0.3886;
  um = 354.0;
  sig = 53.05;
elseif p == 1.01 || p < 1.02
  A1 = -0.05879;
  A2 = 0.1579;
  A3 = -0.3045;
```

```
A4 = 0.3887;
um = 354.3;
sig = 53.09;
elseif p == 1.02 || p < 1.03
    A1 = -0.05876;
    A2 = 0.1578;
    A3 = -0.3044;
    A4 = 0.3888;
    um = 354.7;
    sig = 53.13;
elseif p == 1.03 || p < 1.04
    A1 = -0.05873;
    A2 = 0.1576;
    A3 = -0.3044;
    A4 = 0.3888;
    um = 355.1;
    sig = 53.17;
elseif p == 1.04 || p < 1.05
    A1 = -0.05870;
    A2 = 0.1575;
    A3 = -0.3044;
    A4 = 0.3889;
    um = 355.5;
    sig = 53.21;
elseif p == 1.05 || p < 1.06
    A1 = -0.05867;
    A2 = 0.1574;
    A3 = -0.3044;
    A4 = 0.3890;
    um = 355.8;
    sig = 53.25;
elseif p == 1.06 || p < 1.07
    A1 = -0.05864;
    A2 = 0.1573;
    A3 = -0.3043;
    A4 = 0.3891;
```

```
    um = 356.2;
    sig = 53.29;
elseif p == 1.07 || p < 1.08
    A1 = -0.05861;
    A2 = 0.1572;
    A3 = -0.3043;
    A4 = 0.3891;
    um = 356.6;
    sig = 53.33;
elseif p == 1.08 || p < 1.09
    A1 = -0.05857;
    A2 = 0.1570;
    A3 = -0.3043;
    A4 = 0.3892;
    um = 356.9;
    sig = 53.37;
elseif p == 1.09 || p < 1.10
    A1 = -0.05854;
    A2 = 0.1569;
    A3 = -0.3043;
    A4 = 0.3893;
    um = 357.3;
    sig = 53.40;
elseif p == 1.10 || p < 1.11
    A1 = -0.05851;
    A2 = 0.1568;
    A3 = -0.3042;
    A4 = 0.3893;
    um = 357.7;
    sig = 53.44;
elseif p == 1.11 || p < 1.12
    A1 = -0.05848;
    A2 = 0.1567;
    A3 = -0.3042;
    A4 = 0.3894;
    um = 358.0;
```

```
    sig = 53.48;
elseif p == 1.12 || p < 1.13
    A1 = -0.05845;
    A2 = 0.1566;
    A3 = -0.3042;
    A4 = 0.3895;
    um = 358.4;
    sig = 53.51;
elseif p == 1.13 || p < 1.14
    A1 = -0.05842;
    A2 = 0.1565;
    A3 = -0.3042;
    A4 = 0.3895;
    um = 385.7;
    sig = 53.55;
elseif p == 1.14 || p < 1.15
    A1 = -0.05839;
    A2 = 0.1564;
    A3 = -0.3041;
    A4 = 0.3896;
    um = 359.1;
    sig = 53.59;
elseif p == 1.15 || p < 1.16
    A1 = -0.05837;
    A2 = 0.1563;
    A3 = -0.3041;
    A4 = 0.3897;
    um = 359.4;
    sig = 53.62;
elseif p == 1.16 || p < 1.17
    A1 = -0.05834;
    A2 = 0.1561;
    A3 = -0.3041;
    A4 = 0.3897;
    um = 359.8;
    sig = 53.66;
```

```
elseif p == 1.17 || p < 1.18
    A1 = -0.05831;
    A2 = 0.1560;
    A3 = -0.3041;
    A4 = 0.3898;
    um = 360.1;
    sig = 53.69;
elseif p == 1.18 || p < 1.19
    A1 = -0.05828;
    A2 = 0.1559;
    A3 = -0.3041;
    A4 = 0.3899;
    um = 360.4;
    sig = 53.73;
elseif p == 1.19 || p < 1.20
    A1 = -0.05825;
    A2 = 0.1558;
    A3 = -0.3040;
    A4 = 0.3899;
    um = 360.8;
    sig = 53.76;
elseif p == 1.20 || p < 1.21
    A1 = -0.05822;
    A2 = 0.1557;
    A3 = -0.3040;
    A4 = 0.3900;
    um = 361.1;
    sig = 53.80;
elseif p == 1.21 || p < 1.22
    A1 = -0.05819;
    A2 = 0.1556;
    A3 = -0.3040;
    A4 = 0.3901;
    um = 361.4;
    sig = 53.81;
elseif p == 1.22 || p < 1.23
```

```
A1 = -0.05816;  
A2 = 0.1555;  
A3 = -0.3040;  
A4 = 0.3901;  
um = 361.8;  
sig = 53.87;  
elseif p == 1.23 || p < 1.24  
  A1 = -0.05814;  
  A2 = 0.1554;  
  A3 = -0.3039;  
  A4 = 0.3902;  
  um = 362.1;  
  sig = 53.9;  
elseif p == 1.24 || p < 1.25  
  A1 = -0.05811;  
  A2 = 0.1553;  
  A3 = -0.3039;  
  A4 = 0.3903;  
  um = 362.4;  
  sig = 53.93;  
elseif p == 1.25 || p < 1.26  
  A1 = -0.05808;  
  A2 = 0.1552;  
  A3 = -0.3039;  
  A4 = 0.3903;  
  um = 362.7;  
  sig = 53.97;  
elseif p == 1.26 || p < 1.27  
  A1 = -0.05805;  
  A2 = 0.1551;  
  A3 = -0.3039;  
  A4 = 0.3904;  
  um = 363.1;  
  sig = 54.00;  
elseif p == 1.27 || p < 1.28  
  A1 = -0.05803;
```

```
A2 = 0.1550;
A3 = -0.3039;
A4 = 0.3904;
um = 363.4;
sig = 54.03;
elseif p == 1.28 || p < 1.29
    A1 = -0.05800;
    A2 = 0.1549;
    A3 = -0.3038;
    A4 = 0.3905;
    um = 363.7;
    sig = 54.07;
elseif p == 1.29 || p < 1.30
    A1 = -0.05797;
    A2 = 0.1548;
    A3 = -0.3038;
    A4 = 0.3906;
    um = 364.0;
    sig = 54.1;
elseif p == 1.30 || p < 1.31
    A1 = -0.05795;
    A2 = 0.1547;
    A3 = -0.3038;
    A4 = 0.3906;
    um = 364.3;
    sig = 54.13;
elseif p == 1.31 || p < 1.32
    A1 = -0.05792;
    A2 = 0.1546;
    A3 = -0.3038;
    A4 = 0.3907;
    um = 364.7;
    sig = 54.16;
elseif p == 1.32 || p < 1.33
    A1 = -0.05789;
    A2 = 0.1545;
```

```
A3 = -0.3038;
A4 = 0.3907;
um = 365.0;
sig = 54.20;
elseif p == 1.33 || p < 1.34
  A1 = -0.05787;
  A2 = 0.1544;
  A3 = -0.3038;
  A4 = 0.3908;
  um = 365.3;
  sig = 54.23;
elseif p == 1.34 || p < 1.35
  A1 = -0.05784;
  A2 = 0.1543;
  A3 = -0.3037;
  A4 = 0.3909;
  um = 365.6;
  sig = 54.26;
elseif p == 1.35 || p < 1.36
  A1 = -0.06109;
  A2 = 0.1542;
  A3 = -0.3037;
  A4 = 0.3909;
  um = 365.9;
  sig = 54.29;
elseif p == 1.36 || p < 1.37
  A1 = -0.05779;
  A2 = 0.1541;
  A3 = -0.3037;
  A4 = 0.3910;
  um = 366.2;
  sig = 54.32;
elseif p == 1.37 || p < 1.38
  A1 = -0.05776;
  A2 = 0.1540;
  A3 = -0.3037;
```

```
A4 = 0.3910;
um = 366.5;
sig = 54.35;
elseif p == 1.38 || p < 1.39
    A1 = -0.05774;
    A2 = 0.1539;
    A3 = -0.3037;
    A4 = 0.3911;
    um = 366.8;
    sig = 54.38;
elseif p == 1.39 || p < 1.40
    A1 = -0.05771;
    A2 = 0.1538;
    A3 = -0.3036;
    A4 = 0.3912;
    um = 367.1;
    sig = 54.41;
elseif p == 1.40 || p < 1.41
    A1 = -0.05768;
    A2 = 0.1537;
    A3 = -0.3036;
    A4 = 0.3912;
    um = 367.4;
    sig = 54.44;
elseif p == 1.41 || p < 1.42
    A1 = -0.05766;
    A2 = 0.1537;
    A3 = -0.3036;
    A4 = 0.3913;
    um = 367.7;
    sig = 54.47;
elseif p == 1.42 || p < 1.43
    A1 = -0.05763;
    A2 = 0.1536;
    A3 = -0.3036;
    A4 = 0.3913;
```

```
    um = 368.0;
    sig = 54.50;
elseif p == 1.43 || p < 1.44
    A1 = -0.05761;
    A2 = 0.1535;
    A3 = -0.3036;
    A4 = 0.3914;
    um = 368.3;
    sig = 54.53;
elseif p == 1.44 || p < 1.45
    A1 = -0.05758;
    A2 = 0.1534;
    A3 = -0.3036;
    A4 = 0.3914;
    um = 368.6;
    sig = 54.56;
elseif p == 1.45 || p < 1.46
    A1 = -0.05756;
    A2 = 0.1533;
    A3 = -0.3035;
    A4 = 0.3915;
    um = 368.8;
    sig = 54.59;
elseif p == 1.46 || p < 1.47
    A1 = -0.05753;
    A2 = 0.1532;
    A3 = -0.3035;
    A4 = 0.3915;
    um = 369.1;
    sig = 54.62;
elseif p == 1.47 || p < 1.48
    A1 = -0.05751;
    A2 = 0.1531;
    A3 = -0.3035;
    A4 = 0.3916;
    um = 369.4;
```

```
    sig = 54.65;
elseif p == 1.48 || p < 1.49
    A1 = -0.05749;
    A2 = 0.1530;
    A3 = -0.3035;
    A4 = 0.3916;
    um = 369.7;
    sig = 54.68;
elseif p == 1.49 || p < 1.50
    A1 = -0.05746;
    A2 = 0.1529;
    A3 = -0.3035;
    A4 = 0.3917;
    um = 370.0;
    sig = 54.71;
elseif p == 1.50 || p < 1.51
    A1 = -0.05744;
    A2 = 0.1529;
    A3 = -0.3035;
    A4 = 0.3918;
    um = 370.3;
    sig = 54.74;
elseif p == 1.51 || p < 1.52
    A1 = -0.05741;
    A2 = 0.1528;
    A3 = -0.3034;
    A4 = 0.3918;
    um = 370.5;
    sig = 54.77;
elseif p == 1.52 || p < 1.53
    A1 = -0.05739;
    A2 = 0.1527;
    A3 = -0.3034;
    A4 = 0.3919;
    um = 370.8;
    sig = 54.79;
```

```
elseif p == 1.53 || p < 1.54
    A1 = -0.05737;
    A2 = 0.1526;
    A3 = -0.3034;
    A4 = 0.3919;
    um = 371.1;
    sig = 54.82;
elseif p == 1.54 || p < 1.55
    A1 = -0.05734;
    A2 = 0.1525;
    A3 = -0.3034;
    A4 = 0.3920;
    um = 371.4;
    sig = 54.85;
elseif p == 1.55 || p < 1.56
    A1 = -0.05732;
    A2 = 0.1524;
    A3 = -0.3034;
    A4 = 0.3920;
    um = 371.7;
    sig = 54.88;
elseif p == 1.56 || p < 1.57
    A1 = -0.05729;
    A2 = 0.523;
    A3 = -0.3034;
    A4 = 0.3921;
    um = 371.9;
    sig = 54.91;
elseif p == 1.57 || p < 1.58
    A1 = -0.05727;
    A2 = 0.1523;
    A3 = -0.3034;
    A4 = 0.3921;
    um = 372.2;
    sig = 54.93;
elseif p == 1.58 || p < 1.59
```

```
A1 = -0.05725;
A2 = 0.1522;
A3 = -0.3033;
A4 = 0.3922;
um = 372.5;
sig = 54.96;
elseif p == 1.59 || p < 1.60
    A1 = -0.05723;
    A2 = 0.1521;
    A3 = -0.3033;
    A4 = 0.3922;
    um = 372.7;
    sig = 54.99;
elseif p == 1.60 || p < 1.61
    A1 = -0.05720;
    A2 = 0.1520;
    A3 = -0.3033;
    A4 = 0.3923;
    um = 373.0;
    sig = 55.01;
elseif p == 1.61 || p < 1.62
    A1 = -0.05718;
    A2 = 0.1519;
    A3 = -0.3033;
    A4 = 0.3923;
    um = 373.3;
    sig = 55.04;
elseif p == 1.62 || p < 1.63
    A1 = -0.05716;
    A2 = 0.1518;
    A3 = -0.3033;
    A4 = 0.3924;
    um = 373.5;
    sig = 55.07;
elseif p == 1.63 || p < 1.64
    A1 = -0.05713;
```

```
A2 = 0.1518;
A3 = -0.3033;
A4 = 0.3924;
um = 2373.8;
sig = 55.10;
elseif p == 1.64 || p < 1.65
    A1 = -0.05711;
    A2 = 0.1517;
    A3 = -0.3033;
    A4 = 0.3925;
    um = 374.1;
    sig = 55.12;
elseif p == 1.65 || p < 1.66
    A1 = -0.05709;
    A2 = 0.1516;
    A3 = -0.3032;
    A4 = 0.3925;
    um = 374.3;
    sig = 55.15;
elseif p == 1.66 || p < 1.67
    A1 = -0.05707;
    A2 = 0.1515;
    A3 = -0.3032;
    A4 = 0.3926;
    um = 374.6;
    sig = 55.17;
elseif p == 1.67 || p < 1.68
    A1 = -0.05704;
    A2 = 0.1515;
    A3 = -0.3032;
    A4 = 0.3926;
    um = 374.8;
    sig = 55.20;
elseif p == 1.68 || p < 1.69
    A1 = -0.05702;
    A2 = 0.1514;
```

```
A3 = -0.3032;
A4 = 0.3927;
um = 375.1;
sig = 55.23;
elseif p == 1.69 || p < 1.70
  A1 = -0.05700;
  A2 = 0.1513;
  A3 = -0.3032;
  A4 = 0.3927;
  um = 375.4;
  sig = 55.25;
elseif p == 1.70 || p < 1.71
  A1 = -0.05698;
  A2 = 0.1512;
  A3 = -0.3032;
  A4 = 0.3927;
  um = 375.6;
  sig = 55.28;
elseif p == 1.71 || p < 1.72
  A1 = -0.05696;
  A2 = 0.1511;
  A3 = -0.3032;
  A4 = 0.3928;
  um = 375.9;
  sig = 55.30;
elseif p == 1.72 || p < 1.73
  A1 = -0.05693;
  A2 = 0.1511;
  A3 = -0.3032;
  A4 = 0.3928;
  um = 376.1;
  sig = 55.33;
elseif p == 1.73 || p < 1.74
  A1 = -0.05691;
  A2 = 0.1510;
  A3 = -0.3031;
```

```
A4 = 0.3929;
um = 376.4;
sig = 55.35;
elseif p == 1.74 || p < 1.75
    A1 = -0.05689;
    A2 = 0.1509;
    A3 = -0.3031;
    A4 = 0.929;
    um = 376.6;
    sig = 55.38;
elseif p == 1.75 || p < 1.76
    A1 = -0.05687;
    A2 = 0.1508;
    A3 = -0.3031;
    A4 = 0.3930;
    um = 376.9;
    sig = 55.41;
elseif p == 1.76 || p < 1.77
    A1 = -0.05685;
    A2 = 0.1508;
    A3 = -0.3031;
    A4 = 0.3930;
    um = 377.1;
    sig = 55.43;
elseif p == 1.77 || p < 1.78
    A1 = -0.05683;
    A2 = 0.1507;
    A3 = -0.3031;
    A4 = 0.3931;
    um = 377.4;
    sig = 55.45;
elseif p == 1.78 || p < 1.79
    A1 = -0.05680;
    A2 = 0.1506;
    A3 = -0.3031;
    A4 = 0.3931;
```

```
    um = 377.6;
    sig = 55.48;
elseif p == 1.79 || p < 1.80
    A1 = -0.05678;
    A2 = 0.1505;
    A3 = -0.3031;
    A4 = 0.3932;
    um = 377.9;
    sig = 55.50;
elseif p == 1.80 || p < 1.81
    A1 = -0.05676;
    A2 = 0.1505;
    A3 = -0.3031;
    A4 = 0.3932;
    um = 378.1;
    sig = 55.53;
elseif p == 1.81 || p < 1.82
    A1 = -0.05674;
    A2 = 0.1504;
    A3 = -0.3030;
    A4 = 0.3932;
    um = 378.4;
    sig = 55.55;
elseif p == 1.82 || p < 1.83
    A1 = -0.05672;
    A2 = 0.1503;
    A3 = -0.3030;
    A4 = 0.3933;
    um = 378.6;
    sig = 55.58;
elseif p == 1.83 || p < 1.84
    A1 = -0.05670;
    A2 = 0.1502;
    A3 = -0.3030;
    A4 = 0.3933;
    um = 378.8;
```

```
    sig = 55.60;
elseif p == 1.84 || p < 1.85
    A1 = -0.05668;
    A2 = 0.1502;
    A3 = -0.3030;
    A4 = 0.3934;
    um = 379.1;
    sig = 55.63;
elseif p == 1.85 || p < 1.86
    A1 = -0.05666;
    A2 = 0.1501;
    A3 = -0.3030;
    A4 = 0.3934;
    um = 379.3;
    sig = 55.65;
elseif p == 1.86 || p < 1.87
    A1 = -0.05664;
    A2 = 0.1500;
    A3 = -0.3030;
    A4 = 0.3935;
    um = 379.6;
    sig = 55.67;
elseif p == 1.87 || p < 1.88
    A1 = -0.05662;
    A2 = 0.1500;
    A3 = -0.3030;
    A4 = 0.3935;
    um = 379.8;
    sig = 55.70;
elseif p == 1.88 || p < 1.89
    A1 = -0.05660;
    A2 = 0.1499;
    A3 = -0.3030;
    A4 = 0.3936;
    um = 380.0;
    sig = 55.72;
```

```
elseif p == 1.89 || p < 1.90
    A1 = -0.05658;
    A2 = 0.1498;
    A3 = -0.3030;
    A4 = 0.3936;
    um = 380.3;
    sig = 55.74;
elseif p == 1.90 || p < 1.91
    A1 = -0.05656;
    A2 = 0.1498;
    A3 = -0.3029;
    A4 = 0.3936;
    um = 380.5;
    sig = 55.77;
elseif p == 1.91 || p < 1.92
    A1 = -0.05354;
    A2 = 0.1497;
    A3 = -0.3029;
    A4 = 0.3937;
    um = 380.7;
    sig = 55.79;
elseif p == 1.92 || p < 1.93
    A1 = -0.056652;
    A2 = 0.1496;
    A3 = -0.3029;
    A4 = 0.3937;
    um = 381.0;
    sig = 55.81;
elseif p == 1.93 || p < 1.94
    A1 = -0.05650;
    A2 = 0.1495;
    A3 = -0.3029;
    A4 = 0.3938;
    um = 381.2;
    sig = 55.84;
elseif p == 1.94 || p < 1.95
```

```
A1 = -0.05648;
A2 = 0.1495;
A3 = -0.3029;
A4 = 0.3938;
um = 381.4;
sig = 55.86;
elseif p == 1.95 || p < 1.96
  A1 = -0.05646;
  A2 = 0.1494;
  A3 = -0.3029;
  A4 = 0.3938;
  um = 381.7;
  sig = 55.88;
elseif p == 1.96 || p < 1.97
  A1 = -0.05644;
  A2 = 0.1493;
  A3 = -0.3029;
  A4 = 0.3939;
  um = 381.9;
  sig = 55.91;
elseif p == 1.97 || p < 1.98
  A1 = -0.05642;
  A2 = 0.1493;
  A3 = -0.3029;
  A4 = 0.3939;
  um = 382.1;
  sig = 55.93;
elseif p == 1.98 || p < 1.99
  A1 = -0.05640;
  A2 = 0.1492;
  A3 = -0.3029;
  A4 = 0.3940;
  um = 382.3;
  sig = 55.95;
elseif p == 1.99 || p < 2.00
  A1 = -0.05638;
```

```
A2 = 0.1491;
A3 = -0.3029;
A4 = 0.3940;
um = 382.6;
sig = 55.97;
elseif p == 2.00 || p < 2.01
    A1 = -0.05636;
    A2 = 0.1491;
    A3 = -0.3028;
    A4 = 0.3941;
    um = 382.8;
    sig = 56.00;
elseif p == 2.01 || p < 2.02
    A1 = -0.05634;
    A2 = 0.1490;
    A3 = -0.3028;
    A4 = 0.3941;
    um = 383.0;
    sig = 56.02;
elseif p == 2.02 || p < 2.03
    A1 = -0.05632;
    A2 = 0.1489;
    A3 = -0.3028;
    A4 = 0.3941;
    um = 383.2;
    sig = 56.04;
elseif p == 2.03 || p < 2.04
    A1 = -0.05630;
    A2 = 0.1489;
    A3 = -0.3028;
    A4 = 0.3942;
    um = 383.5;
    sig = 56.06;
elseif p == 2.04 || p < 2.05
    A1 = -0.05628;
    A2 = 0.1488;
```

```
A3 = -0.3028;
A4 = 0.3942;
um = 383.7;
sig = 56.09;
elseif p == 2.05 || p < 2.06
  A1 = -0.05626;
  A2 = 0.1487;
  A3 = -0.3028;
  A4 = 0.3943;
  um = 383.9;
  sig = 56.11;
elseif p == 2.06 || p < 2.07
  A1 = -0.05625;
  A2 = 0.1487;
  A3 = -0.3028;
  A4 = 0.3943;
  um = 384.1;
  sig = 56.13;
elseif p == 2.07 || p < 2.08
  A1 = -0.05623;
  A2 = 0.1486;
  A3 = -0.3028;
  A4 = 0.3943;
  um = 384.3;
  sig = 56.15;
elseif p == 2.08 || p < 2.09
  A1 = -0.05621;
  A2 = 0.1486;
  A3 = -0.3028;
  A4 = 0.3944;
  um = 384.6;
  sig = 56.17;
end
B = (T - um)/sig;
X =A1*B^3 + A2*B^2 +A3*B + A4;
if X > 1 || X < 0
```

```
X = NaN;  
disp('"ERROR" OUT OF RANGE')  
end  
end
```

C. Temperature - concentration plot

Temperature - composition relation of Aqua-Ammonia for $x = 0.0:0.1:1.0$, and pressure in MPa 0.01 to 0.09 (0.1bar to 0.9bar)

```
Tp200 = [486.3045 456.8367 431.3044 407.6716 385.9955 367.1732 352.0423 340.8330 33
```

```
Tp201 = [486.5613 457.0925 431.5515 407.9095 386.2252 367.3957 352.2583 341.0428 33
```

```
Tp202 = [486.8170 457.3472 431.7976 408.1465 386.4540 367.6174 352.4734 341.2518 33
```

```
Tp203 = [487.0718 457.6010 432.0428 408.3825 386.6819 367.8382 352.6877 341.4600 33
```

```
Tp204 = [487.3256 457.8538 432.2870 408.6177 386.9090 368.0582 352.9013 341.6674 33
```

```
Tp205 = [487.5785 458.1056 432.5303 408.8519 387.1352 368.2773 353.1140 341.8740 33
```

```
Tp206 = [487.8303 458.3565 432.7727 409.0853 387.3606 368.4957 353.3259 342.0799 33
```

```
Tp207 = [488.0813 458.6064 433.0141 409.3178 387.5852 368.7132 353.5371 342.2850 33
```

```
Tp208 = [488.3312 458.8553 433.2547 409.5494 387.8088 368.9299 353.7475 342.4893 33
```

```
Tp209 = [488.5803 459.1034 433.4944 409.7802 388.0317 369.1458 353.9570 342.6929 33
```

```
x = 0:0.1:1;
```

```
plot(Tp200,x,'--r','LineWidth',2)  
ylabel('Ammonia mole fraction')  
xlabel('Temperature (K)')
```

```
hold on
plot(Tp201,x,'g','LineWidth',2)
plot(Tp202,x,'o','LineWidth',2)
plot(Tp203,x,':','LineWidth',2)
plot(Tp204,x,'d','LineWidth',2)
plot(Tp205,x,'<k','LineWidth',2)
plot(Tp206,x,'*c','LineWidth',2)
plot(Tp207,x,'.r','LineWidth',2)
plot(Tp208,x,'-.','LineWidth',2)
plot(Tp209,x,'--','LineWidth',2)
hold off
title('Ammonia Temperature - concentration plot')
legend('P = 2.00MPa','P = 2.01MPa','P = 2.02MPa','P = 2.03MPa','P = 2.04MPa','P = 2.05MPa',
'P = 2.06MPa','P = 2.07MPa','P = 2.08MPa','P = 2.09MPa')
```

D. State Point Enthalpy - Liquid phase

Contents

- Coefficients/Constants of the Correlation
- General

```
function[H_liq,Hw,Ha,He,Hsa] = H_liquid(t,p,x)
```

Coefficients/Constants of the Correlation

For Water

```
a1 = 2.748796e-2;
```

```
a2 = -1.016665e-5;
```

```
a3 = -4.452025e-3;
```

```
a4 = 8.389246e-4;
```

```
b1 = 1.214557e1;
```

```
b2 = -1.898065;
```

```
b3 = 2.911966e-1;
```

```
hw = 21.821141;
```

Trw = 5.0705;

Prw = 3.000;

% For Ammonia

m1 = 3.971423e-2;

m2 = -1.790557e-5;

m3 = -1.308905e-2;

m4 = 3.752836e-3;

n1 = 1.634519e1;

n2 = -6.508119;

n3 = 1.448937;

ha = 4.878573;

Tra = 3.2252;

Pra = 2.0000;

General

R = 8.341;

T = t + 273;

Tb = 100;

Tr = T/Tb;

P = p;

Pb = 10;

Pr = P/Pb;

E1 = -41.733398; E2 = 0.02414; E3 = 6.702285; E4 = -0.011475;
E5 = 63.608967; E6 = -62.490768; E7 = 1.761064; E8 = 0.008626;
E9 = 0.387983; E10 = 0.004772; E11 = -4.648107; E12 = 0.836376;
E13 = -3.553627; E14 = 0.000904; E15 = 21.361723; E16 = -20.736547;

Not enough input arguments.

Error in H_liquid (line 35)

T = t + 273;

```

He = ((-R*Tb*x*(1-x))/(17*x + (18*(1-x))))*((-E1-E2*Pr-(2*E5/Tr)-...
(3*E6/Tr^2))+((2*x-1)*((-E7-E8*Pr-2*E11/Tr)-(3*E12/Tr^2)))+((2*x-1)^2*...
((-E13-E14*Pr)-(2*E15/Tr)-(3*E16/Tr^2))));

Hw = (-R*Tb*(1-x)/18)*((-hw+b1*(Trw-Tr))+((b2/2)*(Trw^2-Tr^2))+((b3/3)*...
(Trw^3-Tr^3))+((a4*Tr^2)-a1)*(Pr-Prw))-(a2/2*(Pr^2-Prw)+a3/3*(Pr^3-Prw));
Ha = (-R*Tb*x/17)*((-ha+n1*(Tra-Tr))+((n2/2)*(Tra^2-Tr^2))+((n3/3)*...
(Tra^3-Tr^3))+((m4*Tr^2)-m1)*(Pr-Pra))-(m2/2*(Pr^2-Pra)+m3/3*(Pr^3-Prw));
Hliq = (Hw + Ha);%*0.85;
H_liq = Hliq + He;
Hsa = Ha + He;

disp(He)
disp(Ha)
disp(Hw)

end

```

E. State Point Enthalpy - Vapour phase

Contents

- Enthalpy of the Vapour Phase
- general/Input parameters
- Equations

```
function [H_vap,Hvw,Hva] = Hvapour(t,p,x)
```

Enthalpy of the Vapour Phase

for water

```

C1 = 2.136131e-2;
C2 = -3.169291e1;
C3 = -4.634611e4;
C4 = 0.0000;

D1 = 4.019170;

```

D2 = -5.175550e-2;

D3 = 1.951939e-2;

Trw = 5.0705;

Prw = 3.000;

hvw = 60.965058;

% for Ammonia

Ca = -1.049377e-2;

Cb = -8.288224;

Cc = -6.647257e2;

Cd = -3.045352e3;

Da = 3.673647;

Db = 9.989629e-2;

Dc = 3.617622e-2;

hva = 26.468879;

Tra = 3.2252;

Pra = 2.0000;

general/Input parameters

%t = 100;

% p = 13.5;

% x = 0.95;

%s = 0.999;

%[~, ~, x, ~] = TP_Flash(s, t);

R = 8.341;

T = t + 273;

Tb = 100;

Tr = T/Tb;

P = p;

Pb = 10;

Pr = P/Pb;

Not enough input arguments.

Error in Hvapour (line 43)

```
T = t + 273;
```

Equations

```
Hvw = (-R*Tb*(1-x)/18)*(-hvw+(D1*Trw)+((D2/2)*(Tr^2+Trw^2))+((D3/3)*...  
(2*Tr^3+Trw^3))-((D1*Tr)-(D2*Tr^2))-(D3/2*(Tr^2+Trw^2))-(C1*(Pr-Prw))+...  
(C2*((4*Prw/Trw^3)-(4*Pr/Tr^3)))+(C3*((12*Prw/Trw^11)-(12*Pr/Tr^11)))+...  
((C4/3)*(12*Prw^3/Trw^11)-(12*Pr^3/Tr^11)));
```

```
Hva = (-R*Tb*x/17)*(-hva+(Da*Tra)+((Db/2)*(Tr^2+Tra^2))+((Dc/3)*...  
(2*Tr^3+Tra^3))-((Da*Tr)-(Db*Tr^2))-(Dc/2*(Tr^2+Tra^2))-(Ca*(Pr-Pra))+...  
(Cb*((4*Pra/Tra^3)-(4*Pr/Tr^3)))+(Cc*((12*Pra/Tra^11)-(12*Pr/Tr^11)))+...  
((Cd/3)*(12*Pra^3/Tra^11)-(12*Pr^3/Tr^11)));
```

```
H_vap = Hvw + Hva;
```

```
%disp(H_vap)
```

```
%disp(Hvw)
```

```
%disp(Hva)
```

F. State Point Enthalpy - Mixed phase

Contents

- FLASH CALCULATION
- Flash calculation is necessary for the determination of vapour-liquid (mix)phase composition.
- DERIVATION

```
function [x1, x2, y1, y2] = TP_Flash(s,t)
```

```
% i = 1 for ammonia
```

```
% i = 2 for water
```

FLASH CALCULATION

Flash calculation is necessary for the determination of vapour-liquid (mix)phase composition.

The vapour and the liquid is assumed to be in equilibrium. $Fz(i) = Lx(i) + Vy(i)$ F is the feed with composition $z(i)$. V is the vapour $y(i)$ composition while L is the liquid of $x(i)$. $y(i)=K(i)x(i)$. $K(i) = K(i)(T,P,x(i),y(i))$ - computed from the VLE model. There are two equations with four unknowns, therefore two additional equations need to be specified to make it solvable. PT flash specifies PT in the function as K depends on P and T.

DERIVATION

$Fz(i) = Lx(i) + Vy(i)$ (1) $y(i) = K(i) x(i)$ (2) substituting (1) in (2), $Fz(i) = Lx(i) + VK(i)x(i)$ (3) $x(i) = Fz(i)/(L+VK(i))$ (4) Introducing $L = F - V$ (total mass balance) $x(i) = z(i)/(1 + V/F(K(i)-1))$ (5)

% Note that $x(i)$ cannot be calculated directly due the vapour split V/F is
% not known. To find V/F the relationship $\sum(i)y(i) = \sum K(i)x(i)=1$ is
% used. The combination $\sum(i)(y(i) - x(i))=0$ result in an equation with
% good numerical properties. This is so-called Rachford-Rice flash equation
% $\sum(i)= z(i)(K(i) - 1)/1+V/F(K(i) - 1)=0$. $0 \leq V/F \leq 1$. Assuming ideal
% situation, then $K(i)$ depends on P and T only. $K(i)=p_{sat}(i)/p$. For
% non-ideal cases, $K(i)$ depends also on $x(i)$ and $y(i)$ which could be
% approached by the an additional iteration loop on $K(i)$.

A1 = 4.48540;

B1 = 926.132;

C1 = -32.98;

A2 = 5.11564;

B2 = 1687.537;

C2 = -42.98;

%s = 0.3; % s is the ammonia fraction of the binary composition.

z = s/17;

z1 = (z)/((z)+(1-(17*z))/18);

z2 = 1 - z1;

```
%t = 70;
T = t + 273.15;

psat1 = 10^(A1 - B1/(T + C1));
psat2 = 10^(A2 - B2/(T + C2));

p = psat1*z1 + psat2*z2;

K1 = psat1/p;
K2 = psat2/p;
k1 = 1/(K1 - 1);
k2 = 1/(K2 - 1);
% Solving the Rachford-Rice numerically to find a = V/F
a = fzero(@(a) z1/(k1+a) + z2/(k2+a),0.5);
%if nargout > 1 disp('calculatiing parameters')
    x1 = z1/(1+(a*(K1 - 1)));
    x2 = z2/(1+(a*(K2 - 1)));
    y1 = K1*x1;
    y2 = K2*x2;

Not enough input arguments.

Error in TP_Flash (line 42)
z = s/17;

end
```


Appendix B

Biomass Cooling

B.1 Oxygen Bomb Experiment

Weight 1	Weight 2	Average
1.1096	0.9630	1.0363

Wire Length 1	Wire Length 2	Average
10.0000	10.0000	10.0000

Wire Left 1	Wire Left 2	Average
3.2000	3.3000	3.2500

Alkali 1	Alkali 2	Average
6.3000	6.7000	6.5000

a (min)	0.0833
b (min)	12.3050
c (min)	11.0000
ta	16.6830
tc	16.6830
r1	0.1830
r2	1.6040
c1	6.5000
c2	0.0102
c3	6.7500
W	2500.0000
m	1.0363
e1	6.5000
e2	0.1448
e3	15.5250
M average	9.2640

	Cal/g	MI/Kg
t	-0.1433	
HHV	-367.2028	-1.5370
HHVd	-404.6936	-1.6940
NCVd	-640.8936	-2.6827

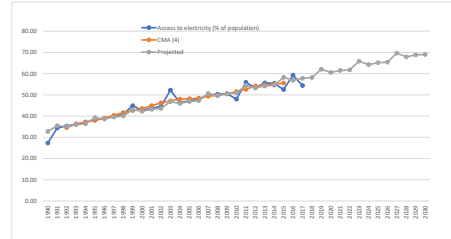
	Test1	Test2	Test3
M1	24.9656	28.0668	27.0189
M2	25.9135	29.1927	28.0982
M3	25.8257	29.0885	27.9981
Msd (g)	9.2626	9.2548	9.2745

Time	Sawdust	Wood chip	Average	Temp3	Temp4	Miscanthus	Temp6	Temp7	Rice husks	Straw
0.00	16.500	16.500	16.500	16.500	16.500	16.500	16.500	16.500	16.500	16.500
5.00	16.500	16.500	16.500	16.500	16.500	16.500	16.500	16.500	16.500	16.500
6.00	16.500	16.500	16.500	16.500	16.500	16.500	16.500	16.500	16.500	16.500
7.00	16.500	16.500	16.500	16.500	16.500	16.500	16.500	16.500	16.500	16.500
8.00	16.500	16.500	16.500	16.500	16.500	16.500	16.500	16.500	16.500	16.500
9.00	16.500	16.500	16.500	16.500	16.500	16.500	16.500	16.500	16.500	16.500
10.00	16.500	16.500	16.500	16.500	16.500	16.500	16.500	16.500	16.500	16.500
11.00	16.616	16.750	16.683	16.623	16.643	16.786	16.845	16.613	16.600	16.567
11.45	17.055	17.095	17.075	17.058	17.063	17.225	17.190	17.005	16.875	16.635
12.00	17.336	17.312	17.324	17.311	17.322	17.506	17.407	17.254	17.156	16.916
12.15	17.522	17.504	17.513	17.532	17.514	17.692	17.599	17.443	17.342	17.102
12.30	17.660	17.675	17.668	17.670	17.685	17.830	17.770	17.598	17.480	17.240
12.45	17.817	17.767	17.792	17.825	17.774	17.987	17.862	17.722	17.637	17.397
13.00	17.926	17.876	17.901	17.934	17.777	18.096	17.971	17.831	17.746	17.506
13.15	17.992	17.944	17.968	17.997	17.956	18.162	18.039	17.898	17.812	17.572
13.30	18.065	17.996	18.031	18.074	18.123	18.235	18.091	17.961	17.885	17.645
13.45	18.123	18.101	18.112	18.133	18.111	18.293	18.196	18.042	17.943	17.703
14.00	18.167	18.103	18.135	18.175	18.114	18.337	18.198	18.065	17.987	17.747
14.15	18.193	18.129	18.161	18.197	18.139	18.363	18.224	18.091	18.013	17.773
14.30	18.232	18.156	18.194	18.241	18.162	18.402	18.251	18.124	18.052	17.812
14.45	18.255	18.174	18.215	18.261	18.182	18.425	18.269	18.145	18.075	17.835
15.00	18.275	18.196	18.236	18.279	18.206	18.445	18.291	18.166	18.095	17.855
15.15	18.292	18.210	18.251	18.311	18.221	18.462	18.305	18.181	18.112	17.872
15.30	18.308	18.222	18.265	18.318	18.230	18.478	18.317	18.195	18.128	17.888
15.45	18.319	18.234	18.277	18.327	18.241	18.489	18.329	18.207	18.139	17.899
16.00	18.332	18.242	18.287	18.337	18.249	18.502	18.337	18.217	18.152	17.912
16.15	18.339	18.250	18.295	18.347	18.261	18.509	18.345	18.225	18.159	17.919
16.30	18.346	18.254	18.300	18.354	18.262	18.516	18.349	18.230	18.166	17.926
16.45	18.351	18.261	18.306	18.358	18.270	18.521	18.356	18.236	18.171	17.931
17.00	18.356	18.264	18.310	18.361	18.271	18.526	18.359	18.240	18.176	17.936
17.15	18.362	18.268	18.315	18.370	18.274	18.532	18.363	18.245	18.182	17.942
17.30	18.364	18.271	18.318	18.372	18.280	18.534	18.366	18.248	18.184	17.944
17.45	18.367	18.273	18.320	18.375	18.282	18.537	18.368	18.250	18.187	17.947
18.00	18.370	18.275	18.323	18.380	18.285	18.540	18.370	18.253	18.190	17.950
18.15	18.371	18.277	18.324	18.382	18.287	18.541	18.372	18.254	18.191	17.951
18.30	18.373	18.278	18.326	18.384	18.288	18.543	18.373	18.256	18.193	17.953
18.45	18.375	18.280	18.328	18.385	18.291	18.545	18.375	18.258	18.195	17.955
19.00	18.376	18.280	18.328	18.386	18.292	18.546	18.375	18.258	18.196	17.956
19.15	18.377	18.281	18.329	18.387	18.294	18.547	18.376	18.259	18.197	17.957
19.30	18.377	18.282	18.330	18.389	18.296	18.547	18.377	18.260	18.197	17.957
19.45	18.378	18.283	18.331	18.390	18.299	18.548	18.378	18.261	18.198	17.958
20.00	18.379	18.283	18.331	18.391	18.301	18.549	18.378	18.261	18.199	17.959
21.00	18.380	18.283	18.332	18.393	18.320	18.550	18.378	18.262	18.200	17.960
22.00	18.379	18.284	18.332	18.390	18.299	18.549	18.379	18.262	18.199	17.959
23.00	18.378	18.283	18.331	18.388	18.293	18.548	18.378	18.261	18.198	17.958
24.00	18.378	18.282	18.330	18.385	18.287	18.548	18.377	18.260	18.198	17.958
25.00	18.376	18.282	18.329	18.383	18.285	18.546	18.377	18.259	18.196	17.956
26.00	18.375	18.281	18.328	18.379	18.280	18.545	18.376	18.258	18.195	17.955
27.00	18.374	18.280	18.327	18.372	18.277	18.544	18.375	18.257	18.194	17.954
28.00	18.373	18.280	18.327	18.369	18.274	18.543	18.375	18.257	18.193	17.953
29.00	18.371	18.279	18.325	18.367	18.270	18.541	18.374	18.255	18.191	17.951

Fig. B.1 Computation of HHV from test data

B.2 Time Series Analysis

t	Year	Y _t Access to electricity (% of population)	MA(4)	baseline CMA(4)	Y _t /CMA(4)	S _{t-1}	De-seasonalised Y _t /S _t	Tt	Component Tt	Projected
1	1990	27.30					0.98	27.87	33.46665	32.78
2	1991	34.39					1.03	33.35	34.30405	35.46
3	1992	35.31	33.31	34.54	1.02	0.99	35.51	35.31424	35.12	
4	1993	36.23	35.77	36.23	1.00	0.99	36.47	36.23804	36.00	
1	1994	37.15	36.69	37.15	1.00	0.98	37.91	37.16184	36.42	
2	1995	38.08	37.62	38.08	1.00	1.03	36.97	38.05661	39.23	
3	1996	39.01	38.54	39.01	1.00	0.99	39.40	39.00943	38.62	
4	1997	39.94	39.47	40.33	0.99	0.99	40.34	39.91323	39.53	
1	1998	40.88	41.18	41.65	0.98	0.98	41.71	40.85703	40.04	
2	10 1999	44.90	42.12	42.58	1.05	1.03	43.59	41.78082	43.03	
3	11 2000	42.75	43.05	43.51	0.98	0.99	43.18	42.70462	42.28	
4	12 2001	43.67	43.98	44.89	0.97	0.99	44.11	43.62842	43.19	
1	13 2002	44.58	45.80	46.25	0.96	0.98	45.49	44.55221	43.66	
2	14 2003	52.20	46.70	47.14	1.11	1.03	50.68	45.47601	46.84	
3	15 2004	46.34	47.58	48.00	0.97	0.99	46.81	46.29993	45.34	
4	16 2005	47.18	48.43	48.17	0.98	0.99	47.66	47.3236	46.85	
1	17 2006	48.01	47.91	48.41	0.99	0.98	48.99	48.2474	47.28	
2	18 2007	50.13	48.90	49.32	1.02	1.03	48.67	49.3721	50.65	
3	19 2008	50.30	49.74	49.74	1.01	0.99	50.81	50.09499	49.59	
4	20 2009	50.52	49.74	50.46	1.00	0.99	51.04	51.01879	50.51	
1	21 2010	48.00	51.18	51.56	0.93	0.98	48.98	51.94259	50.90	
2	22 2011	55.90	51.95	52.58	1.06	1.03	54.27	52.86688	54.45	
3	23 2012	53.36	53.22	54.15	0.99	0.99	53.90	53.79018	53.25	
4	24 2013	55.60	55.08	54.65	1.02	0.99	56.16	54.71398	54.17	
1	25 2014	55.44	54.23	54.97	1.01	0.98	56.57	55.63778	54.53	
2	26 2015	52.50	55.71	55.56	0.94	1.03	50.97	56.56157	58.26	
3	27 2016	58.30				0.99	58.90	57.48337	58.91	
4	28 2017	54.40	55.41			0.99	54.95	58.49917	57.83	
1	29 2018					0.98		59.33296	58.15	
2	30 2019					1.03		60.26876	62.06	
3	31 2020					0.99		61.18056	60.57	
4	32 2021					0.99		62.10435	61.48	
1	33 2022					0.98		63.02815	61.77	
2	34 2023					1.03		63.95195	65.87	
3	35 2024					0.99		64.87574	64.23	
4	36 2025					0.99		65.79954	65.14	
1	37 2026					0.98		66.72334	65.39	
2	38 2027					1.03		67.64713	69.68	
3	39 2028					0.99		68.57093	67.89	
4	40 2029					0.99		69.49473	68.80	
1	41 2030					0.98		70.41853	69.01	
2	42									
3	43									
4	44									
1	45									
2	46									
3	47									
4	48									



Quarter	St	Stefancy
1	0.98	0.98
2	1.03	1.03
3	0.99	0.99
4	0.99	0.99

SUMMARY OUTPUT

Regression Statistics	
Multiple R	0.96255827
R Square	0.922287622
Adjusted R	0.919298085
Standard E	2.247689026
Observatio	28

ANOVA					
	df	SS	MS	F	Significance F
Regression	1	1559.163063	1559.163	308.567	6.07E-16
Residual	26	121.3757941	4.6683		
Total	27	1680.538857			

	Coefficients	Standard Error	t Stat	P-value	Lower 95%	Upper 95%	Lower 95.0%	Upper 95.0%
Intercept	32.54283311	0.873986056	37.28148	4.22E-24	30.74809	34.33712	30.74809	34.33712
t	0.923796889	0.052589825	17.56608	6.07E-16	0.815697	1.031897	0.815697	1.031897

Fig. B.2 Energy access projection

Appendix C

Drax Power Station - Biomass Power Plant

C.1 Drax - Reduced Carbon Footprint



Fig. C.1 Biomass Sample - Drax Power Station



Fig. C.2 Biomass Sample - Drax Power Station

Renewable power

We only source from working forests that grow back and stay as forests. We source wood fibre from the US and compressed wood pellets from suppliers around the world.

Six generating units at Drax Power generate up to 8% of the UK's electricity needs. Each of our six generators produces enough electricity to supply a city the size of Leeds.

It's **20 times** more carbon efficient to ship rather than road haul our wood pellets.

Using biomass in place of coal cuts our carbon footprint by more than **80%**

Fig. C.3 Drax carbon footprint reduction

C.2 Drax - Biomass Power Plant



Fig. C.4 Biomass combustion unit - Drax Power Staion



Fig. C.5 Steam turbine unit - Drax Power Staion